

UNIVERSITÉ DU QUÉBEC À MONTRÉAL

ÉTUDE DU COMPORTEMENT DES GAZ RARES ET DES MÉTAUX
VOLATILES DU SYSTÈME MAGMATIQUE-HYDROTHERMAL ACTIF DE
THEISTAREYKIR, ISLANDE

THÈSE
PRÉSENTÉE
COMME EXIGENCE PARTIELLE
DU DOCTORAT EN SCIENCES DE LA TERRE ET DE L'ATMOSPHÈRE

PAR
MARION SABY

AOÛT 2022

UNIVERSITÉ DU QUÉBEC À MONTRÉAL
Service des bibliothèques

Avertissement

La diffusion de cette thèse se fait dans le respect des droits de son auteur, qui a signé le formulaire *Autorisation de reproduire et de diffuser un travail de recherche de cycles supérieurs* (SDU-522 – Rév.04-2020). Cette autorisation stipule que «conformément à l'article 11 du Règlement no 8 des études de cycles supérieurs, [l'auteur] concède à l'Université du Québec à Montréal une licence non exclusive d'utilisation et de publication de la totalité ou d'une partie importante de [son] travail de recherche pour des fins pédagogiques et non commerciales. Plus précisément, [l'auteur] autorise l'Université du Québec à Montréal à reproduire, diffuser, prêter, distribuer ou vendre des copies de [son] travail de recherche à des fins non commerciales sur quelque support que ce soit, y compris l'Internet. Cette licence et cette autorisation n'entraînent pas une renonciation de [la] part [de l'auteur] à [ses] droits moraux ni à [ses] droits de propriété intellectuelle. Sauf entente contraire, [l'auteur] conserve la liberté de diffuser et de commercialiser ou non ce travail dont [il] possède un exemplaire.»

REMERCIEMENTS

Je tiens tout d'abord à remercier mon directeur de thèse Daniele Pinti pour son encadrement, sa présence, mais aussi pour son humour et sa franchise. Depuis toutes ces années, je peux dire que Daniele est devenu un mentor et nos échanges et discussions scientifiques m'ont beaucoup apporté dans mon apprentissage du travail de chercheur mais aussi comme personne. Je peux dire sans hésitation que j'ai eu la chance d'avoir un directeur présent, disponible et toujours prêt à m'aider en cas de besoin et sans qui je ne serais sûrement pas arrivée au bout de l'aventure! Merci.

Je tiens ensuite à remercier mon co-directeur de thèse Vincent van Hinsberg. Par son esprit brillant, Vincent m'a toujours remise dans le droit chemin de recherche quand je tendais à perdre le fil. Il a toujours été disponible et prêt à prendre le temps de revoir ensemble les concepts plus compliqués. Il m'a aussi toujours laissé beaucoup de liberté dans mes réflexions et m'a toujours encouragée dans l'exploration de pistes de recherche parfois exotiques!

Je tenais enfin à souligner la chance que j'ai eu d'avoir deux directeurs aussi présents, compréhensifs et qui se complétaient aussi bien. Chacun à sa façon, ils m'ont permis d'avoir une vision très différente et complémentaire de la science et de la vie! Merci à vous deux, je vous souhaite de continuer à encadrer des étudiants ensemble, vous faites une belle équipe!

Je tiens aussi à remercier chaleureusement Bjarni Gautason du service géologique d'Islande (ÍSOR), sans qui toute cette épopée n'aurait vu le jour. Bjarni a dès le début embarqué dans notre projet un peu fou et a tout mis en œuvre pour le rendre possible.

Il nous a aussi soutenu tout au long de ces années de doctorat pour nous permettre d'aller au bout de nos idées. Nous avons été chanceux de le compter parmi nous.

Je te tiens à remercier également Ásgerdur Sigurdardóttir, de Landsvirkjun qui nous a permis d'avoir accès à ce fabuleux site d'étude et qui nous a soutenu afin que nous puissions échantillonner tout ce dont nous avons besoin. Sa passion pour la géochimie m'a permis d'explorer plusieurs avenues de recherche et d'avoir le soutien de Landsvirkjun pour la réalisation.

Je voudrais remercier particulièrement Clara Castro et Chris Hall pour leur soutien dans l'analyse des gaz rares quand notre laboratoire n'était plus fonctionnel, ainsi que Océane Rocher et Marie Haut-Labourdette pour leur aide sur le terrain et dans le labo. Je tiens aussi à remercier très chaleureusement toute l'équipe de recherche du laboratoire du Geotop, pour leur soutien technique et plus particulièrement Jean-François Hélie, Julien Gogot et André Poirier.

Je voudrais remercier mes compagnons de route à l'UQAM et à McGill, qui ont été étudiants en même temps que moi et avec qui j'ai partagé mes joies et mes peines : Lucille, Manon, Rocio, Nico, Williams, Nathaly, Giselle, Adina, Vanessa, Cat, Shane, Stan et Haylea. Merci à tous!

J'aimerais maintenant remercier tous mes amis, pour m'avoir supporté dans les moments difficiles et d'avoir célébré avec moi à d'autres : Ariane, Clyde, Mona, Sacha, Ludo et Sylvie, Lola et tous les autres!

Je veux remercier très chaleureusement toute ma famille pour leur soutien : mon frère pour nos moments de déconne et nos moments de déprime; mon père, mon soutien infaillible, pour toutes nos discussions sur la vie et bien sûr ma mère et mon beau-père ainsi que Louna. Je veux aussi remercier mes beaux-parents pour leur soutien, pour

m'avoir accepté avec tellement générosité dans leur famille. Sans toutes ces personnes, je n'en serais pas là aujourd'hui.

Enfin, je réserve mes derniers remerciements à mon partenaire de vie, Christophe et à mon petit coconut, Raphaël, les deux amours de ma vie. Christophe, plus qu'un conjoint, tu es mon meilleur ami, mon collègue préféré, mon meilleur compagnon de soirées, et le père de mon enfant, tout ça à la fois et tellement plus encore. Tu as su me redonner confiance dans les moments de doutes, m'encourager et me soutenir jusqu'à la fin de ma thèse. Raphaël, ma petite perle, tu es arrivé en plein dans une période mouvementée sur la planète et tu as été la lumière qui a éclairée nos vies. Tu es le fruit d'un grand amour et tu nous le rends chaque jour. On t'aime...

DÉDICACE

À mon mari et meilleur ami, Christophe.
Nos discussions inspirantes et ton soutien
infaillible depuis toutes ces années m'ont
donné la force d'aller au bout de cette grande
aventure et de tant d'autres.

À mes parents, qui m'ont toujours inspirés à
faire ce qui me passionne dans la vie, à rêver
et à ne jamais abandonner.

À Raphaël, mon coconut, à jamais...

AVANT-PROPOS

Cette thèse a été rédigée sous forme de trois articles en anglais, l'un publié et les autres deux prêt à être soumis dans des revues à comité de lecture, avec une introduction et une conclusion en anglais. Le premier chapitre intitulé « *Fluid sources and dynamics at the newly developed Theistareykir Geothermal Field, Iceland* », a été publié en décembre 2020 dans la revue *Journal of Volcanology and Geothermal Research*. Le deuxième chapitre nommé « *The Behaviour of Metals in the Deep Fluids of NE Iceland* » est en préparation pour soumission dans la revue *Geochemical Perspective Letters*. Enfin, le troisième chapitre, intitulé « *Estimating the Relative Magma Degassing and Water-Rock Interaction Contributions to the Metals Load of an Active Magmatic-Hydrothermal System using Noble Gases and Trace Metals* » est en préparation pour soumission dans la revue *Geochimica et Cosmochimica Acta*.

Mon doctorat avait comme but principal de comprendre le comportement des métaux dans un champ géothermal moderne, comme analogue de gisements minérales (Au-Ag-Cu) épithermaux fossiles. Le travail a consisté à échantillonner pendant trois été (2017, 2018 et 2019) des échantillons de fluides et de roches dans le champs géothermique de Theistreykir, au Nord-Est de l'Islande. Les échantillons de roches ont été analysés pour les oxydes et éléments traces, tandis que les métaux et les gaz rares ont été mesurés dans les fluides prélevés en profondeur à partir des puits de production, et à la surface dans les manifestations de type fumeroles et volacns de boue *mud pot*. J'ai aussi coordonné l'organisation de l'échantillonnage de fluides profonds (1600m) lors du troisième été de terrain. Tous les résultats sont présentés et interprétés dans cette thèse. J'ai été responsable de l'interprétation des résultats et de la rédaction des articles scientifiques, le tout sous la supervision de mon directeur, le Pr. Daniele L. Pinti et de mon co-directeur, le Pr. Vincent van Hinsberg.

TABLE DES MATIÈRES

AVANT-PROPOS	vi
LISTE DES FIGURES.....	x
RÉSUMÉ	xv
ABSTRACT	xvii
INTRODUCTION	1
0.1 General introduction.....	1
0.2 State-of-the art	6
0.3 Scope and significance of research.....	10
0.4 Objectives	12
0.5 Theistareykir geothermal field	13
0.6 Methods and analytical approach	14
0.7 Structure of the thesis	16
REFERENCES.....	18
CHAPTER I SOURCES AND TRANSPORT OF FLUID AND HEAT AT THE NEWLY-DEVELOPED THEISTAREYKIR GEOTHERMAL FIELD, ICELAND	28
1.1 Abstract.....	29
1.2 Introduction	31
1.3 Geology of the investigated area	33
1.4 Methods	37
1.4.1 Water and gas sampling.....	37
1.4.2 Isotopic analyses.....	38
1.4.3 Geochemical computations.....	40
1.5 Results	45

1.6 Discussion.....	47
1.6.1 Fluid sources in the Theistareykir geothermal field	47
1.6.2 Sources of meteoric water	48
1.6.3 Meteoric water residence times	50
1.6.4 Origin of helium and related magmatic fluids.....	55
1.6.5 Magma degassing and heat transfer.....	58
1.6.6 Water-rock interaction and effects on ¹⁸ O and helium isotopic composition 60	
1.6.7 Conceptual model of the Theistareykir geothermal field and implications 62	
1.7 Conclusions	64
1.8 Acknowledgements	65
1.9 References	66
1.10 Figures	75
CHAPTER II THE BEHAVIOUR OF METALS IN THE DEEP FLUIDS OF NE ICELAND	83
2.1 Abstract.....	84
2.2 Introduction	85
2.3 Study area	87
2.4 Methods	88
2.5 Results	90
2.6 Evolution of fluids in the geothermal well.....	92
2.7 Metal behavior patterns	94
2.8 Implications for element mobility in magmatic-hydrothermal systems.....	96
2.9 Acknowledgements	97
2.10 References.....	97
2.11 Figures	103
2.12 Supplementary material	108
2.12.1 Sampling of Deep and Surface Fluids, and Fresh and Altered Rocks.....	108
2.12.2 Sample Preparation and Analysis	110
2.12.3 Supplementary Figures	115
2.12.4 Supplementary Information References	118

CHAPTER III Estimating Relative Contributions OF Magma Degassing and Water-Rock Interaction to the Metal Load at the theistareykir (Iceland) Hydrothermal System using Noble Gases and Trace Metals	119
3.1 Abstract.....	120
3.2 Introduction	121
3.3 Rock leaching vs. Magma degassing: a long-standing debate	125
3.4 Geology of the area and geochemistry of fluids and altered rocks	127
3.4.1 Geology	127
3.4.2 Fluid chemical composition.....	128
3.4.3 Secondary mineralogy of reservoir rocks	130
3.5 Analytical methods and data processing	131
3.5.1 Noble gas sampling and analyses	131
3.5.2 Major and trace metal analyses in water and rocks	132
3.6 Results	133
3.7 Discussion.....	135
3.7.1 Water-rock interaction and magma degassing contributions to the deep geothermal fluids	135
3.7.2 Magma degassing constrained using noble gases.....	137
3.8 Conclusions	140
3.9 Acknowledgements	141
3.10 References.....	142
3.11 Figures	152
3.12 Supplementary material	159
CONCLUSION.....	167
BIBLIOGRAPHY.....	172

LISTE DES FIGURES

- Figure 0-1 : Schematic view of a magmatic-hydrothermal system with relation to fluid flow and localisation of different features of such systems (Hedenquist et al., 2000) 6
- Figure 0-2 : Schematic view of a geothermal system with relation to noble gases systematics and sources..... 10
- Figure 1-1 : Simplified map of the Theistareykir geothermal field with major alteration zones and positions of the sampled sites (wells, mud pots, and fumaroles) indicated. Numbers on the X- and Y-axes indicate the latitudinal and longitudinal geographical coordinates respectively on the World Geodetic System 1984 (WGS84). NVZ = Northern Volcanic Zone; WVZ = Western Volcanic Zone; EVZ = Eastern Volcanic Zone..... 75
- Figure 1-2 : Plot of $\delta^2\text{H}$ vs. $\delta^{18}\text{O}$ corrected for total discharge (TD) of the Theistareykir production fluids, mud pots, and fumaroles sampled over a 20-year period (data from this study and archived ÍSOR data; Table 2 *In Electronic Supplementary Table*). The global meteoric water line (GMWL; dashed line) was calculated following Craig (1961). Pre-Holocene recharge composition is from data of Sveinbjörnsdóttir et al. (2013), and the regional highlands recharge is from Stéfansson et al. (2017). Primary magmatic water composition is from Sheppard and Epstein (1970). The dashed curves represent the evolution of $\delta^2\text{H}_{\text{TD}}$ vs. $\delta^{18}\text{O}_{\text{TD}}$ in the vapor and residual liquid after phase segregation, starting from an initial composition (yellow star), and causing isotopic fractionation. Water isotopic

compositions thus evolve along these lines according to their final equilibrium temperature. The f values correspond to the fraction of residual liquid. Blue dashed areas group stable isotopic compositions measured over the years for wells 03, 05, 07, 16, and 17. Zone A: Ketilfjall, Zone B: Bóndhólsskard, Zone C: Theistareykjagrundir, Zone D: Tjarnarás..... 76

Figure 1-3 : $^3\text{He}/^{36}\text{Ar}$ vs. $^{40}\text{Ar}/^{36}\text{Ar}$ of Theistareykir geothermal fluids. Expected MORB and Icelandic mantle source arrays are indicated for comparison, as calculated following Mukhopadhyay (2012). The black dashed line is extrapolated through data from this study, excluding wells 16 and 17, which fall on the Icelandic mantle source. Wells 7 and 13 show values below that of the Icelandic mantle source (note the broken x-axis and change in scale). The two curved thin black dashed lines correspond to a confidence interval of 95%. 77

Figure 1-4 : The measured $^3\text{He}/^4\text{He}$ ratio (R), normalized to that of the atmosphere (R_a), versus $^4\text{He}/^{20}\text{Ne}$ ratios. Extrapolated mixing hyperbola obtained by data inversion suggests mixing between an atmospheric helium component (ASW or air) and a local mantle helium component with a R/R_a of 11.45, resulting from the mixing of a depleted MORB-type mantle (DMM) and a plume-type mantle. The values from literature are from Hilton et al., (1990), Poreda et al., (1992), and Fűri et al. (2010). 78

Figure 1-5 : $^3\text{He}/Q$ vs. $^4\text{He}/^{36}\text{Ar}$ for Theistareykir well fluid samples showing the heat transport in the field. Dilution of magmatic fluids by meteoric fluids will decrease $^4\text{He}/^{36}\text{Ar}$ at a constant $^3\text{He}/Q$, whereas addition of radiogenic ^4He from the crust (magmatic-type or water-rock interaction-type fluids) will increase $^4\text{He}/^{36}\text{Ar}$ at constant $^3\text{He}/Q$ 79

- Figure 1-6 : $^4\text{He}/^3\text{He}$ vs. $Q/^3\text{He}$ for Theistareykir well fluid samples. Samples are mainly undergoing either magma degassing or magma aging and boiling. The small dashed line corresponds to the fraction of vapor removed from the fluids during boiling. The triangle reports the He isotopic composition and the $Q/^3\text{He}$ ratio of the main sources of helium in fluids (MOR, crust, and ASW). 80
- Figure 1-7 : Helium isotopic composition (R/Ra) vs. the $\delta^{18}\text{O}$ values of Theistareykir well fluids. Dashed lines show mixing between meteoric fluid (a mixture of local recharge, more distant regional recharge, and pre-Holocene recharge with a mean $\delta^{18}\text{O}$ of -15.4‰) and magmatic fluid (with a theoretical initial composition of $R/Ra > 11.9$ and $\delta^{18}\text{O} \approx +4.7\text{‰}$ (Macpherson et al., 2005b), and the effect of water-rock interactions with the addition of radiogenic ^4He to fluids and heavier $\delta^{18}\text{O}$ (with $R/Ra \geq 8.0$ and $\delta^{18}\text{O} \leq -6.5\text{‰}$) respectively. 81
- Figure 1-8 : Conceptual model of the Theistareykir geothermal field, with main fluid and heat sources and transport processes. 82
- Figure 2-1 : Simplified maps of the Theistareykir and Krafla geothermal fields with positions of the wells sampled for the deep fluids (ÞG-01 and K-21). Numbers on the X- and Y-axes indicate the latitudinal and longitudinal geographical coordinates respectively on the World Geodetic System 1984 (WGS84). NVZ = Northern Volcanic Zone; WVZ = Western Volcanic Zone; EVZ = Eastern Volcanic Zone 103
- Figure 2-2 : Plot of $\delta^2\text{H}$ vs. $\delta^{18}\text{O}$ corrected for total discharge (TD) of the Theistareykir production fluids, mud pots, and fumaroles sampled over a 20-year period (data from this study and archived ÍSOR data, in addition to the values of the deep samples at Theistareykir and Krafla; Saby et al., 2020; Table 1 In Electronic Supplementary Material). The global meteoric water line (GMWL; dashed line)

was calculated following Craig (1961). Pre-Holocene recharge composition is from data of Sveinbjörnsdóttir et al. (2013), and the regional highlands recharge is from Stéfansson et al. (2017). Primary magmatic water composition is from Sheppard and Epstein (1970). The dashed curves represent the evolution of $\delta^2\text{HTD}$ vs. $\delta^{18}\text{OTD}$ in the vapor and residual liquid after phase segregation, starting from an initial composition (purple star), and causing isotopic fractionation for Theistareykir. Water isotopic compositions thus evolve along these lines according to their final equilibrium temperature. The f values correspond to the fraction of residual liquid. 104

Figure 2-3 : Diagram of the chemical composition of the fluids sampled at the surface (as condensed vapor) normalized to the deep fluids at depths of 1420 and 1600 m for Theistareykir and 850 m for Krafla. The composition of Theistareykir acidic fumarole fluids is also shown, as are vapor/fluid partition coefficients from Pokrovski et al (2005). The maximum value is shown as a triangle for elements where the concentrations in the surface fluid were below the detection limit, calculated from the respective detection limit. b. Composition of the fluids normalized to their respective fresh local basalt. c. Composition of the altered rock cuttings at a depth of 1600 m, normalized to the fresh local basalt for Theistareykir. The elements have been grouped first by their geochemical behaviour and then their mass. 107

Figure 2-4 : Profile of pressure and temperature in wells ÞG-01 (a) and K-21(b) just before the sampling of deep fluids. 116

Figure 2-5: Evolution of pH depending on the HCl concentration of the fluids..... 117

Figure 3-1 : Simplified map of the Theistareykir geothermal field with major alteration zones and positions of the sampled sites (wells) indicated. Numbers on the X- and

Y-axes indicate the latitudinal and longitudinal geographical coordinates respectively on the World Geodetic System 1984 (WGS84). NVZ = Northern Volcanic Zone; WVZ = Western Volcanic Zone; EVZ = Eastern Volcanic Zone.	152
Figure 3-2 : Alteration trends of variably altered rocks and fresh rocks at Theistareykir for Co, Zn, Ni, Li against MgO.....	153
Figure 3-3 : Comparison between altered rock fresh basalt. a. Concentration of 8 sub-samples of variably altered rocks against the average concentration in fresh rocks. b. Variably altered rocks normalized to the fresh rocks.....	154
Figure 3-4 : Estimation of the magmatic and water-rock interaction contributions using the enrichment factors (EF) for every element. Results are compared to the deep fluids compositions.	155
Figure 3-5 : The Rc/Ra ratio compared to the major gases CO ₂ and H ₂ S, and to SO ₄	156
Figure 3-6 : The Rc/Ra ratio compared to the most volatile metals (Hg, Bi, Tl, Cd, As and Sb) normalized to chlorine.	157
Figure 3-7 : Volatile metals Hg, Bi, Tl, Cd, As and Sb normalized to chlorine compared to the major gases CO ₂ and H ₂ S.....	158

RÉSUMÉ

L'étude des systèmes magmatiques-hydrothermaux actifs au sein de la croûte continentale et/ou océanique a conduit à de grandes améliorations dans notre connaissance du rôle des magmas et des fluides associés en tant que transporteurs de chaleur et d'éléments du manteau à la surface de la Terre. Parmi ces éléments, les métaux ont été d'un intérêt particulier pour leur importance économique, et des années de recherche ont conduit à la reconnaissance de ces systèmes magmatiques-hydrothermaux comme analogues modernes des gisements porphyres et épithermaux fossiles. Malgré des progrès significatifs dans la compréhension des processus conduisant à la mobilisation, au transport et à la concentration des métaux au sein de la croûte terrestre, des questions clés subsistent, notamment en ce qui concerne les sources de fluides et de métaux associés. Dans cette contribution, nous visons à déchiffrer les sources de fluides et de métaux dans un système magmatique-hydrothermal actif en combinant deux types de traceurs : les isotopes des gaz rares et les signatures métalliques des fluides profondes et superficiels des champs géothermiques de Theistareykir et Krafla dans le nord de l'Islande.

Pour répondre à cette question importante, une diversité d'environnements et de matériaux représentant une coupe transversale d'un système géothermique actif ont été échantillonnés pour contraindre trois paramètres principaux :

(1) Les sources de fluides. Les fluides à la sortie du puits ainsi que les manifestations naturelles de surface (fumeroles et mud pot) ont été échantillonnés. Dans ces fluides, les isotopes stables de l'eau $\delta^2\text{H}$ et $\delta^{18}\text{O}$ et les concentrations élémentaires et isotopiques des gaz rares (He, Ne, Ar, Kr, Xe) ont été analysés afin de déterminer les sources des fluides hydrothermaux dans ce système. Les isotopes de l'eau indiquent la présence de quatre principales sources d'eau, trois étant de l'eau météorique et glaciaire moderne et une glaciaire Holocène et une source de fluides magmatique. Les isotopes de gaz rares montrent deux sources du manteau sous Theistareykir : le basalte de manteau de la dorsale médio-océanique (MORB) appauvri (DMM) et, avec une influence moindre, le panache du manteau islandais. Cela aide également à identifier les sources de chaleur, suggérant que le transport de chaleur par convection domine la partie orientale du champ où se trouve l'intrusion magmatique, tandis que dans d'autres parties du champ, la conduction thermique est dominante.

(2) Comportement des éléments depuis la profondeur jusqu'à la surface. Nous présentons les premières données sur la composition et la signature élémentaire des fluides des réservoirs profonds dans un système géothermique basaltique à faible teneur en carbone. En combinant des échantillons de fluides en profondeur avec des

échantillons de vapeur condensée en surface, de roche altérée et de basalte frais, nous montrons que les fluides profonds sont relativement enrichis en métaux de base et en métaux (semi) volatils (en particulier Te, Hg, Re et Tl) par rapport au basalte environnant, et que cela reflète l'apport d'éléments provenant à la fois du dégazage du magma et de l'interaction eau-roche. L'ébullition de ce fluide profond entraîne une composition de surface qui est considérablement appauvrie en la plupart des éléments et possède sa propre signature élémentaire. La teneur en éléments et les modèles dans les fluides de surface ne peuvent donc pas être interprétés comme reflétant ceux du fluide profond. Le comportement des éléments dans les fluides est cohérent et s'accorde largement avec des données similaires obtenues pour un autre système géothermique dans le sud-ouest de l'Islande modifié par l'interaction eau-roche.

(3) Les sources de métaux. Nous pensons que les métaux dans les fluides magmatiques-hydrothermaux proviennent du dégazage du magma et de l'interaction eau-roche. Ici, nous quantifions l'importance relative de ces deux sources en estimant la signature élémentaire de la composante du dégazage du magma, et déterminons directement le transfert de masse dans l'interaction eau-roche. Les résultats indiquent que le fluide du réservoir profond est dominé par l'apport de dégazage magmatique, à l'exception de Mn, Fe, Co, Cu, V et Ti. Les données isotopiques de l'hélium pour les fluides de surface le confirment, les deux sources de données suggérant une contribution d'environ 80 à 99 % du magma et de 1 à 20 % de l'interaction eau-roche. Les échantillons de fluide géothermique provenant des puits de production montrent des rapports $^3\text{He}/^4\text{He}$ normalisés à l'atmosphère (R_c/R_a) de 10,05 à 11,45 qui sont interprétés comme représentant la dilution d'un fluide transportant un composant magmatique enrichi en ^3He avec de ^4He radiogénique d'origine crustale. Ce dernier est considéré comme une mesure de l'interaction eau-roche. R_c/R_a montre une variabilité dans le dégazage du magma et les contributions de l'interaction eau-roche à travers le champ. Les métaux volatils corrélaient avec R_c/R_a et varient de manière similaire à travers le champ, Hg et Bi étant les meilleurs indicateurs de la contribution magmatique. Les gaz rares et les métaux volatils fournissent ainsi les outils pour identifier et quantifier les contributions relatives du dégazage magmatique et de l'interaction eau-roche à la charge métallique des fluides géothermiques, et permettent de suivre leur variation dans l'espace et dans le temps.

Ensemble, ces trois études dressent un portrait complet des sources et de la dynamique des fluides dans un système magmatique-hydrothermal. Cela jette les bases pour comprendre le comportement des éléments dans les fluides profonds et de surface, et la mobilité des éléments dans les fluides crustaux profonds en général. La compréhension de ces multiples contributions et processus fournit aussi des informations pour les modèles de formation de gisements.

Mots-clés : Systèmes géothermiques, Gaz rares, Métaux, Dégazage magmatique, Interaction eau-roche, Système magmatique-hydrothermal, Theistareykir, Islande.

ABSTRACT

The study of active magmatic-hydrothermal systems within the continental and/or oceanic crust has led to great improvements in our knowledge of the role of magmas and associated fluids as carriers of heat and elements from the mantle to the surface of the Earth. Among these elements, metals have been of particular interest for their economic importance, and years of research have led to the recognition that active magmatic-hydrothermal systems are modern analogues of fossil porphyry and epithermal ore-forming systems. Despite significant progress in understanding the processes leading to the mobilisation, transport and concentration of metals within the Earth's crust, key questions still remain, especially regarding the sources of fluids and metals. In this contribution, we aim to decipher the sources of fluids and metals in an active magmatic-hydrothermal system by combining noble gas isotopes and deep and surface fluid metal signatures from the basalt-hosted Theistareykir and Krafla geothermal fields in northern Iceland.

To address this important question, a diversity of environments and materials representing a cross-section of an active geothermal system were sampled to constrain three main parameters:

- (1) **The sources of fluids.** Fluids at the well-head and from natural surface manifestations (fumaroles and mud pots) were sampled and water stable isotopes $\delta^2\text{H}$ and $\delta^{18}\text{O}$ and noble gas elemental and isotope concentrations (He, Ne, Ar, Kr, Xe) were analyzed. Water isotopes indicate the presence of four main water sources, three being meteoric and glacial waters of different ages and a magmatic fluid. Noble gas isotopes show two mantle sources below Theistareykir: the depleted mid-ocean ridge basalt (MORB) mantle (DMM), and — with lesser influence — the Icelandic mantle plume. This also helps to identify the sources of heat, suggesting that convective heat transport dominates the eastern part of the field where the magmatic heat source is located, while in other parts of the field, heat conduction is dominant.
- (2) **Element behavior from depth to surface.** We present some of the first data on the composition and elemental signature of deep reservoir fluids in a basalt-hosted, low-Cl geothermal system. Combining down-hole fluid samples with well-head samples of condensed vapor, altered rock cuttings, and fresh basalt, we show that deep fluids are relatively enriched in base metals and (semi)-

volatile metals (in particular Te, Hg, Re and Tl) compared to local basalt, and that this reflects element input from both magma degassing and water-rock interaction. Boiling of this deep fluid results in a well-head composition that is significantly depleted in most elements, and has its own distinct elemental signature. The element content and patterns in surface fluids can thus not be interpreted to reflect that of the deep fluid. The behavior of elements in the fluids is consistent, and largely agrees with similar data obtained for The Reykjanes geothermal system in SW Iceland, and we therefore posit that our results are representative for this geological setting and indicate a significant magmatic degassing input to deep fluids, variably modified by water-rock interaction.

- (3) **The sources of metals.** Metals in magmatic-hydrothermal fluids are thought to be sourced from magma degassing and water-rock interaction. Here, we quantify the relative importance of these two sources by estimating the elemental signature of the magma degassing component, and determine the mass transfer in water-rock interaction directly. Results indicate that the deep reservoir fluid is dominated by magma degassing input, except for Mn, Fe, Co, Cu, V and Ti. Helium isotopic data for well-head fluids confirm this, both data sources suggesting an approximately 80-99% contribution from magma, and 1-20% from water-rock interaction. Geothermal fluid samples from production wells show atmosphere-normalized $^3\text{He}/^4\text{He}$ ratios (Rc/Ra) from 10.05 to 11.45 which are interpreted to represent dilution of a fluid carrying a pure magmatic ^3He -enriched component with radiogenic ^4He of crustal origin. The latter is considered a measure of water-rock interaction. Rc/Ra shows variability in magma degassing and WRI contributions across the field. Volatile metals correlate with Rc/Ra and similarly vary across the field, with Hg and Bi the best indicators of the magmatic contribution. Noble gases and volatile metals thus provide the tools to identify and quantify the relative contributions of magma degassing and water-rock interaction to the metal load of geothermal fluids, and to track how these vary in space and time.

Together, these three studies draw a complete portrait of the sources and dynamics of fluids in a magmatic-hydrothermal system. This sets the basis for understanding the behaviour of elements in both deep and surface fluids, and the mobility of elements in deep crustal fluids in general. Understanding these multiple contributions and processes, provides insights for models of ore-formation.

Keywords : Geothermal Systems, Noble gases, Metals, Magma Degassing, Water-rock interaction, Magmatic-hydrothermal system, Theistareykir, Iceland.

INTRODUCTION

0.1 General introduction

The concentrations, sources and transport mechanisms of metals in the Earth's crust have been studied for decades to enhance our understanding of the cycling of elements through Earth systems and the processes resulting in the formation of economically-valuable ore deposits (Robb, 2005; Ridley, 2013; Hattori and Keith, 2001; Petrov, 2004; Berning et al., 1976; Cerny et al., 1996; Simon et al., 2006; Burnham, 1979; Candela, 1989; Heinrich et al., 1992). Fluids represent the most important agent of metal mobility and redistribution in the crust (e.g., Yardley and Bodnar, 2014).

Fluids with high metal concentrations are found in active magmatic-hydrothermal systems – which are now assumed to be the modern analogues of epithermal ore deposits (Weissberg et al., 1979; Henley et al., 1984; Hedenquist and Henley, 1985; Berger and Bethke, 1985; Krupp and Seward, 1987; Clark and Williams-Jones, 1990; Hedenquist et al., 1993; Todsdal et al., 2009; Sillitoe, 2010); in volcanic emissions (Delmelle and Bernard, 1994; Christenson and Wood, 1993); and in industrial emissions, including geothermal energy production where they can lead to pollution (Kristmannsdóttir and Ármannsson, 2003). This thesis will focus on understanding the sources and transport mechanisms of metals in an active magmatic-hydrothermal system, particularly as such geothermal areas are of interest for energy production.

Crustal magmatic-hydrothermal systems and their associated geothermal areas are initiated by magma bodies intruded at shallower depths of 5-10 km (Figure 0-1). In these systems, hydrothermal aqueous fluids are a complex mixture of meteoric water,

groundwater, water exsolved from melt upon crystallization, and local seawater (Norton, 1984; Giggenbach, 1992). Geothermal systems are assumed to be mainly composed of meteoric water with little input (often less than 5% in volume; Craig, 1963) from fluids of magmatic origin. Their elemental load is derived in part from their magmatic source and in part from the interaction of fluids with reservoir host rocks. An often dominantly CO₂ gas phase originates from magmatic gases released by the melt, and includes other gaseous components such as HCl, H₂S, N₂, primordial noble gas isotopes (such as ³He), and volatile trace elements (including metals). In many cases, these fluids are emitted to the surface in fumaroles, hot springs, or in more extreme examples, crater lakes and acid rivers (Delmelle and Bernard, 1994; Christenson and Wood, 1993). Combined, these features are referred to as a magmatic-hydrothermal system.

Magmatic-hydrothermal systems contain complex mixtures of fluids and metals from various sources which are not always easily identifiable, even with the most recent progress in geochemistry and engineering. It is thus critical to identify tracers of fluid and metal sources to decipher their contributions to the geothermal system, which is the primary goal of this thesis. Among the fluids that directly contribute water to a hydrothermal system, only the magmatic fluid is expected to be a significant contributor for metals. Meteoric water and seawater are both very low in metals (e.g. 0.5 and 0.2 ppb for Cu, 0.1 and 0.5 ppb Ni and 0.1 and 2.5 ppb V in pristine rain and seawater, respectively; Reimann and de Caritat 1998), as is circumneutral (pH \approx 7) groundwater. However, water-rock interaction can modify the metal content of meteoric water, significantly. Groundwater – here assumed to be meteoric water having interacted long enough with the reservoir rocks to efficiently exchange elements with it – can be enriched progressively in metals and play a key role in their mobilisation, distribution and precipitation in the reservoir. Given that magmatic water is generally only a minor contributor to the water budget of geothermal systems compared to

groundwater, combined with very long residence times for fluids in a geothermal reservoir and hence a long time for element exchange, water-rock interaction is regarded as an important source of elements, possibly the dominant one.

In magmatic systems, several processes can occur to lead to the mobilization and/or deposition of metals, and these are directly linked to processes occurring in the magma chamber including partial melting, progressive and extreme fractionation during crystallization, separation of immiscible melts, assimilation of elements or mixing with other magmas in the ascending path, and, finally, degassing (Robb, 2005). Each of these processes can be seen as one or several steps in the same dynamic system, and at each step, chemical partitioning of elements between phases takes place. In extreme cases each step can result in the concentration of elements to form ore deposits (Ridley, 2013). Generally, however, it is the succession of all these steps that will lead to the concentration of metals in the exsolved magmatic fluids. In the case of magmatic-hydrothermal ore deposit formation, all these steps are crucial to pre-concentrating the mineralizing fluids that will feed the porphyry and epithermal deposits in ore metals (Hattori and Keith, 2001). Magma degassing is a critical process in the transport and concentration of metals from the magmatic to the hydrothermal system. As pressure drops, the solubility of water in silicate melts also decreases, leading hydrous magma to exsolve an aqueous volatile phase at shallow crustal levels or during an eruption (Burnham, 1979; Eichelberger, 1995). As the magma approaches its solvus at depths of ~5–10 km, the bulk of the magmatic water content tends to exsolve rather rapidly, depending on the composition and the water content of the magma (Burnham, 1979). This exsolved magmatic volatile phase is mostly aqueous and contains sulfur species (SO_2 and/or reduced S species), CO_2 , NaCl, KCl, HCl, and metal chlorides, the exact composition being dependent on a number of parameters such as the depth of degassing, magma composition with $\text{H}_2\text{O}/\text{Cl}$ ratio and alkali content (Candela, 1989; Candela and Piccoli, 2005; Cline and Bodnar, 1991; Webster, 1992). However, studies have

estimated that generally, for a single phase, supercritical fluid exsolved at depths below the H₂O–NaCl solvus are ~2–13 wt.% NaCl equivalent (average 5 wt.% NaCl equivalent) with minor CO₂ (Audétat and Pettke, 2003; Burnham, 1979; Candela, 1989; Hedenquist et al., 1998; John, 1991;), and up to 1.3 wt.% Cu and 0.3 wt.% Fe (Rusk et al., 2004, 2008; Sawkins and Scherkenbach, 1981). These relatively elevated metal solubilities are consistent with experimental observations and theoretical predictions based on chloride complexing alone (e.g., Candela and Holland, 1984, 1986), and point towards the presence of other volatile ligands such as sulfide species that could increase the solubility of chalcophile elements such as Cu and Au in high temperature aqueous fluids (e.g., Heinrich et al., 1992; Pokrovski et al., 2005, 2008; Seo et al., 2009; Simon et al., 2006; Zajacz et al., 2008, 2011). Magma emplaced at shallower depths will exsolve fluids resulting in immediate formation of an immiscible low-salinity vapor and high-salinity brine that will feed the upper hydrothermal system.

In virtually all cases, the hydrothermal fluids are not in equilibrium with their host rocks, and therefore water-rock interactions and element exchanges ensue (Winter, 2001). In magmatic systems, the host rocks are commonly magmatic rocks, and their primary magmatic minerals will be replaced by a secondary paragenesis that reflects the new physical and chemical conditions (e.g. replacement of olivine, pyroxene and calcic plagioclase in basalt by chlorite, epidote and albite). These secondary minerals invariably have different elemental preferences compared to the primary magmatic phases, resulting in both the release of some elements into the fluid and sequestration of others. Studies of progressively altered rocks allow for a mass balance on the elemental fluxes that result. For example, a study by Libbey and William-Jones (2016) on the Reykjanes geothermal basaltic reservoir showed large differences in behavior of trace metals within the altered reservoir with the net mass change of altered material ranging from –26 to +22 g/100 g. Trace elements with the greatest net mass changes

were $Ba > Zn > Cu, Ni > Sr > Rb > As > Cd$, with Zn, Ni and Ba mainly gained, and Cu mainly released.

Metal mobility is controlled to a large extent by the ligand content, the temperature, as well as pH (Seward et al., 2014). The main solvent of metals in hydrothermal systems is water, which itself changes phase, activity and bonding with modifications in the physico-chemical state of the system, thereby impacting its interaction with metal and other more complex molecular phases (Fernandez et al., 1997). The input of more acidic magmatic fluids will lead to more efficient leaching of the host rocks with associated release of elements and metals in the system (Saunders et al., 2014). These metals will interact with the elements already dissolved in the fluid phase and will be transported and eventually precipitated further away in the system. Metal mobility is also highly correlated to the concentration and types of ligands present in the systems (Zajacz, 2011). The ligands correspond to negatively charged molecules and serve as a bonding structure for positively charged metals (Seward 2014; Sherman, 2010). They are usually found in the form of hydroxides (OH^-), halide ions (F^- , Cl^- , Br^- , I^-) and sulfur species (HS^- , SO_3^{2-} , SO_4^{2-}). But ligand availability and stability can be affected by various reactions occurring within the hydrothermal solution (Seward et al., 2014). Metal mobility in the crust varies by orders of magnitude depending on the presence of a mobile phase (fluid or melt), the availability and concentrations of ligands in the mobile phase, and variables including pressure and temperature (PT), pH, fO_2 and XCO_2 (Seward et al., 2014).

Geothermal systems provide an opportunity to enhance our knowledge of this dynamic by sampling both deep fluids (below the level where the fluids segregate between water and vapor, i.e. the boiling horizon) and the alteration minerals formed from these. Obtaining such deep fluid samples and preserving them up to the surface is complicated and expensive, which is why only a very limited set of such samples has been published

to date (Simmons and Brown, 2006; Hannington et al., 2016). However, access to information from a natural setting is important to confirm experimental results and add new data and understanding to these complex natural systems.

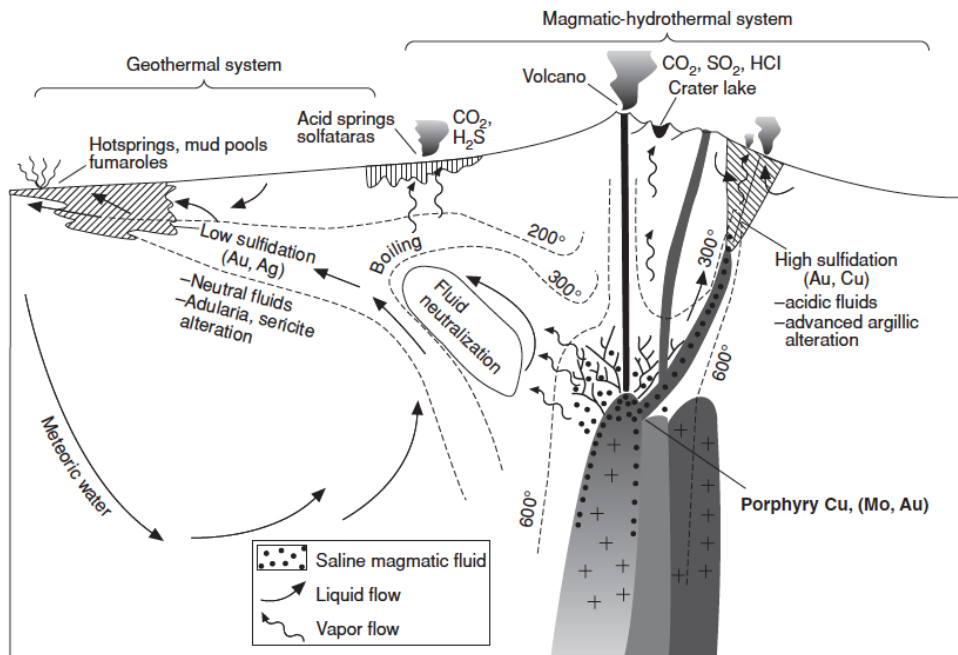


Figure 0-1 : Schematic view of a magmatic-hydrothermal system with relation to fluid flow and localisation of different features of such systems (Hedenquist et al., 2000)

0.2 State-of-the art

What are the sources of metals in magmatic-hydrothermal systems ? This question is the focus of numerous studies, but is still much debated. The respective contributions of magma degassing and rock leaching to the metal content of active magmatic-hydrothermal systems is contentitious.

It is well established that fluids released by magma are relatively enriched in metals compared to their host magma (Hedenquist et al., 1993), and that these fluids therefore sequester the metals and inject them into the hydrothermal system. On the other hand, mass balance on altered rocks and their fresh counterparts commonly shows extensive metal mobilization, which has been attributed to the elevated temperatures of the hydrothermal fluids and their high ligand concentrations (e.g. Cl^- , SO_4^{2-}) making them effective leaching agents (Williams-Jones and Migdisov, 2014, Seward et al., 2014). Water-rock interaction thus appears to be an efficient mechanism for concentrating metals in hydrothermal fluids. The ligands, particularly Cl, are dominantly derived from magma (e.g., Aiuppa et al., 2009), and proponents of host-rock leaching as the dominant metal source therefore still have to invoke a degassing contribution (Hedenquist and Lowenstern, 1994). The nature of the sources also varies in their associated timing. Whereas a dominant magmatic source would allow for time-limited emission of metals, water-rock interaction is more gradual and long-lived.

To tackle this question of the source of metals, researchers have used a large spectrum of scientific approaches from thermal modelling (Seewald and Seyfried, 1990), to O and H isotopes (Craig, 1963; Giggenbach, 1992), from metal isotopes (Cu, Zn, Fe, Moynier et al., 2017; Dauphas and Rouxel, 2006) to volcanic gas compositions (Nadeau et al., 2016), from fluid inclusions (Samson et al., 2008; Heinrich et al., 1999) to laboratory experiments and geochemical modelling (Williams-Jones and Heinrich, 2005), and to noble gases (Burnard and Polya, 2004).

The idea that the leaching of host rocks by heated surface water is the dominant process of metal concentration in the crust is supported by a number of strong arguments. For example, the study of mid-ocean ridge vents shows that the main process involved in the concentration of metals is the interaction between seawater and basaltic crust, with minor additions of magmatic fluids, as shown by the study of the chemical assemblages

of fluids and geochemical modeling involving timing, volume and concentration of metals in modern fluids (Weiss et al., 1977; Tivey, 2007; Yang and Scott, 1996, 2006; Shanks, 2012). In the mid-20th century, the boom in ore exploration led to extensive studies of magmatic-hydrothermal systems associated with active volcanism, as modern analogues of the equivalent fossil mineralized systems, particularly porphyry and epithermal ones. These active equivalents were increasingly considered as actively-forming ore deposits (Barnes and Seward, 1997; Clark and Williams-Jones, 1990; Krupp and Seward, 1987, 1990; Weissberg et al., 1979; Henley et al., 1984; Berger and Bethke, 1985). These studies showed that, unlike submarine magmatic-hydrothermal systems, aerial or sub-aerial volcanic systems in arcs and near-arc settings were more influenced by magmatic fluids, possibly by as much as 25% (Reeves et al., 2011). Over time, magmatic fluids are increasingly being considered as an additional source of economic metals (Cu, Zn, Ag and Au) in excess of what is possible to dissolve by leaching of host rocks alone (Hedenquist and Lowenstern, 1994; Yang and Scott, 1996, 2006; Sun et al., 2004; Simmons and Brown, 2006).

The study of volcanic gases also brings interesting insights, even though they are not directly representative of the reservoir's fluid composition. In addition to water vapor, they can contain >30 mol% CO₂, >20 mol% SO₂, >5 mol% H₂S, >2mol% HCl, and >0.2 mol% HF (Halmer, 2002) and up to 6 ppm Cu, 12 ppm Pb, 11 ppm Zn, 7 ppm Sn, 250 ppb Ag, and 24 ppb Au (e.g., Symonds et al., 1987; Wahrenberger et al., 2002; Williams- Jones et al., 2002, Nadeau et al., 2016). These concentrations are significant in terms of ore-forming potential and thus provide more evidence in favor of magma degassing as the origin of metals in magmatic-hydrothermal systems.

Noble gases, especially helium, have long been studied both in active magmatic-hydrothermal environments and in rocks, to decipher the origin of fluids and melts in different geological settings (Simmons et al., 1987; Hu et al., 1998a,b, 2004; Stuart et

al., 1995; Burnard et al., 1999; Burnard and Polya, 2004; Landis and Rye, 2005; Sano and Fisher, 2013; Manning and Holfstra, 2017; Wu et al., 2017). These studies show that noble gases can define the contributions of purely magmatic fluids versus fluids impacted by leaching of host rocks using, for example, the helium isotope ratio $^3\text{He}/^4\text{He}$ (Figure 0-2). The ^3He isotope is a primordial noble gas isotope, i.e. added to Earth during its accretion. Thus, ^3He is enriched over ^4He in the mantle and in its degassed product, the terrestrial atmosphere. On the contrary, ^4He is the product of U and Th α -decay and thus it is enriched in the felsic continental crust where these elements are concentrated. Thus, $^3\text{He}/^4\text{He}$ variations in fluids can be explained as mixing between magmas (bringing more ^3He than ^4He into the system) and the crust (where radiogenic ^4He produced by U-Th decay in rocks is brought to fluids by water-rock interaction). Meteoric water will finally bring purely atmospheric helium.

Studies have also looked at noble gases as tracers of ore-forming fluid dynamics in magmatic-hydrothermal related deposits including porphyry and epithermal ones (Manning and Holfstra, 2017; Wu et al., 2017; Landis and Rye, 2005; Burnard and Polya, 2004; Hu et al., 1998a,b; 2004; Burnard et al., 1999; Stuart et al., 1995; Simmons et al., 1987). Noble gases, and especially helium, have long been studied both in active magmatic-hydrothermal environments and in rocks, to decipher the origin of fluids and melts in different geological settings. These studies show that noble gases can be a powerful tool to help constrain the metal content of ore-forming fluids by defining the contributions of purely magmatic fluids versus fluids impacted by leaching of host rocks using, for example, the helium isotope ratio $^3\text{He}/^4\text{He}$. Argon isotopes and elemental ratios of noble gases are helpful in determining the proportion of crustal fossil fluids within hydrothermal environments (Pinti et al., 2017) and to constrain solubility-driven processes such as boiling and steam condensation, which are crucial processes in metal redistribution within the hydrothermal system (Burnard, 2001; Fisher, 1997).

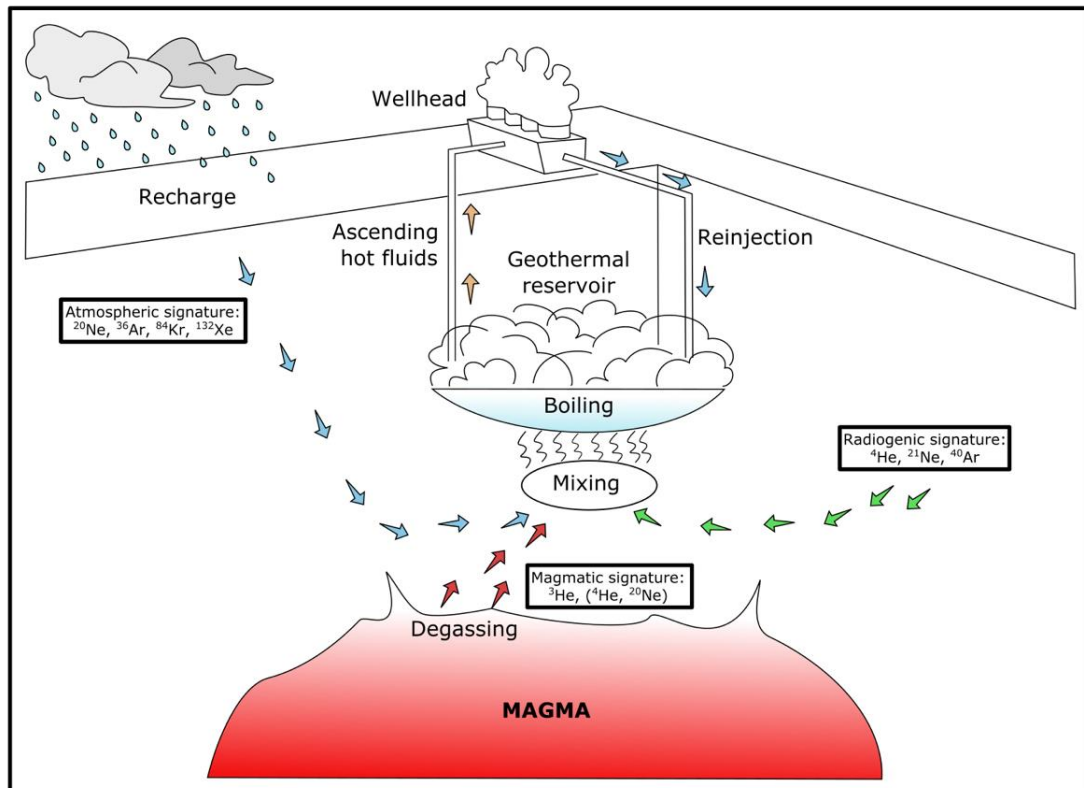


Figure 0-2 : Schematic view of a geothermal system with relation to noble gases systematics and sources.

0.3 Scope and significance of research

Although much is known regarding the origins of metals in magmatic-hydrothermal systems, the question of the relative and absolute contributions of the two main sources – magma degassing and water-rock interaction – remains unclear. Due to the lack of access to deep fluid samples to directly characterize the magmatic contribution, it is still extremely challenging to identify and quantify the contributions from the analysis

of surface samples. Moreover, since metals complex with ligands and solvate as different species, the characterization of sources and relative contributions is highly dependent on ligand abundances, which complicates the attempts to properly assess the metal sources.

In this project, volcanic-related geothermal areas have been studied to understand the abundance, mobility and sources of metals in deep Earth fluids. Geothermal systems, where surface meteoritic fluids meet deep hot fluids related to shallow magma intrusions, are ideal environments to observe the mobility of elements among mineral, water and gas phases for three main reasons:

1. They provide access to samples of almost all components of the system (gases, aqueous fluids, rocks);
2. They involve extensive interaction between these components with large changes in composition and element mobility; and
3. The various sources have distinct elemental and isotopic signatures that allow for tracing of sources as they interact and evolve (Giggenbach, 1992; Burnard et al., 1999; Stuart et al., 1995).

In these geothermal systems, the alteration of primary magmatic minerals due to interaction with hot fluids is one of the major processes leading to metal mobilisation and differentiation, commonly referred to as water-rock interaction (Williams-Jones and Migdisov, 2014, Seward et al., 2014). A second major input of metals into the geothermal system is the release of volatile metals in magma degassing as the magma becomes volatile-saturated during decompression, cooling and crystallisation (Hedenquist and Lowenstern, 1994). Secondary or alteration minerals form in response to the imposed conditions and fluid chemistry, and thereby provide an avenue to

reconstruct the composition of the fluid from which the mineral grew, and hence the abundance of metals in deep fluids resulting from magma degassing and water-rock interaction (Gamo et al., 1997, 2006; Gena et al., 2001; Yang and Scott, 2006).

In this context, the research presented in this thesis aims to assess the relative contributions of magma degassing and rock leaching to the metal content of magmatic-hydrothermal systems by using the chemical inert nature of noble gases as a tracer of metal behavior, thus removing the problematic complexation of metals with other chemical species. Moreover, this research proposes a unique method for calculating the relative contribution using both rock and fluids samples, at depth and on the surface.

An enhanced understanding of the sources, concentrations and mobility of elements in active geothermal systems has broad implications. It addresses major questions regarding;

- 1) Metal cycling on Earth, including the relative importance of fluids and the differences therein among metals with varying geochemical affinity,
- 2) Ore deposit formation, by understanding the sources of elements (magma degassing versus rock leaching) and the dynamics of the fluids that carry these elements,
- 3) Geothermal exploration and exploitation management, by determining the sources of fluids and heat, as well as the dynamics of the fluids under natural and exploitation conditions.

0.4 Objectives

The general objective of this study is to determine the contributions of water-rock interaction and magma degassing to the metal content of fluids in magmatic-

hydrothermal settings. Our hypothesis is that both magma degassing and water-rock interactions contribute to the metal load of a hydrothermal system, and we seek to establish the relative contributions of these two sources through analyses of deep fluids and noble gases. Moreover, we aim to investigate how the composition of surface emissions, both gaseous and liquid, correlates with sources, and can thereby provide easier access to this information.

Specifically, this comes in three sub-objectives which are each the focus of one scientific article:

- 1) To investigate the dynamics of fluids and their sources in a newly-developed geothermal area in northern Iceland (Theistareykir) by using noble gas and water stable isotopes.
- 2) To determine the concentrations of metals in rocks, surface fluids sampled at the well-head and deep reservoir fluids sampled at depth in this geothermal system, as well as their compositional systematics.
- 3) To show the relative contribution of magma degassing and water-rock interaction as a source of metals in basalt-hosted geothermal systems from noble gas systematics combined with determining the elemental signature of magma degassing and water-rock interaction.

0.5 Theistareykir geothermal field

The main area studied in this thesis is the Theistareykir geothermal field and its associated magmatic-hydrothermal system and volcanic and intrusive rocks. The area is known for its abundant surface volcanic features and the geothermal field is newly exploited for its geothermal energy resources, with 18 wells drilled since 2017.

Theistareykir is part of the Northern Volcanic Zone where volcanism is related to spreading. Magmas are dominantly derived from depleted MOR mantle, but a distinct plume signature is present, as traced by the $^3\text{He}/^4\text{He}$ ratios of fluids. Basalt-hosted extensional magmatic-hydrothermal systems are regarded as less interesting than arcs in terms of ore-forming potential, and considerably less is known about the behaviour, mobilisation, transport and deposition of metals in these systems. But Theistareykir provides a unique opportunity to study this type of magmatic setting without the interference of the slab and its contributions to metal emissions. Moreover, the Theistareykir geothermal field is newly developed, and the fluids studied are considered as almost pristine and thus reflecting the primary composition of the system with only minor disturbances from exploitation. All the details on the geology of the area can be found in the first chapter of this thesis, or in Saby et al. (2020).

0.6 Methods and analytical approach

This study uses noble gases as tracers of element sources and processes in geothermal fluids of Iceland, and correlates these to metal abundances in surface and deep fluids to understand and quantify the relative contributions of magmatic degassing and water-rock interaction to the metal budget of these systems.

The surface and deep sources of fluids and metals have distinct chemical signatures, which allows them to be traced throughout the geothermal system. In this study, noble gases have been chosen as a powerful tool to decipher the sources and dynamics of the fluids in geothermal systems. Noble gases owe this potential to their unique properties of chemical inertia, volatility, rarity and their large spectrum of behavior due to large mass differences (Sano and Fisher, 2013). They represent a chemical tool that can provide information on both the physical behavior of phases such as the boiling into a liquid and vapor phase, and a tracer of compositional fluxes such as magma degassing

and meteoric input (Torgensen et al., 1982). Noble gases can thus help decipher not only the potential sources of metals but also their specific behaviour inside the system and also allow for the identification of the presence of fresh magma (Kennedy et al., 2000).

In this thesis, we make the assumption that the R/Ra ratio ($(^3\text{He}/^4\text{He})_{\text{sample}}/(^3\text{He}/^4\text{He})_{\text{air}}$) can be used at a local scale to characterize the two dominant processes in the mobilization of metals in magmatic-hydrothermal systems: the degassing of magma and the leaching of rocks by hot fluids. If He is purely sourced from the mantle, more of a ^3He mantle signature is present in the fluid. In contrast, if He is derived from the decay of U and Th from the host rocks, this results in a ^4He -enriched signature, and more of a crustal contribution will be identified. We also make the assumption that the magma $^3\text{He}/^4\text{He}$ signature is homogeneous at the scale of the geothermal field and that the smaller variations in the R/Ra ratio throughout the field are mainly due to the amount of radiogenic ^4He added by water-rock interaction. Making these assumptions, the R/Ra ratio becomes a powerful tool to discriminate between the two processes of magma degassing and rock leaching.

Quantifying the relative contributions of magma degassing and water-rock interaction to the metal content of geothermal fluids requires knowledge of the relative preference of the elements for the magmatic fluid phase over the magma, and the compatibility of the elements in the secondary minerals formed in water-rock interaction. The preference for the magmatic fluid phase is referred to as the magmatic volatility of the element and depends on the magma composition as well as on the composition of the fluid phase, especially its $X(\text{CO}_2)$ and ligand concentrations. A combination of experimental studies (Zajacz et al., 2011; Mackenzie and Canil, 2008) and work on natural systems (Mather et al., 2012; Moune et al., 2006) provides a reasonable consensus on the relative magmatic volatilities of metals. Here, we therefore focus on

determining the metal signature of water-rock interaction by characterising the mobility of metals between the geothermal fluid and bulk altered rock from samples of variably altered reservoir host rocks.

Until recently, it was only possible to sample deep fluids at the well-head. These fluids have generally experienced boiling and phase separation, and metals commonly precipitate in the deeper parts of the system. Thus, the composition of reservoir fluids can differ drastically from the fluids sampled at the surface. Recently, down-hole devices have been developed and used to sample fluids at depth to measure the metal concentrations at fluid pre-boiling conditions (Simmons and Brown, 2006). For example, down-hole sampling carried out at the Taupo volcanic zone, New Zealand, showed that the reservoir fluid contains up to 23 ppb Au, 2400 ppb Ag, and 4850 ppb As, which is significantly higher than in surface emissions (Ellis, 1979; Seward, 1989, Simmons and Brown, 2006). Similar work in the Reykjanes geothermal field (Iceland) showed concentrations up to 6 ppb Au and 34 ppb Ag, and 16 and 26 ppb for Cu and Zn, and again a strong depletion of the elements in surface fluids (Hardardottir et al., 2009, Hannington et al., 2016).

0.7 Structure of the thesis

This thesis is presented in three chapters, one published, and two in the process of being submitted to peer-reviewed journals.

Chapter 1, published in the *Journal of Volcanology and Geothermal Research* in December 2020, provides a detailed study of the different sources of fluids composing the reservoir fluids at the Theistareykir Geothermal Field, in NE Iceland, using water isotopes and the elemental and isotopic composition of noble gases. It also allowed for

the identification of the sources of heat and the magma contribution to the hydrothermal system.

Chapter 2, will be submitted to the journal *Geochemical Perspective Letters*. It presents the compositions of fluids sampled at up to 1600m depth from wells of the Theistareykir and Krafla Geothermal Fields, combined with analysis of fresh and altered rocks, in order to characterise the sources of elements and their behaviour from depth to the surface. This contribution also highlights the complex interactions between the different sources of fluids in the system and their impact on the chemical composition of the reservoir fluids.

Chapter 3 will be submitted to the journal *Geochimica et Cosmochimica Acta*. It presents how noble gas isotopic signature of fluids can help discriminating between the metal load signature of magma degassing and water-rock interaction. It is shown that metals are predominantly sourced from degassing magma, and identifies He-isotopes and volatile metals in surface fluids as tracers of the relative importance of the magmatic contribution. This has broad implications for the understanding of sources of metals in basalt-hosted magmatic-hydrothermal systems as well as for geothermal system monitoring and their sustainable exploitation.

REFERENCES

- Aiuppa, A., Baker, D.R. and Webster, J.D., 2009. Halogens in volcanic systems. *Chem Geol* 263, 1-18.
- Audétat, A. and Pettke, T., 2003. The magmatic-hydrothermal evolution of two barren granites: a melt and fluid inclusion study of the Rito del Medio and Canada Pinabete plutons in northern New Mexico (USA). *Geochimica et Cosmochimica Acta*, 67(1): 97-121.
- Barnes, H. and Seward, T., 1997. Geothermal systems and mercury deposits. *Geochemistry of hydrothermal ore deposits*, 3: 699-736.
- Berger, B.R. and Bethke, P.M., 1985. *Geology and geochemistry of epithermal systems*. Society of economic geologists.
- Berning, J., Cooke, R., Hiemstra, S. and Hoffman, U., 1976. The Rössing uranium deposit, south west Africa. *Economic Geology*, 71(1): 351-368.
- Burnard, P.G. and Polya, D.A., 2004. Importance of mantle derived fluids during granite associated hydrothermal circulation: He and Ar isotopes of ore minerals from Panasqueira 1. Associate editor: R. Wieler. *Geochimica et Cosmochimica Acta*, 68(7): 1607-1615.
- Burnard, P., 1999. The bubble-by-bubble volatile evolution of two mid-ocean ridge basalts. *Earth and Planetary Science Letters*, 174(1): 199-211.
- Burnard, P., 2001. Correction for volatile fractionation in ascending magmas: noble gas abundances in primary mantle melts. *Geochimica et Cosmochimica Acta*, 65(15): 2605-2614.
- Burnard, P., Graham, D. and Farley, K., 2004. Fractionation of noble gases (He, Ar) during MORB mantle melting: a case study on the Southeast Indian Ridge. *Earth and Planetary Science Letters*, 227(3): 457-472.
- Burnham, C.W., 1979. Magmas and hydrothermal fluids. *Geochemistry of Hydrothermal Ore Deposits*: 71-136.

- Candela, P., 1989. Magmatic ore-forming fluids: thermodynamic and mass-transfer calculations of metal concentrations. In ore deposition associated with magmas. *Rev. Econ. Geol.*, 4: 203-221.
- Candela, P. and Piccoli, P., 2005. Magmatic processes in the development of porphyry-type ore systems. *Economic Geology*, 100: 25-37.
- Candela, P.A. and Holland, H.D., 1984. The partitioning of copper and molybdenum between silicate melts and aqueous fluids. *Geochimica et Cosmochimica Acta*, 48(2): 373-380.
- Candela, P.A. and Holland, H.D., 1986. A mass transfer model for copper and molybdenum in magmatic hydrothermal systems; the origin of porphyry-type ore deposits. *Economic Geology*, 81(1): 1-19.
- Černý, P. and Ercit, T.S., 2005. The classification of granitic pegmatites revisited. *The Canadian Mineralogist*, 43(6).
- Christenson, B. and Wood, C., 1993. Evolution of a vent-hosted hydrothermal system beneath Ruapehu Crater Lake, New Zealand. *Bulletin of volcanology*, 55(8): 547-565.
- Clark, J.R. and Williams-Jones, A.E., 1990. Analogues of epithermal gold-silver deposition in geothermal well scales. *Nature*, 346(6285): 644-645.
- Cline, J.S. and Bodnar, R.J., 1991. Can economic porphyry copper mineralization be generated by a typical calc-alkaline melt? *Journal of Geophysical Research: Solid Earth*, 96(B5): 8113-8126.
- Craig, H., 1963. The isotopic geochemistry of water and carbon in geothermal areas, Nuclear geology on geothermal areas, Spoleto Conference Proceedings, 1963, pp. 17-53.
- Dauphas, N., & Rouxel, O. (2006). Mass spectrometry and natural variations of iron isotopes. *Mass Spectrometry Reviews*, 25(4), 515–550. doi:10.1002/mas.20078
- Delmelle, P. and Bernard, A., 1994. Geochemistry, mineralogy, and chemical modeling of the acid crater lake of Kawah Ijen Volcano, Indonesia. *Geochimica et cosmochimica acta*, 58(11): 2445-2460.
- Eichelberger, J.C., 1995. Silicic volcanism: ascent of viscous magmas from crustal reservoirs. *Annual Review of Earth and Planetary Sciences*, 23(1): 41-63.

- Ellis, A., 1979. Explored geothermal systems. *Geochemistry of hydrothermal ore deposits*: 465-514.
- Fernández, D. P., Goodwin, A. R. H., Lemmon, E. W., Levelt Sengers, J. M. H., & Williams, R. C. (1997). A Formulation for the Static Permittivity of Water and Steam at Temperatures from 238 K to 873 K at Pressures up to 1200 MPa, Including Derivatives and Debye–Hückel Coefficients. *Journal of Physical and Chemical Reference Data*, 26(4), 1125–1166. doi:10.1063/1.555997
- Fischer, T.P., Sturchio, N.C., Stix, J., Arehart, G.B., Counce, D. and Williams, S.N., 1997. The chemical and isotopic composition of fumarolic gases and spring discharges from Galeras Volcano, Colombia. *Journal of Volcanology and Geothermal Research*, 77(1): 229-253.
- Gamo, T., Ishibashi, J., Tsunogai, U., Okamura, K. and Chiba, H., 2006. Unique Geochemistry of Submarine Hydrothermal Fluids from Arc-Back-Arc Settings of the Western Pacific. *Back-arc spreading systems: geological, biological, chemical, and physical interactions*: 147-161.
- Gamo, T., Okamura, K., Charlou, J.-L., Urabe, T., Auzende, J.-M., Ishibashi, J., Shitashima, K. and Chiba, H., 1997. Acidic and sulfate-rich hydrothermal fluids from the Manus back-arc basin, Papua New Guinea. *Geology*, 25(2): 139-142.
- Gena, K., Mizuta, T., Ishiyama, D. and Urabe, T., 2001. Acid-sulphate Type Alteration and Mineralization in the Desmos Caldera, Manus Back-arc Basin, Papua New Guinea. *Resource Geology*, 51(1): 31-44.
- Giggenbach, W., 1992. Isotopic shifts in waters from geothermal and volcanic systems along convergent plate boundaries and their origin. *Earth and planetary science letters*, 113(4): 495-510.
- Hannington, M., Harðardóttir, V., Garbe-Schönberg, D. and Brown, K.L., 2016. Gold enrichment in active geothermal systems by accumulating colloidal suspensions. *Nature Geoscience*, 9(4): 299-302.
- Hardardottir, V., Brown, K.L., Fridriksson, T., Hedenquist, J.W., Hannington, M.D. and Thorhallsson, S., 2009. Metals in deep liquid of the Reykjanes geothermal system, southwest Iceland: Implications for the composition of seafloor black smoker fluids. *Geology*, 37(12): 1103-1106.
- Hattori, K.H. and Keith, J.D., 2001. Contribution of mafic melt to porphyry copper mineralization: evidence from Mount Pinatubo, Philippines, and Bingham Canyon, Utah, USA. *Mineralium Deposita*, 36(8): 799-806.

- Hedenquist, J.W., 1998. The influence of geochemical techniques on the development of genetic models for porphyry copper deposits. *Rev. Econ. Geol.*, 10: 235-256.
- Hedenquist, J.W., Arribas, A. and Gonzalez-Urien, E., 2000. Exploration for epithermal gold deposits. *Reviews in Economic Geology*, 13(2): 45-77.
- Hedenquist, J.W., Arribas, A. and Reynolds, T.J., 1998. Evolution of an intrusion-centered hydrothermal system; Far Southeast-Lepanto porphyry and epithermal Cu-Au deposits, Philippines. *Economic Geology*, 93(4): 373-404.
- Hedenquist, J.W. and Henley, R.W., 1985. Hydrothermal eruptions in the Waiotapu geothermal system, New Zealand; their origin, associated breccias, and relation to precious metal mineralization. *Economic geology*, 80(6): 1640-1668.
- Hedenquist, J.W. and Lowenstern, J.B., 1994. The role of magmas in the formation of hydrothermal ore deposits. *Nature*, 370(6490): 519-527.
- Hedenquist, J.W., Simmons, S.F., Giggenbach, W.F. and Eldridge, C.S., 1993. White Island, New Zealand, volcanic-hydrothermal system represents the geochemical environment of high-sulfidation Cu and Au ore deposition. *Geology*, 21(8): 731-734.
- Heinrich, C., Günther, D., Audétat, A., Ulrich, T. and Frischknecht, R., 1999. Metal fractionation between magmatic brine and vapor, determined by microanalysis of fluid inclusions. *Geology*, 27(8): 755-758.
- Heinrich, C.A., Ryan, C.G., Mernagh, T.P. and Eadington, P.J., 1992. Segregation of ore metals between magmatic brine and vapor; a fluid inclusion study using PIXE microanalysis. *Economic Geology*, 87(6): 1566-1583.
- Henley, R.W., Barton, P., Truesdell, A. and Whitney, J., 1984. Fluid-mineral equilibria in hydrothermal systems, 1. Society of Economic Geologists El Paso, TX.
- Hu, R., Burnard, P., Turner, G. and Bi, X., 1998. Helium and argon isotope systematics in fluid inclusions of Machangqing copper deposit in west Yunnan Province, China. *Chemical Geology*, 146(1): 55-63.
- Hu, R., Turner, G., Burnard, P., Zhong, H., Ye, Z. and Bi, X., 1998. Helium and argon isotopic geochemistry of Jinding superlarge Pb-Zn deposit. *Science in China Series D: Earth Sciences*, 41(4): 442-448.
- John, D.A., 1991. Evolution of hydrothermal fluids in the Alta stock, central Wasatch mountains, Utah. US Department of the Interior, US Geological Survey.

- Kristmannsdóttir, H., & Ármannsson, H. 2003. Environmental aspects of geothermal energy utilization. *Geothermics*, 32(4-6), 451–461. doi:10.1016/s0375-6505(03)00052-x
- Krupp, R.E. and Seward, T.M., 1987. The Rotokawa geothermal system, New Zealand; an active epithermal gold-depositing environment. *Economic Geology*, 82(5): 1109-1129.
- Krupp, R.E. and Seward, T.M., 1990. Transport and deposition of metals in the Rotokawa geothermal system, New Zealand. *Mineralium Deposita*, 25(1): 73-81.
- Landis, G.P. and Rye, R.O., 2005. Characterization of gas chemistry and noble-gas isotope ratios of inclusion fluids in magmatic-hydrothermal and magmatic-steam alunite. *Chemical Geology*, 215(1-4): 155-184.
- Libbey, R. and Williams-Jones, A., 2016. Lithogeochemical approaches in geothermal system characterization: An application to the Reykjanes geothermal field, Iceland. *Geothermics*, 64: 61-80.
- MacKenzie, J. M., & Canil, D. (2008). Volatile heavy metal mobility in silicate liquids: Implications for volcanic degassing and eruption prediction. *Earth and Planetary Science Letters*, 269(3-4), 488–496. doi:10.1016/j.epsl.2008.03.005
- Manning, A.H. and Hofstra, A.H., 2017. Noble gas data from Goldfield and Tonopah epithermal Au-Ag deposits, ancestral Cascades Arc, USA: Evidence for a primitive mantle volatile source. *Ore Geology Reviews*, 89: 683-700.
- Mather, T. A., Witt, M. L. I., Pyle, D. M., Quayle, B. M., Aiuppa, A., Bagnato, E., et al., 2012. Halogens and trace metal emissions from the ongoing 2008 summit eruption of Kīlauea volcano, Hawaii. *Geochimica Et Cosmochimica Acta*, 83(C), 292–323. <http://doi.org/10.1016/j.gca.2011.11.029>
- McKennedy, B.M., Fischer, T.P., Schuster, D.L., 2000. Heat and helium in geothermal systems, Twenty-Fifth Workshop on Geother. Reser. Engin., Standord University, Stanford, California, SGP-TR-165.
- Moune, S., Sigmarsson, O., Thordarson, T. and Gauthier, P.-J., 2006. Recent volatile evolution in the magmatic system of Hekla volcano, Iceland. *Earth and Planetary Science Letters*, 255(3-4): 373-389.
- Moynier, F., Vance, D., Fujii, T., & Savage, P., 2017. The Isotope Geochemistry of Zinc and Copper. *Reviews in Mineralogy and Geochemistry*, 82(1), 543–600. doi:10.2138/rmg.2017.82.13

- Nadeau, O., Williams-Jones, A.E. and Stix, J., 2010. Sulphide magma as a source of metals in arc-related magmatic hydrothermal ore fluids. *Nature Geoscience*, 3(7): 501-505.
- Norton, D.L., 1984. Theory of Hydrothermal Systems. *Annu. Rev. Earth Planet. Sci.* 12, 155-177.
- Petrov, S., 2004. Economic deposits associated with the alkaline and ultrabasic complexes of the Kola Peninsula. Phoscorites and carbonatites from mantle to mine: the key example of the Kola Alkaline Province. *Mineral. Soc. Ser.*, 10: 469-490.
- Pinti, D.L., Castro, M.C., Lopez-Hernandez, A., Han, G., Shouakar-Stash, O., Hall, C.M. and Ramírez-Montes, M., 2017. Fluid circulation and reservoir conditions of the Los Humeros Geothermal Field (LHGF), Mexico, as revealed by a noble gas survey. *Journal of Volcanology and Geothermal Research*, 333: 104-115.
- Pokrovski, G.S., Borisova, A.Y. and Harrichoury, J.-C., 2008. The effect of sulfur on vapor-liquid fractionation of metals in hydrothermal systems. *Earth and Planetary Science Letters*, 266(3): 345-362.
- Pokrovski, G.S., Roux, J. and Harrichoury, J.-C., 2005. Fluid density control on vapor-liquid partitioning of metals in hydrothermal systems. *Geology*, 33(8): 657-660.
- Poreda, R., Craig, H., Arnorsson, S. and Welhan, J., 1992. Helium isotopes in Icelandic geothermal systems: I. ^3He , gas chemistry, and ^{13}C relations. *Geochimica et cosmochimica acta*, 56(12): 4221-4228.
- Reeves, E.P., Seewald, J.S., Saccocia, P., Bach, W., Craddock, P.R., Shanks, W.C., Sylva, S.P., Walsh, E., Pichler, T. and Rosner, M., 2011. Geochemistry of hydrothermal fluids from the PACMANUS, Northeast Pual and Vienna Woods hydrothermal fields, Manus basin, Papua New Guinea. *Geochimica et Cosmochimica Acta*, 75(4): 1088-1123.
- Reimann, C., & de Caritat, P. (1998). *Chemical Elements in the Environment*. doi:10.1007/978-3-642-72016-1
- Robb, L., 2005. *Introduction to ore-forming processes*. John Wiley & Sons.
- Ridley, J., 2013. *Ore deposit geology*. Cambridge University Press.

- Rusk, B.G., Reed, M.H. and Dilles, J.H., 2008. Fluid inclusion evidence for magmatic-hydrothermal fluid evolution in the porphyry copper-molybdenum deposit at Butte, Montana. *Economic Geology*, 103(2): 307-334.
- Rusk, B.G., Reed, M.H., Dilles, J.H., Klemm, L.M. and Heinrich, C.A., 2004. Compositions of magmatic hydrothermal fluids determined by LA-ICP-MS of fluid inclusions from the porphyry copper–molybdenum deposit at Butte, MT. *Chemical Geology*, 210(1): 173-199.
- Saby, M. Pinti, D.L. van Hinsberg V., Gautason B., Sigurðardóttir Á., Castro M.C., Hall C., Óskarsson, F., Rocher O., Hélie, J-F., Mejean P., 2020. Sources and transport of fluid and heat at the newly-developed Theistareykir Geothermal Field, Iceland. *Journal of Volcanology and Geothermal Research*. 405. 107062. 10.1016/j.jvolgeores.2020.107062.
- Samson, I.M., Williams-Jones, A.E., Ault, K.M., Gagnon, J.E. and Fryer, B.J., 2008. Source of fluids forming distal Zn-Pb-Ag skarns: Evidence from laser ablation–inductively coupled plasma–mass spectrometry analysis of fluid inclusions from El Mochito, Honduras. *Geology*, 36(12): 947-950.
- Sano, Y. and Fischer, T.P., 2013. The analysis and interpretation of noble gases in modern hydrothermal systems, *The Noble Gases as Geochemical Tracers*. Springer, pp. 249-317.
- Saunders, J.A., Hofstra, A.H., Goldfarb, R.J. and Reed, M.H., 2014. 13.15 - Geochemistry of Hydrothermal Gold Deposits A2 - Holland, Heinrich D. In: K.K. Turekian (Editor), *Treatise on Geochemistry (Second Edition)*. Elsevier, Oxford, pp. 383-424.
- Sawkins, F.J. and Scherkenbach, D.A., 1981. High copper content of fluid inclusions in quartz from northern Sonora: Implications for ore-genesis theory. *Geology*, 9(1): 37-40.
- Seewald J.F. and Seyfried W.E., 1990. The effect of temperature on metal mobility in subseafloor hydrothermal systems: constraints from basalt alteration experiments. *Earth and Planetary Science Letters*, 101 : 2–4, 388-403.
- Seo, J.H., Guillong, M. and Heinrich, C.A., 2009. The role of sulfur in the formation of magmatic–hydrothermal copper–gold deposits. *Earth and Planetary Science Letters*, 282(1): 323-328.

- Seward, T.M., 1989. The hydrothermal chemistry of gold and its implications for ore formation: Boiling and conductive cooling as examples. *Econ. Geol. Monogr.*, 6: 398-404.
- Seward, T.M., Williams-Jones, A.E. and Migdisov, A.A., 2014. The Chemistry of Metal Transport and Deposition by Ore-Forming Hydrothermal Fluids. 29-57.
- Shanks, W.C. and Thurston, R., 2012. Volcanogenic massive sulfide occurrence model. US Department of the Interior, US Geological Survey.
- Sherman, L.A. and Barak, P., 2000. Solubility and dissolution kinetics of dolomite in Ca–Mg–HCO₃/CO solutions at 25 C and 0.1 MPa carbon dioxide. *Soil Science Society of America Journal*, 64(6): 1959-1968.
- Sillitoe, R.H., 2010. Porphyry Copper Systems. *Economic Geology*, 105(1): 3.
- Simmons, S.F. and Brown, K.L., 2006. Gold in magmatic hydrothermal solutions and the rapid formation of a giant ore deposit. *Science*, 314(5797): 288-91.
- Simmons, S.F., Sawkins, F. and Schlutter, D., 1987. Mantle-derived helium in two Peruvian hydrothermal ore deposits. *Nature*, 329(6138): 429-432.
- Simon, A.C., Pettke, T., Candela, P.A., Piccoli, P.M. and Heinrich, C.A., 2006. Copper partitioning in a melt–vapor–brine–magnetite–pyrrhotite assemblage. *Geochimica et Cosmochimica Acta*, 70(22): 5583-5600.
- Stuart, F., Burnard, P., Taylor, R.e.a. and Turner, G., 1995. Resolving mantle and crustal contributions to ancient hydrothermal fluids: He-Ar isotopes in fluid inclusions from Dae Hwa W-Mo mineralisation, South Korea. *Geochimica et Cosmochimica Acta*, 59(22): 4663-4673.
- Sun, W., Arculus, R.J., Kamenetsky, V.S. and Binns, R.A., 2004. Release of gold-bearing fluids in convergent margin magmas prompted by magnetite crystallization. *Nature*, 431(7011): 975-978.
- Symonds, R.B., Rose, W.I., Reed, M.H., Lichte, F.E. and Finnegan, D.L., 1987. Volatilization, transport and sublimation of metallic and non-metallic elements in high temperature gases at Merapi Volcano, Indonesia. *Geochimica et Cosmochimica Acta*, 51(8): 2083-2101.
- Tivey, M.K., 2007. Generation of seafloor hydrothermal vent fluids and associated mineral deposits. *Oceanography*, 20(1): 50-65.

- Toddsdal, R.M., Dilles, J.H. and Cooke, D.R., 2009. From Source to Sinks in Auriferous Magmatic-Hydrothermal Porphyry and Epithermal Deposits. *Elements*, 5(5): 289-295.
- Torgersen, T. and Jenkins, W., 1982. Helium isotopes in geothermal systems: Iceland, the geysers, raft river and steamboat springs. *Geochimica et Cosmochimica Acta*, 46(5): 739-748.
- Wahrenberger, C., Seward, T. and Dietrich, V., 2002. Volatile trace-element transport in high-temperature gases from Kudriavyy volcano (Iturup, Kurile Islands, Russia). *Geochemical Society Special Publication*, 7: 307-327.
- Webster, J.D., 1992. Water solubility and chlorine partitioning in Cl-rich granitic systems: effects of melt composition at 2 kbar and 800 C. *Geochimica et Cosmochimica Acta*, 56(2): 679-687.
- Weiss, R.F., Lonsdale, P., Lupton, J.E., Bainbridge, A.E. and Craig, H., 1977. Hydrothermal plumes in the Galapagos Rift. *Nature*, 267: 600.
- Weissberg, B.G., Browne, P.R. and Seward, T.M., 1979. Ore metals in active geothermal systems. *Geochemistry of hydrothermal ore deposits*: 738-780.
- Williams-Jones, A. and Migdisov, A., 2014. Experimental constraints on the transport and deposition of metals in ore-forming hydrothermal systems. *Society of Economic Geologists*, 18: 77-96.
- Williams-Jones, A.E. and Heinrich, C.A., 2005. 100th Anniversary Special Paper: Vapor Transport of Metals and the Formation of Magmatic-Hydrothermal Ore Deposits. *Economic Geology*, 100(7): 1287-1312.
- Williams-Jones, A.E., Migdisov, A.A., Archibald, S.M. and Xiao, Z., 2002. Vapor-transport of ore metals. *Water–Rock Interaction, Ore Deposits, and Environmental Geochemistry: A Tribute to David A. Crerar*: 279-306.
- Winter, J.D., 2001 *An introduction to igneous and metamorphic petrology*: Upper Saddle River. Prentice-Hall Inc., New Jersey.: 697.
- Wu, L.-Y., Hu, R.-Z., Li, X.-F., Stuart, F.M., Jiang, G.-H., Qi, Y.-Q. and Zhu, J.-J., 2017. Mantle volatiles and heat contributions in high sulfidation epithermal deposit from the Zijinshan Cu-Au-Mo-Ag orefield, Fujian Province, China: Evidence from He and Ar isotopes. *Chemical Geology*.

- Yang, K. and Scott, S.D., 2006. Magmatic fluids as a source of metals in seafloor hydrothermal systems. Back-arc spreading systems: geological, biological, chemical, and physical interactions: 163-184.
- Yardley, B.W.D. and Bodnar, R.J., 2014. Fluids in the Continental Crust. *GeochemPersp* 3, 1-127; Harlov, D.E., Austrheim, H. (Eds.), *Metasomatism and the Chemical Transformation of Rock: The Role of Fluids in Terrestrial and Extraterrestrial Processes*. Springer Berlin Heidelberg, Berlin, Heidelberg).
- Zajacz, Z., Halter, W.E., Pettke, T. and Guillong, M., 2008. Determination of fluid/melt partition coefficients by LA-ICPMS analysis of co-existing fluid and silicate melt inclusions. *Geochimica et cosmochimica acta*, 72(8): 2169-2197.
- Zajacz, Z., Seo, J.H., Candela, P.A., Piccoli, P.M. and Tossell, J.A., 2011. The solubility of copper in high-temperature magmatic vapors: a quest for the significance of various chloride and sulfide complexes. *Geochimica et Cosmochimica Acta*, 75(10): 2811-2827.

CHAPTER I

SOURCES AND TRANSPORT OF FLUID AND HEAT AT THE NEWLY- DEVELOPED THEISTAREYKIR GEOTHERMAL FIELD, ICELAND

Marion Saby^{1,*}, Daniele L. Pinti¹, Vincent van Hinsberg², Bjarni Gautason³, Ásgerdur Sigurdardóttir⁴, Clara Castro⁵, Chris Hall⁵, Finnbogi Óskarsson³, Océane Rocher^{1,6}, Jean-François Hélie¹ and Pauline Méjean⁷

1-Geotop & Département des sciences de la Terre et de l'atmosphère, Université du Québec à Montréal, CP.8888 Succ. Centre Ville, H3C 3P8, Montréal, Canada.

2-Geotop & Department of Earth and Planetary sciences, McGill University, 34, University Street, Montréal, Canada.

3-ÍSOR Iceland GeoSurvey, Grensásvegur 9, Reykjavik, Iceland.

4-Landsvirkjun, Háaleitisbraut 68, Reykjavik, Iceland.

5-Department of Earth and Environmental sciences, University of Michigan, Ann Arbor, USA.

6 - École Nationale Supérieure de Géologie, 2 Rue du doyen Marcel Roubault, 54518 Vandœuvre-lès-Nancy

7 -Laboratoire des Geosciences Environnement Toulouse (GET) and Observatoire Midi-Pyrénées (OMP), 14 avenue Edouard Belin, 31400 Toulouse, France

Article publié en décembre 2020 dans la revue Journal of Volcanology and Geothermal Research

1.1 Abstract

Successful management of geothermal energy requires detailed understanding of physical and chemical conditions within the field prior to exploitation. It is thus crucial to identify the fluids involved and their duration of residency, as well as the heat source, in order to assess the potential of the resource in terms of energy production. To this end, a geochemical study of relatively undisturbed fluids from the newly-developed Theistareykir geothermal field, Northern Volcanic Zone, Iceland was carried out on production wells, fumaroles, and mud pots. Noble gas (He, Ne, Ar, Kr, and Xe) elemental and isotopic abundances and stable isotopes ($\delta^{18}\text{O}$ and $\delta^2\text{H}$) were measured to determine the system fluid sources and dynamics as exploitation proceeds. Results of this study, together with previously published data, show that four fluid sources are present: modern and local meteoric water (48.9%); sub-modern meteoric water from regional highlands precipitation (10.6%); pre-Holocene glaciated meteoric water (40.4%) with strongly depleted $\delta^2\text{H}$ values of -127‰ , calculated ^{40}K - ^{40}Ar * fluid residence times from $57\pm 20\text{ ka}$ to $92\pm 30\text{ ka}$ and a (U/Th)- ^4He fluid residence times from $96\pm 50\text{ ka}$ to $160\pm 80\text{ ka}$; and, finally, ^3He -rich magmatic fluids. Concomitant enrichment in ^{18}O and radiogenic ^4He suggests that some fluids reside a long time in the reservoir, exchanging O and He with reservoir rocks. Maximum estimated helium isotopic ratios, $^3\text{He}/^4\text{He}$ (R), of 11.45 Ra (Ra= atmospheric ratio) show that the magma beneath Theistareykir is a depleted mid-ocean ridge basalt (MORB) mantle (DMM), with less influence (8.7 to 12.7%) of the Icelandic mantle plume source. Calculated heat (Q)/ ^3He ratios plotted vs. R/Ra and $^4\text{He}/^{36}\text{Ar}$ ratios suggest that convective heat transport dominates the eastern part of the field where the magmatic heat source is located, while in other parts of the field, heat conduction seems to be dominant. Boiling and phase separation exists in the field, as indicated by $\delta^{18}\text{O}$ values which fall to the left of the Global Meteoric Water Line in a $\delta^{18}\text{O}$ vs. $\delta^2\text{H}$ plot, but Q/ ^3He ratios indicate that boiling affects only 1-10% of the fluid reservoir. With this obtained knowledge,

any subsequent changes in the field conditions during the exploitation phase of Theistareykir can be better understood, helping to sustainably manage the resource.

1.2 Introduction

Iceland exhibits intense volcanic, hydrothermal, and seismic activity given its location at the intersection of the Icelandic plume and a series of active rifts and transform segments belonging to the Mid-Atlantic Oceanic Ridge (e.g., Sigmundsson et al., 2018). This leads to significant geological hazards, but also to energy opportunities, including exploitable geothermal resources.

Over the years, the exploration of natural geothermal areas throughout Iceland has revealed a great potential for energy production. Geothermal areas have been commercially exploited for electricity production since the 1960s, with the development of the first plant at Námafjall, located in the Northern Volcanic Zone (NVZ) (Gudmundsson, 1983). Today, Iceland is the world leader in geothermal energy utilization, with 6.26 MWt per 1000 inhabitants (Lund and Boyd, 2016) and an installed electricity generation capacity of 753 MWe (Ragnarsson et al., 2020).

The most recent geothermal field developed for energy production in Iceland is at Theistareykir, also located in the NVZ, ca. 30 km north of Námafjall and 20 km north of the Krafla caldera (Figure 1-1), one of the most active volcanoes of the NVZ. Because the field is still in the initial phase of exploitation, this study allows the flow, dynamics, and chemistry of the geothermal fluids to be understood prior to exploitation-related changes to the original fluid signature. It is expected that this primary fluid pattern will be progressively lost as a result of phase segregation and boiling induced by exploitation and re-injection. The current study also provides a baseline against which later states of the system, following production, can be compared to assess and maintain the sustainability of the geothermal field.

Here, the results of a noble gas (He, Ne, Ar, Kr, and Xe) survey of the geothermal fluids of Theistareykir is presented, along with complementary stable isotopes of water ($\delta^2\text{H}$, $\delta^{18}\text{O}$). Noble gases are used as fluid tracers because of their chemically-inert nature and their distinct isotopic signatures for terrestrial fluid sources (i.e., the mantle, crust, and atmosphere, e.g., Ballentine et al., 2002; Ballentine and Burnard, 2002; Saar et al., 2005). Noble gas isotopes are able to be used to trace the sources of geothermal fluids (e.g., Mazor and Truesdell, 1984; Kennedy et al., 1991; Kennedy and Van Soest, 2007; Stefánsson et al., 2017), which are a mixture of a magmatic source (e.g., Hedenquist and Lowenstern; 1994) and a meteoric water source, either modern and/or fossil (Birkle et al., 2016; Pinti et al., 2017; Stefánsson et al., 2017; Pinti et al., 2019).

Mantle-derived fluids are enriched in primordial ^3He compared to ^4He with respect to the atmosphere. The $^3\text{He}/^4\text{He}$ ratio (R) of the depleted mid-ocean ridge basalt (MORB) mantle (DMM), normalized to that of the atmosphere ($R_a = 1.384 \times 10^{-6}$; Clarke et al., 1976) – or R/R_a – is rather homogeneous, at 8 ± 1 (e.g., Allègre et al., 1995). Fluids in plume-related settings, where volatiles are sourced from a primitive non-degassed mantle, are often more ^3He -rich compared to ^4He with respect to the DMM. The resulting R/R_a values are in excess of 8 and as high as $50R_a$ (Stuart et al., 2003), although in a few places values lower than 8 have been measured (e.g., Tristan de Cunha and Gough Islands; $5-7R_a$; Kurz et al., 1982). In Iceland, the highest R/R_a value reported for a hot spring is 30.4, at Vestfirðir, in the northwestern part of Iceland (Hilton et al., 1998), approximately 350 km away from the present position of the Icelandic plume. This clearly shows how widespread the primordial helium input from the plume into the geothermal fluids is across Iceland (Breddam et al., 2000).

Crustal fluids, representing the fossil meteoric component in geothermal reservoirs (e.g., Pinti et al., 2019), contain mainly radiogenic ^4He from the decay of U

and Th, together with little ^3He produced from neutron reactions with ^6Li (Andrews and Kay, 1983). The resulting crustal R/Ra values are typically in the range of 0.02-0.03 (e.g., Mamyrin and Tolstikhin, 1984). Radiogenic ^{40}Ar ($^{40}\text{Ar}^*$) can also be present in geothermal fluids and is derived from the decay of ^{40}K . It is usually retained in rocks, but because the temperature in geothermal reservoirs commonly exceed 300°C , which is equal to the closure temperature of argon in typical K-bearing minerals (Ballentine and O’Nions, 1994), it can accumulate in geothermal fluids (e.g., Pinti et al., 2017).

Modern meteoric fluids are dominated by atmosphere-derived noble gases. The resulting R/Ra ratio is thus assumed to be close to that of the atmosphere (i.e., 0.983; Benson and Krause, 1980). Noble gas abundances are those of solubility equilibrium between water at the recharge temperature and the atmosphere, Air-Saturated Water (ASW; Mazor and Truesdell, 1984).

1.3 Geology of the investigated area

Iceland has been divided into volcanic zones based on the volcanic eruption style, the magmatic products, and the position relative to the mid-ocean ridge (MOR) and the Icelandic mantle plume (Sigmundsson et al., 2018, Figure 1-1). The volcanic rift zones are the Reykjanes Volcanic Zone, the Eastern and Western Volcanic Zones, set along the two southern branches of the North Atlantic MOR, and the Northern Volcanic Zone, on the main active MOR rift in the northern part of Iceland (Figure 1-1; Sigmundsson et al., 2018). The Northern Volcanic Zone has been the main spreading zone in the north of Iceland for the past 6–7 Ma (Pedersen et al., 2009). It is characterized by oblique extension (i.e., the direction of spreading is oblique to the regional trend of the deformation zone). This creates five *en echelon* spreading segments in the NVZ, each having a fissure swarm and an associated central volcano that is the focus of volcanic and high-temperature geothermal activities (Pedersen et

al., 2009). From south to north, these volcanic centers are Kverkfjöll, Askja, Fremrinámar, Krafla, and Theistareykir (Pedersen et al., 2009; Figure 1-1).

The Theistareykir geothermal field is located in the northernmost segment of the NVZ, and represents the westernmost of the five NVZ *en echelon* volcanic systems (Figure 1-1). High-temperature geothermal activity has been related to magma intrusions associated with recent volcanic activity that occurred 2.5-3 ka ago (MacLennan et al., 2002; Óskarsson et al., 2013). At the surface, four lava units are present, mainly related to the activity of the Theistareykjarbunga shield volcano: Skildingahraun (>14.5 ka) lava shield; Stórávíti, a widespread (30 km³) post-glacial lava shield that erupted approximately 10.5 ka ago (MacLennan et al., 2002); the picritic basalt, Borgarhraun (10-8 ka); and the youngest Theistareykjahraun lava shield (2400 a) (Saemundsson, 2007).

Tectonically, Theistareykir developed at the intersection of the N-S-oriented Northern Rift Zone (corresponding to the NVZ) and the WNW-ESE-oriented transform zone, called the Tjörnes Fracture Zone (TFZ; Khodayar et al., 2018). This particular structural setting created the Theistareykir fissure swarm, a 7-8 km-wide and 70-80 km-long tectonic assemblage (Saemundsson, 2007). Until recently, it was assumed that only the N-S structures underlie the permeability of the geothermal reservoir, but relationships between deep-derived gas manifestations and tectonic features now suggest that the main WNW, ENE, NW, and N-S fault segments all contribute to the reservoir permeability (Khodayar et al., 2018).

The development of the Theistareykir geothermal field began with nine wells drilled between 2002 and 2011. Exploitation of the field began in 2017, after a total of 18 wells had been drilled to depths ranging from 1,723 m to 2,799 m. The plant

currently has two generating units of 45MWe, making Theistareykir the fourth largest station in Iceland in terms of power generated.

The geothermal area of the Theistareykir system is 25-30 km², but surface manifestations are confined to the eastern part of the fissure swarm, northwest and north of Mt. Bæjarfjall, over a surface restricted to 11 km² (Kristinsson et al., 2013; Figure 1-1). The geothermal surface manifestations consist of warm soil, mud-pools, fumaroles, and solfataras, as well as steam areas. Mud pots have a wide range of colors related to hydrothermal clay alteration (white, grey, blueish, reddish, greenish), and are generally bubbling (Óskarsson et al., 2013). The temperatures of the fumaroles are all just below 100°C, but reconstructed gas temperatures at depth are between 257 and 310°C (Óskarsson et al., 2013). The Theistareykir thermal area has historically been divided into five N-S oriented sub-areas, which from east to west are: Ketilfjall (A), Bóndhólsskard (B), TheistareykjagrunDIR (C), Tjarnarás (D), and Theistareykjahraun (E) (Figure 1-1). These areal subdivisions are based on the reservoir temperatures estimated by gas geothermometry, ranging from 230°C to 315°C (ÁrmanSSon et al., 1986). Among these areas, Ketilfjall (A), TheistareykjagrunDIR (C), and Tjarnarás (D) were regarded as more promising for drilling. Previous studies on the stable isotopes, $\delta^2\text{H}$ and $\delta^{18}\text{O}$, of both deep water from the wells and shallow water from springs and mud pots, show the most depleted values among the studied geothermal fields of Iceland (Stefánsson et al., 2017). Lower $\delta^2\text{H}$ values are found in the Tjarnarás (D) and Ketilfjall (A) areas (Darling and ÁrmanSSon, 1989), whereas lower fumarole and mud pot $\delta^{18}\text{O}$ values are found in the Tjarnarás (D) area (ÁrmanSSon et al., 1986). The Theistareykir fumaroles and mud pots also exhibit low Na/Cl ratios, due to relatively high Cl concentration in comparison to the majority of seawater-absent geothermal areas in Iceland, suggesting the presence of more HCl-rich acidic brines, especially in the TheistareykjagrunDIR (C) and Tjarnarás (D) areas (ÁrmanSSon et al., 1986). In fluids extracted from the geothermal wells, the Na/Cl ratio is higher than in surface

manifestations, which suggests a mixing of the acidic brines with more neutral fluids in the latter, with no specific spatial distribution across the field. The highest fumarole and well gas concentrations ($\text{CO}_2 = 24,723$ ppm, $\text{H}_2\text{S} = 4\,673$ ppm, $\text{H}_2 = 122.1$ ppm, $\text{CH}_4 = 149.03$ ppm) are found in the Ketilfjall (A) and Tjarnarás (D) areas, and are probably due to subsurface steam condensation, at least in Tjarnarás, as suggested by Darling and Ármannsson (1989).

Although gas measurements in Theistareykir have been undertaken for over half a century (Hermannsson and Línadal, 1951), noble gas data remains scarce, obtained only at fumaroles and mud pots (Hilton et al., 1990; Poreda et al. 1992, Füre et al., 2010). The helium isotopic ratio in the area ranges from 6.9 to 10.6Ra, similar to the range measured in the nearby Krafla (5.6 to 10.4Ra; compiled data in Harðardóttir et al., 2018) and Námafjall geothermal field (8 to 10.3Ra; compiled data in Harðardóttir et al., 2018). These helium isotopic signatures are close to or slightly higher than those in MORBs, suggesting that the helium in the area is predominantly sourced by the DMM (Harðardóttir et al., 2018).

The heat source of the field has been related to the most recent mafic volcanic activity in the area (Theistareykjahraun lava shield; 2.4ka), and the distribution of fumarole gases suggests that it is supplied by an E-W-oriented magmatic intrusion (Óskarsson et al., 2013). The meteoric recharge of the Theistareykir geothermal system was long thought to be controlled by modern water (rainfall) flowing into the reservoir from the surrounding highlands (Ármannsson et al. 1986). However, the very low water isotopic composition measured in subarea C by Sveinbjörnsdóttir et al. (2015), with $\delta^2\text{H}$ and $\delta^{18}\text{O}$ values of -141.0 ‰ and -13.2 ‰, well below local precipitation values (-80 ‰ and -11 ‰ for $\delta^2\text{H}$ and $\delta^{18}\text{O}$), suggests that the recharge of the system is older, possibly having occurred during a colder period than at present (Sveinbjörnsdóttir et al., 2013, 2015; Stefánsson, 2017).

Based on stable isotope signatures of geothermal water in the NVZ, Darling and Ármannsson (1989) suggested that the Krafla geothermal field was recharged locally by rainwater, while both Námafjall and Theistareykir were recharged by a combination of surface water and groundwater flowing from the south. Sveinbjörnsdóttir et al., (2015) observed variable degrees of $\delta^2\text{H}$ depletion, with extreme values of $\leq 120\text{‰}$ vs. SMOW in geothermal fluids of the NVZ, suggesting that fluids from the Askja caldera, Fremrinámar, Krafla, Námafjall, and Theistareykir derived from variable mixing of at least three components: 1) modern local meteoric water; 2) sub-actual meteoric water, originating from higher elevations and further away – likely the Kverkfjöll glaciated highlands at the northern border of the Vatnajökull glacier ($\delta^2\text{H} \leq -102\text{‰}$ vs. SMOW; Árnason, 1977) and flowing through the NVZ; and 3) pre-Holocene meteoric water with even more depleted $\delta^2\text{H}$ values, flowing deeper into the rift system. This latter water component, defined by Stefánsson (2017) as “ice age” water, greatly influences the isotopic composition of thermal water in geothermal areas across Iceland (Gudmundsson et al., 2008; Sveinbjörnsdóttir et al., 2013; Óskarsson, et al., 2013; Stefánsson et al., 2017).

1.4 Methods

1.4.1 Water and gas sampling

Fluid and gas samples from surface manifestations and geothermal wells were collected in the summers of 2017, 2018, and 2019, with some sites sampled in multiple years. Water from five warm to hot springs (prefixed PG-S; Table 1 *In Electronic Supplementary Table*) was collected for stable isotope ($\delta^2\text{H}$, $\delta^{18}\text{O}$) analysis. Among the surface manifestations, a total of eleven mud pots and two fumaroles (prefixed PG-F; Table 2 *In Electronic Supplementary Table*) were sampled for noble gas analysis. A total of eleven geothermal wells (prefixed PG-; Tables 1 and 2 *In Electronic Supplementary Table*) were sampled for noble gas and water stable isotope analysis.

The water phase was collected from boiling hot springs. Mud pots were sampled for gases and not water, because the mud is extremely dense, and water filtration proved unfeasible on site. At the geothermal well sites, the water and gas phases were collected using a portable steam/fluid separator installed at the exit of the wellhead, given that the wellheads were deprived of the classic Webre-type steam/water separator (Bangma, 1961). Water collected for the analysis of water stable isotopes was poured into a 30 ml HDPE bottle filled to the top and closed avoiding air bubbles. The gas phase was collected using a standard refrigeration-grade 3/8" (14 cm³ internal volume) copper tube. The copper tube was directly installed at the gas exit of the portable fluid/steam separator using all stainless-steel Swagelok[®] NPT connections. After letting the gas flow for several minutes, the tubes were sealed using stainless steel pinch-off clamps, closed using an electric drill to minimize air contamination (Pinti et al., 2017). Gases were collected from the mud pots using armored-PVC tubing connected at one end to a plastic funnel. The funnel was placed directly above the bubbling mud pot, with the mud acting as a seal to prevent air contamination. At the other end of the PVC tubing, the tube itself was placed in a bottle filled with water to check for gas flow and to avoid flowback air contamination. Due to the relatively elevated H₂S content of Iceland gases, compared to, for example, Mexican geothermal gases (Pinti et al., 2017; 2019), sampling Icelandic volcanic gases with copper tubes is thwarted by the corrosion of the Cu tubing (Sano and Fischer, 2013). To minimize this problem, isotopic analyses were carried out shortly after sampling. Helium isotopic ratios and He/Ne ratios measured in the wells (see results section and Table 1 *In Electronic Supplementary Table*) show little to no air contamination, and the method is thus be considered to be successful.

1.4.2 Isotopic analyses

Water isotopes were analyzed at Geotop, Montréal, using a Los Gatos Research (LGR) model T-LWIA-45-EP Off-Axis Integrated Cavity Output Spectroscopy (OA-

ICOS). Three internal reference waters ($\delta^2\text{H} = 1.28 \pm 0.27\text{‰}$, $-98.89 \pm 1.12\text{‰}$, and $-155.66 \pm 0.69\text{‰}$; $\delta^{18}\text{O} = 0.23 \pm 0.06\text{‰}$, $-13.74 \pm 0.07\text{‰}$, and $-20.35 \pm 0.10\text{‰}$) were used to normalize the results to the VSMOW-SLAP scale. A fourth reference water ($\delta^2\text{H} = -25.19 \pm 0.83\text{‰}$ and $\delta^{18}\text{O} = -4.31 \pm 0.08\text{‰}$) was analyzed as a control. Results are given in delta units (δ) in ‰ (or mUr) vs. V-SMOW. The total mean analytical uncertainty (1σ) is $\pm 0.12\text{‰}$ for $\delta^2\text{H}$ and $\pm 0.2\text{‰}$ for $\delta^{18}\text{O}$.

Noble gas analyses of fumaroles, mud pots, and wells were carried out at the Noble Gas Laboratory, University of Michigan, except for well PG-17 and mud pot replicates PG-F12 and PG-F15, for which noble gas analyses were carried out at the Noble Gas Laboratory, Geotop. At the University of Michigan, gas samples connected to a stainless-steel purification line were expanded in a known volume and gas pressure was reduced by computer-controlled sequential pumping until reaching an acceptable value for analyses. The gas sample was successively dried on a molecular sieve trap and reactive gases removed using three Ti-getters at 600°C for three minutes each. The He, Ne, Ar, Kr, and Xe were quantitatively extracted using a computer-controlled cryo-separator at temperatures of 49 K, 84 K, 225 K, 280 K, and 320 K respectively, and sequentially allowed to enter a Thermo Scientific® Helix SFT mass spectrometer for He and Ne isotope analyses, and a Thermo Scientific® ARGUS VI mass spectrometer for Ar, Kr, and Xe isotope analyses. All noble gas isotopes were measured using a Faraday detector, except for ^3He , which was measured using an electron multiplier in ion counting mode. Blank analyses using the same procedures were run frequently throughout analyses. Typical blanks are 0.04 to 0.15% of the measured sample value respectively. Quantitative analyses were obtained by calibrating the two mass spectrometers with a known aliquot of standard air. Typical standard reproducibility for ^4He , ^{20}Ne , and ^{36}Ar is 0.4-0.5%, while for both $^{20}\text{Ne}/^{22}\text{Ne}$ and $^{40}\text{Ar}/^{36}\text{Ar}$ ratios the reproducibility is 0.07%. Calculated standard errors for concentrations range from 1.3 to 2.2% of the measured values.

At Geotop, copper tubes were degassed offline on a small stainless-steel vacuum line connected to a turbo pump, with vacuum pressure reaching more than 10^{-8} mbar to remove any steam condensate. The extracted gases were collected in a 12 cc volume stainless-steel vacuum finger closed by a NUPRO $\frac{1}{2}$ inch BG-Valve with copper seal. The finger was connected to a stainless-steel extraction line and the connection pumped overnight to reach vacuum conditions of 10^{-8} mbar. Gases were diluted manually in a specific volume until pressure, measured on a Baratron Gauge, reached values of less than 10 mbar, a value acceptable for analyses. The reactive gases were removed using two Ti-getters at 600°C for 15 min each and a SAES ST-707 getter at 100°C for 15 min. Gases were then adsorbed onto an ARS[®] cryogenic trap containing activated charcoal, and released sequentially at 40K, 110K, 210K, and 280K for He, Ne, Ar, and Kr-Xe respectively. Noble gas isotopes were measured on a Thermo[®] HELIX-MC using the axial Faraday by peak jumping, except for ^3He , which was measured by ion counting on the axial Compact Discrete Dynode[™] (CDD). Blanks were routinely measured and were typically on the order of 0.01% for ^4He to 0.15% for ^{132}Xe . Quantitative analyses were obtained by calibrating with a known aliquot of standard air. Typical standard reproducibility for ^4He , ^{20}Ne , ^{36}Ar , ^{84}Kr , and ^{132}Xe was usually 1.5-3.4%. Calculated standard errors for concentrations range from 1 to 3% of the measured values.

1.4.3 Geochemical computations

Total discharge stable isotope fluid composition

The stable isotope ($\delta^2\text{H}$, $\delta^{18}\text{O}$) composition of geothermal water usually needs to be recalculated for reservoir conditions (i.e., prior to the separation of steam and liquid at the wellhead separator). Indeed, this phase separation induces isotopic fractionation that needs to be corrected for (e.g., Arnórsson and Stefánsson, 2005).

The $\delta^{2}\text{H}_{\text{TD}}$ and $\delta^{18}\text{O}_{\text{TD}}$ (where TD stands for “Total Discharge”) were calculated using the following equation:

$$\delta_{\text{TD}} = y_{\text{SEP}} \cdot \delta_{\text{V}} + (1 - y_{\text{SEP}}) \cdot \delta_{\text{L}} \quad (1),$$

where δ_{V} and δ_{L} are the stable isotopic composition under reservoir conditions in the vapor (δ_{V}) and liquid water (δ_{L}) phases measured at the separator. y_{SEP} corresponds to the fraction of steam at the separator. It ranges between 0.16 and 0.28, and was calculated based on the following equation (e.g., Nieva et al., 1983):

$$y_{\text{SEP}} = \frac{(H_{\text{well}} - H_{\text{L}})}{(H_{\text{V}} - H_{\text{L}})} \quad (2),$$

where H_{well} is the enthalpy measured at the well (from 1181 to 2748 kJ/kg; Landsvirkjun internal company data), and H_{V} and H_{L} are the theoretical enthalpies of the steam and liquid phases at the separation temperature, T_{SEP} . δ_{V} is calculated using the relationship:

$$1000 \ln \alpha \cong \delta_{\text{L}} - \delta_{\text{V}} \quad (3),$$

where α is the fractionation factor of H and O between the liquid and the steam phases of water, calculated using the equations of Horita and Wesoloski (1994) at wellhead temperatures varying between 178°C (PG-17) and 208°C (PG-07; Hauksson, 2018). Wellhead separation temperatures (T_{sep}) were calculated using steam pressure values found at <https://www.tlv.com/global/TI/calculator/steam-table-pressure.html>

Fluid residence time calculation using ^{40}K - $^{40}\text{Ar}^$ and (U/Th) - ^4He chronometers*

Fluid residence times can be semi-quantitatively calculated based on the accumulation rates in fluids of the radiogenic noble gas isotopes produced by the radioactive decay of U, Th, and K in rocks. The most widely-used radiogenic isotope in groundwater chronology is ^4He , produced by α -decay of ^{238}U , ^{235}U , and ^{232}Th (e.g., Torgersen and Clarke, 1985; Kulongoski and Hilton, 2011), because the closure temperature for the U/Th-He system is usually low (50-70°C) and can be attained in shallow sedimentary basins (Ballentine and O’Nions, 1994). Radiogenic $^{40}\text{Ar}^*$, produced by the electron capture of ^{40}K , has rarely been used as a groundwater chronometer (e.g., Torgersen et al., 1989), because the typical temperatures in shallow sedimentary basins are below the closure temperature of argon in most K-bearing minerals, which is around 300°C (Ballentine and O’Nions, 1994). However, in high-enthalpy geothermal reservoirs such as Theistareykir, where temperatures are often in excess of 300°C, radiogenic $^{40}\text{Ar}^*$ should be efficiently released into fluids. Hydrothermal clay alteration of the reservoir rocks could also facilitate the release of $^{40}\text{Ar}^*$ even at lower temperatures of 150°C, as suggested by the high $^{40}\text{Ar}^*$ content ($^{40}\text{Ar}/^{36}\text{Ar}$ up to 865.3 ± 15.6) measured in the geothermal fluids of the Los Humeros Geothermal Field in Mexico (Pinti et al., 2017). The problem is that geothermal waters often show very little radiogenic $^{40}\text{Ar}^*$, because it is largely diluted by meteoric water which contains large amounts of atmospheric argon (Pinti et al., 2017).

In numerous instances, it has been suggested that a second source of radiogenic noble gas isotopes may be present in crustal fluids, identified by basal degassing flux from the deeper crust (e.g., Torgersen, 2010). This would be particularly true in volcanic settings such as Theistareykir, which is in the middle of a mid-ocean ridge, where the mantle is continuously degassing volatiles (Craig et al., 1975). If we assume that both sources of radiogenic and mantle noble gas isotopes are present (i.e., local production in rocks and a mantle flux), then the geothermal water residence time, t , can be calculated as follows (e.g., Torgersen and Clarke, 1985; Torgersen et al., 1989):

$$t = [X^*] \left(\Lambda_X J'_X \rho_{rock} \frac{1-\Phi}{\Phi} + \frac{\Sigma F_X}{\rho_{H_2O} \cdot Z \cdot \Phi} \right)^{-1} \quad (4),$$

where $[X^*]$ is the amount of radiogenic noble gas isotope in the fluid phase (with X being either ^4He or $^{40}\text{Ar}^*$) in $\text{cm}^3\text{STP g}^{-1}\text{H}_2\text{O}$; Λ_X is the gas retention factor ($X^*_{\text{released}}/X^*_{\text{produced}}$), which can be presumed to be 1 for high-temperature fluids; J'_X is the production rate of the given radiogenic noble gas isotope in the rock in $\text{cm}^3\text{STP g}^{-1}\text{rock}$; ρ_{rock} is the rock density in $\text{g}_{\text{rock}} \text{cm}^{-3}\text{rock}$; ρ_{H_2O} is the water density in $\text{g}_{\text{water}} \text{cm}^{-3}\text{water}$; Φ is the porosity in $\text{cm}^3_{\text{rock}} \text{cm}^{-3}_{\text{total}}$; ΣF_X are the boundary fluxes of the considered noble gas isotope into/out of the reservoir in $\text{cm}^3\text{STP m}^{-2} \text{yr}^{-1}$; and z is the distance between the bedrock, where the flux enters the reservoir, and the bottomhole of the sampled wells in centimeters.

To calculate the most reliable (U/Th)- ^4He or ^{40}K - $^{40}\text{Ar}^*$ fluid age, considering the numerous uncertainties for all the variables used in eqn. 4, a Monte Carlo simulation can be run (M ejan et al., 2020). Monte Carlo simulations make use of the uncertainty domains for all variables of a specific model, here the fluid residence time model of Eqn. (4). By running the algorithm multiple times (a hundred thousand times here) and randomly sampling those variables, a comprehensive output dataset is generated. The probability distribution of the output is usually reported as a Gaussian curve, and the average and standard deviation thereof can be extrapolated. Monte Carlo simulations are carried out using the NIST Uncertainty Machine (<https://uncertainty.nist.gov/>), which is a web-based software application used to evaluate the measurement uncertainty associated with an output quantity defined by a measurement model of the form $y = f(x_1, \dots, x_n)$ (Lafarge and Possolo, 2015). Input parameters, such as those reported above, are defined, the number of iterations is selected, and the measurement model (Eqn. 4) is compiled in an ‘‘R’’ script.

Mixing hyperbola inverse method

To identify the sources of helium in a terrestrial reservoir, a classic Craig's diagram is used, where the $^3\text{He}/^4\text{He}$ ratios (expressed as R/Ra) are plotted against the $^4\text{He}/^{20}\text{Ne}$ ratios (Craig et al., 1978). In this diagram (Figure 1-3 in the Discussion), the mantle, air, and crustal sources have distinct isotopic R/Ra and $^4\text{He}/^{20}\text{Ne}$ ratios, and data points are expected to plot along hyperbolas that represents mixing between these three possible source (Craig et al., 1978). It is common to arbitrarily plot those mixing hyperbolas. Here, an inverse method is applied to trace the hyperbola that best fits the data points. The mathematical solution is described in detail in Albarède (1995), and is summarized here.

Given m pairs of experimental data, u_i (corresponding to the values on the Y-axis) and v_i (values on X-axis) ($i=1,2,\dots,m$), a general hyperbola equation is:

$$(u - u_\infty) \cdot (v - v_\infty) = c \quad (5),$$

where u_∞ and v_∞ are the positions of the asymptotes on the axes (i.e., the values of the endmember for the isotopic ratio represented on the Y-axis and on the X-axis respectively), and c is a constant characteristic of the extent of the hyperbola curvature (Langmuir et al., 1978). This equation can be written for each pair of measurements as follows:

$$u_i v_i = c - u_\infty v_\infty + v_i u_\infty + u_i v_\infty \quad (6).$$

The m products $u_i v_i$ are lumped together into a m -vector, \mathbf{y} ; $c - u_\infty v_\infty$, u_∞ , and v_∞ are lumped into a 3-vector \mathbf{X} of unknowns, and an $\mathbf{A}_{m \times 3}$ matrix, for which each i th row is composed of 1, u_i , and v_i . The matrix equality $\mathbf{Ax}=\mathbf{y}$ reads as follows:

$$\begin{bmatrix} 1 & u_1 & v_1 \\ 1 & u_2 & v_2 \\ \dots & u_m & v_m \end{bmatrix} = \begin{bmatrix} c - u_\infty v_\infty \\ v_\infty \\ u_\infty \end{bmatrix} \cdot \begin{bmatrix} u_1 v_1 \\ u_2 v_2 \\ u_m v_m \end{bmatrix} \quad (7).$$

The least squares solution of eqn (7) gives the solution for the unknowns, $c - u_\infty v_\infty$, u_∞ , and v_∞ . To calculate the unknowns, the following steps need to taken: 1) the $A_{m \times 3}$ matrix is transposed into an $A_{3 \times m}$ matrix, defined as A^T ; 2) the A^T matrix is multiplied by $A_{m \times 3}$, which results in a 3×3 matrix, $A^T A$; 3) the matrix is inverted to obtain an $(A^T A)^{-1}$ matrix; 4) the A^T matrix is then multiplied by the vector y to obtain the “stripping matrix”, $A^T y$; 5) finally, the least squares solution will be:

$$\begin{bmatrix} c - u_\infty v_\infty \\ v_\infty \\ u_\infty \end{bmatrix} = A^T y \cdot (A^T A)^{-1} \quad (8).$$

The general hyperbola mixing equation will be:

$$u = u_\infty + \frac{c}{v - v_\infty} \quad (9),$$

where the curvature factor, c , is calculated from the obtained $c - u_\infty v_\infty$, u_∞ , and v_∞ values. Calculations were performed in a Microsoft® *Excel* sheet.

1.5 Results

The $\delta^2\text{H}_{\text{TD}}$ and $\delta^{18}\text{O}_{\text{TD}}$ values of the water collected from the wells in the field separator connected to the wellhead range from -127.4 ‰ to -106.9 ‰ and from -13.6 ‰ to -9.0 ‰ respectively. The $\delta^2\text{H}$ and $\delta^{18}\text{O}$ values measured in the warm springs are higher than those from the wells, and range from -74.0 ‰ to -83.3 ‰ and -6.5 ‰ to -10.6 ‰ respectively (Table 1 *In Electronic Supplementary Table*).

Helium-4 abundances range from 0.065 to 17.24 x 10⁻⁶ cm³STP cc⁻¹ in the wells and from 1.24 to 7.03 x 10⁻⁶ cm³STP cc⁻¹ in the fumaroles and mud pots. (Table 2 *In Electronic Supplementary Table*). The ³He/⁴He ratios normalized to the atmosphere (i.e., R/Ra) range from 9.96 ± 0.10 to 11.44 ± 0.30 for the wells and from 1.78 ± 0.01 to 10.41 ± 0.09 for the fumaroles and mud pots (Table 2 *In Electronic Supplementary Table*). Helium isotopic ratios are corrected for the air component (Rc/Ra) using the ⁴He/²⁰Ne ratio as an index of the atmospheric helium contribution (Torgersen and Jenkins, 1982):

$$Rc/Ra = [(R/Ra)_{meas} - r] / (1 - r) \quad (10)$$

$$r = (^4He/^{20}Ne)_{ASW} / (^4He/^{20}Ne)_{meas} \quad (11),$$

where (R/Ra)_{meas} is the measured helium isotopic ratio, and (⁴He/²⁰Ne)_{ASW} and (⁴He/²⁰Ne)_{meas} are the ASW ratios at 3.7°C and the sample ratios (Table 2 *In Electronic Supplementary Table*) respectively. Computation of the total Rc/Ra uncertainty is described in Sano et al. (2006). The Rc/Ra ratios calculated for the wells range from 10.05 ± 0.10 for well PG-11 to 11.45 ± 0.30 for well PG-07, whereas for the fumaroles it ranges from 3.00 ± 0.03 for fumarole PG-F15 to 10.96 ± 0.09 for fumarole PG-F13 (Table 2 *In Electronic Supplementary Table*). For the wells, air contamination is minimal, with a mean difference between the original and corrected values, R/Ra and Rc/Ra, of +0.03. For the fumaroles and mud pots, air contamination is more significant, with a mean difference of +1.37. The mud pot samples contain significant air contamination despite the careful sampling procedures put into place and multiple sample runs, suggesting that air may be present prior to sampling, and thus be intrinsic to the sample.

Results for the well $^{20}\text{Ne}/^{22}\text{Ne}$ and $^{21}\text{Ne}/^{22}\text{Ne}$ ratios show values ranging from 9.16 ± 0.04 to 9.81 ± 0.004 and from 0.0272 ± 0.0012 to 0.0295 ± 0.0004 respectively (Table 2 *In Electronic Supplementary Table*). For the fumaroles and mud pots, values range from 9.54 ± 0.001 to 9.84 ± 0.003 and from 0.0272 ± 0.0012 to 0.0295 ± 0.0004 respectively. These values are close to or lower than the atmospheric $^{20}\text{Ne}/^{22}\text{Ne}$ and $^{21}\text{Ne}/^{22}\text{Ne}$ values of 9.80 and 0.0290 respectively.

The well $^{40}\text{Ar}/^{36}\text{Ar}$ and $^{38}\text{Ar}/^{36}\text{Ar}$ ratios show values ranging from 299.9 ± 1.1 for well ÞG-11 to 307.3 ± 2.2 for well ÞG-07 and from 0.1870 ± 0.003 for well ÞG-11 to 0.1899 ± 0.0032 for well ÞG-17 respectively (Table 2 *In Electronic Supplementary Table*). The $^{40}\text{Ar}/^{36}\text{Ar}$ ratios are slightly higher than the atmospheric value of 295.5, indicating the presence of radiogenic and/or mantle $^{40}\text{Ar}^*$. Kr and Xe isotopic compositions are clearly atmospheric, or slightly mass-fractionated, and will not be discussed further, but can be found in Table A1 *In Electronic Supplementary Table*.

1.6 Discussion

1.6.1 Fluid sources in the Theistareykir geothermal field

Primary thermal fluids in Iceland (those reaching the deepest level of penetration; Stefánsson et al., 2017), including in Theistareykir, can be composed of variable contributions of meteoric precipitation, seawater, and magmatic water. Geothermal systems impacted by seawater, such as Reykjanes on the Reykjanes Peninsula, show high Cl concentrations, of up to $\sim 20,000 \text{ mg kg}^{-1}$ (Arnórsson and Andrésdóttir, 1995), but such values were not found at Theistareykir ($\sim 65\text{-}100 \text{ mg/kg}$), suggesting negligible or no seawater input to the system. Among the potential meteoric contributions, modern rainwater and snowmelt are the most abundant fluid sources across Iceland (Stefánsson et al., 2017), together with pre-Holocene “ice age” water, recharged during colder climates (e.g., Sveinbjörnsdóttir et al. 2015). Magmatic water

is considered to be water in its aqueous or gaseous phase in equilibrium with the magma and originating from the expelled fluids of the crystallized magma (Sheppard et al., 1969). Magmatic water composition depends on the parent magma, but generally exhibits high salinities and $\delta^2\text{H}$ and $\delta^{18}\text{O}$ values ranging from -80 ‰ to -10 ‰ and +6 ‰ to +10 ‰ respectively (Sheppard and Epstein, 1970). Here below, the different fluid sources are discriminated and fluid ages proposed using stable isotopes of water and noble gases.

1.6.2 Sources of meteoric water

On the classic $\delta^2\text{H}$ vs. $\delta^{18}\text{O}$ plot (Figure 1-2), the water isotopic signature of Theistareykir geothermal fluids group into several clusters that broadly correspond to sample types (wells, warm/hot springs, mud pots, etc.). Surface spring waters sampled during the summer of 2017 show values that are very close to the local rain water values and exhibit a positive shift in $\delta^{18}\text{O}$ of $\Delta = +4.19\text{‰}$ compared to the global meteoric water line (GMWL). The samples most enriched in heavy isotopes (PG-S1 and PG-S3) were collected from two boiling surface springs, whereas the two samples most depleted in heavy isotopes (PG-S2 and PG-S4) were collected from the main thermal areas and represent two small resurgent centers with temperatures of approximately 30°C. Consequently, the observed shift in $\delta^{18}\text{O}$ is likely due to mixing between rainwater and either a water component influenced by water-rock interaction or magmatic water. The magmatic water component is less likely given the small proportion of magmatic water in these samples, as highlighted in the $\delta^2\text{H}$ vs $\delta^{18}\text{O}$ plot.

Most of the geothermal wells are influenced by an old regional meteoric water component, as indicated by the $\sim -141\text{‰}$ shift in $\delta^2\text{H}$ and $\sim -19\text{‰}$ shift in $\delta^{18}\text{O}$ toward the endmember (Figure 1-2). The distribution of the wells in Figure 1-2 corresponds to

the sub-areas in the geothermal field defined by Ármannsson (1986), and indicates those which are more heavily impacted by the old meteoric components (Figure 1-2). Two wells, ÞG-03 and ÞG-07, are more strongly influenced by the Pre-Holocene meteoric water component, probably having been drilled closer to the zone where this old water has been channeled deeper in the system (Guðmundsson et al., 2015). Well ÞG-07 exhibits the highest $\delta^{18}\text{O}$, suggesting either extensive water-rock interaction or a larger magmatic water input. The input of magmatic water usually translates into a shift in both $\delta^2\text{H}$ and $\delta^{18}\text{O}$ toward higher values, but the absence of a corresponding $\delta^2\text{H}$ shift could, in this case, result from the pre-Holocene water component's depleted heavy isotopic signature. Both water-rock interaction and magmatic water input are likely involved, given that well ÞG-07 is situated closest to the expected magma intrusion, thereby allowing for a stronger magmatic contribution while facilitating the occurrence of water-rock interaction due to higher reservoir temperatures.

Mud pots show low ^{18}O isotopic signatures that fall to the left of the GMWL (Figure 1-2). In geothermal reservoirs dominated by a liquid phase, P - T conditions are generally insufficient to initiate boiling in the aquifer, which can only take place in the wells. The system is thus considered to be closed and at the boiling adiabatic (Arnórsson et al., 2007). On the other hand, when the reservoir aquifer is composed of both liquid and vapor (i.e., is two-phase), intensive boiling will be induced in the aquifer when the well is discharged, due to depressurization. During boiling, the water stable isotopes fractionate between the vapor phase and the residual liquid (e.g., Pope et al., 2016; Stefánsson et al., 2017), with the residual liquid becoming isotopically heavier than the initial starting fluid, while the vapor becomes lighter. However, the precise isotopic evolution depends on the temperature and degree of boiling, with decreasing in $\delta^2\text{H}$ values upon progressive boiling, (Figure 1-2). Hydrogen and oxygen isotope fractionation between liquid and vapor can be represented as a Rayleigh distillation with the following equation:

$$\delta R = \delta R_0 - 1000[f(\alpha-1) - 1] \quad (12),$$

where δR is the measured $^2\text{H}/^1\text{H}$ or $^{18}\text{O}/^{16}\text{O}$ ratio in delta notation in one of the two phases, δR_0 is the initial ratio in the fluid, α is the fractionation factor for liquid or vapor (calculated from Horita and Wesolowski, 1994) at a given temperature, and f is the fraction of residual liquid. The liquid-vapor fractionation evolution of oxygen and hydrogen water isotopes is shown here for f values of 0.3, 0.5, and 0.7, starting from an average composition of $\delta^2\text{H}_{\text{TD}} = -107.31\text{‰}$ and $\delta^{18}\text{O}_{\text{TD}} = -14.79\text{‰}$ (yellow star; Figure 1-2). These values have been determined by the best fit of the curves through the points in Figure 1-2.

These results show good agreement with earlier studies, which present distinct isotopic signatures of water for the subfields within the Theistareykir geothermal field, suggesting different fluid origins (Ármannsson et al., 1986; Sveinbjörnsdóttir et al. 2015). According to these previous studies, the most recent analysis done by the Iceland GeoSurvey (ÍSOR; unpublished), and this study (Figure 1-2), the Theistareykir reservoir fluids could be influenced by four different sources of water: 1) modern local meteoric water, 2) sub-modern regional meteoric water from the highlands, 3) pre-Holocene meteoric water, and 4) magmatic water.

1.6.3 Meteoric water residence times

In Figure 1-3, the $^{40}\text{Ar}/^{36}\text{Ar}$ vs. $^3\text{He}/^{36}\text{Ar}$ values are plotted. Two lines indicate mixing between an atmospheric component and two distinct mantle sources. The first is the depleted MORB mantle, as sampled by the well-known, gas-rich ‘popping rock’ (2IID43) from the north Mid-Atlantic Ridge (Moreira et al., 1998); the second is the Icelandic mantle source (mantle plume beneath Iceland), as defined by Mukhopadhyay (2012) based on high-precision noble gas analyses of well-known basaltic glass from SW Iceland, approximately 30 km from Reykjavik, on the active ridge (DICE 10;

Harrison et al., 2003). Our data seems to follow the Icelandic mantle source trends defined by Mukhopadhyay (2012), but shifted in parallel for most of the wells, indicating a possible enrichment of radiogenic argon or mixing with the MORB-type magma source.

The presence of an older meteoric water component is supported by the argon isotopic ratios (Figure 1-3). The straight-line correlation plotted in Figure 1-3 can be interpreted as mixing between recharging meteoric water, which should have an atmospheric $^{40}\text{Ar}/^{36}\text{Ar}$ ratio, and a magmatic fluid, enriched in radiogenic and mantle $^{40}\text{Ar}^*$. However, the $^{40}\text{Ar}/^{36}\text{Ar}$ ratio at the y-intercept of the slope is 298.97 ± 0.71 , whereas the modern air value is 295.5 (Ozima and Podosek, 1983). The higher $^{40}\text{Ar}/^{36}\text{Ar}$ ratio value of the meteoric fluid component suggests that this water had time to accumulate some radiogenic $^{40}\text{Ar}^*$. The presence of radiogenic $^{40}\text{Ar}^*$ implies that the meteoric component is older and supports the pre-Holocene water age as suggested by the water stable isotopes (Figure 1-2).

The radiogenic $^{40}\text{Ar}^*$ excess could derive from two sources (e.g., Torgersen et al., 1989): 1) local production from rocks by ^{40}K decay and its accumulation over time, and 2) mantle $^{40}\text{Ar}^*$, diffusing through the NVZ (i.e., the mid-ocean ridge). It has been suggested that the meteoric recharge of the different geothermal areas along the NVZ (Askja, Fremrinámar, Námafjall, Krafla, and Theistareykir) could be sourced by south-to-north regional groundwater flow along the rift (Darling and Ármannsson, 1989; Sveinbjörnsdóttir et al., 2015). In this case, both radiogenic and mantle $^{40}\text{Ar}^*$ could have accumulated in these fluids along the flowpath.

Based on these hypotheses, the ^{40}K - $^{40}\text{Ar}^*$ groundwater age has been calculated based on eqn. (4). Values for each variable in eqn. (4) were chosen as follows. Basaltic lavas of Theistareykir are K-poor with K_2O contents of ca. 0.08 ± 0.03 (Stracke et al.,

2003). The calculated $^{40}\text{Ar}^*$ production ratio is $2.58 \pm 0.96 \times 10^{-15} \text{ cm}^3\text{STP g}^{-1}_{\text{rock yr}^{-1}}$. The average porosity of the reservoir rock calculated by simulating the pressure response to injection and production in Theistareykir wells is 10% (Kajugus, 2012), which is the minimum porosity of dense basalts in the region (10-15%; Eggertsson et al., 2020). It is worth noting that fractured basalts and hyaloclastites in the region have much higher porosities, of up to 35 to 45% (Eggertsson et al., 2020). Basaltic rock density is assumed to be $3.0 \pm 0.1 \text{ g cm}^{-3}$; water density is $0.74 \pm 0.05 \text{ g cm}^{-3}$, calculated at reservoir temperatures of 250-300°C. The effective thickness of the reservoir has been calculated as the distance between the reservoir basement (estimated at ~2750m) and the mean depth of the well bottomholes (estimated at ~2350m), which gives a mean effective thickness of $\sim 400 \pm 50\text{m}$. The mantle $^{40}\text{Ar}^*$ flux from the mid-ocean ridge can be calculated from the mantle ^3He flux at the mid-ocean ridge of $4 \pm 1 \text{ atoms/ cm}^{-2}\text{s}^{-1}$ (Craig et al., 1975) and an average MORB $^4\text{He}/^{40}\text{Ar}^*$ ratio of 1.55 ± 0.35 (Graham, 2002). The resulting $^{40}\text{Ar}^*$ flux from the ridge would be $2.73 \pm 0.62 \times 10^{-7} \text{ cm}^3\text{STP cm}^{-2} \text{ yr}^{-1}$.

The accumulated $^{40}\text{Ar}^*$ in the aquifer can be calculated assuming an initial ASW ^{36}Ar value of $1.52 \times 10^{-6} \text{ cm}^3\text{STP g}_{\text{water}}^{-1}$ at a mean annual average temperature (MAAT) of 3.7°C. Radiogenic $^{40}\text{Ar}^*$ is calculated following the equation of Torgersen et al. (1989):

$$^{40}\text{Ar}^* = \left(\left[^{40}\text{Ar}/^{36}\text{Ar} \right]_{\text{meas}} - \left[^{40}\text{Ar}/^{36}\text{Ar} \right]_{\text{air}} \right) \times {}_{\text{ASW}}^{36}\text{Ar} \quad (13),$$

where $\left[^{40}\text{Ar}/^{36}\text{Ar} \right]_{\text{meas}}$ is the extrapolated value of 298.97 ± 0.71 in Figure 1-3 and $\left[^{40}\text{Ar}/^{36}\text{Ar} \right]_{\text{air}}$ is 295.5. The resulting $^{40}\text{Ar}^*$ is $5.27 \pm 0.01 \times 10^{-6} \text{ cm}^3\text{STP g}_{\text{water}}^{-1}$.

Two Monte Carlo simulations were run assuming that recharging fluids in the Theistareykir reservoir accumulated radiogenic and mantle argon both along the

flowpath from local rock production and from flux from the mid-ocean ridge. The two simulations consider the minimum and maximum porosity of the deep reservoir to vary from 10 to 15%. Porosity (ϕ), or better the void ratio ($1 - \phi/\phi$; $\text{cm}^3_{\text{rock}}/\text{cm}^3_{\text{water}}$) in eqn. (4), is the variable that most influences fluid residence time computations. If porosity is low, a smaller volume of water faces a larger volume of rock in which radiogenic $^{40}\text{Ar}^*$ is produced and a smaller volume of water receives the total flux of mantle argon per unit surface. The resulting $^{40}\text{K}/^{40}\text{Ar}^*$ fluid residence time will be minimal. The opposite is observed for high porosity, which will give a maximum $^{40}\text{K}/^{40}\text{Ar}^*$ fluid residence time.

The output of the Monte Carlo simulations has been reported in Table A2 *In Electronic Supplementary Table*, with the average \pm std and median \pm Median Absolute Deviation (MAD) calculated for porosities of 10 and 15% respectively. The $^{40}\text{K}/^{40}\text{Ar}^*$ -calculated average fluid residence time ranges from 62 ± 30 ka to 92 ± 30 ka. The $^{40}\text{K}/^{40}\text{Ar}^*$ -calculated median value of the fluid residence time ranges from 57 ± 20 ka to 86 ± 20 ka (Table A2; *In Electronic Supplementary Table*).

Radiogenic and mantle helium also accumulate by local production in rocks and flux from the mid-ocean ridge. The total amount of mantle and radiogenic ^4He can be calculated from the $^4\text{He}/^{40}\text{Ar}^*$ ratios (Table 2 *In Electronic Supplementary Table*) and the calculated amount of $^{40}\text{Ar}^*$. The calculated $^4\text{He}/^{40}\text{Ar}^*$ ratios range from 1.58 to 3.62, which are within those typical of a DMM source (1.2-1.8; Graham, 2002) and the crust (4.9; Ballentine and O’Nions, 1994). The exception are wells PG-07, PG-16, and PG-17, which show $^4\text{He}/^{40}\text{Ar}^*$ ratios from 10 to 35. Wells PG-07 and PG-17 are most influenced by local production from rocks (see Figure 1-6 and Figure 1-7 and related discussion) and could have received ^4He and $^{40}\text{Ar}^*$ locally. Diffusive-controlled degassing of the magma source could cause fractionation of the $^4\text{He}/^{40}\text{Ar}^*$ ratios (e.g., Burnard, 2004), as also suggested for wells PG-07 and PG-17 given their relationship

between the heat and helium (see Figure 1-6 and related discussion). Assuming an average $^4\text{He}/^{40}\text{Ar}^*$ ratio of 2.66 ± 0.74 , and $^{40}\text{Ar}^*$ of $5.26 \pm 0.01 \times 10^{-6} \text{ cm}^3\text{STP } g_{\text{water}}^{-1}$, then the expected ^4He content would be $1.40 \pm 0.37 \times 10^{-5} \text{ cm}^3\text{STP } g_{\text{water}}^{-1}$. The flux of ^4He from the mid-ocean ridge would be $4.27 \pm 0.99 \times 10^{-7} \text{ cm}^3\text{STP cm}^{-2} \text{ yr}^{-1}$, based on the ^3He flux at MOR measured by Craig et al. (1975). The calculated ^4He production ratio is $5.56 \pm 1.53 \times 10^{-14} \text{ cm}^3\text{STP } g_{\text{rock}}^{-1} \text{ yr}^{-1}$ based on a U content of 0.39 ± 0.09 ppm and Th content of 0.32 ± 0.16 ppm in Theistareykir basalts (Stracke et al., 2003). Using the same values for the reservoir properties and running two distinct Monte Carlo simulations for 10% and for 15% porosity, the resulting (U/Th)- ^4He average fluid residence time then ranges from 100 ± 50 ka to 160 ± 80 ka. The (U/Th)- ^4He -calculated median value of the fluid residence time ranges from 96 ± 50 ka to 140 ± 60 ka (Table A2; *In Electronic Supplementary Table*). The age difference when calculated using ^4He and $^{40}\text{Ar}^*$ is likely dependent on the $^4\text{He}/^{40}\text{Ar}^*$ ratio used. Indeed, if we assume that the lowest $^4\text{He}/^{40}\text{Ar}^*$ measured, 1.58 (PG-17; Table 2 *In Electronic Supplementary Table*), is the least fractionated, the resulting radiogenic ^4He would be $8.33 \pm 0.22 \times 10^{-6} \text{ cm}^3\text{STP } g_{\text{water}}^{-1}$ and the resulting (U/Th)- ^4He ages will be identical, within uncertainties, to the ^{40}K - $^{40}\text{Ar}^*$ ages (Table A2; *In Electronic Supplementary Table*). It is worth noting that much higher porosities for fractured basalts and hyaloclastites would give much older fluid residence times, which have been calculated to range from 210 to 470ka.

Despite the relatively large errors, these computations seem to support the hypothesis of pre-Holocene, “ice age” water in the Theistareykir reservoir, mixed with local modern recharge. This result is compatible with Pleistocene recharge and possibly long-distance recharge from the south through the rift, as postulated by Darling and Ármannsson (1989). Indeed, the calculated fluid residence times are older than the Theistareykir geothermal reservoir itself ($\leq 10,000$ a), and thus it cannot be assumed to

be local connate water trapped in the porous space of the reservoir, but instead supplied by regional groundwater flow from outside of Theistareykir.

It is possible to calculate the volume of each meteoric fluid component (modern recharge vs. pre-Holocene water vs. sub-modern highland recharge) by using a simple ternary mixing equation based on the stable isotopic composition of water (Figure 1-2):

$$f_1 = \frac{\delta^2\text{H}_s - \delta^2\text{H}_2 - f_3(\delta^2\text{H}_3 - \delta^2\text{H}_2)}{\delta^2\text{H}_1 - \delta^2\text{H}_2} \quad (14)$$

$$f_2 = \frac{\delta^{18}\text{O}_s - \delta^{18}\text{O}_1 - f_3(\delta^{18}\text{O}_3 - \delta^{18}\text{O}_1)}{\delta^{18}\text{O}_2 - \delta^{18}\text{O}_1} \quad (15)$$

$$f_3 = 1 - f_1 - f_2 \quad (16),$$

where f_1 , f_2 , and f_3 are the fractions of modern local meteoric water, sub-actual regional highland groundwater, and pre-Holocene meteoric water respectively; $\delta^2\text{H}_s$ and $\delta^{18}\text{O}_s$ correspond to the respective isotopic values of the Theistareykir fluids and $\delta^2\text{H}_{1,2,3}$ and $\delta^{18}\text{O}_{1,2,3}$ correspond to the respective isotopic values of each meteoric water component (Clark, 2015).

Results show that the Theistareykir meteoric water is a mix of 48.9% modern local meteoric water, 10.6% sub-actual regional highland water, and 40.4% pre-Holocene meteoric water.

1.6.4 Origin of helium and related magmatic fluids

Figure 1-4 shows the classic Craig's diagram in which $^3\text{He}/^4\text{He}$ ratios (expressed as R/Ra), measured here in fumaroles, mud pots, and geothermal wells, are plotted against $^4\text{He}/^{20}\text{Ne}$ ratios (Craig et al., 1978). In this figure, the mantle, air, and

crustal sources have distinct isotopic R/Ra signatures, and data points usually plot on hyperbolic curves representing mixing between these sources. The mantle helium endmember is expected to show higher R/Ra than that of the atmosphere, with a R/Ra of 8 ± 1 for a DMM source (Allègre et al., 1995) or higher if a mantle plume source is involved. In Iceland, maximal R/Ra values of 35-43 have been measured in alkaline lavas by Breddam and Kurz (2001) and of 47.5 in an olivine phenocryst from NW Iceland (Harðardóttir et al., 2018). Typical crustal R/Ra values are on the order of 0.02 (Mamyrin and Tolstikhin, 1984), because of the dominant production of radiogenic ^4He and little nucleogenic ^3He in rocks. Finally, the atmospheric endmember may represent air contamination or atmospheric helium dissolved at solubility equilibrium (ASW) in the meteoric water component recharging the system. This source is expected to have a R/Ra value of close to 1 (0.983; Benson and Krause, 1980). The $^4\text{He}/^{20}\text{Ne}$ ratio for atmospheric helium is 0.318, while the ASW value depends on the temperature at recharge. In Theistareykir, the MAAT is 3.7°C , and the resulting $^4\text{He}/^{20}\text{Ne}$ ASW ratio is 0.249, using solubility data from Smith and Kennedy (1983). The $^4\text{He}/^{20}\text{Ne}$ of the mantle and crust endmembers are more difficult to evaluate. Sano and Wakita (1985) suggested a $^4\text{He}/^{20}\text{Ne}$ for subduction-related settings, but this is extremely variable, with recorded values in geothermal systems as high as 50,000 (e.g., Pinti et al., 2017). Here, we arbitrarily fixed this value at 181, which is the highest $^4\text{He}/^{20}\text{Ne}$ value measured in well PG-07 (Figure 1-4) and close to 202, which is the highest value measured in well K-15 in the nearby Krafla geothermal field (Poreda et al., 1992).

Data from this study show a mixing trend, which can be fit using the hyperbola inverse method described in section 3.3.3. Interestingly, the few data available in the literature are compatible with this mixing trend (Figure 1-4). The resulting equation of the best fit using data from this study is:

$$\frac{R}{Ra} = 11.45 - \frac{38.13}{\left(\frac{^4\text{He}}{^{20}\text{Ne}} + 3.77\right)} \quad (18),$$

and the R/Ra value of the mantle endmember (labelled LOCAL MANTLE in Figure 1-4) is 11.45. Also including data from the literature, the mantle endmember R/Ra value would be 11.40. This value is clearly distinct from what is expected from the convective depleted mantle (DMM), 8 ± 1 (Allègre et al., 1995). It might represent the mixing of approximately 8.7 to 12.7% Icelandic plume helium (R/Ra of 35-47.5; Breddam and Kurz, 2001; Harðardóttir et al., 2018) with 87.2-91.3% DMM helium.

The R/Ra value of 11.45 postulated for the Theistareykir local mantle is close to that of 12.2 ± 0.3 measured in an olivine phenocryst from Theistareykir basalts (Macpherson et al., 2005a). Interestingly, the R/Ra values measured in MORBs collected offshore of NE Iceland in both the Tjornes Fracture Zone (TFZ) and the Kolbeinsey mid-ocean ridge, the latter representing the offshore continuation of the NVZ, are also compatible with the mantle endmember of Theistareykir fluids (Macpherson et al., 2005b). The TFZ R/Ra values measured in MORB glasses range from 9.8 to 13.6, while the southern Kolbeinsey ridge MORB glasses have relatively constant R/Ra values centered around 11.15 ± 0.44 (Macpherson et al., 2005b).

In conclusion, the expected helium isotopic signature of the mantle beneath Theistareykir, of 11.45, is compatible with what is observed in this last inland segment of the NVZ and in the nearby offshore segment. This source is slightly enriched in plume He compared with other geothermal systems of the NVZ, south of the studied zone, such as Askja, Krafla, and Namafjall, or even Kverkfjöll in the southern highlands, whose fluids show a helium isotopic signature centered around 8.96 ± 0.88 (compiled data from Harðardóttir et al., 2018). This precludes that the plume helium component has been transported by regional groundwater flow, as observed in the past for other geothermal systems (Hilton et al., 1990). It is likely that this plume component reached Theistareykir transported by volatile-rich incipient melts, and the subsequent

lateral dispersion of the plume through conduits at shallower levels (e.g., Breddam et al., 2000; Harðardóttir et al., 2018).

1.6.5 Magma degassing and heat transfer

Half of the heat in the Earth is produced through the decay of uranium, thorium, and potassium, with an accompanying production of radiogenic ^4He (and $^{40}\text{Ar}^*$). This results in a coupling of heat and ^4He release in geothermal systems (O’Nions and Oxburgh, 1983; Oxburgh and O’Nions, 1987; Kennedy et al., 2000). The helium isotopic ratio and the heat (Q)/ ^3He ratios measured in mid-ocean ridge geothermal systems are similar to the predicted values and are relatively constant ($^3\text{He}/^4\text{He}$ ratio of $8 \pm 1 \text{ Ra}$, and $Q/^3\text{He}$ ratio of $\sim 2 \times 10^{12} \text{ J/cm}^3\text{STP}$), confirming the relationship between heat and helium (Baker and Lupton, 1990; Poreda and Arnórsson, 1992; Lupton et al., 1999a, 1999b; Kennedy et al., 2000). Poreda and Arnórsson (1992) have shown that concomitant losses of ^3He and heat can provide a link between the extraction of heat and that of volatiles from basaltic magmas. This means that, at high temperatures, there is a direct relationship between heat and volatile loss. However, as the magma body cools, processes including magma degassing and cooling can fractionate helium from heat, breaking down the direct relationship between heat and volatile loss, and thus providing a technique for identifying and calculating the proportion of heat versus gas release in geothermal systems. In more complex continental geothermal settings, adiabatic boiling (i.e., the gas loss and mixing with cold groundwater), complicates the interpretation. Poreda and Arnórsson (1992), studied several Icelandic geothermal fields and showed that the fractionation of heat and ^3He is correlated to the aging of the magmatic intrusions, called “magma aging” and defined as the decreasing loss of ^3He from a magma chamber relative to heat (Kennedy et al., 2000).

The $^4\text{He}/^{36}\text{Ar}$ ratio can be used together with $^3\text{He}/Q$ to differentiate conduction versus convection regimes in geothermal reservoirs (Burnard and Polyá, 2004; Wen et

al., 2018). Cooling of an intrusion by conduction will transfer magmatic heat into the geothermal system, but without magmatic volatiles, inducing fractionation of ^3He relative to heat (Q). In contrast, if convection takes place at the interface of the magmatic and geothermal systems, this will result in the extraction of helium more rapidly than of heat. As a result, the $^3\text{He}/\text{Q}$ ratio can be used to distinguish between convection and conduction of heat (Burnard et Polya, 2004). In comparison, the dilution of magmatic fluids by modern surface fluids will decrease $^4\text{He}/^{36}\text{Ar}$ at constant $^3\text{He}/\text{Q}$, whereas the addition of radiogenic ^4He from the crust will increase $^4\text{He}/^{36}\text{Ar}$ at constant $^3\text{He}/\text{Q}$ (Burnard and Polya, 2004). The $^3\text{He}/\text{Q}$ ratio has been calculated as follows (Turner and Stuart, 1992):

$$^3\text{He}/\text{Q} = ^3\text{He}/^{36}\text{Ar} \times ^{36}\text{Ar}_{\text{ASW}} / (C_p \times \theta) \quad (19),$$

where C_p and θ are specific heat capacity ($4.4 \text{ J K}^{-1} \text{ g}^{-1}$; Burnard et al., 1999) and temperature excess ($^{\circ}\text{C}$) with respect to the local MAAT of 3.7°C . $^3\text{He}/^{36}\text{Ar}$ ratios are measured values while $^{36}\text{Ar}_{\text{ASW}}$ represents ^{36}Ar concentration in ASW at 3.7°C ($1.52 \times 10^{-6} \text{ cm}^3\text{STP g}^{-1}_{\text{water}}$; Smith and Kennedy, 1983). Calculated $^3\text{He}/\text{Q}$ ratios are minimum estimates, as air contamination lowers the $^4\text{He}/^{36}\text{Ar}$ ratios (Burnard and Polya, 2004).

In Theistareykir, the calculated $^3\text{He}/\text{Q}$ ratios plotted against $^4\text{He}/^{36}\text{Ar}$ range from $2.83 \times 10^{-11} \text{ cm}^3\text{STP J}^{-1}$ for well ÞG-13 to $3.04 \times 10^{-14} \text{ cm}^3\text{STP J}^{-1}$ for well ÞG-11, and show that two different processes occur within the system (Figure 1-5). The majority of the wells show conduction, meaning that heat is lost through solid matter on a linear gradient. In contrast, wells ÞG-07 and ÞG-13 show convection, and thus a direct transfer of heat through fluids (liquids and gases) from the magmatic source to the hydrothermal system. Well ÞG-13 is an outlier, probably due to an abnormally low ^4He or high ^{36}Ar content.

The $^4\text{He}/^3\text{He}$ versus $Q/^3\text{He}$ plot (Figure 1-6) shows that, at a constant $^4\text{He}/^3\text{He}$ ratio, high $Q/^3\text{He}$ values indicate that the magma body is cooling, but is still hot in comparison to other geothermal fields fed by magmatic intrusions (Kennedy et al., 2000). This “magma aging” (e.g., cooling with local production of radiogenic ^4He), corresponds to the conductive process in Figure 1-5. These data also show that the Theistareykir geothermal field is minimally affected by boiling (only between 0-1%, Figure 1-6; Kennedy et al., 2000), meaning that very little vapor is removed from the system and that the fluids have experienced low $^3\text{He}/Q$ fractionation. This shows that the field is not significantly impacted by exploitation at the moment. The low $Q/^3\text{He}$ values of wells ÞG-07 and ÞG-13 show that this magma degassing contributes to these two wells, which agrees with the previous conclusion of a convective regime for the eastern sector of the Theistareykir field.

1.6.6 Water-rock interaction and effects on ^{18}O and helium isotopic composition

The oxygen shift toward higher $\delta^{18}\text{O}$ values, up to -9.02 ‰ (Figure 1-2 and Figure 1-7), likely reflects two different processes and mixing. First, it points to water-rock interaction in the geothermal reservoir (Giggenbach, 1992; Hedenquist and Lowenstern, 1994; Pope et al., 2009; 2016), which is supported by the decrease in R/R_a , correlating with the progressive increase in the $\delta^{18}\text{O}$ for almost half of the wells in the area (Figure 1-7). This decrease in R/R_a results from the addition of radiogenic ^4He , the decay product of ^{238}U , ^{235}U , and ^{232}Th contained in rocks and their daughter nuclei. In principle, it could also reflect variations in the mixing proportions of DMM and plume mantle sources (see Figure 1-4), but the strong correlation with $\delta^{18}\text{O}$ makes the local addition of radiogenic ^4He a more likely process. During prolonged water-rock interaction, the radiogenic ^4He produced in the rock slowly accumulates in the porewater (e.g., Torgersen and Clarke, 1985). Therefore, the more a rock is in contact with water, the more it is enriched in radiogenic ^4He . This process is further enhanced at the higher temperatures of geothermal fluids, and in this case also by the long

residence time of the pre-Holocene age of some of the water. As a result, water-rock interaction is an important process in the Theistareykir geothermal field. This has already been shown by the presence of epidote and other secondary alteration minerals in basalt-hosted geothermal systems, including in the Krafla geothermal system (Gautason et al., 2010; Pope et al., 2016).

The second cluster of wells (ÞG-03, 05, 07, 13, 16, and 17) indicates mixing between Theistareykir meteoric water (a mixture of modern, sub-modern, and pre-Holocene components) and the magmatic water endmember. The data have been fitted with a hyperbola calculated using the inverse method described in section 3.3.3. The resulting fit equation is:

$$\frac{R}{Ra} = 11.89 - \frac{6 \times 10^{-6}}{\delta^{18}O - 15.39\text{‰}} \quad (20).$$

The magmatic endmember has a R/Ra value of 11.89, which is fully compatible with the value of 11.45 calculated by the R/Ra vs. $^4\text{He}/^{20}\text{Ne}$ relationship (Figure 1-4). The meteoric endmember has a $\delta^{18}\text{O}$ value of -15.39‰, which is also close to that of -14.79‰, determined on the Craig's plot of Figure 1-2.

Wells ÞG-03, ÞG-07, and ÞG-17 are thus more influenced by this magmatic water endmember, with ÞG-07 also having much higher CO_2 concentrations than the other wells (Kristinsson et al., 2013). The high $\delta^{18}\text{O}$ values coupled with high R/Ra ratios show that the $\delta^{18}\text{O}$ of these particular fluids is more influenced by the magmatic component, although water-rock interaction is also probably more intense given the magmatic volatiles and heat released.

1.6.7 Conceptual model of the Theistareykir geothermal field and implications

Analysis of all available data provided in this and previous studies (Ármannsson et al., 1986; Darling and Ármannsson, 1989; Gudmundsson et al. 2008; Sveinbjörnsdóttir et al., 2013; 2015; Óskarsson, et al., 2013) leads to a better understanding of the dynamics of the Theistareykir geothermal system, described in the conceptual model shown in **Erreur ! Source du renvoi introuvable.**. The Theistareykir geothermal reservoir receives inputs from magmatic fluids, modern precipitation (48.9%), sub-actual meteoric water from the southern highlands (10.6%), and pre-Holocene meteoric water (40.4%). These proportions are important to determine in order to evaluate the sustainability of the geothermal field. Indeed, 40.4% of the water feeding the field is of “fossil” origin, meaning that this water has a limited volume available over time. It is therefore important to closely monitor water flow within the field over time and to adapt production accordingly.

According to the measured helium isotopic composition, the intrusion below Theistareykir is dominated by a MORB-type source with limited influence from the plume source and a calculated R/Ra value of 11.45 (Figure 1-4). This magmatic intrusion feeds the geothermal reservoir with both magmatic fluids and heat (Q). Relationships between heat and noble gas isotopes, ^3He , ^4He , and ^{36}Ar allowed heat and mantle helium sources to be understood. The Theistareykir geothermal field originates from an underlying hot intrusion, which exhibits two different heat regimes depending on the region of the field considered. A convective regime dominates the eastern and southern (sub-areas A and C/D) regions of the field ($^3\text{He}/Q > 1 \times 10^{-12} \text{ cm}^3\text{STP J}^{-1}$), especially below and along the Ketilfjall mountain, along the boundary of the fissure swarm and the western side of the Bæjarfjall mountain (Figure 1-1, Figure 1-5 and **Erreur ! Source du renvoi introuvable.**). $^3\text{He}/Q$ values are as high as $2.83 \times 10^{-11} \text{ cm}^3\text{STP J}^{-1}$, whereas a conductive regime is more important in the central region of the field (sub-areas B and C), with $^3\text{He}/Q$ values ranging from $4.94 \times 10^{-13} \text{ cm}^3\text{STP}$

J^{-1} for well ÞG-17 to $3.04 \times 10^{-14} \text{ cm}^3\text{STP } J^{-1}$ for well ÞG-11. This observation is consistent with the fact that, for example, ÞG-03, which is in the same area, has been known to be the second hottest well on record in Iceland. Also, the work of previous geologists (Arnaldsson et al., 2011; Khodayar et al., 2018) based on the tectonics of the field combined with several chemical and physical parameters (major gas contents, resistivity, fumarole gas monitoring, and geothermometry (Ármansson et al., 1986)) suggested that the eastern area around the Ketilfjall ridge is hotter than the other areas of the field.

In parallel, both modern, sub-modern, and pre-Holocene meteoric water components feed the geothermal reservoir. The three fluid sources are clearly identifiable in the $\delta^2\text{H}$ and $\delta^{18}\text{O}$ values, exhibiting values ranging from local precipitation for the modern water component (-80‰ and -11‰ respectively; Figure 1-2) to extremely low $\delta^2\text{H}$ and $\delta^{18}\text{O}$ for the pre-Holocene water (\sim -141‰ and \sim -19‰ respectively; Figure 1-2). These very low values are mainly found in sub-area A, where ^{40}K - $^{40}\text{Ar}^*$ and (U/Th)- ^4He fluid residence times have been calculated to provide ages ranging from $57 \pm 20 - 92 \pm 30 \text{ ka}$ and $96 \pm 50 - 160 \pm 80 \text{ ka}$ respectively.

Limited phase segregation, induced by the underlying intrusion, provides secondary modification of the isotopic signature of the fluid, as shown by both water stable isotopes. Fumarole water isotopes show very low values of $\delta^{18}\text{O}$, of -20.8‰ (partly due to boiling and condensation), but essentially unmodified $\delta^2\text{H}$, ranging from -105‰ to -125‰, which plots to the left of the GMWL (Figure 1-2). The observed isotopic shift in $\delta^2\text{H}$ and $\delta^{18}\text{O}$ compared to the GMWL (Figure 1-2) indicates that phase segregation and boiling take place in Theistareykir. However, compared to the adjacent Krafla geothermal system (Pope et al., 2016), the isotopic shift is smaller, suggesting that less than 10% of the fluid has been affected by phase segregation with the

separation of a steam phase (Figure 1-2). The $Q/{}^3\text{He}$ relationship (Figure 1-6), suggests even less, closer to 1%.

Finally, the R/Ra ratios and $\delta^{18}\text{O}$ (Figure 1-7) allow areas subjected to more intensive water-rock interaction processes (sub-areas B and central area C) as opposed to the new input of magmatic fluids (sub-areas A and C/D) to be identified. This is highlighted by both the addition of crustal helium, as well as the high $\delta^{18}\text{O}$ values in the fluids, with values ranging from 9.44 ± 0.2 to 11.45 ± 0.30 for R/Ra, and from -13.58‰ to -11.1‰ for $\delta^{18}\text{O}$.

1.7 Conclusions

This study identifies the sources of fluids and heat in the Theistareykir geothermal system situated in the Northern Volcanic Zone (NVZ) of Iceland, and the processes operating in the geothermal reservoir. Noble gases and water isotopes are combined with information on physical parameters to develop a conceptual model. Results show the presence of four fluid sources in the system. These include a small contribution of magmatic fluids, water from past recharge under a colder climate with respect to the present, sub-modern water regionally recharged in the highlands, and a modern meteoric water component. The He isotopic composition and $Q/{}^3\text{He}$ show that there is a direct transfer of magmatic volatiles into the Theistareykir geothermal system. The $\delta^{18}\text{O}$ and He isotope signatures point to a modification of the original fluid chemistry by water-rock interaction. Fractionation of the $Q/{}^3\text{He}$ ratios highlight the limited extent of phase segregation and boiling in the system, which probably affects 0.1-1% of the whole reservoir. It is apparent that the Theistareykir geothermal system has not yet been affected by significant extraction-induced boiling, thereby making it an ideal system to study.

Constraining fluid sources, in terms of location and age, is critical to ensure the long-term sustainability of the field. Indeed, the pre-Holocene water component accounting for almost half of the water content of the geothermal reservoir could limit the longevity of the resource (e.g., Pinti et al., 2019), and re-injection will need to be carefully managed. Magmatic helium and radiogenic and mantle argon allow whether and where convection or conduction are the dominant heat transfer process in the geothermal field exploitation area to be determined. Noble gases provide information on specific wells impacted by direct magma degassing, which is a critical piece of information to estimate both heat release and the chemical load of the system. Knowledge on heat distribution in the system is also essential to maximize the energy production of the geothermal field.

Together, these results permit a predictive evaluation of the potential evolution of the Theistareykir geothermal system. In the eastern sector of the field (ÞG-07, area A and ÞG-13, ÞG-17, south portion of area C), the direct involvement of magma suggests long-term heat potential at human timescales. In the more western and southern portions of the system, where magma aging is observed (area C, except for the south portion, and area D), cooling and boiling remains low compared to other fields (e.g., Krafla), making the Theistareykir geothermal field a viable long-term system if sustainable exploitation of the field is respected.

1.8 Acknowledgements

We warmly thank Sigurður G. Kristinsson and Auður Agla Óladóttir from the Iceland GeoSurvey (ÍSOR) for their help in the field in the first year of sampling, as well as Trausti Hauksson from Kemía Ltd., and Helgi Arnar Alfreðsson and Júlía Katrín Björke from Geochemý for their help in taking samples and for collecting additional samples. This research was funded by the Natural Sciences and Engineering Research

Council of Canada (NSERC) through an Alexander-Graham-Bell-doctorate (BESC D) grant (CGSD3-503679-2017) to M.S. and a Discovery Grant to D.L.P. (RGPIN-2015-05378); by Geotop through a collaborative research project fund, 2018-2020; by ÍSOR and the Landsvirkjun Power company; and by Osisko philanthropy. We also thank ÍSOR, Landsvirkjun, and the University of Iceland for providing access to sampling locations and to their facilities.

1.9 References

- Allègre, C.J., Moreira, M., Staudacher, T., 1995. $4\text{He}/3\text{He}$ dispersion and mantle convection. *Geophys. Res. Lett.* 22, 2325-2328.
- Albarède, F., 1995. *Introduction to geochemical modeling*. Cambridge University Press, Cambridge, England, 543 pp.
- Andrews, J.N., Kay, R.L.F., 1983. The U contents and $^{234}\text{U}/^{238}\text{U}$ activity ratios of dissolved uranium in groundwaters from some Triassic Sandstones in England. *Chem. Geol.* 41, 101-117.
- Ármansson, H, Gíslason, G, Torfason, H, 1986. Surface exploration of the Theistareykir high-temperature geothermal area, Iceland, with special reference to the application of geochemical methods. *Appl. Geochem.* 1, 47-64.
- Arnaldsson, A., Halldórsdóttir, S., Kjarn S.P., Axelsson G., 2011. Computational model of the geothermal system at Theistareykir and initial capacity assessment. ÍSOR report: ÍSOR-2011/049, 58p. (In Icelandic).
- Arnórsson, S., Stefánsson, A., Bjarnason, J.Ö., 2007. Fluid-fluid interaction in geothermal systems. *Rev. Mineral. Geochem.* 65, 259–312. Arnórsson, S. and Stefánsson, A., 2005. Wet-steam well discharges. II. Assessment of aquifer fluid compositions. *Proc. World Geother. Congr.* 2005, Antalya, Turkey, 24-29 April.
- Arnórsson, S., Andrésdóttir, A., 1995. Processes controlling the distribution of boron and chlorine in natural waters in Iceland. *Geochim. Cosmochim. Acta* 59, 4125–4146.

- Árnason, B., 1977. Hydrothermal systems in Iceland traced by deuterium. *Geothermics* 5, 125–151.
- Baker, E.T., Lupton, J.E. 1990. Changes in submarine hydrothermal ^3He /heat ratios as an indicator of magmatic/tectonic activity. *Nature* 346, 556-558.
- Ballentine, C.J., O’Nions, R.K., 1994. The use of natural He, Ne and Ar isotopes to study hydrocarbon-related fluid provenance, migration and mass balance in sedimentary basins. *Geol. Soc. London Spec. Publ.* 78, 347-361.
- Ballentine, C.J., Burgess, R., Marty, B., 2002. Tracing fluid origin, transport and interaction in the crust. *Rev. Mineral. Geochem.* 47, 539-614.
- Ballentine, C.J., Burnard, P.G., 2002. Production, release and transport of noble gases in the continental crust. *Rev. Mineral. Geochem.* 47, 481-538.
- Bangma P., 1961. The Development and Performance of a Steam-Water Separator for use on Geothermal Bores, Mechanical Engineer, Ministry of Works, Wairakei, New Zealand.
- Benson, B.B., Krause Jr, D., 1980. Isotopic fractionation of helium during solution: A probe for the liquid state. *J. Sol. Chem.* 9, 895-909.
- Birkle, P., Portugal Marín, E., Pinti, D.L., Castro, M.C., 2016. Origin and evolution of geothermal fluids from Las Tres Virgenes and Cerro Prieto fields, Mexico—co-genetic volcanic activity and paleoclimatic constraints. *Appl. Geochem.* 65, 36–53.
- Breddam, K., Kurz, M.D., Storey, M., 2000. Mapping out the conduit of the Iceland mantle plume with helium isotopes. *Earth Planet. Sci. Lett.* 176, 45-55.
- Breddam, K., Kurz, M.D., 2001. Helium isotope signatures of Icelandic alkaline lavas. *EOS Trans. Am. Geophys. Union* 82, F1315.
- Burnard, P., 2004. Diffusive fractionation of noble gases and helium isotopes during mantle melting. *Earth Planet. Sci. Lett.* 220, 287-295.
- Burnard, P.G., Polya, D.A., 2004. Importance of mantle derived fluids during granite associated hydrothermal circulation: He and Ar isotopes of ore minerals from Panasqueira. *Geochim. Cosmochim. Acta* 68, 1607-1615.

- Burnard, P.G., Hu, R.Z., Turner, G., Bi, X.W., 1999. Mantle, crustal and atmospheric noble gases in Ailaoshan gold deposits, Yunnan Province, China. *Geochim. Cosmochim. Acta* 63, 1595–1604.
- Clarke, W.B., Jenkins, W.J., Top, Z., 1976. Determination of tritium by mass spectrometric measurement of ^3He . *Appl. Radiat. Isot.* 27, 515-522.
- Clark, I., 2015. *Groundwater Geochemistry and Isotopes*. Boca Raton: CRC Press, <https://doi.org/10.1201/b18347>
- Craig, H., 1961. Isotopic variations in meteoric waters. *Science* 133, 1702-1703.
- Craig, H., Clarke, W.B., Beg, M.A., 1975. Excess ^3He in deep water on the East Pacific Rise. *Earth Planet. Sci. Lett.* 26, 125-132.
- Craig, H., Lupton J.E., Welhan J.A., Poreda R., 1978. Helium isotope ratios in Yellowstone and Lassen Park volcanic gases. *Geophys. Res. Lett.* 5, 897–900.
- Darling, G, Ármannsson H., 1989. Stable isotope aspects of fluid flow in the Krafla, Námafjall and Theistareykir geothermal systems of northeast Iceland. *Chem. Geol.* 76, 197-213.
- Eggertsson, G.H., Lavallée, Y., Kendrick, J.E., Markússon, S.H., 2020. Improving fluid flow in geothermal reservoirs by thermal and mechanical stimulation: The case of Krafla volcano, Iceland. *J. Volcanol. Geotherm. Res.* 391, 106351.
- Füri, E., Hilton, D.R., Halldórsson, S.A., Barry, P.H., Hahn, D., Fischer, T.P., Grönvold, K., 2010. Apparent decoupling of the He and Ne isotope systematics of the Icelandic mantle: the role of He depletion, melt mixing, degassing fractionation and air interaction. *Geochim. Cosmochim. Acta* 74, 3307–3332.
- Gautason, B., Gudmundsson, Á., Hjartarson, H., Blischke, A., Mortensen, A.K., Ingimarsdóttir, A., Gunnarsson, H.S., Sigurgeirsson, M.Á., Árnadóttir, S., Egilson, Th., 2010: Exploration drilling in the Theistareykir high-temperature field, NE-Iceland: Stratigraphy, alteration and its relationship to temperature structure. *Proc. World Geother. Congr.* 2010, Bali, Indonesia, 5 pp.
- Graham, D.W., 2002. Noble gas isotope geochemistry of mid-ocean ridge and ocean island basalts: Characterization of mantle source reservoirs. *Rev. Mineral. Geochem* 47, 247-317.

- Giggenbach, W., 1992. Isotopic shifts in waters from geothermal and volcanic systems along convergent plate boundaries and their origin. *Earth. Planet. Sci. Lett.* 113, 495-510.
- Gudmundsson, J.S., 1983. Geothermal electric power in Iceland: development in perspective. *Energy* 8, 491-513.
- Gudmundsson, Á., Gautason, B., Axelsson, G., Lacasse, C., Thorgilsson, G., Ármannsson, H., Tulinius, H., Saemundsson, K., Karlsdóttir, R., Kjaran, S.P., Pálmarrsson, S.Ó., Halldórsdóttir, S., 2008. A conceptual model of the geothermal system at Theistareykir and a volumetric estimate of the geothermal potential. Iceland GeoSurvey, Mannvit and Vatnaskil Consulting Engineers, report ÍSOR-2008/024 (in Icelandic): 57.
- Guðmundsson A., Myer E. M., Pálmarrsson S.O., 2015. Northeast - flow model revision. Engineer Vatnaskil, report 15.05. 98 p.
- Harðardóttir, S., Halldórsson, S.A., Hilton, D.R., 2018. Spatial distribution of helium isotopes in Icelandic geothermal fluids and volcanic materials with implications for location, upwelling and evolution of the Icelandic mantle plume. *Chem. Geol.* 480, 12-27.
- Harrison, D., Burnard, P.G., Trieloff, M., Turner, G., 2003. Resolving atmospheric contaminants in mantle noble gas analyses. *Geochem. Geophys. Geosyst.* 4, 1023.
- Hauksson T., 2018. Theistareykir, Krafla and Bjarnarflag performance of borehole and chemical content of water and steam in boreholes and production process in 2018. Landsvirkjun report LV-2019-026.
- Hedenquist, J.W., Lowenstern, J.B., 1994. The role of magmas in the formation of hydrothermal ore deposits. *Nature* 370, 519-527.
- Hermannsson, S., Línadal, B., 1951. Chemical analysis of warm and hot springs. Jarðboranir Ríkisins, State Drilling Company (in Icelandic).
- Hilton, D.R., Grönvold, K., O'Nions, R.K., Oxburgh, E.R., 1990. Regional distribution of ^3He anomalies in the Icelandic crust. *Chem. Geol.* 88, 53-67.
- Hilton, D.R., Grönvold, K., Sveinbjörnsdóttir, A.E., Hammerschmidt, K., 1998. Helium isotope evidence for off-axis degassing of the Icelandic hotspot. *Chem. Geol.* 149, 173-187.

- Horita, J., Wesolowski, D.J., 1994. Liquid-vapor fractionation of oxygen and hydrogen isotopes of water from the freezing to the critical temperature. *Geochim. Cosmochim. Acta* 58, 3425-3437.
- Kajugus, 2012. Updated reservoir analysis of the theistareykir high-temperature geothermal field, N-iceland. Geothermal training programme, Orkustofnun, Reykjavik, Iceland.
- Kennedy, B.M., Hiyagon, H., Reynolds, J.H., 1991. Noble gases from Honduras geothermal sites. *J. Volcanol. Geotherm. Res.* 45, 29–39.
- Kennedy, B.M., Fischer, T.P., Schuster, D.L., 2000. Heat and helium in geothermal systems, Twenty-Fifth Workshop on Geother. Reser. Engin., Standord University, Stanford, California, SGP-TR-165.
- Kennedy, B.M., van Soest, M.C., 2007. Flow of mantle fluids through the ductile lower crust: helium isotope trends. *Science* 318, 1433–1436.
- Khodayar, M., Björnsson, S., Kristinsson, S.G., Karlsdóttir, R., Ólafsson, M., Víkingsson, S., 2018. Tectonic control of the Theistareykir geothermal field by rift and transform zones in North Iceland: a multi-disciplinary approach. *Open J. Geol.* 8, 543-584
- Kristinsson, S.G., Fridriksson, Th., Ólafsson, M., Gunnarsdóttir, S.H, Níelsson, S., 2013. The Theistareykir, Krafla and Námafjall high-temperature geothermal areas. Monitoring of surface activity and groundwater. Iceland GeoSurvey, report ÍSOR-2013/037 (in Icelandic), 152 pp.
- Kulongoski, J.T., Hilton, D.R., 2011. Applications of Groundwater Helium, *Handbook of Environmental Isotop Geochemistry*, Vol. 1, 1 ed. Springer Isotope Handbook, Reston, VA, pp. 285-304.
- Kurz, M. D., Jenkins, W. J., Hart, S. R. 1982. Helium isotopic systematics of oceanic islands and mantle heterogeneity. *Nature*, 297, 43.
- Lafarge, T., Possolo, A., 2015. The NIST Uncertainty Machine. *NCSLI Measure J Meas. Sci.* 10, 20-27.
- Langmuir, C.H., Vocke, R.D., Hanson, G.N., Hart, S.R., 1978. A general mixing equation with applications to Icelandic basalts. *Earth Planet. Sci. Lett.* 37, 380-392.

- Lund, J.W., Boyd, T.L., 2016. Direct utilization of geothermal energy 2015 worldwide review. *Geothermics* 60, 66-93.
- Lupton, J.E., Baker, E.T., Massoth, G.J., 1999a. Helium, heat, and the generation of hydrothermal event plumes at mid-ocean ridges. *Earth Planet. Sci. Lett.* 171, 343-350.
- Lupton, J., Baker, E., Embley, R., Greene, R., Evans, L., 1999. Anomalous helium and heat signatures associated with the 1998 axial volcano event, Juan de Fuca ridge. *Geophys. Res. Lett.* 26, 3449-3452.
- Mamyrin, B.A., Tolstikhin, I.N., 1984. Helium isotopes in nature. Elsevier, Amsterdam.
- Mazor, E., Truesdell, A.H., 1984. Dynamics of a geothermal field traced by noble gases: Cerro Prieto, Mexico. *Geothermics* 13, 91-102.
- MacLennan, J., Jull, M., McKenzie, D., Slater, L., Grönvold, K., 2002. The link between volcanism and deglaciation in Iceland, *Geochem Geophys Geosyst*, 3, 1062, doi:10.1029/2001GC000282.
- Macpherson, C.G., Hilton, D.R., Mertz, D.F., Dunai, T.J., 2005. Sources, degassing, and contamination of CO₂, H₂O, He, Ne, and Ar in basaltic glasses from Kolbeinsey Ridge, North Atlantic. *Geochim. Cosmochim. Acta* 69, 5729-5746.
- Macpherson, C.G., Hilton, D.R., Day, J.M.D., Lowry, D., Grönvold, K., 2005. High-³He/⁴He, depleted mantle and low- $\delta^{18}\text{O}$, recycled oceanic lithosphere in the source of central Iceland magmatism. *Earth Planet. Sci. Lett.* 233, 411-427.
- Méjean, P., Pinti, D.L., Kagoshima, T., Roulleau, E., Demarets, L., Poirier, A., Takahata, N., Sano, Y., Larocque, M., 2020. Mantle helium in southern quebec groundwater: a possible fossil record of the New England hotspot. *Earth Planet. Sci. Lett.* In press.
- Moreira, M., J. Kunz, Allègre, C., 1998. Rare gas systematics in Popping Rock: Isotopic and elemental compositions in the upper mantle. *Science* 279, 1178-1181.
- Mukhopadhyay, S., 2012. Early differentiation and volatile accretion recorded in deep-mantle neon and xenon. *Nature* 486, 101-124.
- Nieva, D., Quijano, L., Garfias, A., Barragán, R.M., Laredo, F., 1983. Heterogeneity of the liquid phase, and vapour separation in Los Azufres (Mexico) geothermal

reservoir, Ninth Workshop Geothermal Reservoir Engineering, Stanford University, California, USA, pp. 253-260.

- O'Nions, R.K., Oxburgh, E.R., 1983. Heat and helium in the Earth. *Nature* 306, 429-431.
- Oxburgh, R.E., O'Nions, R.K., 1987. Helium loss, tectonics and the terrestrial heat budget. *Science* 237, 1583-1588.
- Óskarsson, F., Ármannsson, H., Ólafsson, M., Sveinbjörnsdóttir, Á.E., Markússon, S.H., 2013. The Theistareykir geothermal field, NE Iceland: fluid chemistry and production properties. *Proc. Earth Planet. Sci.* 7, 644–647.
- Ozima, M. and Podosek, F.A., 1983. *Noble Gas Geochemistry*. Cambridge University Press, Cambridge.
- Pedersen, R., Sigmundsson, F., Masterlark, T., 2009. Rheologic controls on inter-rifting deformation of the Northern Volcanic Zone, Iceland. *Earth Planet. Sci. Lett.* 281, 14–26.
- Pinti, D.L., Castro, M.C., Lopez-Hernandez, A., Han, G., Shouakar-Stash, O., Hall, C.M., Ramírez-Montes, M., 2017. Fluid circulation and reservoir conditions of the Los Humeros Geothermal Field (LHGF), Mexico, as revealed by a noble gas survey. *J. Volcanol. Geotherm. Res.* 333, 104-115.
- Pinti, D.L., Castro, M.C., López-Hernández, A., Hernández Hernández, M.A., Richard, L., Hall, C.M., Shouakar-Stash, O., Flores-Armenta, M., Rodríguez-Rodríguez, M.H., 2019. Cerro Prieto Geothermal Field (Baja California, Mexico) – A fossil system? Insights from a noble gas study. *J. Volcanol. Geotherm. Res.* 371, 32-45.
- Pope, E.C., Bird, D.K., Arnórsson, S., Fridriksson, Th., Elders, W.A., Fridleifsson, G.Ó., 2009. Isotopic constraints on ice age fluids in active geothermal systems: Reykjanes, Iceland. *Geochim. Cosmochim. Acta*, 73, 4468–88.
- Pope, E.C., Bird, D.K., Arnórsson, S., Giroud, N., 2016. Hydrogeology of the Krafla geothermal system, northeast Iceland. *Geofluids* 16, 1–23.
- Poreda, R.J., Arnórsson, S., 1992. Helium isotopes in Icelandic geothermal systems: II. Helium-heat relationships. *Geochim. Cosmochim. Acta* 56, 4229-4235.

- Poreda, R.J., Craig, H., Arnórsson, S., Welhan, J.A., 1992. Helium isotopes in Icelandic geothermal systems: I. ^3He , gas chemistry, and ^{13}C relations. *Geochim. Cosmochim. Acta* 56, 4221–4228.
- Ragnarsson Á., Steingrímsson B., Thorhallsson S., 2020. Geothermal development in Iceland, 2015-2019. *Proc. World Geother. Congr. 2020*, paper 01063
- Saar, M.O., Castro, M.C., Hall, C.M., Manga, M., Rose, T.P., 2005. Quantifying magmatic, crustal, and atmospheric helium contributions to volcanic aquifers using all stable noble gases: implications for magmatism and groundwater flow. *Geochem. Geophys. Geosyst.* 6, Q03008. <http://dx.doi.org/10.1029/2004GC000828>.
- Sano, Y., Wakita, H., 1985. Geographical Distribution of $^3\text{He}/^4\text{He}$ Ratios in Japan: Implications for Arc Tectonics and Incipient Magmatism. *J. Geophys. Res.* 90, 8729-8741.
- Sano, Y., Takahata, N., Seno, T., 2006. Geographical Distribution of $^3\text{He}/^4\text{He}$ Ratios in the Chugoku District, Southwestern Japan. *Pure Appl. Geoph.* 163, 745-757.
- Sano, Y., Fischer, T.P., 2013. The analysis and interpretation of noble gases in modern hydrothermal systems, *The Noble Gases as Geochemical Tracers*. Springer, pp. 249-317.
- Sheppard, S.M.F., Epstein, S., 1970. D/H and $^{18}\text{O}/^{16}\text{O}$ ratios of minerals of possible mantle or lower crustal origin. *Earth Planet. Sci. Lett.* 9, 232-239.
- Sheppard, S.M.F., Nielsen, R.L., and Taylor, H.P.Jr., 1969. Oxygen and hydrogen isotope ratios of clay minerals from porphyry copper deposits. *Econ. Geol.* 64, 755-777.
- Sigmundsson, F., Einarsson, P., Hjartardóttir, A. R., Drouin, V., Jónsdóttir, K., Árnadóttir, T., Geirsson, H., Hreinsdóttir, S., Li, S., Ófeigsson, B.G., 2018. Geodynamics of Iceland and the signatures of plate spreading. *J. Volcanol. Geotherm. Res.* 391, 106436
- Smith, S. P., Kennedy, B. M. 1983. The solubility of noble gases in water and in NaCl brine. *Geochim. Cosmochim. Acta.* 47, 503-515.
- Stefánsson, A., Hilton, D., Sveinbjörnsdóttir, Á.E., Torsander, P., Heinemeier, J., Barnes, J.D., Ono, S., Halldórsson, S.A., Fiebig, J., Arnórsson, S., 2017. Isotope systematics of Icelandic thermal fluids. *J. Volcanol. Geotherm. Res.* 337, 146-164.

- Stracke, A., Zindler, A., Salters, V.J.M., McKenzie, D., Blichert-Toft, J., Albarède, F., Grönvold, K., 2003. Theistareykir revisited. *Geochem. Geophys. Geosyst.* 4.
- Stuart, F.M., Lass-Evans, S., Fitton, J.G., Ellam, R.M., 2003. High $^3\text{He}/^4\text{He}$ ratios in picritic basalts from Baffin Island and the role of a mixed reservoir in mantle plumes. *Nature* 424, 57-59.
- Sveinbjörnsdóttir, Á., Ármannsson, H., Ólafsson, M., Óskarsson, F., Markússon, S., Magnúsdóttir, S., 2013. The Theistareykir geothermal field, NE Iceland. Isotopic characteristics and origin of circulating fluids. *Proc. Earth. Planet. Sci.* 7, 822-825.
- Sveinbjörnsdóttir, Á.E., Ármannsson, H., Óskarsson, F., Ólafsson, M., Sigurdardóttir, Á.K., 2015. A conceptual hydrological model of the thermal areas within the Northern neovolcanic zone, Iceland using stable water isotopes. *Proc. World Geother. Congr. 2015*, pp. 1–7.
- Torgersen, T., 2010. Continental degassing flux of ^4He and its variability. *Geochem. Geophys. Geosyst.* 11, Q06002, doi:06010.01029/02009GC002930.
- Torgersen, T., Kennedy, B.M., Hiyagon, H., Chiou, K.Y., Reynolds, J.H., Clarke, W.B., 1989. Argon accumulation and the crustal degassing flux of ^{40}Ar in the Great Artesian Basin. *Earth Planet. Sci. Lett.* 92, 43-56.
- Torgersen, T., Clarke, W.B., 1985. Helium accumulation in groundwater, I: an evaluation of sources and the continental flux of crustal ^4He in the Great Artesian Basin, Australia. *Geochim. Cosmochim. Acta* 49, 1211-1218.
- Torgersen, T., Jenkins, W., 1982. Helium isotopes in geothermal systems: Iceland, the geysers, raft river and steamboat springs. *Geochim. Cosmochim. Acta* 46, 739-748.
- Turner, G., Stuart, F., 1992. Helium/heat ratios and deposition temperatures of sulphides from the ocean floor. *Nature* 357, 581-583.

1.10 Figures

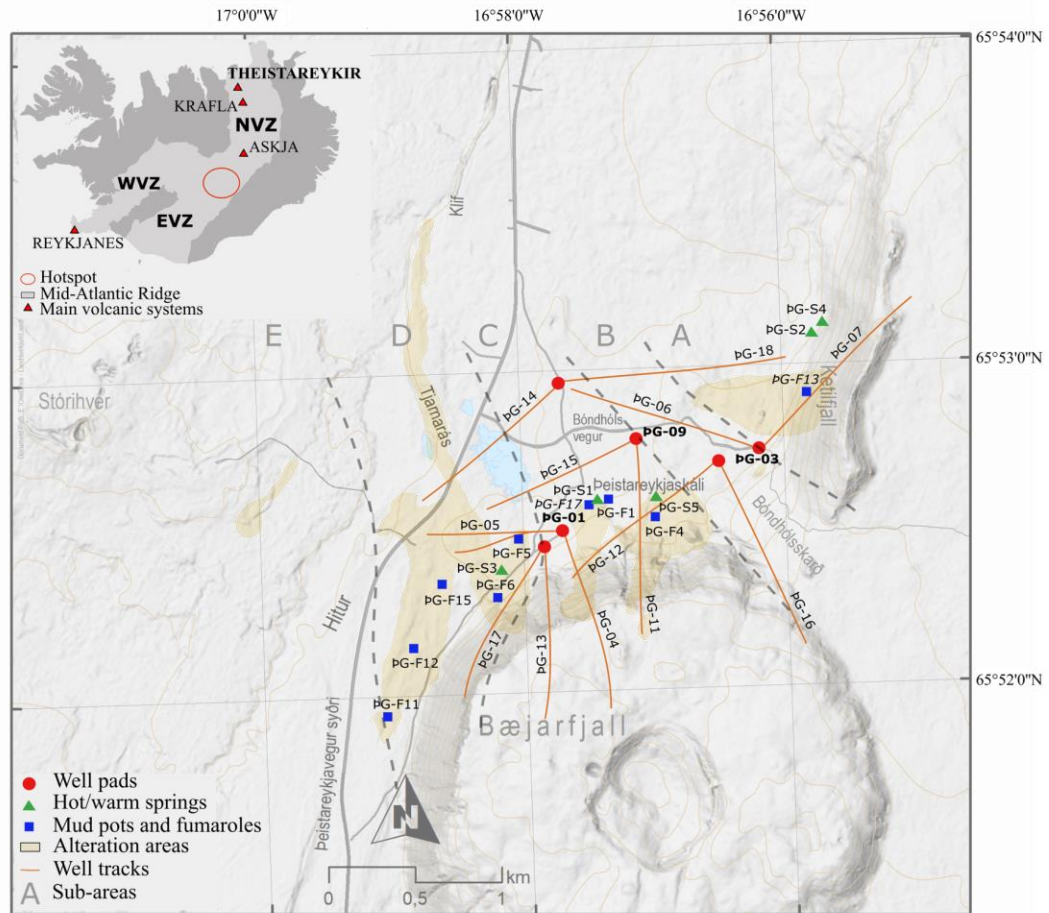


Figure 1-1 : Simplified map of the Theistareykir geothermal field with major alteration zones and positions of the sampled sites (wells, mud pots, and fumaroles) indicated. Numbers on the X- and Y-axes indicate the latitudinal and longitudinal geographical coordinates respectively on the World Geodetic System 1984 (WGS84). NVZ = Northern Volcanic Zone; WVZ = Western Volcanic Zone; EVZ = Eastern Volcanic Zone.

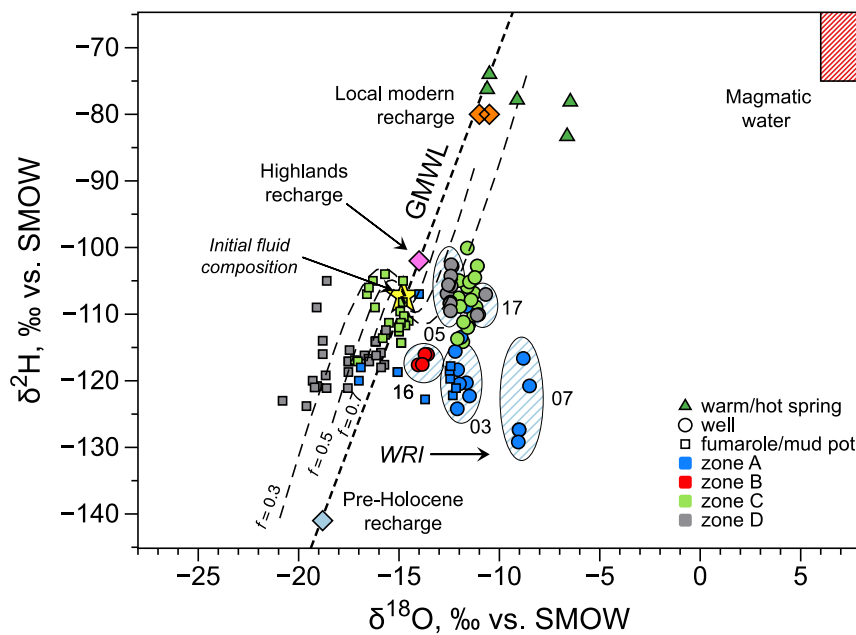


Figure 1-2 : Plot of $\delta^2\text{H}$ vs. $\delta^{18}\text{O}$ corrected for total discharge (TD) of the Theistareykir production fluids, mud pots, and fumaroles sampled over a 20-year period (data from this study and archived ÍSOR data; Table 2 *In Electronic Supplementary Table*). The global meteoric water line (GMWL; dashed line) was calculated following Craig (1961). Pre-Holocene recharge composition is from data of Sveinbjörnsdóttir et al. (2013), and the regional highlands recharge is from Stéfansson et al. (2017). Primary magmatic water composition is from Sheppard and Epstein (1970). The dashed curves represent the evolution of $\delta^2\text{H}_{\text{TD}}$ vs. $\delta^{18}\text{O}_{\text{TD}}$ in the vapor and residual liquid after phase segregation, starting from an initial composition (yellow star), and causing isotopic fractionation. Water isotopic compositions thus evolve along these lines according to their final equilibrium temperature. The f values correspond to the fraction of residual liquid. Blue dashed areas group stable isotopic compositions measured over the years for wells 03, 05, 07, 16, and 17. Zone A: Ketilfjall, Zone B: Bóndhólsskard, Zone C: Theistareykjagundur, Zone D: Tjarnarás.

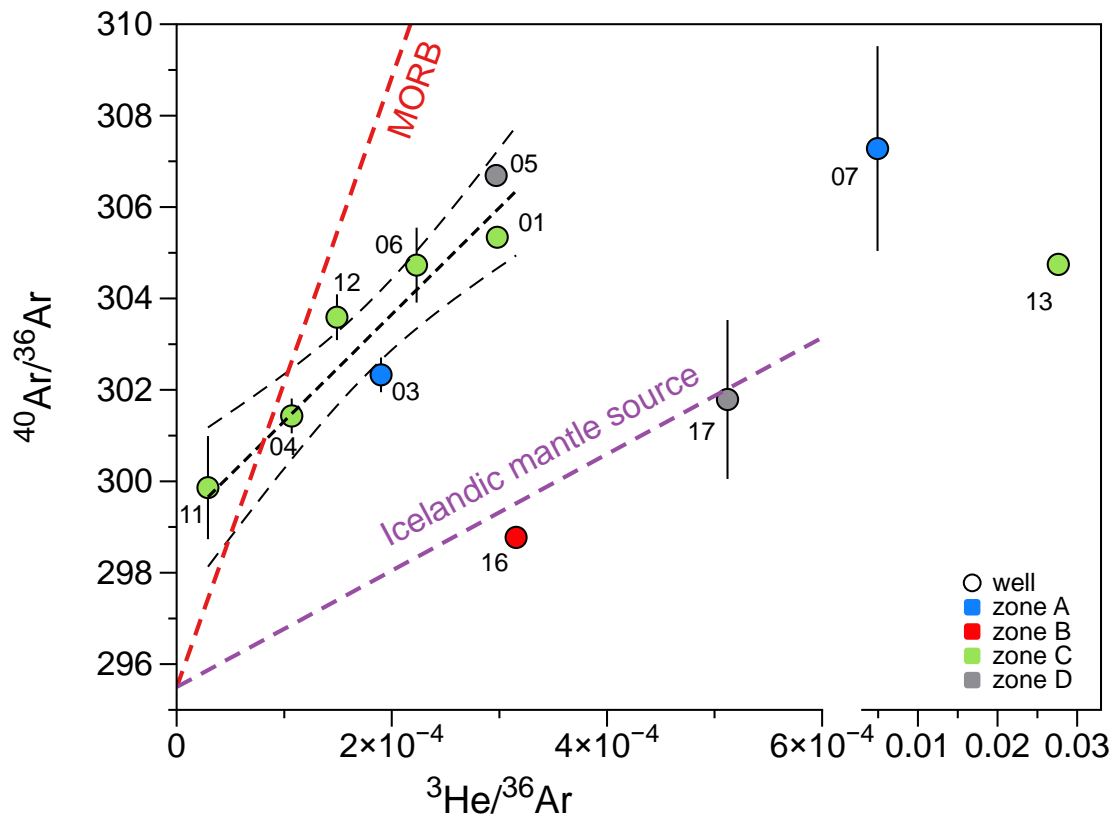


Figure 1-3 : $^3\text{He}/^{36}\text{Ar}$ vs. $^{40}\text{Ar}/^{36}\text{Ar}$ of Theistareykir geothermal fluids. Expected MORB and Icelandic mantle source arrays are indicated for comparison, as calculated following Mukhopadhyay (2012). The black dashed line is extrapolated through data from this study, excluding wells 16 and 17, which fall on the Icelandic mantle source. Wells 7 and 13 show values below that of the Icelandic mantle source (note the broken x-axis and change in scale). The two curved thin black dashed lines correspond to a confidence interval of 95%.

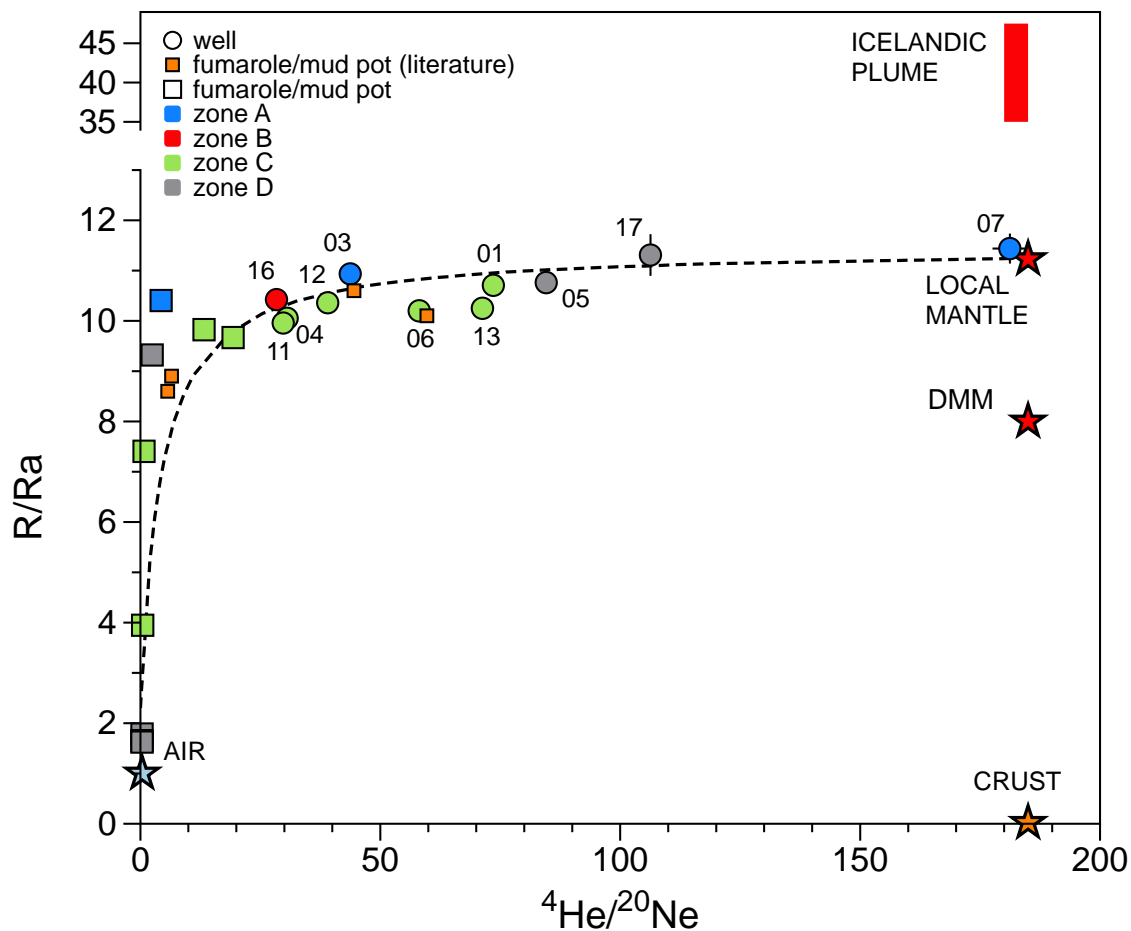


Figure 1-4 : The measured $^3\text{He}/^4\text{He}$ ratio (R), normalized to that of the atmosphere (R_a), versus $^4\text{He}/^{20}\text{Ne}$ ratios. Extrapolated mixing hyperbola obtained by data inversion suggests mixing between an atmospheric helium component (ASW or air) and a local mantle helium component with a R/R_a of 11.45, resulting from the mixing of a depleted MORB-type mantle (DMM) and a plume-type mantle. The values from literature are from Hilton et al., (1990), Poreda et al., (1992), and Fűri et al. (2010).

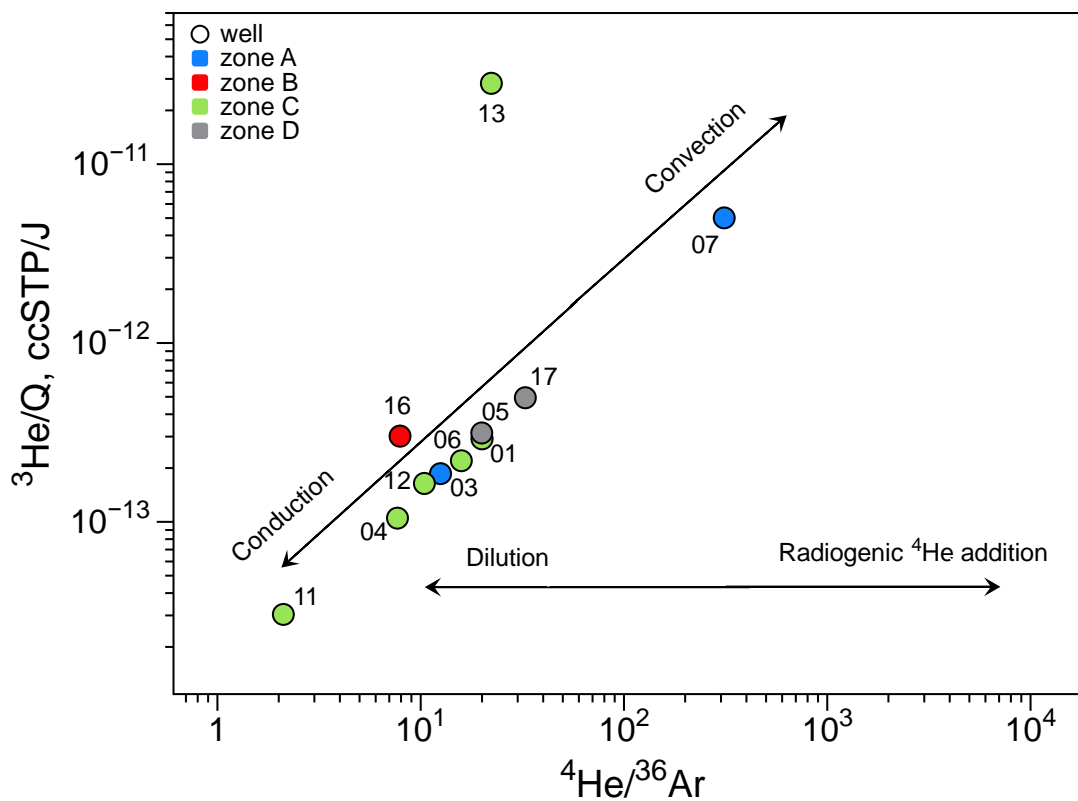


Figure 1-5 : ${}^3\text{He}/Q$ vs. ${}^4\text{He}/{}^{36}\text{Ar}$ for Theistareykir well fluid samples showing the heat transport in the field. Dilution of magmatic fluids by meteoric fluids will decrease ${}^4\text{He}/{}^{36}\text{Ar}$ at a constant ${}^3\text{He}/Q$, whereas addition of radiogenic ${}^4\text{He}$ from the crust (magmatic-type or water-rock interaction-type fluids) will increase ${}^4\text{He}/{}^{36}\text{Ar}$ at constant ${}^3\text{He}/Q$.

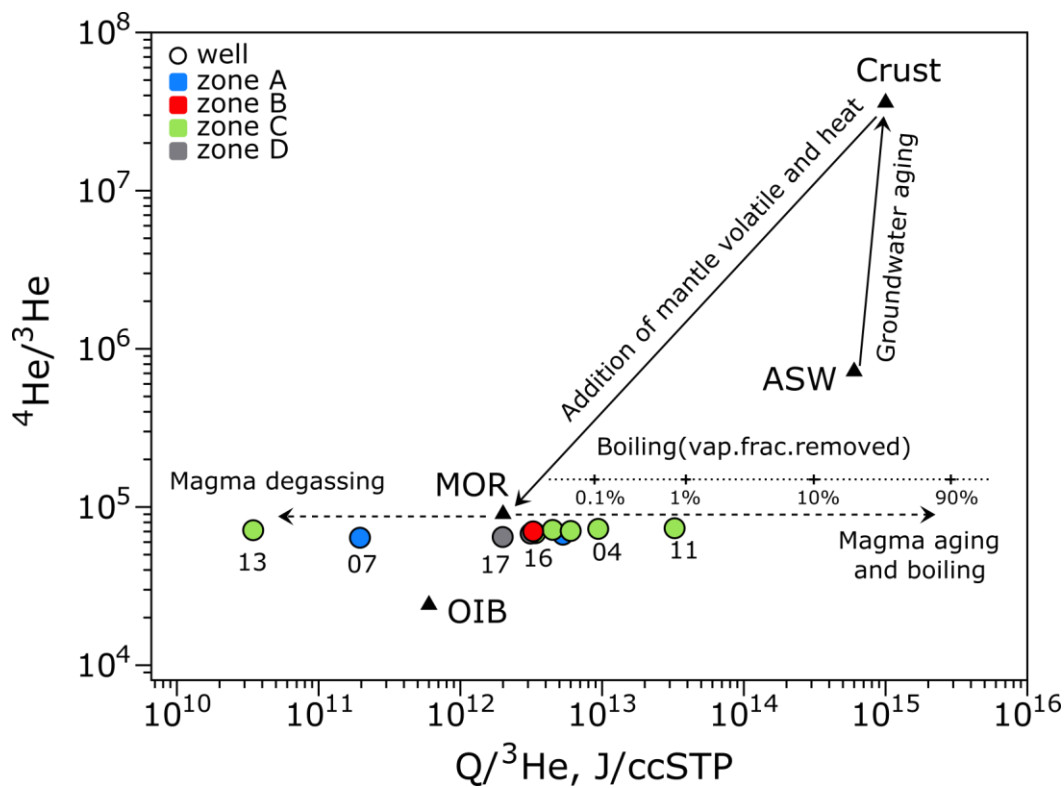


Figure 1-6: $^4\text{He}/^3\text{He}$ vs. $Q/^3\text{He}$ for Theistareykir well fluid samples. Samples are mainly undergoing either magma degassing or magma aging and boiling. The small dashed line corresponds to the fraction of vapor removed from the fluids during boiling. The triangle reports the He isotopic composition and the $Q/^3\text{He}$ ratio of the main sources of helium in fluids (MOR, crust, and ASW).

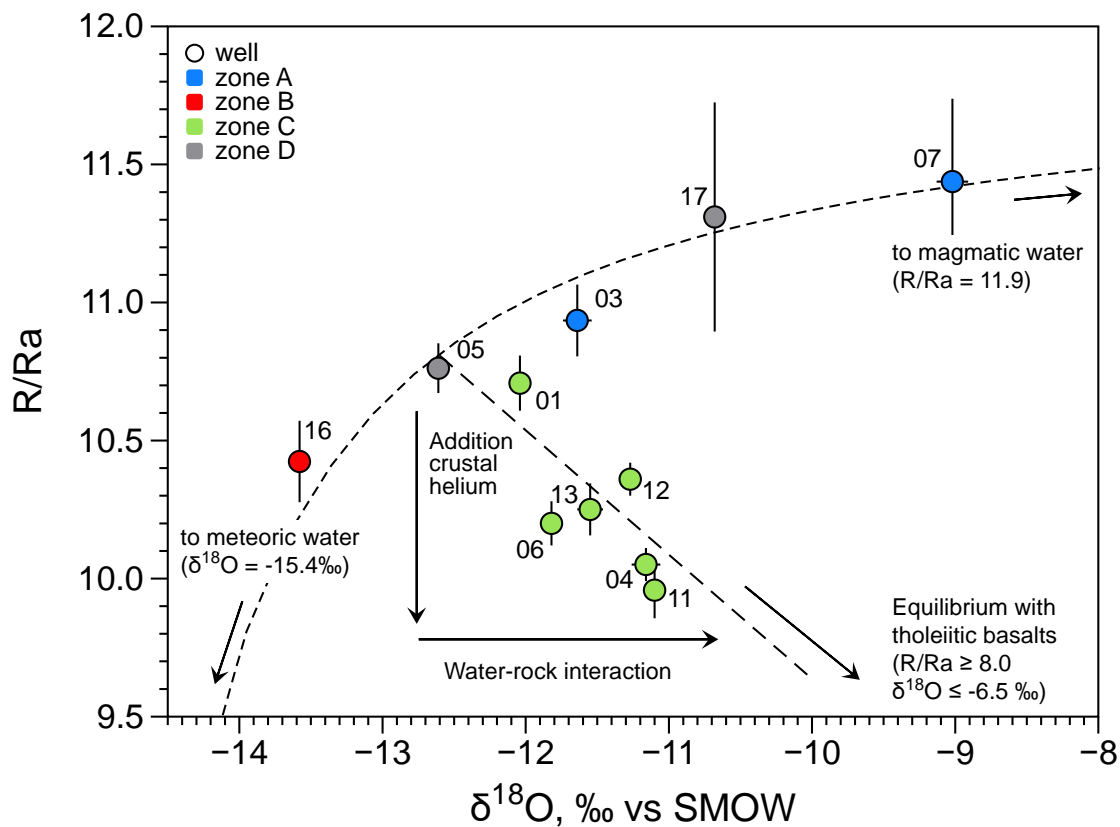


Figure 1-7 : Helium isotopic composition (R/Ra) vs. the $\delta^{18}\text{O}$ values of Theistareykir well fluids. Dashed lines show mixing between meteoric fluid (a mixture of local recharge, more distant regional recharge, and pre-Holocene recharge with a mean $\delta^{18}\text{O}$ of -15.4 ‰) and magmatic fluid (with a theoretical initial composition of R/Ra > 11.9 and $\delta^{18}\text{O} \approx +4.7$ ‰ (Macpherson et al., 2005b), and the effect of water-rock interactions with the addition of radiogenic ^4He to fluids and heavier $\delta^{18}\text{O}$ (with R/Ra ≥ 8.0 and $\delta^{18}\text{O} \leq -6.5$ ‰) respectively.

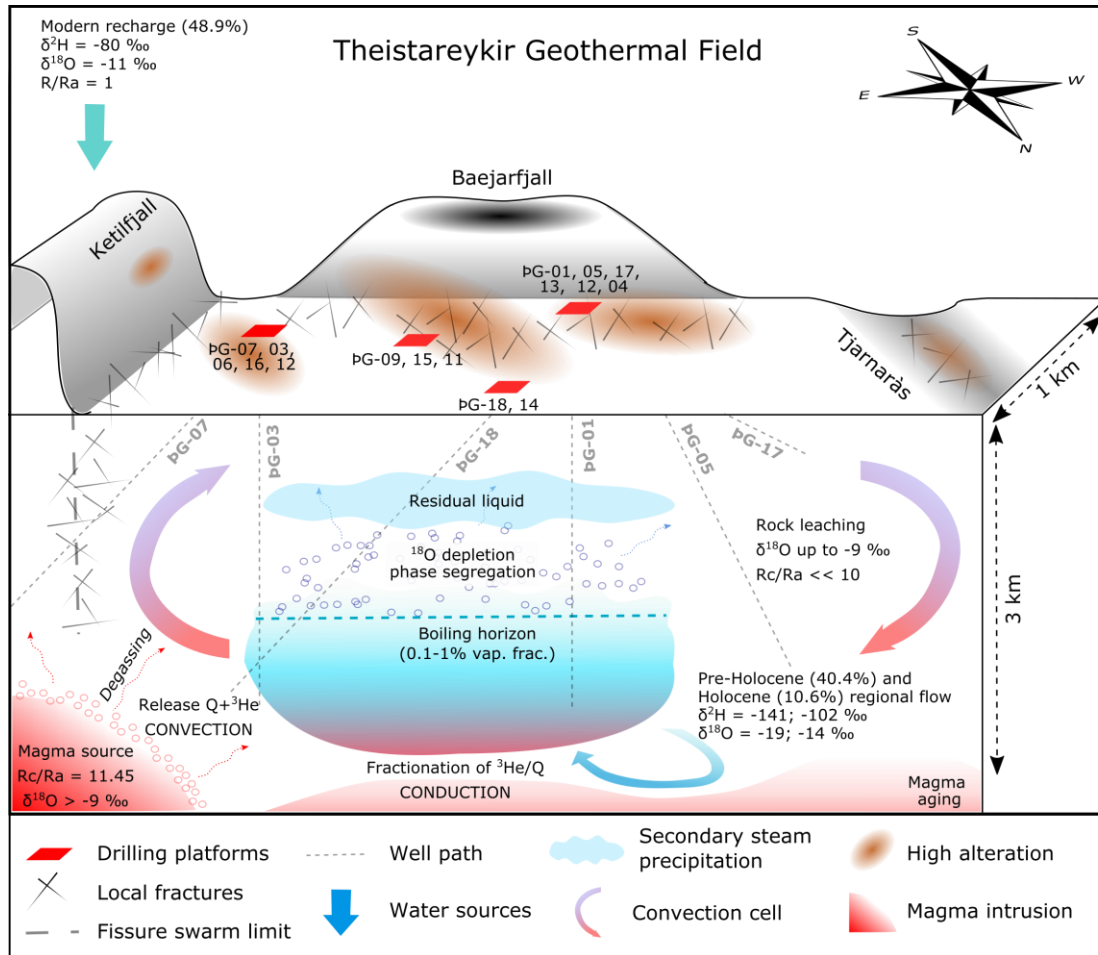


Figure 1-8 : Conceptual model of the Theistareykir geothermal field, with main fluid and heat sources and transport processes.

CHAPTER II

THE BEHAVIOUR OF METALS IN THE DEEP FLUIDS OF NE ICELAND

Marion Saby^{1*}, Vincent van Hinsberg², Daniele L. Pinti¹, Bjarni Gautason³, Ásgerdur Sigurdardóttir⁴, Kevin Brown⁵, Kim Berlo², Océane Rocher⁶

1-GEOTOP & Département des sciences de la Terre et de l'atmosphère, Université du Québec à Montréal, 201 Av. du Président Kennedy, Montréal, Canada.

2-GEOTOP & Department of Earth and Planetary sciences, McGill University, 34, University Street, Montréal, Canada.

3-ÍSOR Iceland GeoSurvey, Orkugardur, Grensásvegur 9, Reykjavik, Iceland.

4-Landsvirkjun, Háaleitisbraut 68, Reykjavik, Iceland.

5- Geokem, P.O. Box 30-125, Barrington, Christchurch 8244, New Zealand

6- GeoRessources - UMR 7359, Université de Lorraine, Vandoeuvre-Les-Nancy, France

*Corresponding author: saby.marion.e@gmail.com

Keywords: Deep fluid composition, Downhole sampling, metal contents, geothermal fluids, magma degassing, water-rock interaction, Krafla, Theistareykir, Iceland

2.1 Abstract

In this contribution, we present some of the first data on the elemental signature of deep crustal fluids in a basalt-hosted, low-chloride magmatic-hydrothermal system. Down-hole fluid samples (850 to 1600 m) from wells in the Theistareykir and Krafla geothermal fields in the Northern Volcanic Zone of Iceland were combined with well-head samples of condensed vapor, cuttings of altered rock, and fresh basalt. Results show that the deep fluids are relatively enriched in base metals and (semi)-volatile metals (in particular Te, Hg, Re and Tl) compared to local basalt. We interpret this enrichment in volatile metals to reflect a significant element input from magma degassing. Boiling of this deep fluid results in a well-head fluid composition that is significantly depleted in most elements. This well-head fluid has a distinct elemental signature, including a depletion in Sb that is mirrored in the altered rocks, and a depletion in the base metals that shows their selective sequestration in scale minerals, likely sulphides. The element content and patterns in surface fluids can thus not be interpreted to directly reflect that of the deep reservoir fluid. The behaviour of elements in Theistareykir and Krafla fluids is consistent, and largely agrees with similar data obtained for the Reykjanes geothermal system in SW Iceland. We therefore posit that our results are representative for this geological setting and indicate a significant magmatic degassing cation input to deep fluids, variably modified by water-rock interaction.

2.2 Introduction

Hot geological fluids are increasingly of interest as a sustainable and clean source of heat and energy and are regarded as one of the cornerstones of transitioning to a CO₂ neutral world (Chambefort and Stefánsson, 2020). Iceland is at the forefront of this development, and currently obtains 62% of its energy needs from geothermal plants (Huttrer, 2020). Sustainable exploitation does require an in-depth understanding of the fluid sources and evolution in these systems and investigating geothermal fluid composition is therefore essential (Arnórsson et al. 2007; Stefánsson et al. 2017; Saby et al., 2020;).

The exploitation of geothermal systems also provides a unique opportunity to access deep fluids in production wells and study the mobility of elements in the crust. For example, geothermal systems related to magma intrusions (i.e., magmatic-hydrothermal systems) are regarded as analogues to ore-forming systems (Henley and Ellis, 1983; Krupp and Seward, 1987; Rae et al., 2011; Simmons et al., 2016; Hannington et al., 2016; Chambefort and Stefánsson, 2020) and can therefore elucidate key questions in economic geology including the sources and fluxes of metals and fluids, and the aqueous concentrations and speciation of ore elements (Hedenquist et al., 1993; Hedenquist and Lowenstern, 1994; Yang and Scott, 2006; Hannington et al., 2016). In particular, the elemental and isotopic composition of geothermal fluids can put constraints on the respective contributions of magma degassing and rock leaching to the metal content of active magmatic-hydrothermal systems (cf. Simmons et al. 2016; Audétat and Edmonds 2020).

Geothermal fluids are normally sampled at the wellhead, given the technical challenges of sampling downhole fluids. The compositions of these surface fluids are commonly regarded as representative of deep fluid element signatures (e.g., Stefánsson et al.,

2005). However, surface fluids have generally experienced boiling, which results in fractionation of the elements between fluid and vapor, and precipitation of scales that selectively sequester elements depending on the scale mineralogy (Simmons et al., 2016). Thus, the composition of reservoir fluids can differ drastically from the fluids sampled at the surface. In addition to fluids, actively exploited geothermal fields can also provide access to fresh and altered reservoir rock cores, cuttings and scale, and thus allow to fully explore the behaviour of elements in the deep system, as well as physical-chemical changes *en route* to the surface.

Down-hole devices have been developed and used to sample reservoir fluids directly and thereby enable the metal concentrations of pre-boiled geothermal fluids to be determined (Simmons and Brown, 2006). In the volcanic arc-related Taupo field, in New Zealand, this has shown reservoir fluids to be metal-laden with up to 23 ppb Au, 2400 ppb Ag, and 4850 ppb As (Ellis, 1979; Seward, 1989; Simmons and Brown, 2006). Basalt-hosted deep fluids in the Reykjanes peninsula in the plume-MOR setting of Iceland are more dilute, despite their equivalent Cl content, with concentrations of up to 6 ppb Au, 34 ppb Ag, <1 ppb As, and concentrations for Cu, Zn, and Pb at 16, 26, and <1 ppb, respectively (Harðardóttir et al., 2009; Hannington et al., 2016). Nonetheless, the Reykjanes fluids result in enrichments in scale precipitates of up to 950 ppm Au and 2.5% Ag (Hardardottir, 2011).

In this contribution, we present compositions of surface and deep-sampled fluids from the Northern Volcanic Zone (NVZ) of Iceland: The newly developed Theistareykir geothermal field hosted in tholeiitic basalts erupted from a Holocene volcanic system (Saemundsson, 2007), and the adjacent Krafla field which is hosted in basalt and rhyolite (Kelley and Barton, 2008). Fluids have been characterized for a full suite of elements, O and H isotopes, and noble gases, allowing us to determine the mobility of elements in the deep reservoir, their fate *en-route* to the surface, the sources of fluids

and metals, and the impact of host rock geology. Direct compositional information on deep fluids is still extremely limited and this new data enables a deeper understanding of fluid-mediated element mobility in magmatic-hydrothermal systems with direct implications for global element cycling. Moreover, we present some of the first concentration data for volatile and semi-volatile elements (Sb, Tl, Bi, Cd and As) in fresh and altered rocks, as well as in deep and surface fluids for this area of Iceland.

2.3 Study area

The Northern Volcanic Zone (NVZ) is a unique geological observatory providing a window into magmatic-hydrothermal systems settled within a sub-aerial mid-ocean ridge and where a minimal interaction with the Icelandic mantle plume exists (Saby et al., 2020). The NVZ has been the main zone of spreading in northern Iceland for the past 6–7 Ma (Pedersen et al., 2009). The NVZ is composed of five NNE striking left-stepping *en échelon* volcanic systems (Saemundsson, 2007), amongst which the Theistareykir shield volcano and the Krafla caldera, both presently exploited for geothermal energy.

The Theistareykir geothermal field is newly developed (Kristinsson et al., 2013) with production started in 2017. A total of 18 deep wells (ranging from 1500 to 3000 m depth) have been drilled to date and the geochemistry of extracted fluids is still under evaluation (Óskarsson et al., 2013; Saby et al., 2020). The Theistareykir reservoir is hosted in olivine-tholeiitic basalts with MgO contents between 7 and 16 wt% to picrites with up to 22 wt% MgO (Stracke et al., 2003, GEOROC database). The helium isotopic composition of fluids suggests a dominant depleted mantle MORB-like source for volatiles, with a small amount (ca. 10%) from the Icelandic mantle plume (Breddam and Kurz, 2001; Harðardóttir et al., 2018; Saby et al., 2020). The recent start of exploitation implies that fluids have been minimally disturbed by exploitation and re-

injection. Fluids sampled at the well-heads are dilute, have chlorine as the dominant anion and show a slightly alkaline pH (7.8-9.1; Óskarsson et al., 2013). Downhole temperatures are among the highest recorded in potential production wells in Iceland at up to 380°C in well ÞG-03 (Figure 2-1; Gautason et al., 2010). The well ÞG--01 studied here is situated in the southern part of the geothermal field.

The adjacent Krafla volcanic system represents the most active part of the Northern Volcanic Zone, last erupting between 1975 and 1984 (Saemundsson, 1974; Einarsson, 2008; Hjartardóttir et al., 2016). The Krafla geothermal system might be fed by a shallow magma chamber of binary rhyolitic – basaltic composition (Kennedy et al., 2018; Lee et al., 2020). The Krafla geothermal field has been exploited since 1978 with reinjection of water starting in 2002 (Juliussón et al., 2015). Surface fluids show near-neutral pH (Arnórsson et al., 2007) and the highest fluid temperature measured in the area is 440°C (well IDDP-1; Figure 2-1; Hermanská et al. 2020). The well K-21 studied here is located at the southern end of the field and is hosted in basalts.

Most Icelandic high-temperature geothermal fields are composed of near-neutral pH and Ca-HCO₃ waters. The Theistareykir and Krafla geothermal fields, however, exhibit some unusual fluid characteristics with water of alkali (Na-K)-chloride type. This type of water composition is quite unusual in Icelandic geothermal systems and reflects water that is more mature (e.g., older; Gunnlaugsson et al., 2014).

2.4 Methods

Fluid samples were collected in August 2019 from wells ÞG-01 (Theistareykir) and K-21 (Krafla) at the well-head and at depths of 850 m for K-21, and for ÞG-01 at 1420 and 1600 m from the surface. Surface fluid samples were collected using a fluid separator while the well was producing, whereas the deep samples were collected when

the well was shut-in to insert the deep sampler. Samples for noble gases were collected and analysed as described in Saby et al. (2020). Deep fluid samples were collected using the in-situ Ti-sampler of Brown and Simmons (2003). Temperature and pressure profiles were collected in the well immediately before sampling and indicate *ca.* 265°C and 55 bar at 1420 m and 290°C and 75 bar at 1600 m in well ÞG-01 and 235°C and 50 bar at 850 m in K-21 (Figure 2-4 du matériel supplémentaire). Between 647 and 860 g of deep fluid was recovered, which was split into several aliquots; unfiltered, 0.45 µm filtered, and acidified with 5 µL of nanopure concentrated HNO₃. Vials were fully filled so as to avoid any air entrapment. The pH was measured in the field with a freshly-calibrated glass electrode on the ÞG-01 deep fluid samples, and was around 2.5 compared to a near neutral pH for the wellhead condensed fluid. Following recovery of the fluid, the sampler was rinsed twice with freshly-prepared *aqua regia* (nanopure grade) to recover any precipitate, and this fluid was also collected. All fluids were stored in pre-cleaned PFA containers. Samples were analysed for O and H isotopes by IRMS at the Light Isotope Laboratory of GEOTOP, for anions by Ion Chromatography at ETS (Montreal, Quebec), and for major and trace elements by HR-ICP-MS at ActLabs (Ancaster, Ontario). Four units of fresh basalt were sampled across the Theistareykir area. Each unit was sampled at 3 different locations for a total of 12 samples. For Krafla, only the most recent lava flow (from the 1984 Krafla Fires) from the Leirhnjúkur area was collected. Samples of altered rock cuttings recovered from well ÞG-01 at 1600 m were provided by ÍSOR. These combined samples are taken here to represent the fresh basalt host rock of the geothermal reservoir and its altered equivalent. However, we acknowledge that basalt taken at the surface is likely to have experienced additional degassing compared to the intrusive rock below the surface. The fresh and altered samples were crushed and milled to below ~1µm. This powder was then pressed into a pellet without additives and analysed by LA-ICP-MS at McGill University following the approach of Garbe-Schönberg and Müller (2014). Full method details are given in the supplementary file.

2.5 Results

The stable isotope composition of surface fluids ($\delta^2\text{H}$, $\delta^{18}\text{O}$) from PG-01 and K-21 are consistent with literature data for these two fields, reflecting contributions from a magmatic source, meteoric water, and at least one source of glacial water (Sveinbjörnsdóttir et al. 2015; Stefánsson et al., 2017), as also confirmed by noble gas isotopic signatures (Saby et al., 2020). Fluids sampled at 1420 m (PG-01) and at 850 m (K-21) show $\delta^2\text{H}$ values (-108.4 ‰ and -90.1 ‰ respectively) that are similar to their respective counterparts sampled at the well-head (Figure 2-2). However, the shift towards the left side of the Global Meteoric Water Line (GMWL) shows that these deep fluids have undergone some boiling (Horita & Wesolowski, 1994), and are likely located close to the boiling horizon. In contrast, the 1600 m PG-01 sample, which is situated on the right side of the GMWL, shows no isotopic evidence for phase separation and this sample reflects the reservoir fluid below the boiling horizon, in agreement with the P-T curve for this well (Figure 2-4a du matériel supplémentaire).

At both sites, the well-head fluids are dilute (TDS ~ 350 mg/L), circumneutral solutions dominated by Na-K-Cl. The deep fluids have a higher TDS (~1650, ~830 and ~700 mg/L for 850 m at K-21, and 1420 and 1600 m at PG-01, respectively), and the Theistareykir deep fluids have an acidic pH between 2 and 2.6. The pH of the K-21 deep fluid was not directly measured, but the charge balance shows a cation deficit that also points towards an acidic fluid. This would be consistent with the acidic character of these waters in some portions of the field (Gíslason and Arnórsson 1976; Hauksson and Gudmundsson 2008; Gunnlaugsson et al., 2014).

Concentrations in the deep fluids at Theistareykir are the same order of magnitude for Ca, Mg, Fe, Sb, Te, Zn, Cu as deep fluids from other geothermal fields including New-Zealand, Iceland (Reykjanes), Japan, USA, and Mexico (Chambefort and Stefánsson,

2020). Aluminium is distinctly higher, whereas As is lower. For Na, K, and Cl, the Theistareykir deep fluid concentrations are between those found in conventional and supercritical reservoir fluids.

Figure 2-3a shows the composition of the surface fluids normalized to their deep counterparts. The behaviour of the elements in the fluids from Theistareykir and Krafla wells is largely consistent, with an overall larger difference between surface and deep fluid element concentrations for Krafla, as a combined result of lower surface and higher deep fluid concentrations. The behaviour of Rb, Cs, Mg, Sr, Ga and Ge differs between Krafla and Theistareykir and mainly reflects lower concentrations for these elements in Krafla surface fluids. This suggests the presence of one or more additional phases in the Krafla scales that sequester these elements. Element concentrations are mostly 1 to 3 orders of magnitude lower in surface fluids than fluids at depth (Figure 2-3a) except for Cl, B, the alkali elements, Sr, Al, Si, Ga and Ge that are essentially the same or somewhat enriched, Re that is strongly enriched in the surface fluid, and the semi-volatile metals As, Te, Hg and Tl that are less depleted than most. Sulphate, Mg, Ba, the base metals, Sb, Pb, Ti and Cr are particularly depleted. The observed behaviour of elements is similar to that observed for surface versus deep fluids (directly sampled and fluid inclusions) from the Reykjanes peninsula in Iceland (Bali et al., 2020).

Figure 2-3b shows the fluid compositions normalised to the fresh Theistareykir and Krafla basalts. The semi-volatile metals are enriched in the fluid compared to the host basalt. The alkali elements, Rb and Cs in particular, are less depleted than the alkali-earth elements. Copper, Zn and Ni are enriched in the fluid relative to Co, Mn and Fe. On the other hand, the refractory elements (e.g. Nb, Zr, Ti, Hf and Al) and the REE are strongly depleted in the fluids compared to the fresh rock, with a small but consistent LREE to HREE decrease.

The altered rock cuttings from the Theistareykir well at 1600 m show an overall enrichment in the elements compared to the fresh Theistareykir basalt, especially for the most refractory elements including Zr, Nb, Hf, Th, U and the REE. These refractory elements have a common enrichment factor of *ca.* 2. We interpret this to reflect residual enrichment of these elements during alteration as a result of their immobile nature, and we therefore normalise the altered rock composition to the content of these elements in the fresh basalt (cf., Grant 1986). The normalized altered over fresh composition is shown in Figure 2-3c, and indicates approximate conservative behaviour for the alkalis, refractory metals and LREE, and depletion in the earth alkalis, base and (semi)-volatile metals, and the HREE. Copper is strongly depleted, whereas Sb is highly enriched. These trends broadly follow alteration-associated element re-distribution in Reykjanes reservoir rocks (Libbey and Williams-Jones, 2016), despite the Reykjanes fluids having much higher Cl-contents.

2.6 Evolution of fluids in the geothermal well

The temperature and pressure profile in the wells (Figure 2-4 du matériel supplémentaire) indicate that the deepest parts are below the boiling horizon, and the resident fluid at depth is a 1-phase solution. As this fluid rises up the well, it reaches the boiling horizon and splits into a vapour and residual liquid phase. Whereas the vapor rises to the surface, the denser residual liquid is thought to descend in the well, mix with the deeper fluid, and/or flow laterally out of the well. Surface fluids are therefore predominantly composed of the vapor fraction. *En route* to the surface, additional fluid or steam can enter the well and mix with the vapour, especially when the well is shut-in to permit the deep fluid sampling. An increase in T indicates an influx of hot fluid or steam, whereas a drop in T shows an inflow of colder water (e.g. groundwater). For well ÞG-01, an inflow of liquid water is noticeable around 1275 m depth in the P-T profile, which is well above the boiling horizon.

The fluids collected at the surface exhibit a near-neutral pH, and given that boiling generally produces a vapor with a lower pH than the 1-phase source fluid (e.g. Reed and Spycher, 1984), this indicates that the deep fluids must also have a near-neutral to slightly alkaline pH. This is consistent with the secondary mineral assemblage (epidote + chlorite + albite + prehnite \pm K-feldspar) observed for Krafla and in the nearby Namafjall geothermal field (Stefánsson and Arnorsson, 2002). However, the fluids sampled at depth – when the wells were shut-in – were acidic (pH 2 to 2.6). We interpret this discrepancy to reflect influx of a low pH fluid into the well, likely a condensate of acidic gases (e.g., SO₂, H₂S, CO₂, and HCl) into groundwater. These acidic gases may have three origins: (1) they could be derived directly from the magmatic intrusions that are associated with the Krafla and Theistareykir geothermal fields but this would result in significant $\delta^2\text{H}$ and $\delta^{18}\text{O}$ shifts of the hydrothermal fluids that are not observed, (2) they could be generated by the condensation of vapor on the way to the surface, but this process would unlikely be able to lower the pH to 2.5 (rather closer to 5 - 6), or (3) represent shallow condensation of the acid vapor formed in secondary boiling and which is emitted in fumaroles in the Theistareykir field close to well PG-01. Given that these geothermal waters have a low capacity of buffering the pH due to their low element concentrations and content of dissolved CO₂, even a small amount of acidic water mixing with deep fluids can result in a significant drop of the pH (Figure 2-5 du matériel supplémentaire).

In this interpretation, the deep fluids do not represent a pristine deep fluid composition. It is unclear to what extent the fluid has been modified by addition of elements from the acidic fluid influx, or by interaction between the acidified fluid and its now-in-disequilibrium host rock mineralogy. The wells were only shut-in for few hours prior to the deep sampling so fluid-rock interaction may not yet have significantly affected the element concentrations. Indeed, carbonates, present in cuttings as a secondary phase, would be expected to dissolve in the acidified fluid, but Ca and Sr concentrations

follow the overall trends of the earth-alkali elements in Figure 2-3b, and mimic the trend for the surface fluids. The acidic surface fumarole fluids sampled in Theistareykir are depleted in most elements compared to surface and deep well fluids with the exception of S, Mg, Ca, Sr, Mn, Fe and Al (Figure 2-3a). Addition of elements from a fumarole-like fluid would thus result in higher concentrations in the deep fluid of these elements, yet this signature is not observed. We therefore conclude that the impact of host-rock re-equilibration and element addition was minimal.

2.7 Metal behavior patterns

The fluid compositions reflect multiple processes at work in the geothermal system, including a primary magmatic input, water-rock interaction with associated element mobilization and sequestration, boiling and its associated element partitioning, scale formation and its associated element sequestration, and dilution by modern and ancient groundwater. The elements and the media analysed here respond variably to these processes, thereby potentially allowing for their impact to be identified and quantified.

The basalt-normalized fluid compositions show higher values for the semi-volatile metals, and particularly low values for the refractory metals and the REE. This can be interpreted as preferential mobilization of the semi-volatile metals during water-rock interaction, addition of the semi-volatile metals from a different source, and/or selective precipitation of the refractory metals and REE. The altered-over-fresh rock composition shows more or less conservative behaviour for the REE (Figure 2-3c), and water-rock interaction therefore does not significantly impact these elements in the fluid. The same can be argued for the majority of the refractory metals and alkalis, but the earth alkalis, base metals and semi-volatile metals are depleted in the altered rock and are therefore released during water-rock interaction. In contrast, Sb is highly enriched in the altered rock and is preferentially sequestered. This is mirrored in the

singular depletion in Sb for surface fluid relative to the deep fluid (Figure 2-3a). The relative depletion for the 3 groups of elements is approximately the same. However, their behaviour in the fluid/basalt plot is distinctly different, with the earth alkalis the lowest, and the (semi)-volatile metals the highest (Figure 2-3b). This requires a source other than water-rock interaction for the base and (semi)-volatile metals. The semi-volatile metals are preferentially enriched in magmatic gases, as are the base metals albeit to lower extent (Williams-Jones and Heinrich, 2005; Mather et al., 2012; van Hinsberg et al., 2017). We therefore interpret this additional source to be magma degassing and for the behaviour of these elements in the Theistareykir and Krafla deep fluids to reflect a strong contribution from the magmatic system. This is supported by noble gases, which indicate a direct transfer of material from the magma to the geothermal fluid, as evident in the $^3\text{He}/^4\text{He}$ ratio (Saby et al. 2020).

The fluids are enriched in LREE over HREE. This is not the result of water-rock interaction, because the LREE act conservatively in the altered rocks whereas the HREE, Y and Sc are leached (Figure 2-3c). Rather, we interpret this to reflect the higher stability constants for LREE over HREE-species in the fluid (Migdisov et al. 2009), and therefore a stronger mobilization of the LREE from the magma.

The differences between surface and deep fluids can be expected to mainly reflect boiling and the associated element partitioning between vapour and residual liquid, with the surface fluid dominantly, or even exclusively, reflecting vapour. The volatile metals are less depleted than, for example, the base metals in the surface fluids, which is consistent with their preferential fractionation into the vapour, and the element pattern in surface vs. deep fluid follows, to some extent, vapour-liquid partition coefficients (Pokrovski et al., 2005 –Figure 2-3a). Concentrations of Cl, B, the alkali metals, Al, Si, Ga and Ge are somewhat enriched in the surface fluids. Several processes can contribute to this enrichment, including (1) the loss of steam from depth

to the surface, thus residually concentrating the surface fluids compared to the deep fluids, and (2) metastable persistence of elements above their solubility, aided by the thermal state of the system - excess enthalpy - and the type of fluid - NaCl-type rather than steam-heated acid-sulphate waters (Kaasalainen and Stefánsson, 2012).

The base metals are among the most depleted in the surface fluids compared to the deep fluids (Figure 2-3a), yet they are released during water-rock interaction. We therefore interpret this to reflect precipitation in scale along the walls of the well or in the host rocks. Well scales of geothermal sites throughout Iceland contain silica, iron-silicate, iron-magnesium-silicate as well as pyrite, pyrrhotite, magnetite and other metal sulphides (Kristmansdóttir, 1989; Kaasalainen and Stefánsson, 2012; Gunnlaugsson et al., 2014). The sulphides, in particular, can be an important host for base metals, as observed in sulphides from Reykjanes well fluid precipitates (Hardardottir, 2011).

2.8 Implications for element mobility in magmatic-hydrothermal systems

Geothermal production fields in magmatic settings provide a unique opportunity to study the behaviour of elements in magmatic-hydrothermal fluids, in particular by providing direct access to deep fluids. The Theistareykir and Krafla fluids provide a consistent story of metal enrichment and depletion patterns. The two fields share common background conditions for the mobilisation of metals in deep geothermal fluids with similar reservoir host rocks and secondary mineralogy, fluid temperatures, and the same local meteoric water and regional groundwater. These conditions are typical for basaltic magmatic settings and we therefore posit that the results obtained here are representative for such systems, showing that element concentrations reflect a magmatic degassing input variably modified by water-rock interaction. There are significant changes between the deep fluid composition and that at the surface, in absolute concentrations, but especially in the element signature as a result of boiling

and scale precipitation. This means that element content and pattern from surface fluids cannot be interpreted as directly reflecting the deep reservoir fluid composition.

2.9 Acknowledgements

Thanks to A. Poirier and J. Gogot for helping with sample preparation and analyses. This research was funded by the NSERC through an Alexander-Graham-Bell-doctorate grant (CGSD3-503679-2017) to MS and Discovery Grant to DLP (RGPIN-2015-05378 and RGPIN-2020-04684), KB (RGPIN-2014-03882) and VvH (RGPIN-2020-04173); by Geotop Collaborative Research Project fund, 2018-001; by ÍSOR and the Landsvirkjun Power company; and by Osisko philanthropy. We also thank ÍSOR, Landsvirkjun, and the University of Iceland for providing access to sampling locations and to their facilities.

2.10 References

- Arnórsson, S., Stefánsson, A., Bjarnason, J.O., 2007. Fluid-fluid interactions in geothermal systems. *Reviews in Mineralogy and Geochemistry* 65:259-312.
- Audétat, A. and Edmonds, M., 2020. Magmatic-hydrothermal fluids. *Elements*, 16: 401-406.
- Bali, E., Aradi, L. E., Zierenberg, R., Diamond, L. W., Pettke, T., Szabo, A., et al., 2020. Geothermal energy and ore-forming potential of 600 °C mid-ocean-ridge hydrothermal fluids. *Geology*, 48(12), 1221–1225).
- Breddam K., Kurz, M.D., 2001. Helium isotope signatures of Icelandic alkaline lavas. *EOS Trans. Am. Geophys. Union* 82, F1315.
- Brown, K.L., Simmons, S.F., 2000. Precious metals in high-temperature geothermal systems in New Zealand. *Geothermics* 32, 619–625.
- Chambefort, I., & Stefansson, A., 2020. Fluids in Geothermal Systems. *Elements*, 16, 407–411

- Einarsson, P., 2008. Plate boundaries, rifts and transforms in Iceland: *J kull*, v. 58, p. 35-58.
- Ellis, A., 1979. Explored geothermal systems. *Geochemistry of hydrothermal ore deposits*: 465-514.
- Gautason, B., Gudmundsson, Á., Hjartarson, H., Blischke, A., Mortensen, A.K., Ingimarsdóttir, A., Gunnarsson, H.S., Sigurgeirsson, M.Á., Árnadóttir, S., Egilson, Th., 2010. Exploration drilling in the Theistareykir high-temperature field, NE-Iceland: Stratigraphy, alteration and its relationship to temperature structure. *Proc. World Geother. Congr. 2010, Bali, Indonesia*, 5 pp.
- Gíslason, G., and Arnórsson, S., 1976. Framvinduskýrsla um breytingar á rennsli og efnainnihaldi í borholum 3 og 4 í Kröflu (A progress report on flow and chemical composition of fluids from boreholes 3 and 4 in Krafla). Orkustofnun, report OS-JHD-7640 (in Icelandic), 14 pp.
- Gunnlaugsson, E., Ármannsson, H., Thorhallsson, S., and Steingrímsson, B., 2014. Problems in geothermal operation – Scaling and corrosion. Presented at “Short Course VI on Utilization of Low- and Medium-Enthalpy Geothermal Resources and Financial Aspects of Utilization”, organized by UNU-GTP and LaGeo, in Santa Tecla, El Salvador, March 23-29, 2014. 18 pp.
- Hannington, M., Harðardóttir, V., Garbe-Schönberg, D. and Brown, K.L., 2016. Gold enrichment in active geothermal systems by accumulating colloidal suspensions. *Nature Geoscience*, 9(4): 299-302.
- Harðardóttir, V., Brown, K.L., Fridriksson, T., Hedenquist, J.W., Hannington, M.D. and Thorhallsson, S., 2009. Metals in deep liquid of the Reykjanes geothermal system, southwest Iceland: Implications for the composition of seafloor black smoker fluids. *Geology*, 37(12): 1103-1106.
- Harðardóttir, V., 2011. Metal-rich Scales in the Reykjanes Geothermal System, SW Iceland: Sulfide Minerals in a Seawater-dominated Hydrothermal Environment. Thesis (Ph.D.)--University of Ottawa (Canada), 2011, 312 pp
- Harðardóttir, S., Halldórsson, S.A., Hilton, D.R., 2018. Spatial distribution of helium isotopes in Icelandic geothermal fluids and volcanic materials with implications for location, upwelling and evolution of the Icelandic mantle plume. *Chem. Geol.* 480, 12-27.
- Hauksson, T., and Gudmundsson, 2008: Krafla. Acid wells. *Landsvirkjun*, report, 17 pp.

- Hedenquist, J.W. and Lowenstern, J.B., 1994. The role of magmas in the formation of hydrothermal ore deposits. *Nature*, 370(6490): 519-527.
- Hedenquist, J.W., Simmons, S.F., Giggenbach, W.F. and Eldridge, C.S., 1993. White Island, New Zealand, volcanic-hydrothermal system represents the geochemical environment of high-sulfidation Cu and Au ore deposition. *Geology*, 21(8): 731-734.
- Henley, R.W. and Ellis, A.J., 1983. Geothermal systems ancient and modern: a geochemical review. *Earth-science reviews*, 19(1): 1-50.
- Hermanská, M., Kleine, B.I., Stefánsson, A., 2020. Geochemical constraints on supercritical fluids in geothermal systems. *Journal of Volcanology and Geothermal Research* 394, doi:10.1016/j.jvolgeores.2020.106824
- Hjartardóttir, Á. R., Einarsson, P., Magnúsdóttir, S., Björnsdóttir, Þ., and Brandsdóttir, B., 2016, Fracture systems of the Northern Volcanic Rift Zone, Iceland: an onshore part of the Mid-Atlantic plate boundary, in Wright, T. J., Ayele, A., Ferguson, D. J., Kidane, T. & Vye-Brown, C., eds., Geological Society, London, Special Publication 420, p. 297-314.
- Horita, J., Wesolowski, D.J., 1994. Liquid-vapor fractionation of oxygen and hydrogen isotopes of water from the freezing to the critical temperature. *Geochim. Cosmochim. Acta* 58, 3425-3437.
- Huttrer, G.W., 2020. Geothermal power generation in the world 2015-2020 Update Report. Proceedings of the World Geothermal Congress 2020. <https://www.geothermal-energy.org/pdf/IGAstandard/WGC/2020/01017.pdf> , 17 pp
- Juliusson, E., Markusson, S., Sigurdardóttir, A., 2015. Phase-specific and phase-partitioning tracer experiment in the Krafla reservoir, Iceland. Proceedings, World Geothermal Congress.
- Kaasalainen, H., & Stefánsson, A. (2012). The chemistry of trace elements in surface geothermal waters and steam, Iceland. *Chemical Geology*, 330-331, 60–85. doi:10.1016/j.chemgeo.2012.08.019
- Kelley, D. F., and Barton, M., 2008, Pressures of crystallization of Icelandic magmas: *Journal of Petrology*, v. 49, p. 465-492.

- Kennedy, B. M., Holohan, E. P., Stix, J., Gravely, D. M., Davidson, J. R. J., and Cole, J. W., 2018, Magma plumbing beneath collapse caldera volcanic systems: *Earth-Science Reviews*, v. 177, p. 404-424.
- Kristinsson, S.G., Fridriksson, Th., Ólafsson, M., Gunnarsdóttir, S.H, Níelsson, S., 2013. The Theistareykir, Krafla and Námafjall high-temperature geothermal areas. Monitoring of surface activity and groundwater. Iceland GeoSurvey, report ÍSOR-2013/037 (in Icelandic), 152 pp.
- Kristmannsdóttir, H., 1989. Types of scaling occurring by geothermal utilization in Iceland. *Geothermics*, 18(1-2), 183–190. doi:10.1016/0375-6505(89)90026-6
- Krupp, R.E., Seward, T.M., 1987. The Rotokawa geothermal system, New Zealand: an active epithermal gold depositing environment. *Economic Geology* 82: 1109-1129
- Lee, B., Unsworth, M., Árnason, K., and Cordell, D., 2020. Imaging the magmatic system beneath the Krafla geothermal field, Iceland: A new 3-D electrical resistivity model from inversion of magnetotelluric data: *Geophysical Journal International*, v. 220, p. 541-567.
- Libbey, R. and Williams-Jones, A., 2016. Lithochemical approaches in geothermal system characterization: An application to the Reykjanes geothermal field, Iceland. *Geothermics*, 64: 61-80.
- Mather, T. A., Witt, M. L. I., Pyle, D. M., Quayle, B. M., Aiuppa, A., Bagnato, E., et al. (2012). Halogens and trace metal emissions from the ongoing 2008 summit eruption of Kīlauea volcano, Hawaii. *Geochimica Et Cosmochimica Acta*, 83(C), 292–323. <http://doi.org/10.1016/j.gca.2011.11.029>
- Migdisov, A.A., Williams-Jones, A.E., & Wagner, T., 2009. An experimental study of the solubility and speciation of the Rare Earth Elements (III) in fluoride- and chloride-bearing aqueous solutions at temperatures up to 300 degrees C. *Geochimica Et Cosmochimica Acta*, 73(23), 7087–7109. <http://doi.org/10.1016/j.gca.2009.08.023>
- Óskarsson, F., Ármannsson, H., Ólafsson, M., Sveinbjörnsdóttir, Á.E., Markússon, S.H., 2013. The Theistareykir geothermal field, NE Iceland: fluid chemistry and production properties. *Proc. Earth Planet. Sci.* 7, 644–647.
- Pedersen, R., Sigmundsson, F., Masterlark, T., 2009. Rheologic controls on inter-rifting deformation of the Northern Volcanic Zone, Iceland. *Earth Planet. Sci. Lett.* 281, 14–26.

- Pokrovski, G. S., Roux, J., Harrichoury, J.-C. 2005. Fluid density control on vapor-liquid partitioning of metals in hydrothermal systems. *Geology*, 33,657–660
- Rae, A.J., Cooke, D.R., Brown, K.L., 2011. The trace metal chemistry of deep geothermal water, Palinpinon Geothermal Field, Negros Island Philippines: implications for precious metal deposition in epithermal gold deposits. *Economic Geology* 106:1425-1446
- Reed, M.H. and Spycher, N.F., 1984. Calculation of pH and mineral equilibria in hydrothermal waters with application to geothermometry and studies of boiling and dilution. *Geochim. Cosmochim. Acta* 48, 1479–1492.
- Saby, M. Pinti, D.L. van Hinsberg V., Gautason B., Sigurðardóttir Á., Castro M.C., Hall C., Óskarsson, F., Rocher O., Hélie, J-F., Mejean P., 2020. Sources and transport of fluid and heat at the newly-developed Theistareykir Geothermal Field, Iceland. *Journal of Volcanology and Geothermal Research*. 405. 107062. 10.1016/j.jvolgeores.2020.107062.
- Saemundsson, K., 1974, Evolution of the axial rifting zone in northern Iceland and the Tjarnes Fracture Zone: *Geological Society of America Bulletin*, v. 85, p. 495-504.
- Saemundsson, K., 2007. The geology of Theistareykir. Iceland GeoSurvey, short report ÍSOR-07270 (in Icelandic): 23.
- Seward, T.M., 1989. The hydrothermal chemistry of gold and its implications for ore formation: Boiling and conductive cooling as examples. *Econ. Geol. Monogr.*, 6: 398-404.
- Simmons, S.F. and Brown, K.L., 2006. Gold in magmatic hydrothermal solutions and the rapid formation of a giant ore deposit. *Science*, 314(5797): 288-91.
- Simmons, SF, Brown, KL, Tutolo, B.M., 2016. Hydrothermal transport of Ag, Au, Cu, Pb, Te, Zn, and other metals and metalloids in New Zealand geothermal systems: spatial patterns, fluid-mineral equilibria, and implications for epithermal mineralization. *Economic Geology* 111: 589-618
- Stefánsson, A., Arnórsson, S., 2002. Gas pressures and redox reactions in geothermal fluids in Iceland. *Chem. Geol.* 190, 251–271.
- Stefánsson, A., Arnórsson, S., Sveinbjörnsdóttir, Á.E., 2005. Redox reactions and potentials in natural waters at disequilibrium. *Chem. Geol.* 221, 289–311.

- Stefánsson, A., Hilton, D., Sveinbjörnsdóttir, Á.E., Torsander, P., Heinemeier, J., Barnes, J.D., Ono, S., Halldórsson, S.A., Fiebig, J., Arnórsson, S., 2017. Isotope systematics of Icelandic thermal fluids. *J. Volcanol. Geotherm. Res.* 337, 146-164.
- Sveinbjörnsdóttir, Á.E., Ármannsson, H., Óskarsson, F., Ólafsson, M., Sigurdardóttir, Á.K., 2015. A conceptual hydrological model of the thermal areas within the Northern neovolcanic zone, Iceland using stable water isotopes. *Proc. World Geother. Congr. 2015*, pp. 1–7.
- van Hinsberg, V., Vigouroux, N., Palmer, S., Berlo, K., Mauri, G., Williams-Jones, A., et al., 2017. Element flux to the environment of the passively degassing crater lake-hosting Kawah Ijen volcano, Indonesia, and implications for estimates of the global volcanic flux. *Geological Society London Special Publications*, 1–26. <http://doi.org/10.6084/m9.figshare.c.2134359>
- Yang, K. and Scott, S.D., 2006. Magmatic fluids as a source of metals in seafloor hydrothermal systems. *Back-arc spreading systems: geological, biological, chemical, and physical interactions*: 163-184.
- Williams-Jones, A., & Heinrich, C., 2005. 100th Anniversary special paper: Vapor transport of metals and the formation of magmatic-hydrothermal ore deposits. *Economic Geology*, 100(7), 1287–1312.

2.11 Figures

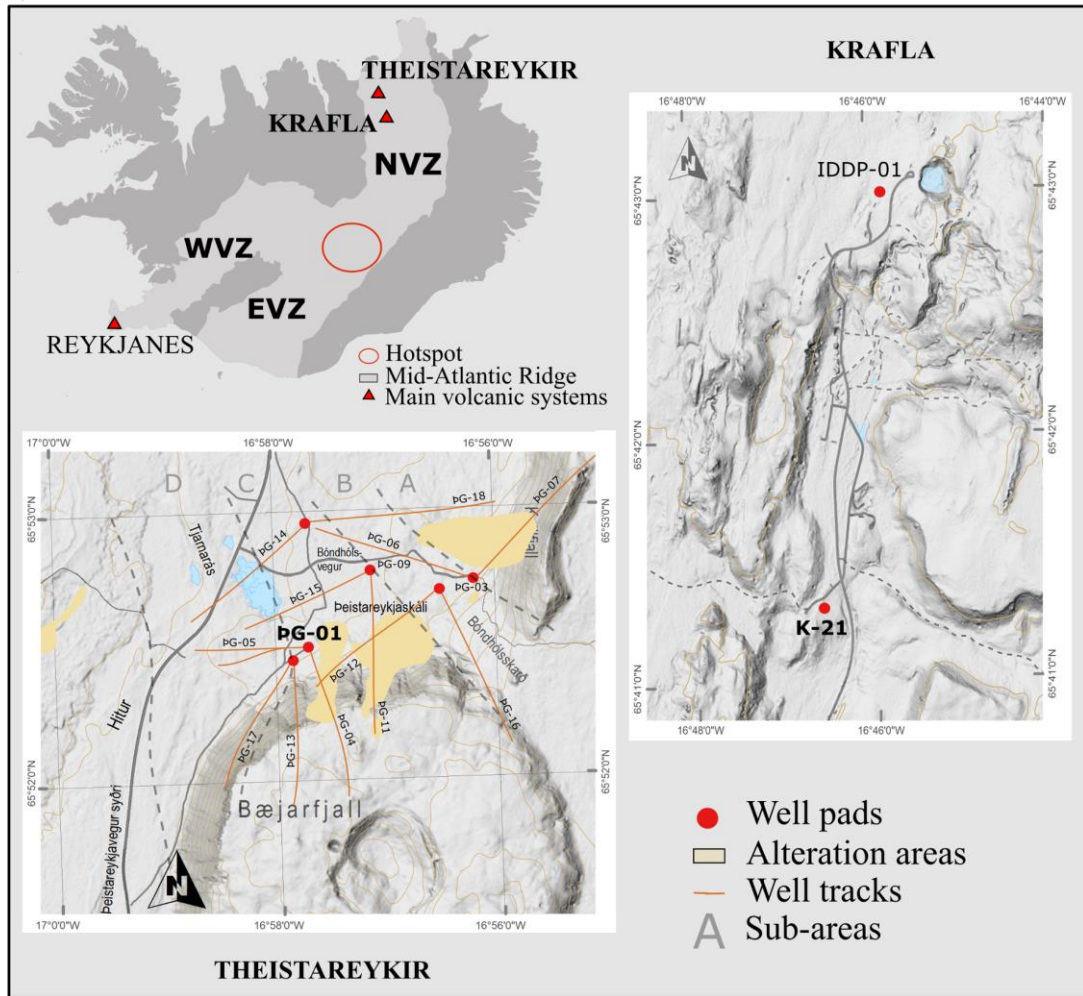


Figure 2-1 : Simplified maps of the Theistareykir and Krafla geothermal fields with positions of the wells sampled for the deep fluids (PG-01 and K-21). Numbers on the X- and Y-axes indicate the latitudinal and longitudinal geographical coordinates respectively on the World Geodetic System 1984 (WGS84). NVZ = Northern Volcanic Zone; WVZ = Western Volcanic Zone; EVZ = Eastern Volcanic Zone

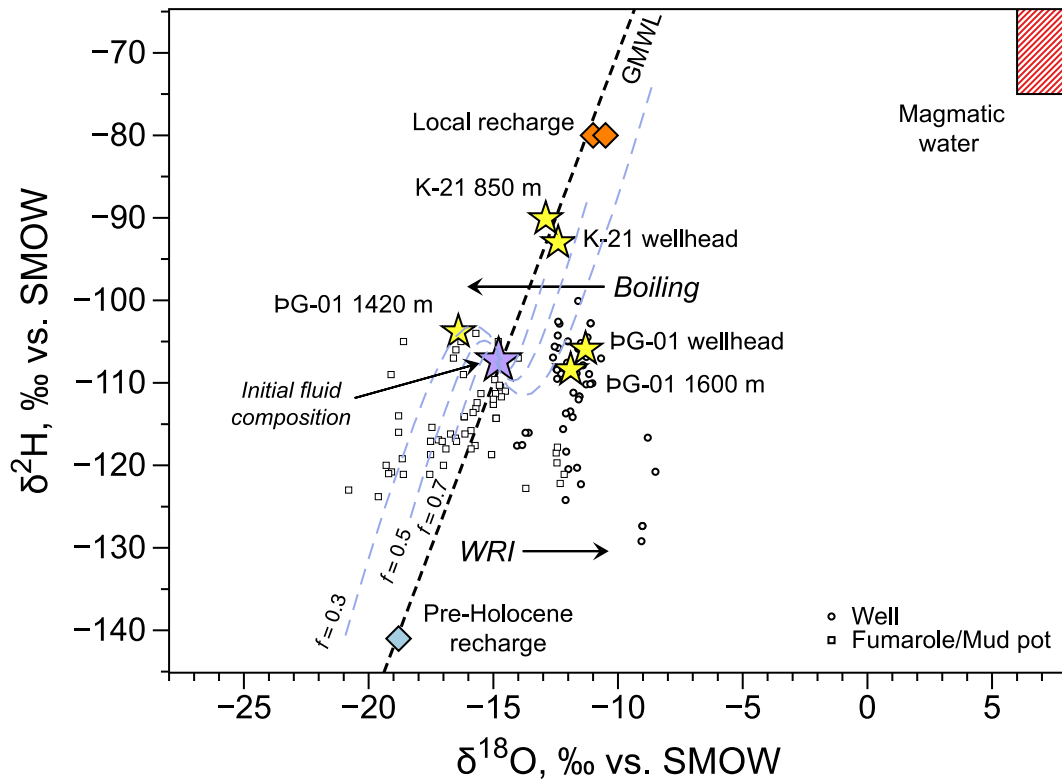


Figure 2-2 : Plot of $\delta^2\text{H}$ vs. $\delta^{18}\text{O}$ corrected for total discharge (TD) of the Theistareykir production fluids, mud pots, and fumaroles sampled over a 20-year period (data from this study and archived ÍSOR data, in addition to the values of the deep samples at Theistareykir and Krafla; Saby et al., 2020; Table 1 In Electronic Supplementary Material). The global meteoric water line (GMWL; dashed line) was calculated following Craig (1961). Pre-Holocene recharge composition is from data of Sveinbjörnsdóttir et al. (2013), and the regional highlands recharge is from Stéfansson et al. (2017). Primary magmatic water composition is from Sheppard and Epstein (1970). The dashed curves represent the evolution of $\delta^2\text{HTD}$ vs. $\delta^{18}\text{OTD}$ in the vapor and residual liquid after phase segregation, starting from an initial composition (purple star), and causing isotopic fractionation for Theistareykir. Water isotopic compositions

thus evolve along these lines according to their final equilibrium temperature. The f values correspond to the fraction of residual liquid.

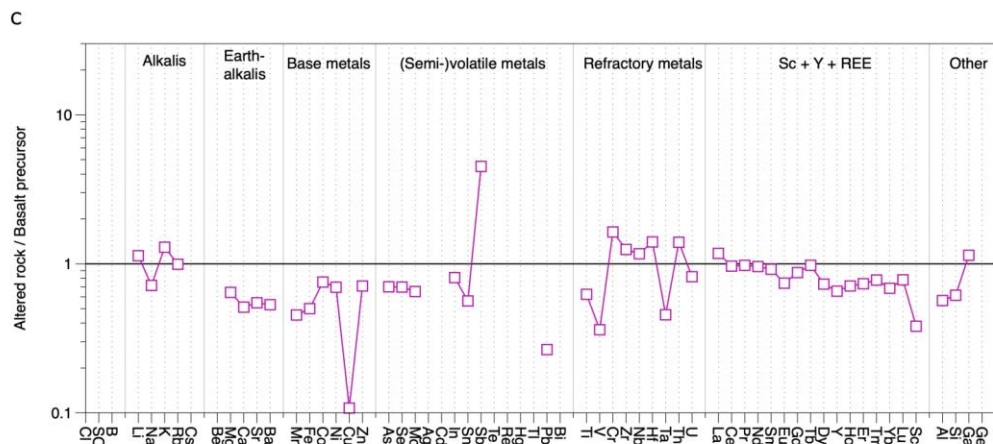
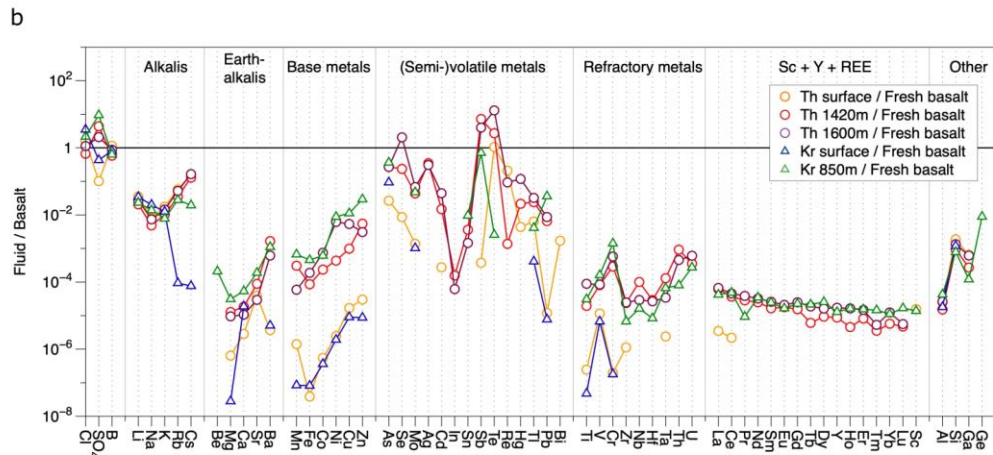
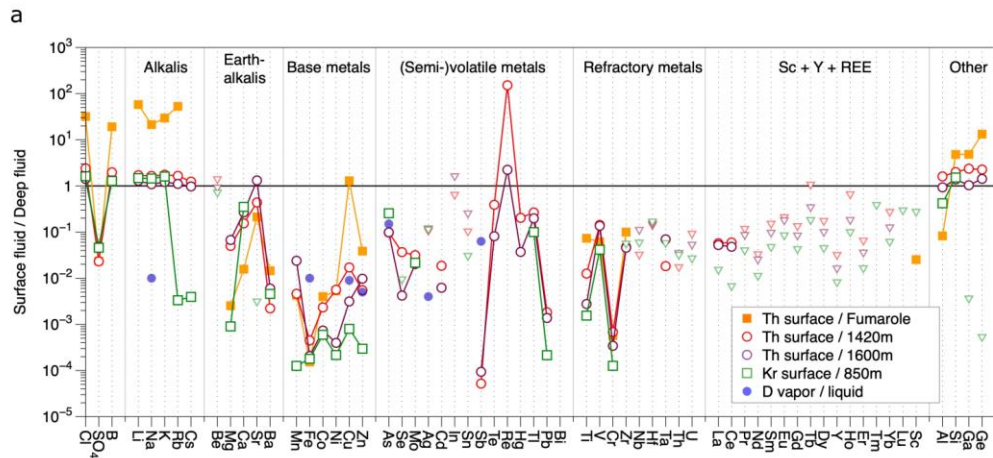


Figure 2-3 : Diagram of the chemical composition of the fluids sampled at the surface (as condensed vapor) normalized to the deep fluids at depths of 1420 and 1600 m for Theistareykir and 850 m for Krafla. The composition of Theistareykir acidic fumarole fluids is also shown, as are vapor/fluid partition coefficients from Pokrovski et al (2005). The maximum value is shown as a triangle for elements where the concentrations in the surface fluid were below the detection limit, calculated from the respective detection limit. b. Composition of the fluids normalized to their respective fresh local basalt. c. Composition of the altered rock cuttings at a depth of 1600 m, normalized to the fresh local basalt for Theistareykir. The elements have been grouped first by their geochemical behaviour and then their mass.

2.12 Supplementary material

2.12.1 Sampling of Deep and Surface Fluids, and Fresh and Altered Rocks

Two vertical wells were sampled for this study: one in the Theistareykir Geothermal Field, with a bottom depth of 1953 m (PG-01), and the second in the Krafla Geothermal Field, with a bottom depth of 1200 m (K-21). Both wells are active production wells and were shut-in several hours prior to sampling to allow for the deep sampler to be inserted into the well. The wells were logged with a Kuster K-10 tool immediately prior to sampling to determine P and T profiles (Fig. S1a,b). Deep fluid samples were collected using a pacified Ti-metal sampler developed by Kevin Brown and described in detail in Brown and Simmons, 2003. The evacuated sampler was lowered into the well with a steel cable the length of which was monitored to determine the depth of the sampler. The sample was collected by physically puncturing a rupture disc at the desired depth with the pressure-differential forcing the fluid into the sampler. This same fluid pressure subsequently pushed a spring-loaded valve closed during ascent to keep the sample chamber sealed. At the surface, the sampler was quenched in water and then opened to recover the fluid.

A total of three samples were collected: two from PG-01 (1420 m and 1600 m below the surface) and one from K-21 (850 m). The 1420 m sample from PG-01 and the 850 m sample from K-21 have been collected close to the boiling horizon while the 1600 m from PG-01 was collected below the boiling horizon as indicated by the down-hole pressure and temperature measurements (e.g., Fig. S-1a,b). 860.2 g of liquid was recovered for K-21, 647.37 g for well PG-01 at 1420 m, and at 1600 m, 841.84 g of fluid was recovered. After collecting the fluid, the sample was divided into three sub-samples: (1) an unacidified aliquot for the analysis of anions and water isotopes, (2) a sample acidified with ultra-pure HNO₃, and (3) a sample filtered through a 0.45 µm disposable filter and acidified with ultra-pure HNO₃. Sample vials were fully filled to

avoid entrapping any air. Then, the titanium sampler was rinsed twice with a freshly-prepared, concentrated solution of trace-metal grade aqua regia (~ 40 ml) to dissolve any precipitates followed by ~ 40 ml of distilled water, and these rinse solutions were collected. All solutions were stored separately in PFA or PFA-lined HDPE bottles. The original element content was then reconstituted from all the subsamples after being analysed separately (see below).

A method blank has been determined in the study of geothermal wells in New Zealand in which this exact sampler was filled with deionized and lowered close to 1 km depth (255 °C) for 10 min. The blank solution was recovered and the sampler washed with the aqua regia and deionized water, with these rinse solutions added to the blank. These method blanks consistently returned concentrations at least 10 times lower than the lowest measured concentration in our samples (cf. Brown and Simmons, 2003).

Surface fluids were sampled at the well head of ThG-01 and K-21 while the well was producing. Fluids were collected in HDPE 30 mL bottles, unfiltered for the analysis of anions and 0.45 µm filtered, and acidified with 5 µL of nanopure concentrated HNO₃ for the analysis of cations. Bottles were fully filled to avoid air entrapment.

Four units of outcropping basalt were sampled across the Theistareykir area to represent the fresh basalts in the subsurface of well ÞG-01. Each unit was sampled at 3 different locations for a total of 12 samples. Only one lava sample has been taken for Krafla, on the most recent lava flow, from the Leirhnjúkur area. ÍSOR provided a sample of rock cuttings from 1600 m of Theistareykir well ÞG-01 consisting of fragments of variably altered rock. The cuttings were washed in deionized water and air dried, and then split into 8 sub-samples to create a mixing array with variable alteration. The fresh Theistareykir lava at the end of this mixing array is used here as the precursor basalt and as the normalizing basalt for Theistareykir in Figure 3.

2.12.2 Sample Preparation and Analysis

2.12.2.1 Surface Fluids

Chemical analyses of anions and cations were carried out at the Krafla Power Station's laboratory using ICP-SFMS and ICP-AES, and were conducted by Helgi A. Alfreðsson and Júlía Björke of Geochemý. The heavy metals in the fluids were analyzed by ALS Global in Sweden. Full details can be found in Hauksson, 2020.

The volatile metals (Hg, Bi, Cd, Sb and Tl) were analyzed at McGill University by ICP-MS using an optimized method with long dwell times to obtain low detection limits. The McGill ICP-MS analyses were conducted using a Thermo-Finnigan iCAP-Qc ICP-QMS. All samples and standards were analysed in triplicate. The precision for these analyses is better than 7.7 % as determined from the triplicate analyses.

2.12.2.2 Deep Fluids

The deep fluid composition was reconstituted from the direct fluid samples and the compositions of the sampler rinse solutions. Moreover, precipitates were observed in the direct deep fluid sample vials after a few days, likely resulting from cooling, degassing and associated REDOX changes. The elements in these precipitates were also determined and added to the dissolved element content of the fluids. The following analytical protocol was applied:

STEP 1

10 mL of the supernatant fluid of the deep fluid samples was extracted after allowing the precipitates to settle for several weeks and ensuring that all precipitates were at the bottom of the vials and nothing was in suspension.

The remaining supernatant fluid was transferred to another Teflon vial for storage. As much fluid as possible was extracted, but none of the precipitate. The vials were subsequently dried in a desiccator overnight and weighed before and after to determine the amount of remaining fluid. It is assumed that only water is lost in this drying.

12 mL of an aqua regia – HF mixture was added to the precipitate to bring it into solution, and the closed vial heated to 80°C for two and a half days and weighed before and after to make sure no fluid was lost. This acid was prepared from nano-pure HF, aqua regia and water, in the proportion 1:1:1. No visible solids remained at the end. The resulting solution was transferred to a Teflon vial and the original vial cleaned and weighed to determine the total amount of sample it had originally contained.

STEP 2

A small amount of nano-pure HF was added to the aqua regia rinse solution to obtain the same HF concentration as in the precipitate-dissolution solution above. The fluid was heated at 40°C overnight on a hot plate to dissolve any silicate precipitates, and weighed before and after to make sure no fluid was lost. No visible solids remained after the heating.

STEP 3

The various solutions were analysed by ActLabs as follows;

The undiluted supernatant fluid sample was analysed by method HydroChem using ICP-MS, ICP-OES and HR-ICP-MS.

The aqua regia precipitate digest solution and aqua regia sampler rins were analysed by method ultratrace 2 using ICP-OES and ICP-MS analysis, including a blank of the digest solution.

STEP 4

The masses of the various fluid components were used to reconstitute the fluid from the partial analyses and determine its original total composition. The blank digestion solution only had measurable concentrations of Si, Al, Ti, V, Co, Zr, Nb, Sb, Cs, Ce, Ta and Th, and in all cases concentrations of these elements in the blank were low compared to the concentrations in the digested precipitates. Blank subtraction was applied to remove this blank contribution. The precipitates contain base metals (Fe, Co, Ni, V, Cr) and refractory elements (Ti, Al, REE), but no significant concentrations of soluble elements including the alkalis, as would be expected. For most elements, the final concentration predominantly reflects the supernatant fluid.

Precision and accuracy were determined by ActLabs on in-house and international reference samples analysed with our samples. These indicate precisions below 7.5% for all the elements except for B (39.2%). The accuracy is better than 12% for all the elements except for Li (388%), Zn (19.5%) and Se (34.2%).

2.12.2.3 Pellet analyses of altered and fresh rocks

A set of 20 samples (12 for the fresh rocks and 8 for the altered rocks) was analysed using a pellet laser-ablation ICP-MS method after Garbe-Schönberg and Müller (2014). Fresh rock samples were hand crushed wrapped in brown Kraft paper with a steel hammer and an aliquot was dry milled in a WC ring mill. The milled powders and selected reference materials were then wet milled in a Micro Mill Pulverisette 7 WC ball mill to a nanoparticulate powder. Mixtures of 2 g powder and 5 mL nanowater

were milled in a WC vessel for intervals of 3 minutes, with 1-minute pauses over a period of 40 minutes, at 500 Hz. Between samples, the milling vessels were cleaned using high purity ethanol and fresh quartz powder was milled between each sample. Altered samples were hand crushed in an agate mortar to below $\sim 1\mu\text{m}$. All the powdered samples were then dried in an oven at 60°C and re-homogenised with high purity ethanol in an agate mortar. A 2 to 5 g aliquot of this fine-milled powder was pressed into a 10 mm diameter, 3 to 5 mm tall pellet in a polished steel piston-cylinder at a pressure of 20 MPa without an additive and was subsequently stored in a desiccator. The resulting pellets are hard, robust, and encased in aluminium cups, with a smooth upper surface.

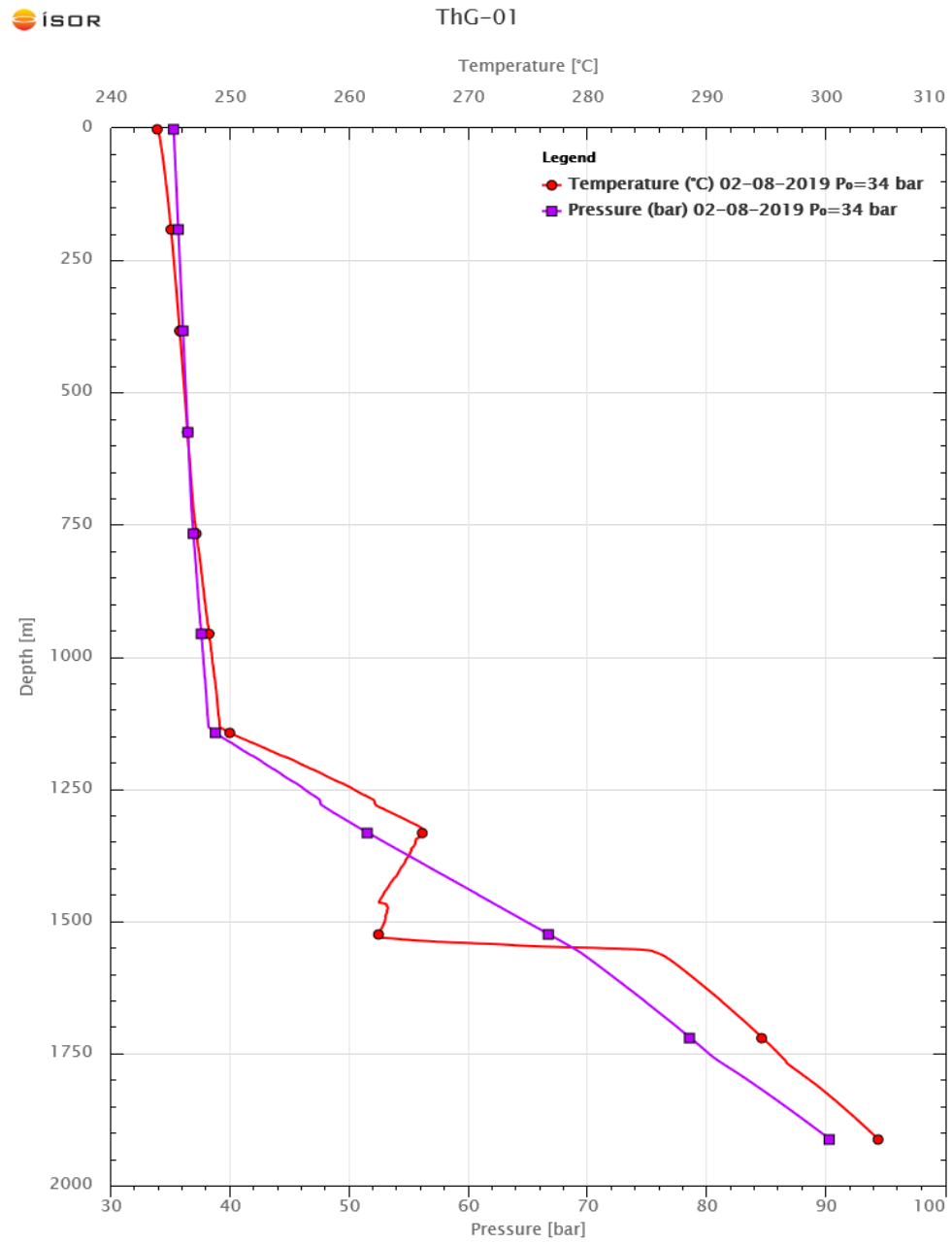
Pellets were analysed by laser ablation ICP-QMS on a NewWave 213 nm Nd:YAG laser-ablation system coupled to a Thermo Finnigan iCapQc ICP-QMS. The ablated material was transferred to the ICP-MS in a 800 mL/min He flow, mixed with Argon prior to injection of material into the plasma. Concentrations for 60 elements were determined. The surface of each analysis spot was pre-ablated before analysis, to obtain a clean surface. Five spot replicates were analysed per sample at 160 μm spot size, 20 Hz laser repetition rate, 120 s dwell time, a 40 s washout, and a laser fluence of 4.2 J/cm². Analyses of NIST SRM 610 glass bracketed the analyses and were used to correct for drift, using Mg as the internal reference element. The data were processed using Iolite (v.2.5, Paton et al., 2011) with integration windows set using the Mg-divided signals. A background window was defined before and after each analysis with linear interpolation between these used to subtract the background for each integration window. Analyses in the same session of pelletized reference materials were used to construct a multi-standard calibration curve, following Peters and Pettke (2017). For the fresh basalt, three reference materials of varying bulk rock composition were included in this calibration, bracketing the compositions of the samples: PCC1, Jb_1a and Ja_1. For the altered basalt samples, 15 reference materials of varying bulk rock

composition were included in this calibration, bracketing the compositions of the samples: PCC1, Jb_1a, Ja_1, BCR-2, BHVO-2, SY-3, SY-4, TILL-1, JR-1, JR-2, SARM2, SARM3, SARM44, NGRI-UMR, and OOKO201. Certified values for these reference materials were taken from the GEOREM database, using the GEOREM preferred values where available (Jochum et al., 2005 and <http://georem.mpch-mainz.gwdg.de/> accessed August 2019). For the fresh rocks, the precision on the analyses as determined from duplicates is better than 22% for elements less than 10 ppm, 8% for elements between 10-100 ppm, and 12% for elements that are 100 ppm+. For the altered rocks, the precision on the analyses as determined from duplicates is better than 10% for all elements except Mo (11%). For the fresh rocks, the accuracy, as determined by the residuals of the calibration on the reference material, is better than 21% on all elements. For the altered rocks, the accuracy is better than 15% on all elements, except B at 30% and Se at 36%.

Major element compositions were determined by powder EDS-XRF on an Olympus X-5000 instrument. Approximately 5 g of milled material was placed in a plastic cup with a 6 μm Mylar window and counted in air at 35 and 10 kV incoming X-Ray beam for 180 s each. Fourteen reference materials were included to construct a multi-standard calibration curve, and precision was determined from duplicate analyses on samples and reference materials. Certified values for the reference materials were taken from the GEOREM database (<http://georem.mpch-mainz.gwdg.de/> accessed Oct 2020). The precision of the analyses is better than 2.5% relative.

Concentrations for Pb, Cl and S in the fresh Theistareykir and Krafla basalts are from the GEOROC database (<http://georoc.mpch-mainz.gwdg.de/> - extracted Jan 2022). Rhenium is from Schilling and Kingsley (2017) and Se + Te are from Forest et al. (2017) both for sub-aerial Reykjanes basalts. For B, a value of 1 mg/kg was assumed based on the typical MORB range of 0.5 to 1.5 mg/kg.

2.12.3 Supplementary Figures



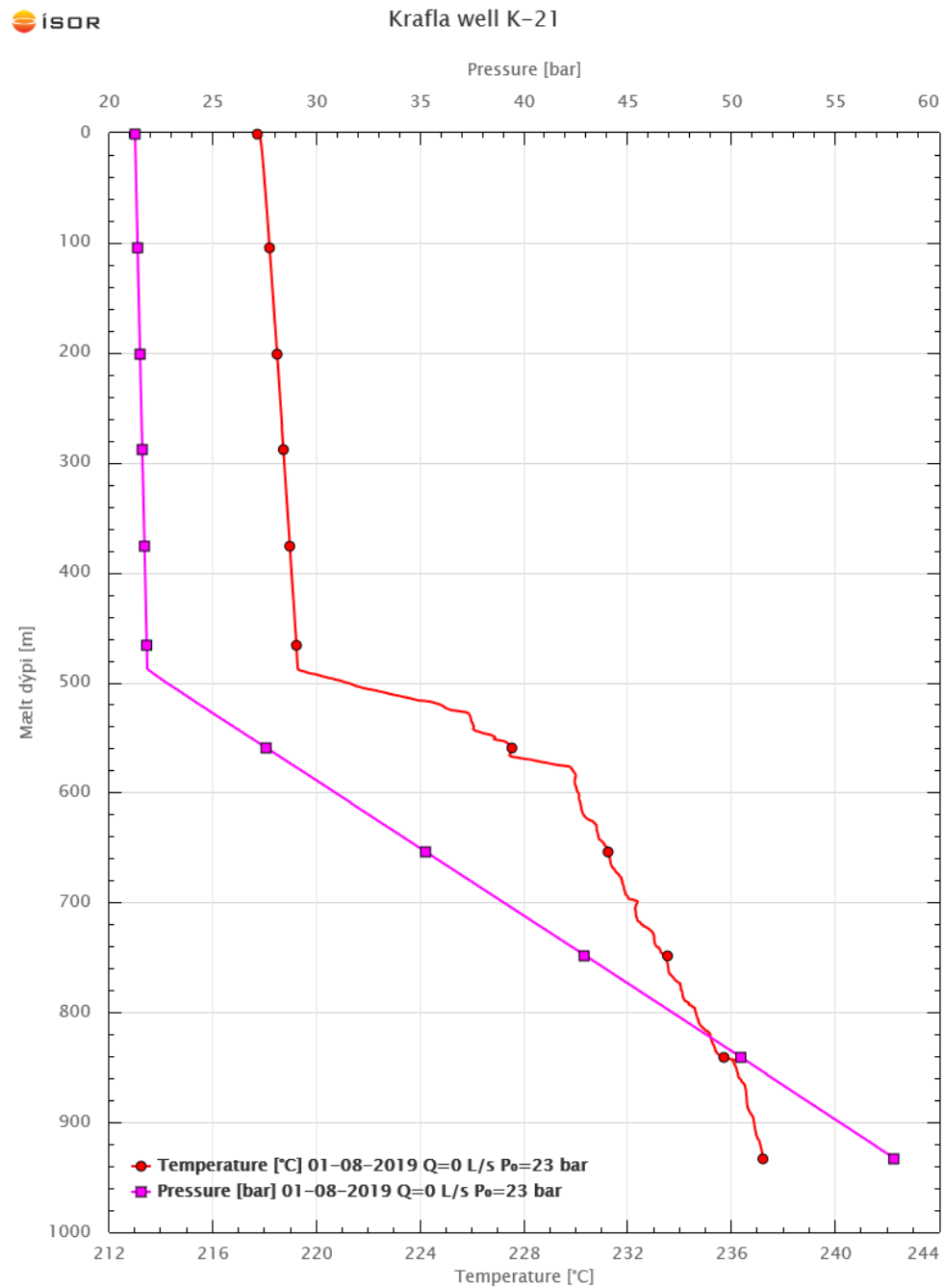


Figure 2-4 : Profile of pressure and temperature in wells ÞG-01 (a) and K-21(b) just before the sampling of deep fluids.

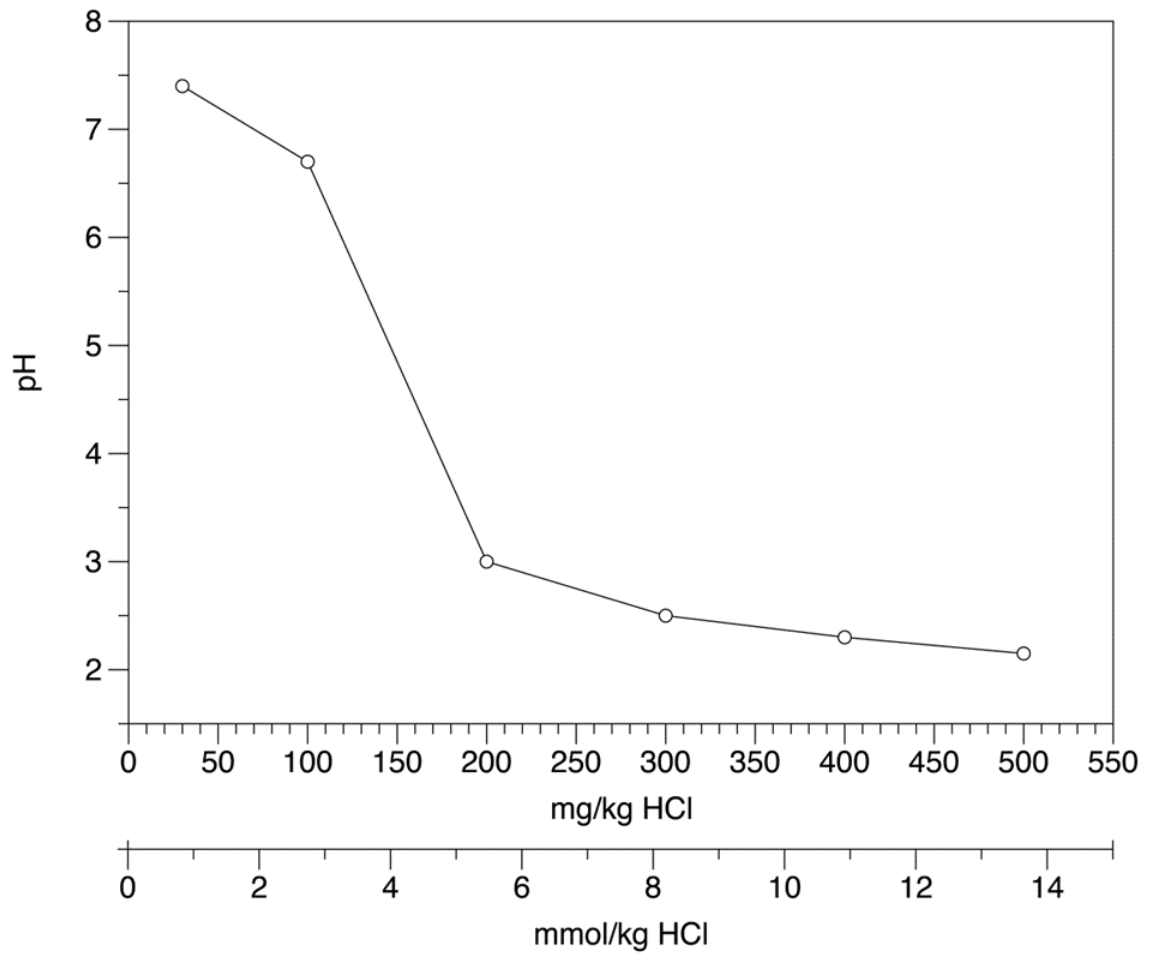


Figure 2-5: Evolution of pH depending on the HCl concentration of the fluids

2.12.4 Supplementary Information References

- Brown, K.L., Simmons, S.F. (2003) Precious metals in high-temperature geothermal systems in New Zealand. *Geothermics* 32, 619–625.
- Forest, A., Kelley, K. A., & Schilling, J. G. (2017). Selenium, tellurium and sulfur variations in basalts along the Reykjanes Ridge and extension over Iceland, from 50°N to 65°N (pp. 1–49). Interdisciplinary Earth Data Alliance.
- Hauksson, T., and Gudmundsson, 2008: Krafla. Acid wells. Landsvirkjun, report, 17 pp.
- Jochum, K. P., Nohl, U., Herwig, K., Lammel, E., Stoll, B., & Hofmann, A. W. (2005). GeoReM: A new geochemical database for reference materials and isotopic standards. *Geostandards and Geoanalytical Research*, 29(3), 333–338.
- Paton, C., Hellstrom, J., Paul, B., Woodhead, J., & Hergt, J. (2011). Iolite: Freeware for the visualisation and processing of mass spectrometric data. *Journal of Analytical Atomic Spectrometry*, 26(12), 2508–2518. <http://doi.org/10.1039/c1ja10172b>
- Schilling and Kingsley (2017) Platinum-group elements (PGE), Re, Ni, Cu, Ag and Cd variations along the Reykjanes Ridge and Iceland South-West Neovolcanic Rift Zone, from 50°N to 65°N: Implications on sulfide bearing PGE mantle source heterogeneities and partial melting effects. <https://www.researchgate.net/publication/319354915>

CHAPTER III

ESTIMATING RELATIVE CONTRIBUTIONS OF MAGMA DEGASSING AND WATER-ROCK INTERACTION TO THE METAL LOAD AT THE THEISTAREYKIR (ICELAND) HYDROTHERMAL SYSTEM USING NOBLE GASES AND TRACE METALS

Marion Saby^{1,*}, Vincent van Hinsberg², Daniele L. Pinti¹, Bjarni Gautason³, Ásgerdur Sigurdardóttir⁴, Kim Berlo², M. Clara Castro⁵

1-GEOTOP & Département des sciences de la Terre et de l'atmosphère, Université du Québec à Montréal, 201 Av. du Président Kennedy, Montréal, Canada.

2-GEOTOP & Department of Earth and Planetary Sciences, McGill University, 34, University Street, Montréal, Canada.

3-ÍSOR Iceland GeoSurvey, Orkugardur, Grensásvegur 9, Reykjavik, Iceland.

4-Landsvirkjun, Háaleitisbraut 68, Reykjavik, Iceland.

5-Department of Earth and environmental sciences, University of Michigan, Ann Arbor, USA.

*Corresponding author: saby.marion.e@gmail.com

Keywords: Volatile Metals, Noble Gases, Magma Degassing, Water-rock interaction, Iceland

3.1 Abstract

Magmatic-hydrothermal systems are of great interest as probes of the Earth's dynamic interior. They are sites of mobilization and re-distribution of elements in the crust and represent a preferential pathway for transfer of elements from the deep Earth to the surface. The behavior of metals in these systems led to active magmatic-hydrothermal systems being recognized as analogues for fossil magmatic-hydrothermal ore deposits. Although our understanding of these systems has improved dramatically, there is still uncertainty regarding the sources of fluids and metals, specifically the relative contribution of magma degassing and water-rock interactions. Here, we combine analyses of noble gases and volatile metals in fluids and rocks from the Theistareykir geothermal field in northern Iceland to provide constraints on the relative contribution of these two sources. Helium isotope data obtained from well-head fluids suggest 80-85% of helium originating from magma degassing. Similarly, using the elemental signature of magmatic degassing and water-rock interaction, we show that the deep geothermal reservoir fluid is dominated by magmatic input at ca. 80%, with host-rock leaching contributing the remaining 20%. By comparing the estimated element release from magma degassing to the composition of deep fluids, it is clear that the dominant source of elements is fluid released from the magma, except for Mn, Fe, Co, Cu, Ti and V. The $^3\text{He}/^4\text{He}$, corrected for atmospheric contamination (R_c/R_a) correlates with volatile metal abundances and indicates that Bi and Hg are predominantly derived from magma degassing. The variations in R_c/R_a and volatile metal contents among the wells allow for the magmatic contributions to be mapped out across the geothermal field and show that the wells with the highest magmatic contribution are the ones closest to the local topographic highs, suggesting the impact of local and regional structures on the fluid's pathway from depth to surface.

3.2 Introduction

Crustal convective hydrothermal systems are predominantly initiated by magma bodies intruded at shallow crustal depths, often of 5-10 km. In these systems, hydrothermal (or, synonymously, “geothermal”) aqueous fluids are a complex mixture of meteoric water, groundwater, sometimes sea water and water exsolved from the melt (e.g., Giggenbach, 1992) either found under conventional P,T or supercritical conditions (e.g., Chambefort and Stefansson, 2020). A volatile phase can coexist with this aqueous phase, mainly formed by magmatic gases released by the melt (CO₂, H₂S, N₂, noble gases etc.), with a minor contribution from radiogenic gases produced within the reservoir (e.g., ⁴He, ⁴⁰Ar*; Pinti et al., 2019) and atmospheric gases introduced by meteoric recharge.

Metals contained in these geothermal fluids can be brought into the system by magmas and/or by the interaction and element exchange with reservoir rocks (Weiss et al., 1977; Hedenquist and Lowenstern, 1994). In some cases, these fluids are emitted to the surface in fumaroles, hot springs, or, in more extreme examples, as crater lakes and acid rivers (Christenson and Wood, 1993; Varekamp et al., 2001). The mobilization and redistribution of metals which take place in these systems can lead to ore formation, particularly porphyry Cu-Mo-W deposits and epithermal Ag-Au ores (Tosdal et al., 2009; Sillitoe, 2010; Hedenquist and Henley, 1985; Hedenquist et al., 1993, 1998).

Numerous studies in the last 50 years focused on the origins of hydrothermal fluids and metals within these systems (see section 2 of this manuscript for a general review), yet the relative contribution of magma degassing and rock leaching to the metal content of magmatic-hydrothermal systems remains unclear. It is commonly assumed that most of the water circulating in high-temperature geothermal fields is of meteoric origin, but the same may not be true for their volatile and metal contents (e.g., Yardley and Bodnar, 2014 for a general review). There is consensus that the thermal energy driving the hydrothermal system is supplied by the magma, and it would

therefore seem reasonable to assume the magma to also contribute to some extent to the metal content of the hydrothermal fluids, especially for the most volatile elements. However, it is unclear if the composition of hydrothermal fluids is dominated by the input of magmatic fluids or if the re-mobilization of metals from the host rock during water-rock interactions (WRI) is the dominant process. Both processes are implicated in the formation of ore deposits, especially porphyry and epithermal deposits (Bodnar, 1995; Sillitoe, 2010). Water-rock interaction can be favored by the fact that large volumes of meteoric water are available in the system (10 to 100 times the volume of magmatic fluids; Norton, 1984) and reservoir residence times for those fluids can exceed thousands (e.g., Birkle et al., 2016; Saby et al., 2020) to million-year timescales (Pinti et al., 2019).

Noble gases (He, Ne, Ar, Kr and Xe) are chemically inert and rare in most of the terrestrial reservoirs, two characteristics which make them excellent tracers of geodynamic processes. This includes magma degassing since noble gases preferentially partition into the vapor phase (e.g., Carroll and Draper, 1994). Noble gases, and particularly the helium isotopes ^3He and ^4He , have been pivotal in showing variable mantle, crustal and meteoric inputs of volatiles into magmatic-hydrothermal systems (e.g., Mazor and Truesdell, 1984; Stuart et al., 1995; Burnard et al., 1999; Sano and Fischer, 2013; Pinti et al., 2019). This is because the mantle, the crust and the atmosphere have distinct $^3\text{He}/^4\text{He}$ isotopic signatures, with mantle enriched in primordial ^3He compared to ^4He with respect to the atmosphere and the crust. The expected $^3\text{He}/^4\text{He}$ ratio (R) in the convective depleted MORB-type mantle (or DMM) is essentially constant (Allègre et al., 1995) at 8 ± 1 times the atmospheric ratio ($R_a = 1.384 \times 10^{-6}$; Clarke et al., 1976). In regions affected by mantle plumes, the R/ R_a ratio is much higher, with 43-45 being the highest R/ R_a measured in the Icelandic mantle plume-derived Miocene alkali basalts of NW Iceland (Breddam and Kurz, 2001) and the picritic basalts of Baffin Island (Stuart et al., 2003). In contrast, crustal fluids are dominated by ^4He , which is produced by decay of ^{235}U , ^{238}U and ^{232}Th contained

in the reservoirs rocks with only little ^3He from neutron reaction with ^6Li (Ballentine and Burnard, 2002), resulting in an R/Ra typically in the range of 0.02-0.03 (e.g., Mamyrin and Tolstikhin, 1984). Finally, meteoric fluids exclusively contain atmospheric noble gases, which are dissolved at the recharge at solubility equilibrium (ASW or Air Saturated Water) and have an R/Ra of 1 (by definition).

Several studies have looked at noble gases as tracers of ore-forming fluids in fossil magmatic-hydrothermal-related ore deposits (e.g., Simmons et al., 1987; Stuart et al., 1995; Hu et al., 1998a,b; Burnard et al., 1999, 2004; Burnard and Poly, 2004; Landis and Rye, 2005; Manning and Holfstra, 2017; Wu et al., 2017), by analyzing these in fluid inclusions trapped in sulfides. Helium (and argon) isotopic compositions were pivotal in discriminating magmatic from crustal fluids involved in the ores. Noble gases have been combined with halogen contents in these inclusions (e.g., Kendrick et al., 2006) given the importance of ligands in metal transport, but the actual metal load could not be measured in these micro-fluid pockets. There are only a handful of studies where noble gases have been studied directly together with the metal load in hydrothermal fluids (e.g., Simmons et al., 1987; 2016).

For the magma sourcing of metals, their relative volatility or emanation coefficient predicts which elements are preferentially released (Zoller et al., 1983; Crowe et al., 1987; Hinkley, 1991, 1999), thereby producing an elemental fingerprint for magma degassing (commonly expressed as the enrichment factor relative to solid magmatic deposits). The highest enrichment factors are found for volatile metals (e.g. Hg, Bi, Cd, Te and Se) and ligands (Cl, S), and distinct differences are observed for different geotectonic settings with arc emissions particularly enriched in Sb, As and Pb while MORB/plume setting are more enriched in Te, Se and Tl (Mather et al., 2012; van Hinsberg et al., 2017; Edmonds et al., 2018). A similar compositional fingerprint can be determined for water-rock interaction from chemical characterization of a suite of

progressively altered rocks (e.g. Libbey and Williams-Jones, 2016). A complication in differentiating the two contributors is that WRI commonly acts on magmatic rocks, which often derive from the same magma intrusion. Moreover, magmatic element volatility depends on the availability and concentrations of ligands, as do element solubility and leachability, leading to cross-correlation with element mobilization in water-rock interaction.

Here, elemental and isotopic signatures of noble gases in geothermal fluids from the high-enthalpy Theistareykir geothermal field in NE Iceland are combined with a suite of trace metals with varying geochemical affinity to bring new constraints on the sources of fluids and metals in magmatic hydrothermal systems. Fluids have been sampled both at the surface for all the wells, and at depth in one well at Theistareykir and one well at Krafla. The Theistareykir Geothermal Field is in the initial phase of exploitation and this study thus allows chemistry of the geothermal fluids to be understood prior to exploitation-related changes to the original fluid signature. It is expected that this primary fluid pattern will be progressively lost as a result of phase segregation and boiling induced by exploitation and fluid re-injection, as it is the case in many geothermal fields the world over (see Pinti et al., 2013, 2019).

Variably altered rock fragments recovered from the geothermal production wells were sampled to directly determine the water-rock interaction mass transfer. This is the first study where a full isotopic and compositional characterization of noble gases and metals in both fluids and reservoir rocks is available for the same hydrothermal system. The combination of these datasets permits direct insights into the contributions of magma degassing and water-rock interaction to the metal load of a basalt-hosted magmatic-hydrothermal system.

3.3 Rock leaching vs. Magma degassing: a long-standing debate

What do magmas contribute to magmatic hydrothermal systems and what are the sources of volatiles and metals in the associated fluids? These questions have been the focus of many studies, but are still unresolved and very much debated. It is well-established that fluids released by magma are relatively enriched in metals compared to their host magma because of their selective partitioning into the fluid phases (Hedenquist et al., 1993), and that these fluids therefore sequester the metals and inject them into the hydrothermal system. However, it is unclear if sufficient mass of metal can be liberated in this process to lead to the formation of an exploitable ore deposit (Yang and Scott, 2006). On the other hand, mass balance on altered rocks and their fresh counterparts commonly shows extensive metal re-mobilization, which has been linked to the elevated temperatures of the hydrothermal fluids (which acts as a catalyst) and their high ligand (Cl^- , SO_4^{2-}) concentrations which provide anions to create complexes with metals (Seward et al., 2014; Williams-Jones and Migdisov, 2014;). Rock-leaching thus appears to be an efficient mechanism for concentrating metals in hydrothermal fluids. The ligands (such as halogens) are dominantly derived from magma degassing (e.g., Aiuppa et al., 2009), and authors supporting host-rock leaching as the dominant metal source therefore still must invoke a degassing contribution (Hedenquist and Lowenstern, 1994).

The idea that the leaching of host rocks by hydrothermal fluids is the dominant process of metal concentration in the crust is defended with a number of strong arguments. For example, the study of mid-ocean ridge (MOR) vents showed that the main process involved in metal concentration is the interaction between seawater and basaltic crust with only a minor addition from magmatic fluids (Weiss et al., 1977; Tivey, 2007; Shanks, 2012; Yang and Scott, 2006). Unlike MOR environments, felsic magmas often exsolve acid-volatile species (SO_2 , HCl , HF), that can substantially lower the pH of the fluids circulating in the hydrothermal system and increase ligand concentrations. This

changes the types of crustal alteration that take place and enhances metal leaching and transport even more and making these systems also more predisposed to ore-deposit formation (Gamo et al., 1997, 2006; Gena et al., 2001; Yang and Scott, 2006).

The booming in ore deposit exploration led to extensive studies of magmatic-hydrothermal systems associated with active volcanism, as modern analogues of the equivalent fossil mineralized systems (Weissberg et al., 1979; Henley et al., 1984; Berger and Bethke, 1985; Krupp and Seward, 1987, 1990; Clark and Williams-Jones, 1990; Hedenquist et al., 1993; Barnes and Seward, 1997). These studies showed that, unlike submarine systems, magmatic-hydrothermal systems in continental settings such as volcanic arcs are more influenced by magmatic fluids, possibly up to 25% in volume, due to the involvement of felsic magmas (Reeves et al., 2011). Increasingly, magmatic fluids are being considered as a source of metals (i.e. Cu, Zn, Ag and Au) in addition to what is possible to be sourced from rock leaching alone (e.g. Hedenquist and Lowenstern, 1994; Yang and Scott, 1996, 2006; Sun et al., 2004; Simmons and Brown, 2006). The study of volcanic gases also brought interesting insights. Even though they are not directly representative of the reservoir's fluid composition, they do provide information on the mobility of metals in magma degassing. In addition to water vapor and major volatile species (i.e. CO₂, SO₂, H₂S), volcanic gases contain up to 6 ppm Cu, 12 ppm Pb, 11 ppm Zn, 7 ppm Sn, 250 ppb Ag, and 24 ppb Au (e.g., Symonds et al., 1987; Hedenquist et al., 2001; Wahrenberger et al., 2002; Williams-Jones et al., 2002; Moune et al., 2006; Mather et al., 2012; Nadeau et al., 2016; van Hinsberg et al., 2017; Hedenquist et al., 2018; Lowenstern et al., 2018). These concentrations are still lower than those measured in fluid inclusions, which are considered as the most direct source of data on ore forming fluid composition in fossil mineralized systems, but magmatic gases represent the low-density vapor exsolved from such fluids, which explains the lower abundances of metals found in these vapors (Hedenquist and Lowenstern, 1994).

3.4 Geology of the area and geochemistry of fluids and altered rocks

Theistareykir is a high-enthalpy liquid-dominated field located in the Northern Volcanic Zone of Iceland (NVZ, Figure 3-1), which corresponds to the northeastern branch of the Mid-Atlantic oceanic ridge. It is located west of the Krafla geothermal field and north-west of Namafjall, both of which are among the older producing geothermal fields in Iceland. The development of the Theistareykir geothermal field is recent and began with nine wells drilled between 2002 and 2011. Exploitation of the field began in 2017 with a total of 18 wells drilled to depths from 1,723 m to 2,799 m. The plant currently has two generating units of 45MWe, making Theistareykir the fourth largest station in Iceland in terms of power generated.

3.4.1 Geology

Theistareykir is a central volcano system (Theistareykjarbunga shield volcano) created by fissure swarms provoked by the interplay between the spreading extension and local deformation. The Theistareykir volcanic system developed at the intersection between the NVZ rift, and the WNW-ESE-oriented transform zone called the Tjörnes Fracture Zone (TFZ; Khodayar et al., 2018). Volcanism is characterized by a series of olivine-tholeiitic and picritic basalt lava flows, mainly erupted from the Theistareykjarbunga volcano: Skildingahraun (>14.5 ka) lava shield; Stóravíti, a widespread (30 km³) post-glacial lava shield that erupted approximately 10.5 ka ago (MacLennan et al., 2002); the picritic basalt Borgarhraun (10-8 ka); and the youngest Theistareykjahraun lava shield (2.4 ka) (Saemundsson, 2007).

The heat source of the geothermal field has been related to the most recent mafic volcanic activity in the area (the 2.4 ka old Theistareykjahraun basaltic eruption), and the distribution of fumaroles suggests that it is supplied by an E-W-oriented magmatic intrusion, likely of basaltic nature (Óskarsson et al., 2013). The radiogenic isotope (Sr, Nd, Hf, Pb) and major and trace element compositions of the erupted basalts are little

affected by crystal fractionation and are essentially unaffected by interaction with the preexisting crust (Stracke et al., 2003). The Theistareykir basalts are therefore thought to be relatively close in composition to primary melts from the mantle (Stracke et al., 2003). Volcanic reservoir rocks at depth are thought to be compositionally equivalent to the surface exposures with variable alteration owing to water-rock interaction in the geothermal reservoir.

The surface area corresponding to the full extension of the Theistareykir hydrothermal system is 25-30 km², but surface manifestations are confined to the eastern part of the fissure swarm, northwest and north of Mt. Bæjarfjall, over an area of 11 km² (Kristinsson et al., 2013; Figure 3-1). The Theistareykir thermal area has historically been divided into five N-S oriented sub-areas, which from east to west are: Ketilfjall (A), Bóndhólsskard (B), Theistareykjagrundir (C), Tjarnarás (D), and Theistareykjahraun (E) (Figure 3-1). These areal subdivisions are based on the reservoir temperatures estimated by gas geothermometry, ranging from 100°C for area C and E to 330°C for areas A and D (Ármannsson et al., 1986). Among these areas, Ketilfjall (A), Theistareykjagrundir (C), and Tjarnarás (D) were regarded as more promising for drilling.

3.4.2 Fluid chemical composition

Based on stable isotopes of water, noble gas isotopes and ⁸⁷Sr/⁸⁶Sr ratios, four fluid sources were identified in the field: modern, local meteoric water; sub-modern meteoric (glacial) water from regional highlands precipitation; pre-Holocene glaciated meteoric water, characterized by strongly depleted $\delta^2\text{H}$ values and calculated U-Th/He and K-Ar fluid residence times from 57 ± 20 ka to 160 ± 80 ka; and, finally, a ³He-enriched magmatic fluid (Stefánsson, 2017; Sveinbjörnsdóttir et al., 2013, 2015; Saby et al., 2020; Pinti et al., 2022).

The geochemistry of the production well fluids sampled at the surface is dominated by Na-K-Cl with a TDS of about 350 mg/l. Chlorine content varies from 5.4 to 173 ppm

while SO_4 varies from 0.7 to 33 ppm. The Na/Cl ratio is higher in well fluids than in fluids from natural surface manifestations. The fluids sampled at the well-head exhibit a near-neutral pH, while fluids directly sampled at depth during well shut-in showed an acidic pH of ca. 2.5 (Saby et al., See Chapter 2 of this thesis). This is regarded to be a result of shutting in the well and to reflect mixing between deep near-neutral fluids with a shallow inflow of fluids that have been acidified by condensation of volcanic steam in the upper part of the system (see Saby et al., See Chapter 2 of this thesis). Trace metals are significantly diluted in surface fluids (both at the well-head and in hot springs) compared to the deep fluids (Saby et al., Saby et al., See Chapter 2 of this thesis). In the water phase, H_2S is the dominant gas with contents ranging from 31 to 88 ppm, followed by CO_2 with contents ranging from 9.4 to 62 ppm. In the steam phase, the dominant gas is CO_2 with contents ranging from 285 to 5597 ppm, followed by H_2S with contents ranging from 207 to 1141 ppm. Nitrogen contents in the dry gas phase vary from 1.6 to 46 ppm. The highest well gas concentrations measured ($\text{CO}_2 = 24,723$ ppm, $\text{H}_2\text{S} = 4,673$ ppm, $\text{H}_2 = 122.1$ ppm, $\text{CH}_4 = 149.03$ ppm) are found in the Ketilfjall (A) and Tjarnarás (D) areas, and are probably due to subsurface steam condensation, at least in Tjarnarás, as suggested by Darling and Ármannsson (1989).

Although gas measurements in Theistareykir have been undertaken for over half a century (Hermannsson and Línadal, 1951), noble gas data remained scarce and mainly limited to sampling from natural surface manifestations (Hilton et al., 1990; Poreda et al. 1992, Furi et al., 2010), given that Theistareykir wells were drilled only recently. Volatiles from the NVZ have been considered to be mainly sourced from the depleted upper mantle based on the work of Hilton (1990) who measured R/Ra values from 6.9 to 9.4 in fluids and that of Breddam et al. (2000) who measured R/Ra values of 7.99 to 9.75 in picrites of Theistareykir. Both set of values are close the $\text{R/Ra} = 8 \pm 1$ value of the DMM (e.g., Allègre et al., 1995). Successive work by Furi et al. (2010) showed slightly higher values up to 10.7 in fumaroles of nearby Namafjall and Krafla geothermal fields, and Saby et al. (2020) calculated a R/Ra endmember value for the

Theistareykir magmatic fluid of 11.45 (Table A1 in Electronic Supplementary Material). This suggests that even if the DMM source is dominating the release of volatiles in the region, ca. 10% of helium could be derived from the Icelandic mantle plume, which shows R/Ra values of 42-45 (Breddam and Kurz, 2000). The other noble gases in the Theistareykir well mainly show an atmospheric signature with the mantle signal obliterated by the meteoric water which is the dominant fluid component of Icelandic geothermal fields (e.g., Stefansson et al., 2017). Only argon showed a clear, but small, terrigenous (either mantle and/or crustal) component with measured $^{40}\text{Ar}/^{36}\text{Ar}$ ratios ranging from 298.8 to 307.3 (Saby et al. 2020).

3.4.3 Secondary mineralogy of reservoir rocks

Extensive research has been conducted on the secondary mineralogy in the Theistareykir geothermal field based on thin section petrography of cuttings from the wells. This shows strong water-rock interaction and high temperatures close to the surface in almost all the wells (Gudfinnsson, 2014). Quartz and wairakite are found at less than 100 m depth in wells ÞG-07, ÞG-03 and ÞG-06, suggesting that the temperature was at least 200°C at some point at this depth. Then at 342 m, prehnite is seen in ÞG-07, indicating a temperature of at least 240°C. Actinolite appears at about 750 m in ÞG-07, ÞG-03 and ÞG-06, at which point, the temperature should have reached at least 280°C. Traces of hornblende found in ÞG-03 and ÞG-06 below 2300 m suggest that the maximum temperature in this part of the geothermal reservoir is about 350°C. Studies of fluid inclusions in the lower part of ÞG-03 show a range of temperatures, exceeding 350°C at the high end. These results agree with downhole logging after the drilling of the well that recorded over 350°C in the lowest part. Traces of hydrothermal calcite can be found at almost all depths in well ÞG-03 down to the bottom. In contrast, calcite is sporadic in the lower part of ÞG-06 and is absent in well ÞG-07 in the 1400–1700 m range. Wells ÞG-04 and ÞG-05, located close to Bæjarfjall mountain 1 km to the ENE of ÞG-07, ÞG-03 and ÞG-06, show that the high temperature

alteration is equally shallow, with quartz, wairakite, chlorite, epidote and prehnite all present in the shallowest sample from 310 m. Actinolite first appears between 500 and 600 m and calcite is not seen below 800–900 m in either of the two wells. Thus, it is likely that the temperature in the part of the reservoir penetrated by PG-04 and PG-05 exceeds 280–300°C. Accessory phases are present and include sulfides and oxides but were not studied by Gudfinnsson (2014).

3.5 Analytical methods and data processing

3.5.1 Noble gas sampling and analyses

A total of 11 geothermal wells were sampled for analysis of noble gases in the gas phase and the full suite of major and trace elements in the liquid phase. Deep fluid samples were collected from wells PG-01 (Theistareykir) and K-21 (Krafla) at depths of 850 m (K-21) and 1420 and 1600 m (PG-01). Deep fluid samples were collected using the in-situ Ti-sampler of Brown and Simmons (2003). All the details regarding deep fluids sampling and analysis can be found in Saby et al., See Chapter 2 of this thesis. Water and gas phases were also collected directly at the wellhead using a portable steam/fluid separator. Noble gases were collected using a standard refrigeration-grade 3/8" (14 cm³ internal volume) copper tube directly installed at the gas exit of the portable fluid/steam separator. After letting the gas flow for several minutes, the tubes were sealed using stainless steel pinch-off clamps. Helium isotopic ratios were measured in the recovered gas phase at the Noble Gas Laboratory, University of Michigan (UMICH) by using a Thermo Helix SFT, except for well PG - 17, which was analyzed in the Noble Gas Laboratory of Geotop, using a Thermo Helix MC. In both institutions, gases were purified by gettering on Ti-sponges and/or ST-707 alloys and then He was separated from the other noble gases using a cryogenic trap. At UMICH, ³He was measured using an electron multiplier in ion counting mode and ⁴He

on a Faraday cup. At Geotop, ^3He was measured by ion counting on the axial Compact Discrete Dynode™ (CDD) detector, while ^4He was determined on the axial Faraday cup. Typical blanks for He are 0.01-0.04%. Quantitative analyses were obtained by calibrating the two mass spectrometers with a known aliquot of standard air, with typical standard reproducibility for ^4He of 0.5-1%. (see Saby et al., 2020 for details).

3.5.2 Major and trace metal analyses in water and rocks

After collection at the well head, the fluids sampled were divided into two sub-samples stored in pre-cleaned HDPE bottles: (1) an unacidified aliquot for the analysis of anions, (2) a sample filtered (0.45 μm) during collection, acidified with nitric acid (Suprapur, Sigma-Aldrich, Darmstadt, Germany) to preserve the fluid and avoid precipitation and absorption of elements onto the walls of the sample container. Anions were analyzed by ion chromatography (see Saby et al., Chapter 2 of this thesis for details). Most cations were analyzed at the Krafla laboratory by ICP-MS (details for the methods can be found in Hauksson, 2020). Strontium concentrations were determined by ICP-MS at the ALS laboratories, Luleå, Sweden, and volatile metals were analyzed at McGill University, also by ICP-MS. The volatile metal ICP-MS analyses were conducted using a Thermo-Finnigan iCAP-Qc quadrupole MS with long dwell times per mass (100 msec) to achieve low detection limits. The instrument was calibrated against 5 dilutions of three volatile metal standards (two standards for Bi, Cd, Tl and Sb, and one for Hg, all at 1 ppt to 10 ppb). Dilutions were prepared by mass using nano-pure 2% HNO_3 as the diluting acid. Analyses were conducted in triplicate to determine precision.

Four units of fresh basalt were sampled across the Theistareykir area. Each unit was sampled at 3 different locations for a total of 12 samples. Rock cuttings collected at 1600 m depth in well ÞG-01 were provided by ÍSOR and are taken to represent the host rock for the geothermal reservoir. The samples consist of fragments of variably altered rock (from pristine magmatic fragments to chlorite-epidote-plagioclase dominated altered fragments). The fragments were washed in de-ionized water, dried, and then

divided into 8 sub-samples to obtain a range in the degree of alteration. The fresh samples were crushed wrapped in Kraft paper using a steel hammer, dry coarse-milled in a WC ring mill, and wet fine-milled to less than 1 μm in a WC ball mill. The altered samples were crushed in an agate mortar and milled to below 1 micron by hand. The powder was then pressed into pellets (without additive) and analyzed by LA-ICP-MS at McGill University following the method of Garbe-Schönberg and Müller (2014). Further method details of the pellet analyses can be found in Saby et al., See Chapter 2 of this thesis. Further method details of the pellet analyses can be found in Chapter 2 of the thesis.

3.6 Results

The fresh rocks have major and trace element compositions that are within the magmatic trend defined by literature data (extracted Jan-2022 from the GEOROC database - <http://georoc.mpch-mainz.gwdg.de/georoc>). Element concentrations in the altered rocks are higher than in the fresh rocks for most elements (Table 2 and 3 in Electronic Supplementary Material). Major oxides concentrations vary from 50.10 to 50.87 wt% for SiO_2 , to 0.16 to 0.18 wt% for MnO while Sr, V, Cr, Ni, Zn and Zr are the most abundant trace elements. The altered samples define a linear trend extending from the magmatic trend defined for Theistareykir (Figure 3-2), which represents a mixing curve between the precursor basalt and a fully altered endmember. It is unlikely that the alteration endmember is captured in the alteration dataset of the measured values, but the trend defines the direction of alteration. The precursor basalt is predicted to have a MgO content of 7 wt% and is close to the composition of samples PG-01-roc-09 and PG-01-roc-11, which are from the Theistareykjahraun lava flow. The altered rocks show up to 2.0 – 2.5 times enrichment in the immobile elements Zr, Nb, Hf, Th and U compared to the fresh basalt (Table 3 in Electronic Supplementary Material), with this enrichment factor consistent among the elements. The LREE also give the same enrichment factor with the HREE somewhat lower (1.5 – 2.0). We

interpret this to represent residual enrichment in these immobile elements during progressive alteration. The altered sample composition was therefore normalized to the precursor basalt content of these elements (following Grant 2005), which allows for determining the release or sequestration of elements during alteration. This calculation shows leaching for all major elements except K, enrichment in Li, Cr and Sb, and leaching of the base metals, semi-volatile metals and the HREE + Sc (Figure 3-3). The elements with strongest relative change during alteration are Cu (leached) and Sb (enriched).

Fluid compositional data used in this study are reported in Table A1 in Electronic Supplementary Material and include $^3\text{He}/^4\text{He}$ ratios, major elements and trace volatile metals. Additional data for these samples has previously been reported in Saby et al., See Chapter 2 of this thesis. The $^3\text{He}/^4\text{He}$ ratios are reported uncorrected for the atmospheric component (R/Ra) and corrected for this component (Rc/Ra) using the $^4\text{He}/^{20}\text{Ne}$ ratio as an index of the atmospheric helium contribution (following Torgersen and Jenkins, 1982):

$$Rc/Ra = [(R/Ra)_{meas} - r] / (1 - r) \quad (1)$$

$$r = (^4\text{He}/^{20}\text{Ne})_{ASW} / (^4\text{He}/^{20}\text{Ne})_{meas} \quad (2),$$

where (R/Ra)_{meas} is the measured helium isotopic ratio, and ($^4\text{He}/^{20}\text{Ne}$)_{ASW} and ($^4\text{He}/^{20}\text{Ne}$)_{meas} are the ASW ratios at 3.7°C (estimated recharge T) and the sample ratios respectively. Calculation of the Rc/Ra uncertainty is described in Sano et al. (2006).

Metal concentration in fluids sampled at the wellhead are low, as is also the case for the majority of geothermal fields in Iceland (Ármansson, 2015). The volatile metals show values ranging from Hg 0.066 to 0.192 ppb, Bi 0.012 to 0.042 ppb, Cd 0.024 to

0.029 ppb, Tl 0.038 to 0.089 ppb, As 0.41 to 230 ppb and Sb 0.005 to 1.2 ppb respectively (Table 1 in Electronic Supplementary Material).

3.7 Discussion

3.7.1 Water-rock interaction and magma degassing contributions to the deep geothermal fluids

The composition of the deep reservoir fluids has been determined for Theistareykir by direct down-well sampling (Saby et al., See Chapter 2 of this thesis). This study showed that the deep fluids are relatively enriched in base metals and (semi)-volatile metals (in particular Te, Hg, Re and Tl) compared to local basalt, interpreted as element input from both magma degassing and water-rock interaction. To verify and quantify the contributions from these two sources requires knowledge of their respective elemental signature.

The element signature of the fluid released in magma degassing can be estimated from the enrichment factors and the composition of the Theistareykir tholeiitic basalt. Here, we use the element enrichment factors as determined for Kilauea basalt (Mather et al. 2012) and calculate the emitted fluid composition for an element i using the equation:

$$C^{\text{fluid}}_i = EF_i * C^{\text{PG-basalt}}_i \quad (3)$$

where C is the concentration of element i in the respective phase and EF the enrichment factor of a given element from one phase to the other. These enrichment factors for Kilauea represent surface volatility, whereas the magma degassing at Theistareykir is taking place at elevated pressure in the subsurface, and pressure has an impact on the volatility of the elements (e.g. Migdisov et al. 2014). However, enrichment factors at elevated pressure are only available for a small subset of elements, which limits the ability to differentiate between magma degassing and water rock interaction. We therefore use the EF data at atmospheric pressure, with the assumption that the resulting

chemical fingerprint is not overly affected by pressure, although absolute values will be.

To scale the resulting composition to the concentration range found in the deep fluid sample, we then assume that all Cl in the fluid is derived from magma degassing. The Cl content of the unaltered rocks is low (ca. 60 mg/kg, GEOROC) and is generally higher for the altered equivalents, so Cl release from water-rock interaction can be expected to be negligible. Whereas direct Cl degassing is unlikely to be significant at Theistareykir given the low Cl abundance in the basalt and the late degassing of Cl (cf. Witham et al. 2012), partition coefficients indicate that Cl would partition into the exsolving water-rich fluid ($D_{\text{fluid-melt}} > 10$ for Etna basalt – Alletti et al. 2009) and hence be strongly mobilized in magma degassing. It should also be noted that this scaling factor only shifts the elemental signature up and down in concentration and does not change the inter-element trends.

To calculate the mass transfer in water-rock interaction, we use the difference between the immobile-element corrected altered rock composition and that of the precursor basalt, and scale this elemental signature by assuming all Na to be derived from WRI. Sodium was chosen as it has a low EF (1.7), strong release in water rock interaction (40% change in composition), and has precise data for all samples. The resulting compositional signatures are shown in Figure 3-4, together with the measured concentrations in the Theistareykir fluid sampled at 1600 m depth.

Figure 3-4 shows a remarkable agreement between the estimated magmatic degassing fluid and the measured composition of deep Theistareykir geothermal fluid. The elemental patterns trace each other and even the absolute concentrations are within an order of magnitude for most elements. In contrast, the WRI elemental signature is distinctly different (Figure 3-4). This suggests that the deep fluid composition is predominantly controlled by magmatic input rather than by water-rock interaction. The only elements that deviate significantly are the alkalis and the base metals, Cu in

particular. Water-rock interaction acts as a sink of Li and K and can therefore not explain the alkali concentrations, but the leaching of base metals that accompanies WRI can explain these concentrations in the deep fluid. Moreover, WRI can explain the higher concentrations of V and Ti and lower concentrations of Cr, Zr, Nb and Hf with the former two leached and the latter 4 sequestered in WRI.

Using the base and refractory metals, where both magma degassing and rock leaching contribute to the fluid composition, gives a mean magmatic degassing contribution of 80% with the remaining 20% from water-rock interaction. Of the base metals, Cu is most prominently leached in WRI, and this gives values of 77% sourced from degassing and 23% for WRI. Applying the same approach to a deep fluid sample collected in the adjacent Krafla geothermal field gives similar results, with a mean magmatic contribution of 82% and 18% from WRI (using a fresh Krafla basalt to calculate the magmatic signature from the enrichment factors, but the WRI signature from Theistareykir for lack of data on alteration in Krafla well K-21). Despite the larger uncertainty in the Krafla result from the unknown WRI signature for Krafla, it is clear that for both geothermal fields, the dominant source of elements is fluid released from the magma, except for Mn, Fe, Co, Cu, Ti and V.

3.7.2 Magma degassing constrained using noble gases

The deep fluid composition in Theistareykir is unfortunately only known from one well (ÞG-01), and it is therefore not possible to assess any variations in the contributions from magma degassing and WRI spatially throughout the field. However, fluids sampled at the well head are available for the entire field. Noble gases are a robust tool to estimate the contribution of volatiles in geothermal fluids sourced from the mantle (M), the crust (C) and the atmosphere (A – via meteoric recharge). Here, we calculate the percentage contribution for each source from the helium isotopes using ternary mixing equations (Pinti et al., 2019):

$$R/R_{\text{aobserved}} = R/R_{\text{amantle}}*M + R/R_{\text{acrust}}*C + R/R_{\text{aASW}}*A \quad (4)$$

$$1/({}^4\text{He}/{}^{20}\text{Ne})_{\text{observed}} = M/({}^4\text{He}/{}^{20}\text{Ne})_{\text{mantle}} + C/({}^4\text{He}/{}^{20}\text{Ne})_{\text{crust}} + A/({}^4\text{He}/{}^{20}\text{Ne})_{\text{ASW}} \quad (5)$$

$$M + C + A = 1 \quad (6),$$

where the subscripts observed, mantle, crust, and ASW refer to the observed sample, the mantle end-member ($R/R_a = 11.45$ and ${}^4\text{He}/{}^{20}\text{Ne} = 1000$; Sano and Wakita, 1985; Saby et al., 2020), the crustal end-member ($R/R_a = 0.02$ and ${}^4\text{He}/{}^{20}\text{Ne} = 1000$; Sano and Wakita, 1985), and the meteoric water end-member ($R/R_a = 1$ and ${}^4\text{He}/{}^{20}\text{Ne} = 0.251$ calculated at air-saturated water (ASW) conditions of 4°C , the average recharge temperature of Icelandic waters; Stefansson, 2017), respectively, and M, C, and A are the fractions of the mantle, crust and atmospheric components. For well ÞG-11 (which exhibits the lowest measured R/R_a value) with ${}^4\text{He}/{}^{20}\text{Ne} = 29.77$ and an $R/R_a = 9.96$ (Table A1 in Electronic Supplementary Material), the percentage of helium derived from mantle in the mixture is 87.0 %, compared with 12.2 % of crustal helium and 0.82 % of atmospheric helium. Well ÞG-01 gives 93.5%, 6.2% and 0.3%, and for the well with the highest R/R_a value, ÞG-07, the relative contributions are 89.1%, 10.8% and 0.1%. These results are consistent with the previously calculated 80% contribution of magmatic degassing based on the metals in the deep fluid sample, and support a strong magmatic contribution to the fluids, both in noble gases and in metals. The magmatic contribution is higher for the noble gases, which likely reflects their higher volatility than metals and therefore their preferential release from the magma (Paonita, 2005). These results thus indicate a clear and direct transfer of volatiles and metals from the magma to the geothermal fluid reservoir.

The contributions of mantle, crust and atmosphere across the geothermal field indicate that the wells with the highest mantle contributions are the ones closest to the Bæjarfjall and Ketilfjall mountains (Figure 3-1), suggesting the impact of local and regional structures and faults on the fluid pathway from depth to surface (see Khodayar et al., 2018). Those highest contributions are also related to the areas of the field that show the highest major gas species abundances (Khodayar et al., 2018).

These results further indicate that the $^3\text{He}/^4\text{He}$ ratio can be used at the scale of the field as a measure of the relative magma degassing contribution, which, when combined with the metal concentrations in the fluids can then reveal the relative importance of magma and the leaching of rocks by hot fluids to the content of a given metal. A dominant magmatic contribution of metals would be associated with relatively high $^3\text{He}/^4\text{He}$ ratios owing to input of primordial ^3He , while water-rock interaction would favor the release of radiogenic ^4He produced by the decay of U and Th contained in the reservoir rocks, and thus have a lower $^3\text{He}/^4\text{He}$ ratio. We also make the explicit assumption that the magmatic signature of helium is homogeneous at the scale of the field and thus any variation in the $^3\text{He}/^4\text{He}$ in the field is only related to a radiogenic contribution of ^4He . The Rc/Ra ratio shows strong positive correlations with the major magmatic gases (CO_2 , H_2S) and SO_4 (Figure 3-5), which further supports that this represents the magmatic contribution.

Figure 3-6 presents the Rc/Ra ratio of the Theistareykir well gases against the Cl-normalized metal content in the corresponding surface fluids, focusing on the most volatile metals. We normalize to Cl here to remove the effect of any shallow dilution, assuming conservative behavior of Cl. Results show that Hg and Bi, which are among the most volatile of the metals (e.g., Mather et al., 2012) have a well-defined positive correlation with Rc/Ra ratio, with potentially a subtle WRI contribution in Bi for wells PG-04, PG-13 and PG-16. This clear positive correlation suggests that Hg and Bi can be used as a tracer of magma degassing. The behavior of Cd, Tl and As is bimodal. Wells PG-01, PG-03, PG-05, PG-17 and PG-07 show a positive correlation with Rc/Ra, whereas PG-04, PG-06, PG-12, PG-13 and PG-16 display a negative correlation. This suggests sourcing from both magma degassing and WRI, with the relative importance of each source varying among the wells and hence spatially in the geothermal field. The wells that present the highest magmatic contribution for the metals evaluated here are wells PG-07, PG-03, PG-05, PG-01 and PG-17.

The metal/Cl ratios also correlate with the major gas species (CO_2 , H_2S) and with SO_4 content of the fluid (Figure 3-7). This will reflect derivation of the same source, i.e. magma degassing, but may also contain a component related to stronger solvation at higher ligand content.

The trends in the metal/Cl data show larger scatter than in volatiles (Figure 3-6 and Figure 3-7). In part, this may reflect the larger analytical uncertainties in the metal data. In addition, the surface fluids represent the vapor fraction following boiling of the geothermal reservoir fluid, and as shown in Saby et al., See Chapter 2 of this thesis, are strongly depleted in most elements compared to the deep fluid. Transfer of the deep elemental signature to the surface is thus very sensitive to boiling. Boiling also greatly complicates the use of surface fluids sampled at the well head in determining the absolute contributions of the two metal sources for metals that are less volatile, that create strong complexes with ligands, and that prefer the residual fluid phase.

3.8 Conclusions

This study of noble gases and volatile metals in geothermal fluids was conducted to establish the respective contributions of magma degassing and water-rock interaction to the metal content of magmatic-hydrothermal fluids, and to determine the variability in these contributions across the Theistareykir geothermal field in northern Iceland. The estimated magma degassing elemental signature, combined with the measured water-rock interaction mass transfer indicates that the deep geothermal reservoir fluid is dominated by magma degassing input, except for Mn, Fe, Co, Cu, V and Ti. Helium isotopic data for well-head fluids confirm this, both data sources suggesting an approximately 80-85% contribution from magma, and 15-20% from water-rock interaction. Geothermal fluid samples from production wells show atmosphere-normalized $^3\text{He}/^4\text{He}$ ratios (R_c/R_a) from 9.44 to 11.45 which are interpreted to

represent mixing between a fluid carrying a pure magmatic ^3He -enriched component and a crustal component with helium slightly diluted by radiogenic ^4He . The latter is considered a measure of water-rock interaction. R_c/R_a shows variability in magma degassing and WRI contributions across the field. Volatile metals correlate with R_c/R_a and similarly vary across the field, with Hg and Bi the best indicators of the magmatic contribution. Noble gases and volatile metals thus provide the tools to identify and quantify the relative contributions of magma degassing and water-rock interaction to the metal load of geothermal fluids and to track how these vary in space and time.

3.9 Acknowledgements

We warmly thank André Poirier and Julien Gogot for their help with sample preparation, analyses and preparation of sampling material prior to field work. This research was funded by the Natural Sciences and Engineering Research Council of Canada (NSERC) through an Alexander-Graham-Bell-doctorate (BESC D) grant (CGSD3-503679-2017) to M.S. and a Discovery Grant to D.L.P. (RGPIN-2015-05378); by Geotop through a collaborative research project fund, 2018-2020; by ÍSOR and the Landsvirkjun Power company; and by Osisko philanthropy. We also thank ÍSOR, Landsvirkjun, and the University of Iceland for providing access to sampling locations and to their facilities.

3.10 References

- Aiuppa, A., Baker, D.R. and Webster, J.D., 2009. Halogens in volcanic systems. *Chem Geol* 263, 1-18.
- Allègre, C. J., Moreira M., and Staudacher T., 1995. $^4\text{He}/^3\text{He}$ dispersion and mantle convection. *Geophys Res Lett* 22(17), 2325-2328.
- Alletti, M., Baker, D. R., Scaillet, B., Aiuppa, A., Moretti, R., & Ottolini, L., 2009. Chlorine partitioning between a basaltic melt and H₂O–CO₂ fluids at Mount Etna. *Chemical Geology*, 263(1-4), 37–50. doi:10.1016/j.chemgeo.2009.04.003
- Ármannsson, H, Gíslason, G, Torfason, H, 1986. Surface exploration of the Theistareykir high-temperature geothermal area, Iceland, with special reference to the application of geochemical methods. *Appl. Geochem.* 1, 47-64.
- Ármannsson, H., 2015. The fluid geochemistry of Icelandic high temperature geothermal areas. *Appl. Geochem.* 66, 14-64.
- Ballentine, C.J. and Burnard, P.G., 2002. Production, release and transport of noble gases in the continental crust. *Rev. Mineral. Geochem.* 47, 481-538.
- Barnes, H. and Seward, T., 1997. Geothermal systems and mercury deposits. *Geochemistry of hydrothermal ore deposits*, 3: 699-736.
- Berger, B.R. and Bethke, P.M., 1985. *Geology and geochemistry of epithermal systems.* Society of economic geologists.
- Birkle, P., Portugal Marín, E., Pinti, D.L. and Castro, M.C., 2016. Origin and evolution of geothermal fluids from Las Tres Vírgenes and Cerro Prieto fields, Mexico - Co-genetic volcanic activity and paleoclimatic constraints. *Appl. Geochem.* 65, 36-53.
- Bodnar, R.J., 1995. Fluid inclusion evidence for a magmatic source for metals in porphyry copper deposits. In: Thompson, J.F.H. (Ed.) *Magmas, Fluids and Ore Deposits.* Mineralogical Association of Canada Short Course Series Volume 23, pp. 139-152.
- Breddam, K., Kurz, M.D. and Storey, M., 2000. Mapping out the conduit of the Iceland mantle plume with helium isotopes. *Earth Planetary Science Letters* 176, 45-55.

- Breddam, K, Kurz, M.D., 2001. Helium isotope signatures of Icelandic alkaline lavas. EOS Trans Am Geophys Union 82:F1315
- Burnard, P.G., Hu, R., Turner, G., Bi, X.W., 1999. Mantle, crustal and atmospheric noble gases in Ailaoshan Gold deposits, Yunnan Province, China. *Geochim. Cosmochim. Acta*, 63(10): 1595-1604
- Burnard, P.G. and Polya, D.A., 2004. Importance of mantle derived fluids during granite associated hydrothermal circulation: He and Ar isotopes of ore minerals from Panasqueira 1 Associate editor: R. Wieler. *Geochimica et Cosmochimica Acta*, 68(7): 1607-1615.
- Burnard, P., Graham, D. and Farley, K., 2004. Fractionation of noble gases (He, Ar) during MORB mantle melting: a case study on the Southeast Indian Ridge. *Earth and Planetary Science Letters*, 227(3): 457-472.
- Carroll, M.R. and Draper, D.S. (1994) Noble gases as trace elements in magmatic processes. *Chemical Geology* 117, 37-56.
- Chambefort, I., & Stefansson, A., 2020. Fluids in Geothermal Systems. *Elements*, 16, 407-411
- Christenson, B. and Wood, C., 1993. Evolution of a vent-hosted hydrothermal system beneath Ruapehu Crater Lake, New Zealand. *Bulletin of volcanology*, 55(8): 547-565.
- Clarke, W. B., W. J. Jenkins and Z. Top, 1976. "Determination of tritium by mass spectrometric measurement of ^3He ." *The International Journal of Applied Radiation and Isotopes* 27: 515-522.
- Clark, J.R. and Williams-Jones, A.E., 1990. Analogues of epithermal gold-silver deposition in geothermal well scales. *Nature*, 346(6285): 644-645.
- Crowe, B. M., Finnegan, D. L., Zoller, W. H. and Boynton, W. V., 1987. Trace element geochemistry of volcanic gases and particles from 1983-1984 eruption episodes of Kilauea volcano. *J. Geophys. Res.* 92, 13,708-13,714.
- Darling, G, Ármannsson, H., 1989. Stable isotope aspects of fluid flow in the Krafla, Námafjall and Theistareykir geothermal systems of northeast Iceland. *Chem. Geol.* 76, 197-213.

- Edmonds, M., Mather, T.A. & Liu, E.J., 2018. A distinct metal fingerprint in arc volcanic emissions. *Nature Geosci* 11, 790–794, <https://doi.org/10.1038/s41561-018-0214-5>
- Füri, E., Hilton, D.R., Halldórsson, S.A., Barry, P.H., Hahm, D., Fischer, T.P., Grönvold, K., 2010. Apparent decoupling of the He and Ne isotope systematics of the Icelandic mantle: the role of He depletion, melt mixing, degassing fractionation and air interaction. *Geochim. Cosmochim. Acta* 74, 3307–3332.
- Gamo, T., Ishibashi, J., Tsunogai, U., Okamura, K. and Chiba, H., 2006. Unique Geochemistry of Submarine Hydrothermal Fluids from Arc - Back - Arc Settings of the Western Pacific. *Back-arc spreading systems: geological, biological, chemical, and physical interactions*: 147-161.
- Gamo, T., Okamura, K., Charlou, J.-L., Urabe, T., Auzende, J.-M., Ishibashi, J., Shitashima, K. and Chiba, H., 1997. Acidic and sulfate-rich hydrothermal fluids from the Manus back-arc basin, Papua New Guinea. *Geology*, 25(2): 139-142.
- Gena, K., Mizuta, T., Ishiyama, D. and Urabe, T., 2001. Acid - sulphate Type Alteration and Mineralization in the Desmos Caldera, Manus Back - arc Basin, Papua New Guinea. *Resource Geology*, 51(1): 31-44.
- Giggenbach, W., 1992. Isotopic shifts in waters from geothermal and volcanic systems along convergent plate boundaries and their origin. *Earth. Planet. Sci. Lett.* 113, 495-510.
- Grant, J.A. Isocon analysis: A brief review of the method and applications, 2005. *Phys. Chem. Earth Parts A/B/C*, 30, 997–1004.
- Gundfinnsson, G.H., 2014. Alteration in the Theistareykir Geothermal System. A Study of Drill Cuttings in Thin Sections. LV report: LV-2014-063, 110 pp.
- Hauksson, T., and Gudmundsson, 2008. Krafla. Acid wells. Landsvirkjun, report, 17 pp.
- Hedenquist, J. W., S. Taguchi and H. Shinohara, 2018. Features of Large Magmatic–Hydrothermal Systems in Japan: Characteristics Similar to the Tops of Porphyry Copper Deposits. *Resource Geology* 68(2): 164-180.
- Hedenquist, J.W., Arribas, A. and Reynolds, T.J., 1998. Evolution of an intrusion-centered hydrothermal system; Far Southeast-Lepanto porphyry and epithermal Cu-Au deposits, Philippines. *Economic Geology*, 93(4): 373-404.

- Hedenquist, J.W. and Lowenstern, J.B., 1994. The role of magmas in the formation of hydrothermal ore deposits. *Nature*, 370(6490): 519-527.
- Hedenquist, J.W., Simmons, S.F., Giggenbach, W.F. and Eldridge, C.S., 1993. White Island, New Zealand, volcanic-hydrothermal system represents the geochemical environment of high-sulfidation Cu and Au ore deposition. *Geology*, 21(8): 731-734.
- Hedenquist, J.W. and Henley, R.W., 1985. Hydrothermal eruptions in the Waiotapu geothermal system, New Zealand; their origin, associated breccias, and relation to precious metal mineralization. *Economic geology*, 80(6): 1640-1668.
- Henley, R.W., Barton, P., Truesdell, A. and Whitney, J., 1984. Fluid-mineral equilibria in hydrothermal systems, 1. Society of Economic Geologists El Paso, TX.
- Hermannsson, S., Línadal, B., 1951. Chemical analysis of warm and hot springs. Jarðboranir Ríkisins, State Drilling Company (in Icelandic).
- Hilton, D.R., Grönvold, K., O'Nions, R.K., Oxburgh, E.R., 1990. Regional distribution of ^3He anomalies in the Icelandic crust. *Chem. Geol.* 88, 53-67.
- Hinkley, T. K., 1991. Distribution of metals between particulate and gaseous forms in a volcanic plume. *Bull. Volcanol.* 53, 395– 400.
- Hinkley, T. K., Lamothe, P. J., Wilson, S. A., Finnegan, D. L. and Gerlach, T. M., 1999. Metal emissions from Kilauea, and a suggested revision of the estimated worldwide metal output by quiescent degassing of volcanoes. *Earth Planet. Sci. Lett.* 170, 315–325.
- Hu, R., Burnard, P., Turner, G. and Bi, X., 1998. Helium and argon isotope systematics in fluid inclusions of Machangqing copper deposit in west Yunnan Province, China. *Chemical Geology*, 146(1): 55-63.
- Hu, R., Turner, G., Burnard, P., Zhong, H., Ye, Z. and Bi, X., 1998. Helium and argon isotopic geochemistry of Jinding superlarge Pb-Zn deposit. *Science in China Series D: Earth Sciences*, 41(4): 442-448.
- Kendrick, M.A., Duncan, R. and Phillips, D., 2006. Noble gas and halogen constraints on mineralizing fluids of metamorphic versus surficial origin: Mt Isa, Australia. *Chem. Geol.* 235, 325-351.

- Khodayar, M., Björnsson, S., Kristinsson, S.G., Karlsdóttir, R., Ólafsson, M., Víkingsson, S., 2018. Tectonic control of the Theistareykir geothermal field by rift and transform zones in North Iceland: a multi-disciplinary approach. *Open J. Geol.* 8, 543-584
- Kristinsson, S.G., Fridriksson, Th., Ólafsson, M., Gunnarsdóttir, S.H, Níelsson, S., 2013. The Theistareykir, Krafla and Námafjall high-temperature geothermal areas. Monitoring of surface activity and groundwater. Iceland GeoSurvey, report ÍSOR-2013/037 (in Icelandic), 152 pp.
- Krupp, R.E. and Seward, T.M., 1987. The Rotokawa geothermal system, New Zealand; an active epithermal gold-depositing environment. *Economic Geology*, 82(5): 1109-1129.
- Krupp, R.E. and Seward, T.M., 1990. Transport and deposition of metals in the Rotokawa geothermal system, New Zealand. *Mineralium Deposita*, 25(1): 73-81.
- Landis, G.P. and Rye, R.O., 2005. Characterization of gas chemistry and noble-gas isotope ratios of inclusion fluids in magmatic-hydrothermal and magmatic-steam alunite. *Chemical Geology*, 215(1-4): 155-184.
- Libbey, R. and Williams-Jones, A., 2016. Lithochemical approaches in geothermal system characterization: An application to the Reykjanes geothermal field, Iceland. *Geothermics*, 64: 61-80.
- Lowenstern J.B., van Hinsberg V., Berlo K., Liesegang M., Iacovino K., Bindeman I.N. and Wright H.M., 2018. Opal-A in Glassy Pumice, Acid Alteration, and the 1817 Phreatomagmatic Eruption at Kawah Ijen (Java), Indonesia. *Front. Earth Sci.* 6:11. doi: 10.3389/feart.2018.00011
- MacLennan, J., M. Jull, D. McKenzie, L. Slater, Grönvold, K., 2002. The link between volcanism and deglaciation in Iceland, *Geochem Geophys Geosyst*, 3, 1062, doi:10.1029/2001GC000282.
- Mamyrin, B.A., Tolstikhin, I.N., 1984. Helium isotopes in nature. Elsevier, Amsterdam.
- Manning, A.H. and Hofstra, A.H., 2017. Noble gas data from Goldfield and Tonopah epithermal Au-Ag deposits, ancestral Cascades Arc, USA: Evidence for a primitive mantle volatile source. *Ore Geology Reviews*, 89: 683-700.
- Mather, T. A., Witt, M. L. I., Pyle, D. M., Quayle, B. M., Aiuppa, A., Bagnato, E., et al., 2012. Halogens and trace metal emissions from the ongoing 2008 summit

eruption of Kīlauea volcano, Hawaii. *Geochimica Et Cosmochimica Acta*, 83(C), 292–323. <http://doi.org/10.1016/j.gca.2011.11.029>

- Migdisov, A. A., Bychkov, A. Y., Williams-Jones, A. E., & van Hinsberg, V. J., 2014. A predictive model for the transport of copper by HCl-bearing water vapour in ore-forming magmatic-hydrothermal systems: Implications for copper porphyry ore formation. *Geochimica et Cosmochimica Acta*, 129, 33–53. doi:10.1016/j.gca.2013.12.024
- Moune, S., Sigmarsson, O., Thordarson, T. and Gauthier, P.-J., 2006. Recent volatile evolution in the magmatic system of Hekla volcano, Iceland. *Earth and Planetary Science Letters*, 255(3-4): 373-389.
- Mazor, E., Truesdell, A., 1984. Dynamics of a geothermal field traced by noble gases: Cerro Prieto, Mexico. *Geothermics*, 13(1): 91-102.
- Nadeau, O., Stix, J. and Williams-Jones, A.E., 2016. Links between arc volcanoes and porphyry-epithermal ore deposits. *Geology*, 44(1): 11-14.
- Norton, D.L., 1984. Theory of Hydrothermal Systems. *Annu. Rev. Earth Planet. Sci.* 12, 155-177.
- Óskarsson, F., Ármannsson, H., Ólafsson, M., Sveinbjörnsdóttir, Á.E., Markússon, S.H., 2013. The Theistareykir geothermal field, NE Iceland: fluid chemistry and production properties. *Proc. Earth Planet. Sci.* 7, 644–647.
- Paonita, A., 2005. Noble gas solubility in silicate melts: a review of experimentation and theory, and implications regarding magma degassing processes. *Annals of Geophysics*, 48(4-5).
- Pinti, D.L.; Haut-Labourdette, M.; Poirier, A.; Saby, M.; van Hinsberg, V.J.; Berlo, K.; Castro, M.C.; Gautason, B.; Sigurðardóttir, Á.K., 2022. ⁸⁷Sr/⁸⁶Sr Ratios and Atmospheric Noble Gases in Theistareykir Geothermal Fluids: A Record of Glacial Water. *Geosciences*, 12, 119. <https://doi.org/10.3390/geosciences12030119>
- Pinti, D. L., Castro, M. C., López-Hernández, A., Hernández Hernández, M. A., Richard, L., Hall, C. M., Shouakar-Stash, O., Flores-Armenta, M. and Rodríguez-Rodríguez, M. H., 2019. "Cerro Prieto Geothermal Field (Baja California, Mexico) – A fossil system? Insights from a noble gas study." *J. Volcanol. Geother. Res.* 371: 32-45.

- Pinti, D.L., Castro, M.C., Shouakar-Stash, O., Tremblay, A., Garduño, V.H., Hall, C.M., Hélie, J.F. and Ghaleb, B., 2013. Evolution of the geothermal fluids at Los Azufres, Mexico, as traced by noble gas isotopes, $\delta^{18}\text{O}$, δD , $\delta^{13}\text{C}$ and $^{87}\text{Sr}/^{86}\text{Sr}$. *Journal of Volcanology and Geothermal Research*, 249: 1-11.
- Poreda, R.J., Arnórsson, S., 1992. Helium isotopes in Icelandic geothermal systems: II. Helium-heat relationships. *Geochim. Cosmochim. Acta* 56, 4229-4235.
- Reeves, E.P., Seewald, J.S., Saccocia, P., Bach, W., Craddock, P.R., Shanks, W.C., Sylva, S.P., Walsh, E., Pichler, T. and Rosner, M., 2011. Geochemistry of hydrothermal fluids from the PACMANUS, Northeast Pual and Vienna Woods hydrothermal fields, Manus basin, Papua New Guinea. *Geochimica et Cosmochimica Acta*, 75(4): 1088-1123.
- Saby, M., van Hinsberg V., Pinti, D.L., Berlo K., Gautason B., Sigurðardóttir Á., Brown K., Rocher O. The Behaviour of Metals in Deep Fluids of NE Iceland. Submitted to *Scientific Reports* (July 2022)
- Saby, M. Pinti, D.L., van Hinsberg, V., Gautason, B., Sigurðardóttir, Á., Castro, M.C., Hall, C., Óskarsson, F., Rocher, O., Hélie, J-F., Mejean, P., 2020. Sources and transport of fluid and heat at the newly-developed Theistareykir Geothermal Field, Iceland. *Journal of Volcanology and Geothermal Research*. 405. 107062. 10.1016/j.jvolgeores.2020.107062.
- Saemundsson, K., 2007. The geology of Theistareykir. Iceland GeoSurvey, short report ÍSOR-07270 (in Icelandic): 23.
- Sano, Y. and Fischer T.P., 2013. The Analysis and Interpretation of Noble Gases in Modern Hydrothermal Systems. *The Noble Gases as Geochemical Tracers*. P. Burnard. Berlin, Heidelberg, Springer Berlin Heidelberg: 249-317.
- Sano, Y., Takahata, N., Seno, T., 2006. Geographical Distribution of $^3\text{He}/^4\text{He}$ Ratios in the Chugoku District, Southwestern Japan. *Pure Appl. Geoph.* 163, 745-757.
- Sano, Y. and Wakita, H., 1985. Geographical Distribution of $^3\text{He}/^4\text{He}$ Ratios in Japan: Implications for Arc Tectonics and Incipient Magmatism. *Journal of Geophysical Research* 90, 8729-8741.
- Sano, Y., Takahata, N., Seno, T., 2006. Geographical Distribution of $^3\text{He}/^4\text{He}$ Ratios in the Chugoku District, Southwestern Japan. *Pure Appl. Geoph.* 163, 745-757.
- Seward, T.M., Williams-Jones, A.E. and Migdisov, A.A., 2014. The Chemistry of Metal Transport and Deposition by Ore-Forming Hydrothermal Fluids. 29-57.

- Shanks, W.C. and Thurston, R., 2012. Volcanogenic massive sulfide occurrence model. US Department of the Interior, US Geological Survey.
- Sillitoe, R.H., 2010. Porphyry Copper Systems. *Economic Geology*, 105(1): 3.
- Simmons, S.F. and Brown, K.L., 2006. Gold in magmatic hydrothermal solutions and the rapid formation of a giant ore deposit. *Science*, 314(5797): 288-91.
- Simmons, S.F., Brown, K.L., Browne, P.R.L. and Rowland, J.V., 2016. Gold and silver resources in Taupo Volcanic Zone geothermal systems. *Geothermics*, 59: 205-214.
- Simmons, S.F., Sawkins, F. and Schlutter, D., 1987. Mantle-derived helium in two Peruvian hydrothermal ore deposits. *Nature*, 329(6138): 429-432.
- Stefánsson, A., Hilton, D., Sveinbjörnsdóttir, Á.E., Torsander, P., Heinemeier, J., Barnes, J.D., Ono, S., Halldórsson, S.A., Fiebig, J., Arnórsson, S., 2017. Isotope systematics of Icelandic thermal fluids. *J. Volcanol. Geotherm. Res.* 337, 146-164.
- Stracke, A., Zindler, A., Salters, V. J. M., McKenzie, D., Blichert-Toft, J., Albarède, F. and Grönvold, K., 2003. Theistareykir revisited. *Geochemistry, Geophysics, Geosystems* 4(2).
- Stuart, F. M., Lass-Evans S., Godfrey Fitton J. and Ellam R. M., 2003. High $^3\text{He}/^4\text{He}$ ratios in picritic basalts from Baffin Island and the role of a mixed reservoir in mantle plumes. *Nature* 424(6944): 57-59.
- Stuart, F.M., Burnard, P.G., Taylor, R.P., Turner, G., 1995. Resolving mantle and crustal contributions to ancient hydrothermal fluids: He-Ar isotopes in fluid inclusions from Dae Hwa W-Mo mineralisation, South Korea. *Geochim. Cosmochim. Acta*, 59(22): 4663-4673.
- Sun, W., Arculus, R.J., Kamenetsky, V.S. and Binns, R.A., 2004. Release of gold-bearing fluids in convergent margin magmas prompted by magnetite crystallization. *Nature*, 431(7011): 975-978.
- Sveinbjörnsdóttir, Á.E., Ármannsson, H., Óskarsson, F., Ólafsson, M., Sigurdardóttir, Á.K., 2015. A conceptual hydrological model of the thermal areas within the Northern neovolcanic zone, Iceland using stable water isotopes. *Proc. World Geother. Congr. 2015*, pp. 1–7.

- Sveinbjörnsdóttir, Á., Ármannsson, H., Ólafsson, M., Óskarsson, F., Markússon, S., Magnúsdóttir, S., 2013. The Theistareykir geothermal field, NE Iceland. Isotopic characteristics and origin of circulating fluids. *Proc. Earth. Planet. Sci.* 7, 822-825.
- Symonds, R.B., Rose, W.I., Reed, M.H., Lichte, F.E. and Finnegan, D.L., 1987. Volatilization, transport and sublimation of metallic and non-metallic elements in high temperature gases at Merapi Volcano, Indonesia. *Geochimica et Cosmochimica Acta*, 51(8): 2083-2101.
- Tivey, M.K., 2007. Generation of seafloor hydrothermal vent fluids and associated mineral deposits. *Oceanography*, 20(1): 50-65.
- Tosdal, R.M., Dilles, J.H. and Cooke, D.R., 2009. From Source to Sinks in Auriferous Magmatic-Hydrothermal Porphyry and Epithermal Deposits. *Elements*, 5(5): 289-295.
- Torgersen, T., Jenkins, W., 1982. Helium isotopes in geothermal systems: Iceland, the geysers, raft river and steamboat springs. *Geochim. Cosmochim. Acta* 46, 739-748.
- van Hinsberg, V., Vigouroux, N., Palmer, S., Berlo, K., Mauri, G., Williams-Jones, A., et al., 2017. Element flux to the environment of the passively degassing crater lake-hosting Kawah Ijen volcano, Indonesia, and implications for estimates of the global volcanic flux. *Geological Society London Special Publications*, 1–26. <http://doi.org/10.6084/m9.figshare.c.2134359>
- Varekamp, J. C., Ouimette, A. P., Herman, S. W., Bermúdez, A., & Delpino, D., 2001. Hydrothermal element fluxes from Copahue, Argentina: A “beehive” volcano in turmoil. *Geology*, 29(11), 1059. doi:10.1130/0091-7613(2001)029<1059:heffca>2.0.
- Wahrenberger, C., Seward, T. and Dietrich, V., 2002. Volatile trace-element transport in high-temperature gases from Kudriavy volcano (Iturup, Kurile Islands, Russia). *Geochemical Society Special Publication*, 7: 307-327.
- Weiss, R.F., Lonsdale, P., Lupton, J.E., Bainbridge, A.E. and Craig, H., 1977. Hydrothermal plumes in the Galapagos Rift. *Nature*, 267: 600.
- Weissberg, B.G., Browne, P.R. and Seward, T.M., 1979. Ore metals in active geothermal systems. *Geochemistry of hydrothermal ore deposits*: 738-780.

- Williams-Jones, A. and Migdisov, A., 2014. Experimental constraints on the transport and deposition of metals in ore-forming hydrothermal systems. *Society of Economic Geologists*, 18: 77-96.
- Williams-Jones, A.E., Migdisov, A.A., Archibald, S.M. and Xiao, Z., 2002. Vapor-transport of ore metals. *Water–Rock Interaction, Ore Deposits, and Environmental Geochemistry: A Tribute to David A. Crerar*: 279-306.
- Witham, F., Blundy, J., Kohn, S. C., Lesne, P., Dixon, J., Churakov, S. V., & Botcharnikov, R., 2012. SolEx: A model for mixed COHCl-volatile solubilities and exsolved gas compositions in basalt. *Computers & Geosciences*, 45, 87–97. doi:10.1016/j.cageo.2011.09.021
- Wu, L.-Y., Hu, R.-Z., Li, X.-F., Stuart, F.M., Jiang, G.-H., Qi, Y.-Q. and Zhu, J.-J., 2017. Mantle volatiles and heat contributions in high sulfidation epithermal deposit from the Zijinshan Cu-Au-Mo-Ag orefield, Fujian Province, China: Evidence from He and Ar isotopes. *Chemical Geology*.
- Yang, K. and Scott, S.D., 2006. Magmatic fluids as a source of metals in seafloor hydrothermal systems. *Back-arc spreading systems: geological, biological, chemical, and physical interactions*: 163-184.
- Yardley, B.W.D., Bodnar, R.J., 2014. Fluids in the Continental Crust. *Geochem. Perspect.*, 3(1): 1-127.
- Zoller, W. H., Parrington J. R. and Phelan Kotra J. M., 1983. Iridium enrichment in airborne particles from Kilauea volcano – January 1983. *Science* 222, 1118–1121.

3.11 Figures

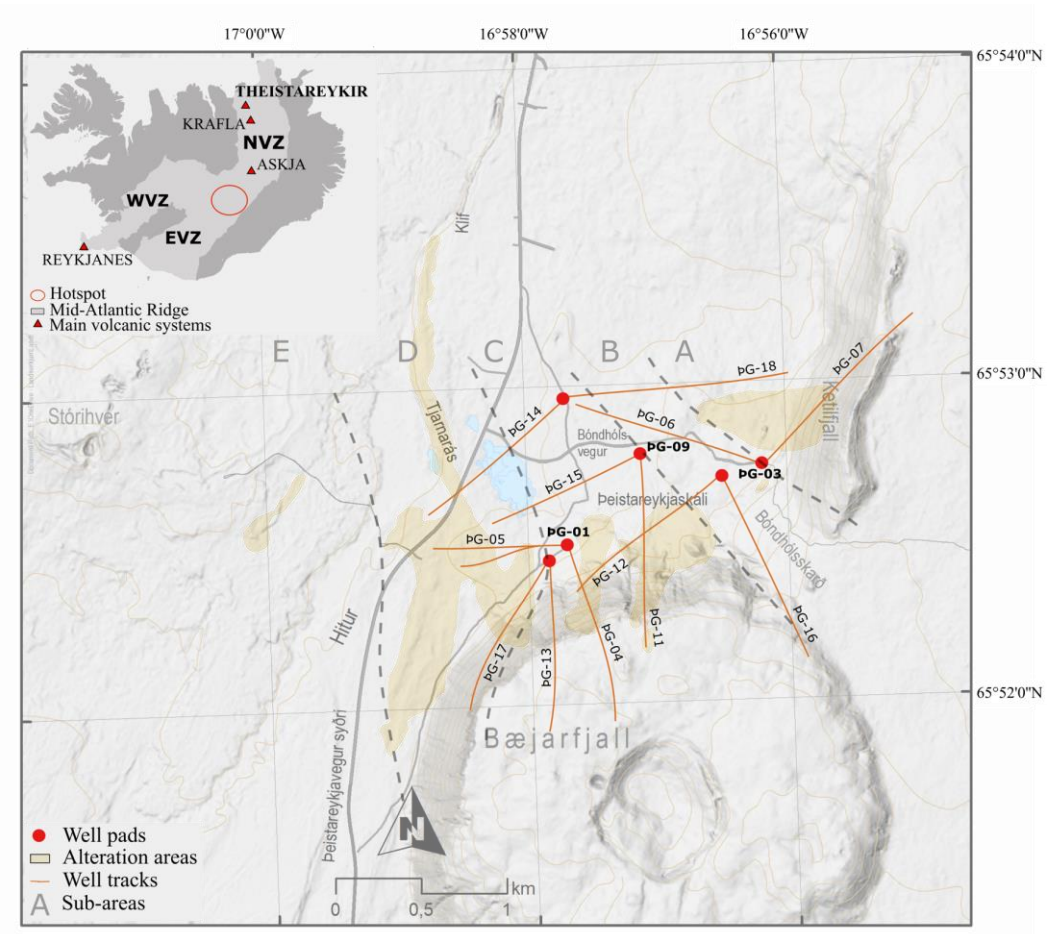


Figure 3-1 : Simplified map of the Theistareykir geothermal field with major alteration zones and positions of the sampled sites (wells) indicated. Numbers on the X- and Y- axes indicate the latitudinal and longitudinal geographical coordinates respectively on the World Geodetic System 1984 (WGS84). NVZ = Northern Volcanic Zone; WVZ = Western Volcanic Zone; EVZ = Eastern Volcanic Zone.

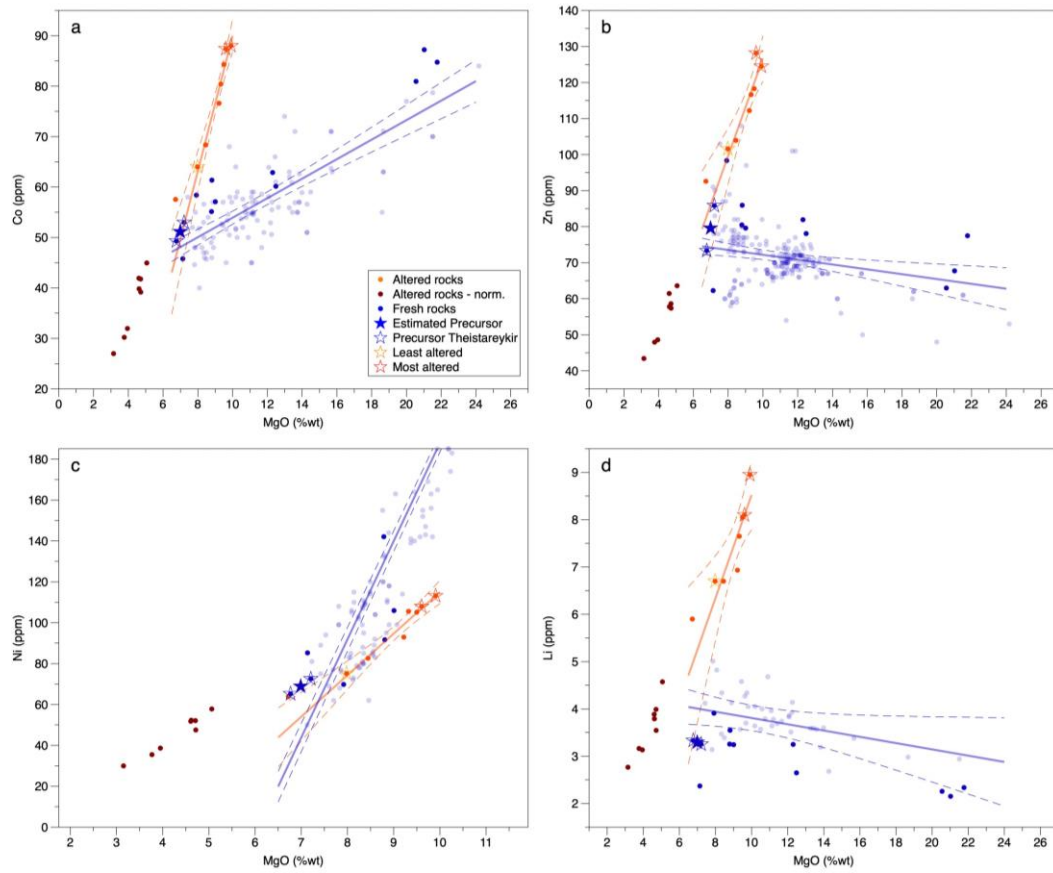


Figure 3-2 : Alteration trends of variably altered rocks and fresh rocks at Theistareykir for Co, Zn, Ni, Li against MgO.

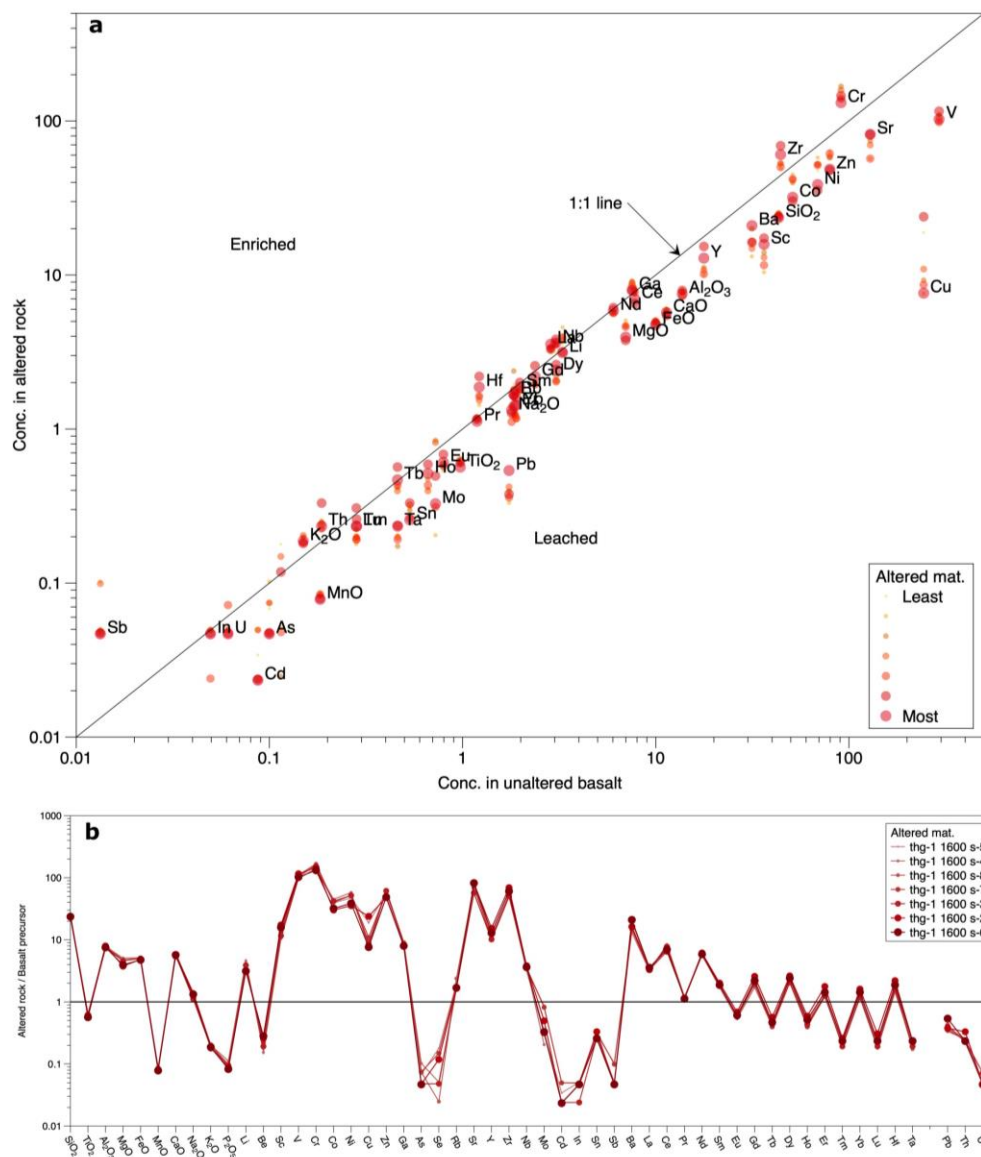


Figure 3-3 : Comparison between altered rock fresh basalt. a. Concentration of 8 sub-samples of variably altered rocks against the average concentration in fresh rocks. b. Variably altered rocks normalized to the fresh rocks.

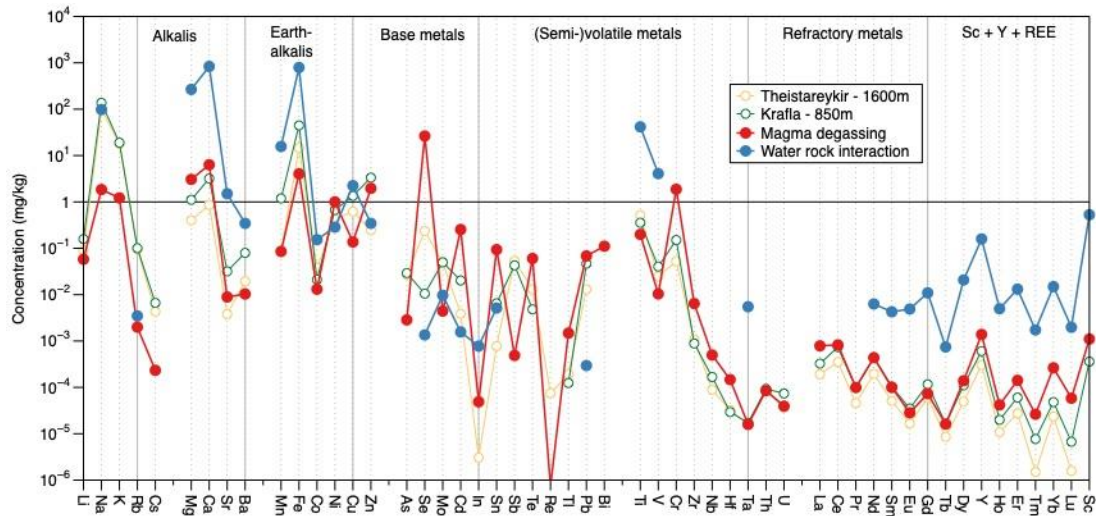


Figure 3-4 : Estimation of the magmatic and water-rock interaction contributions using the enrichment factors (EF) for every element. Results are compared to the deep fluids compositions.

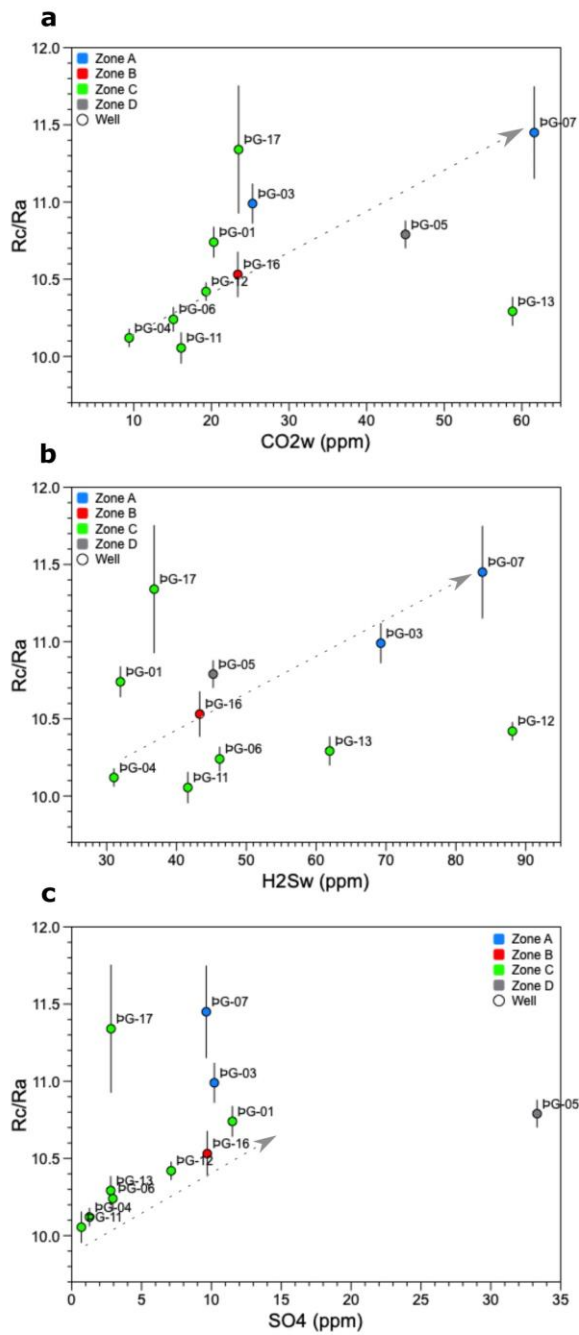


Figure 3-5 : The R_c/R_a ratio compared to the major gases CO_2 and H_2S , and to SO_4 .

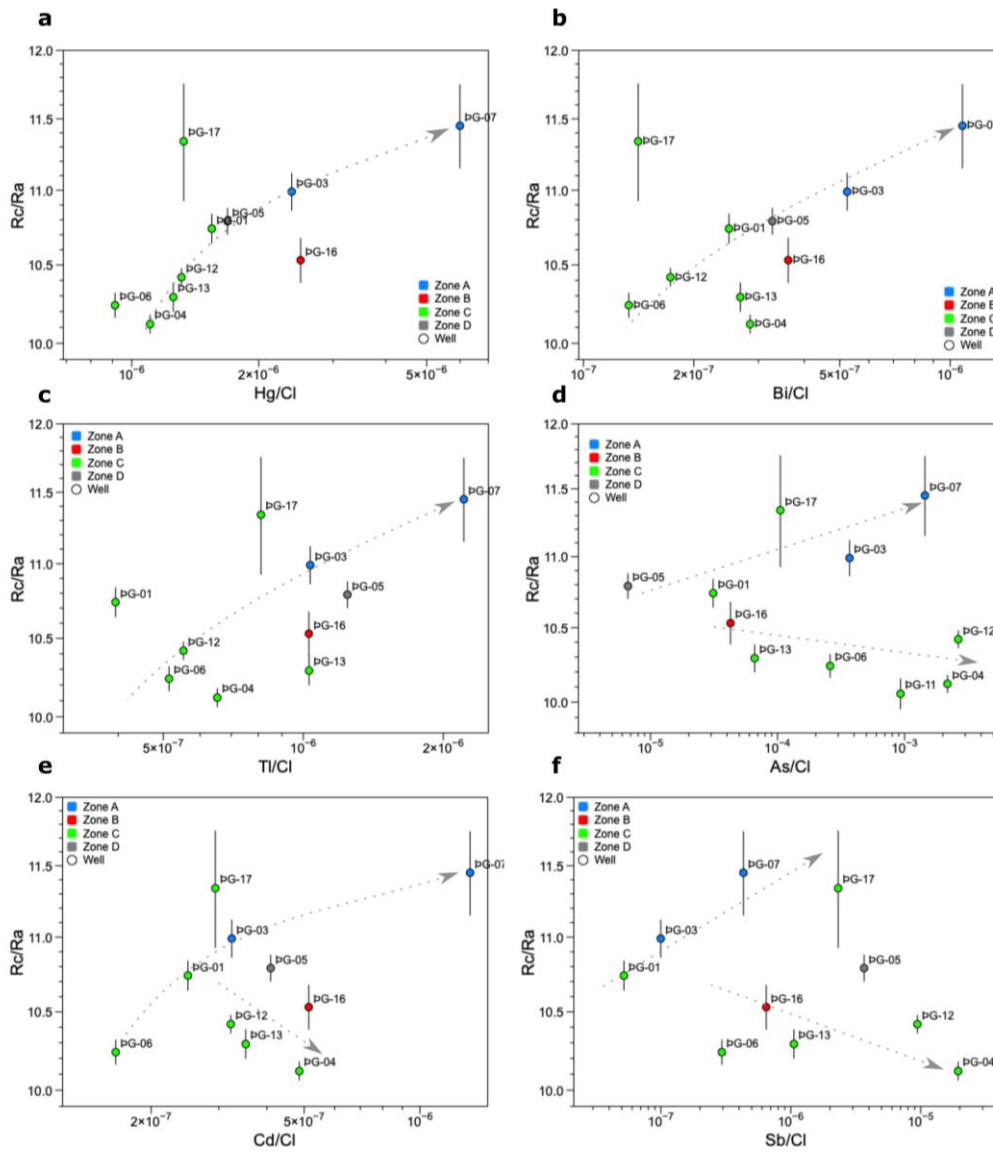


Figure 3-6 : The R_c/R_a ratio compared to the most volatile metals (Hg, Bi, Tl, Cd, As and Sb) normalized to chlorine.

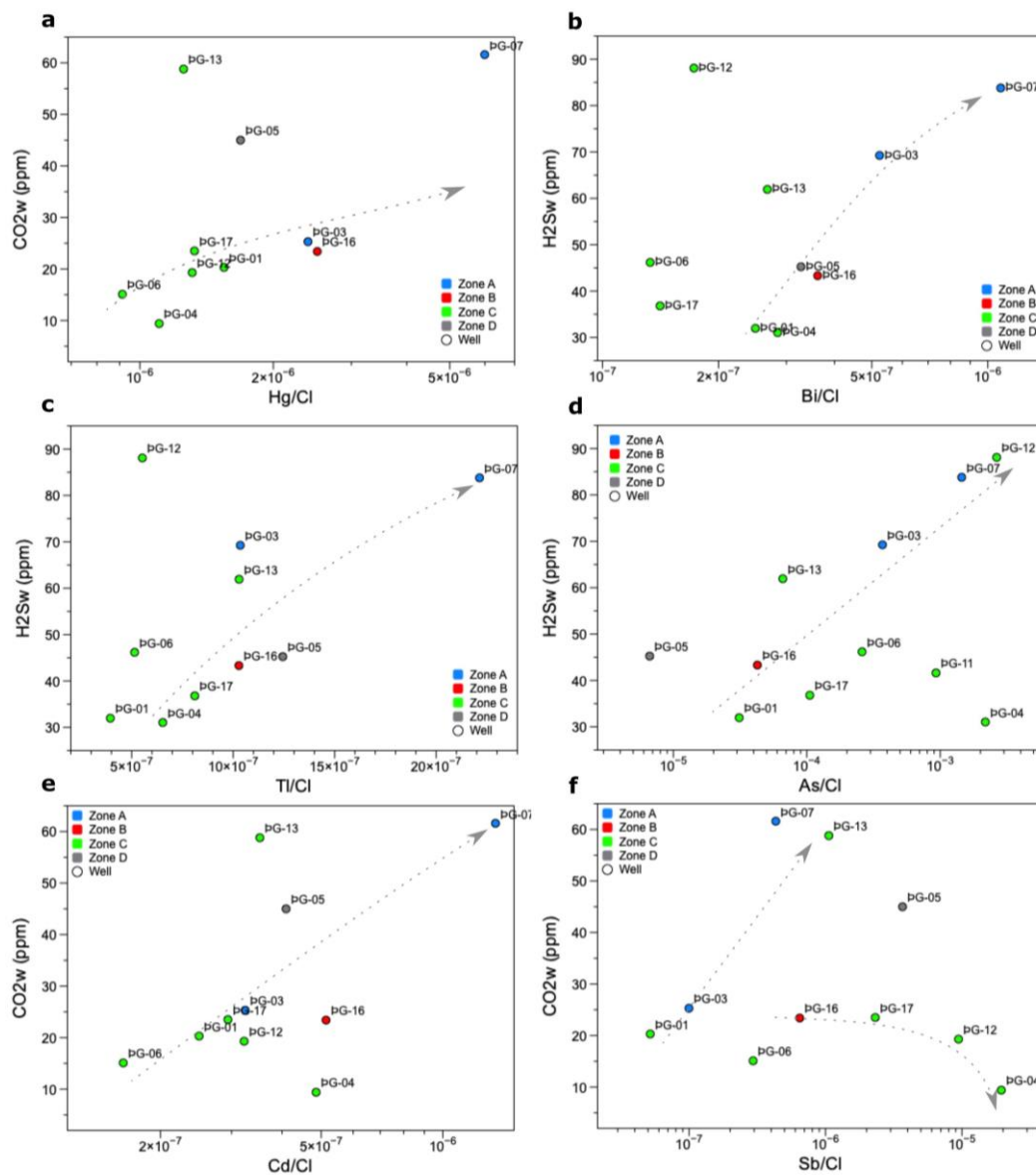
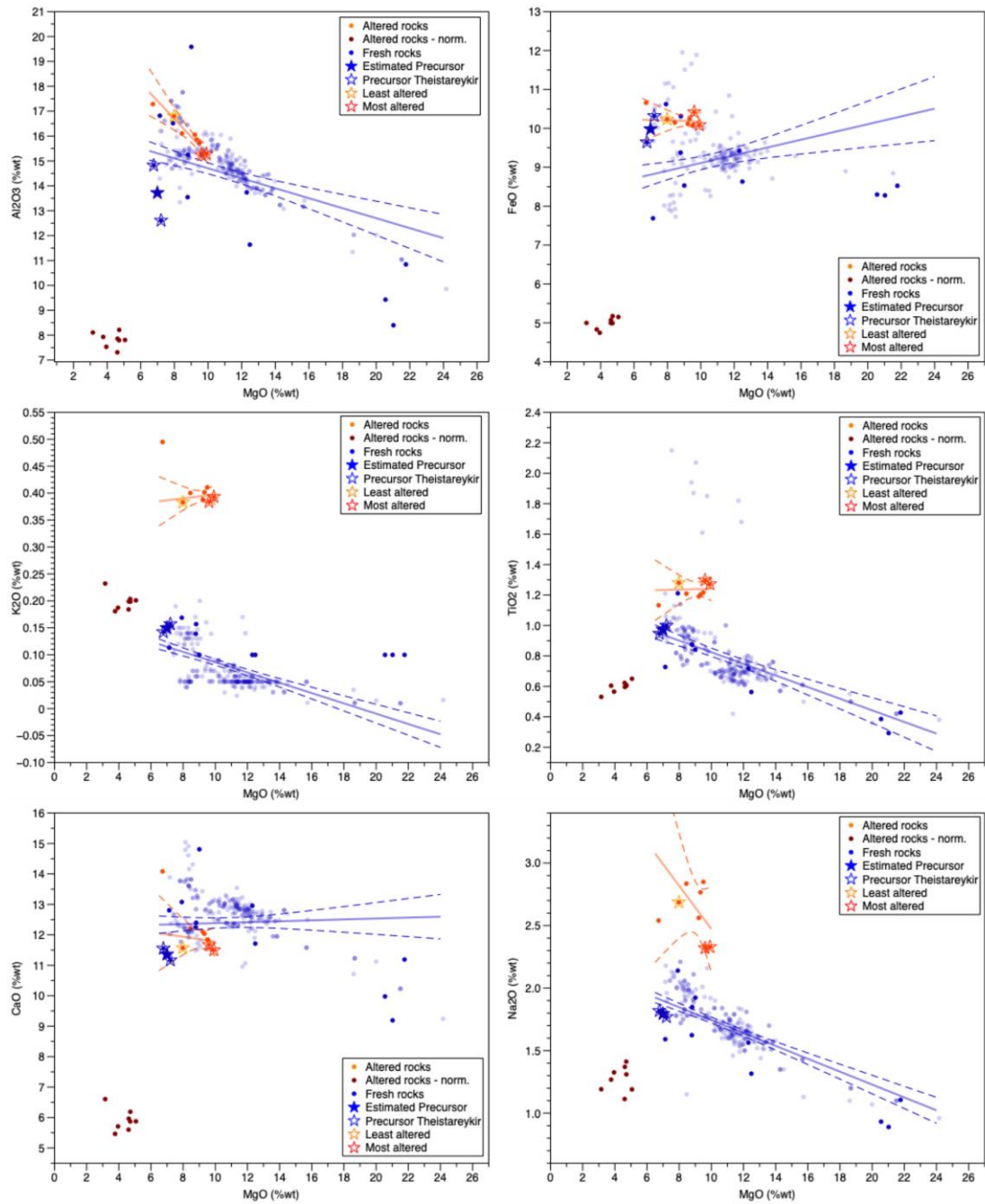
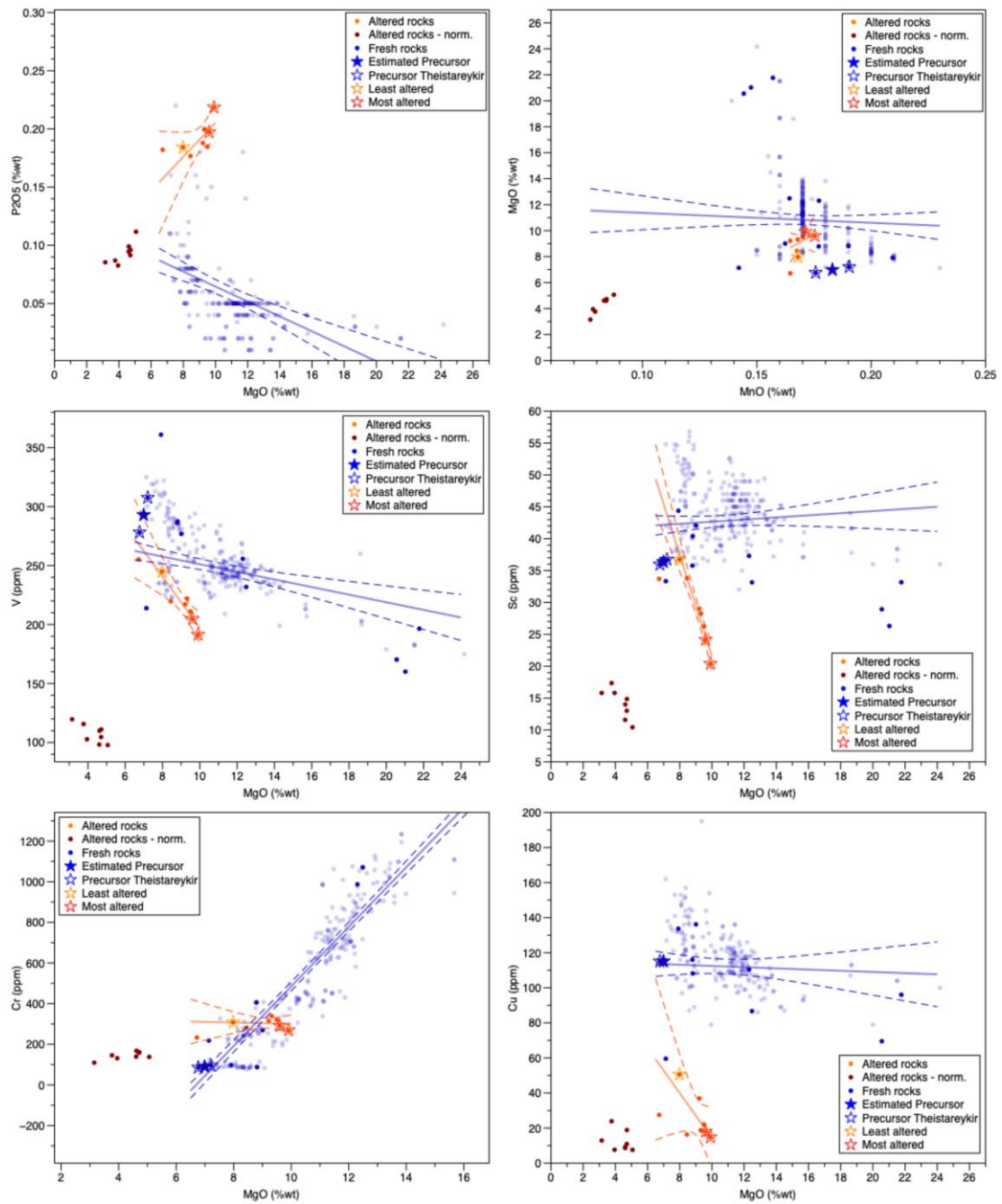


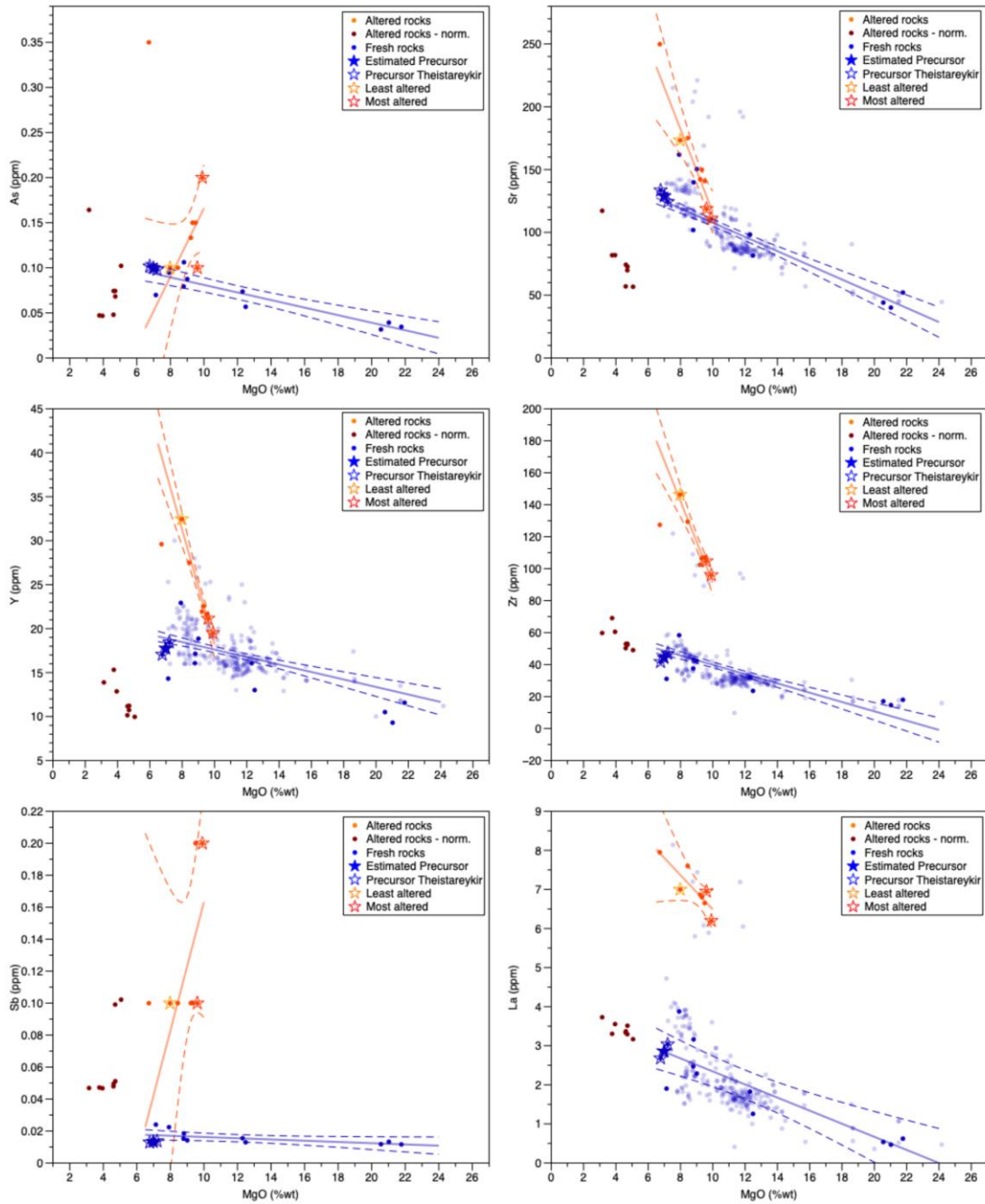
Figure 3-7 : Volatile metals Hg, Bi, Tl, Cd, As and Sb normalized to chlorine compared to the major gases CO_2 and H_2S .

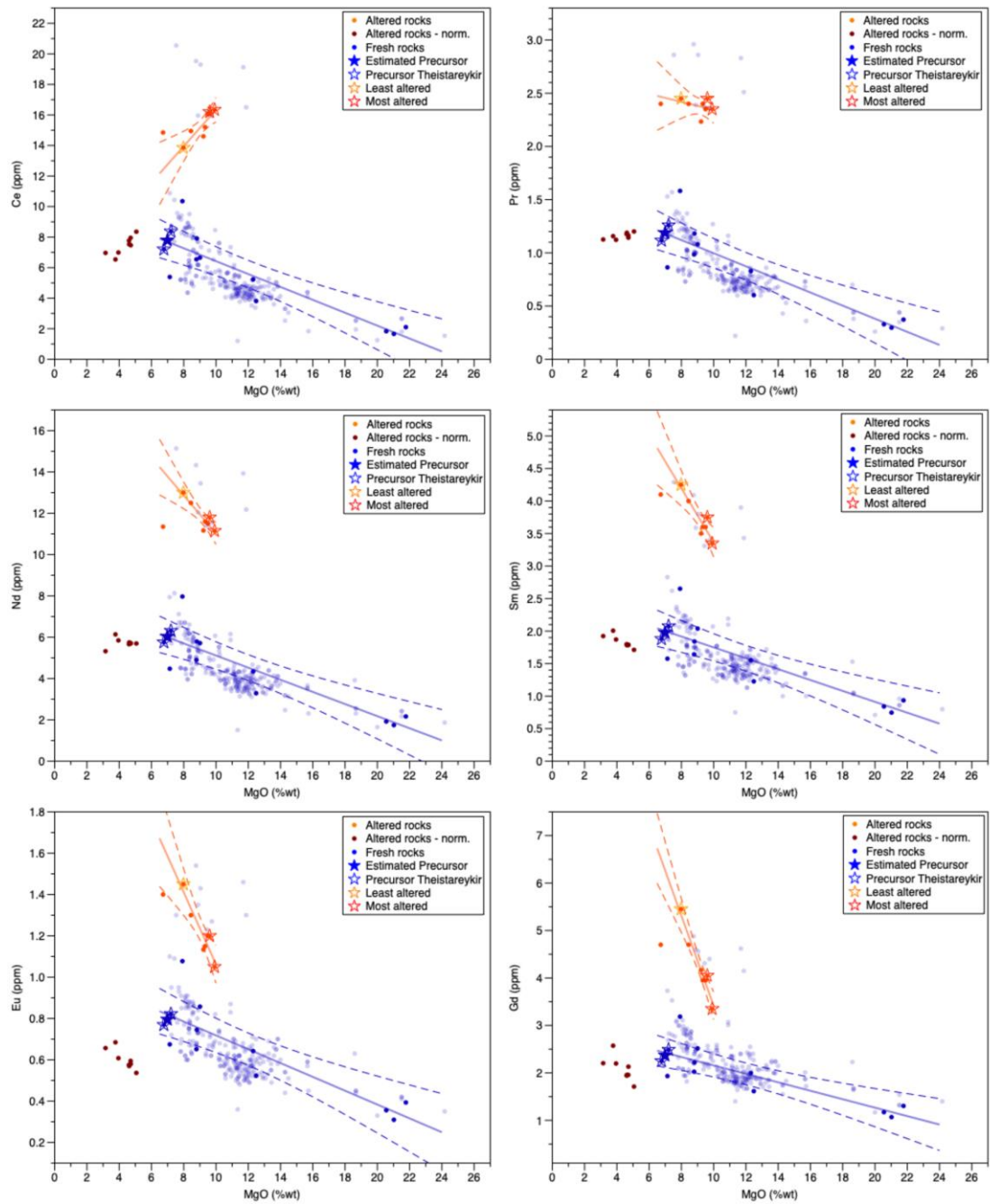
3.12 Supplementary material

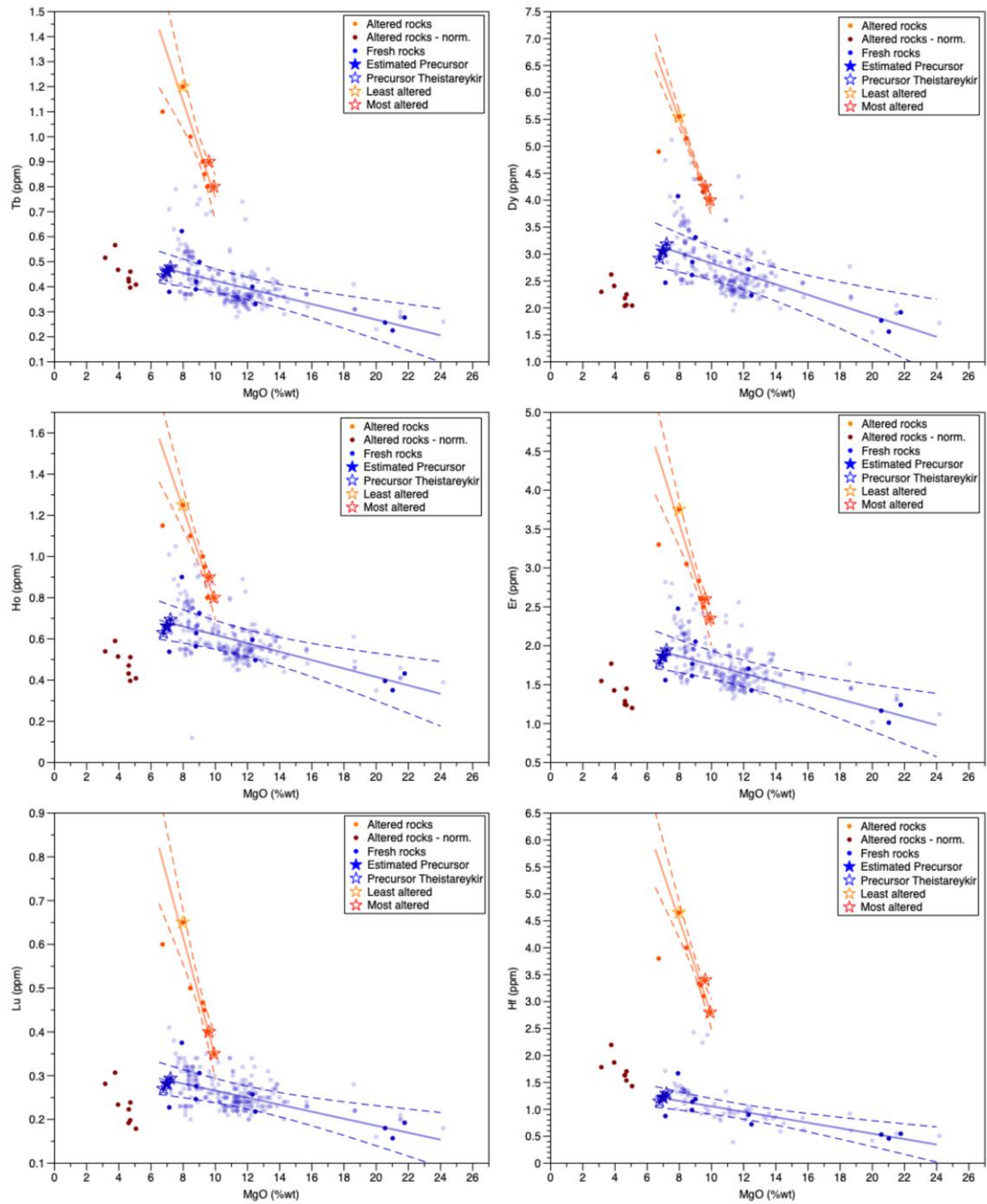
The following figures correspond to the alteration trends for all the elements relative to MgO except for the ones presented in Figure 3-2 of this thesis.

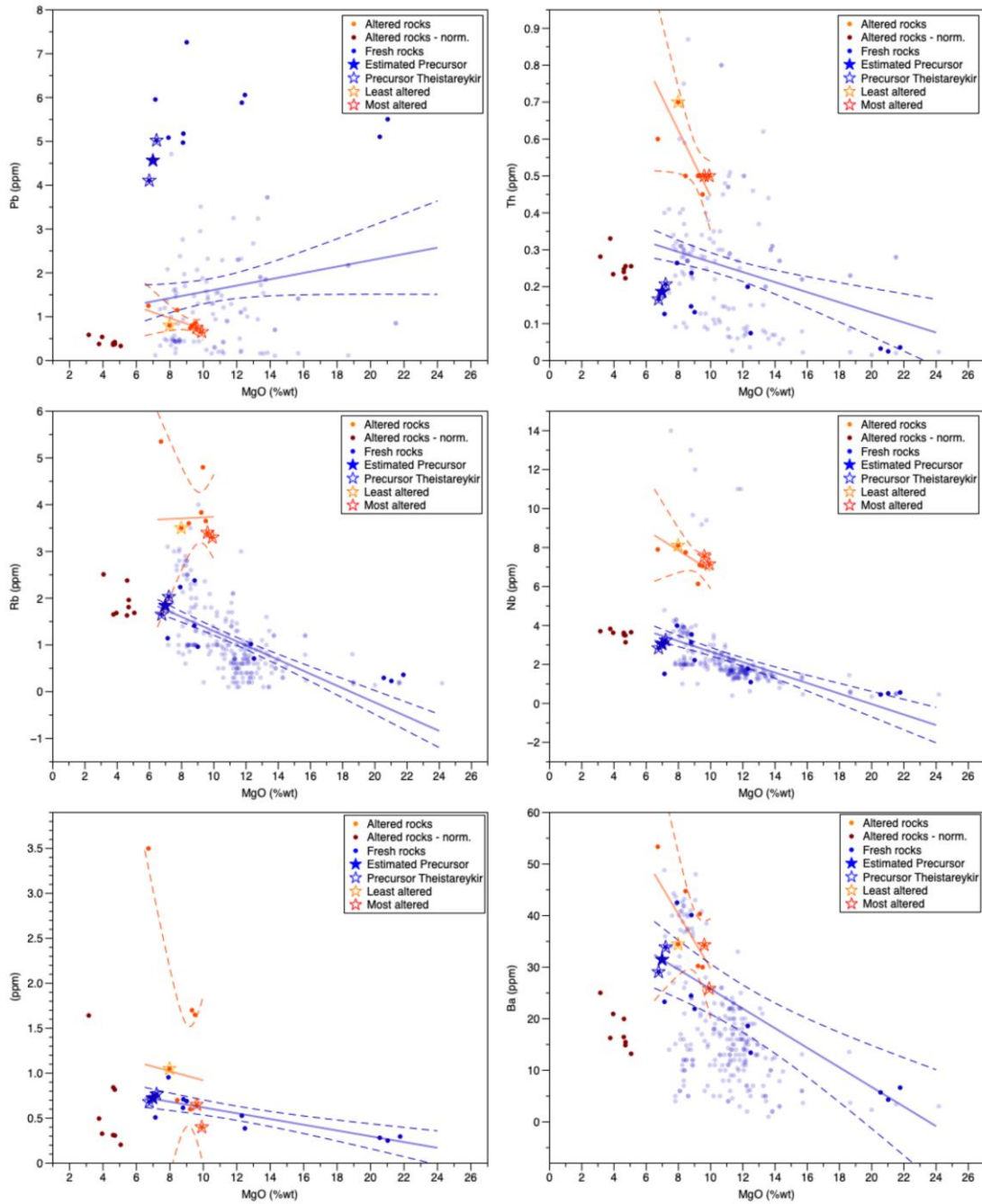


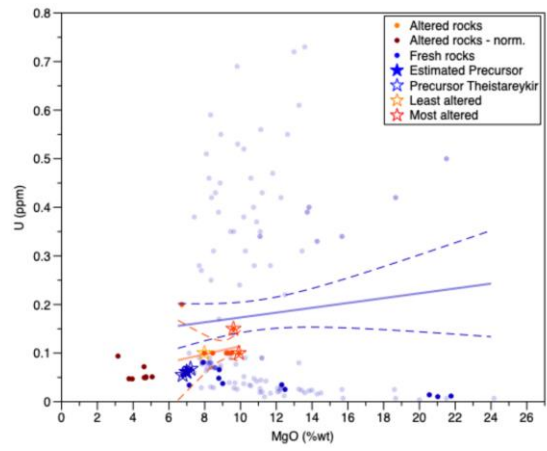
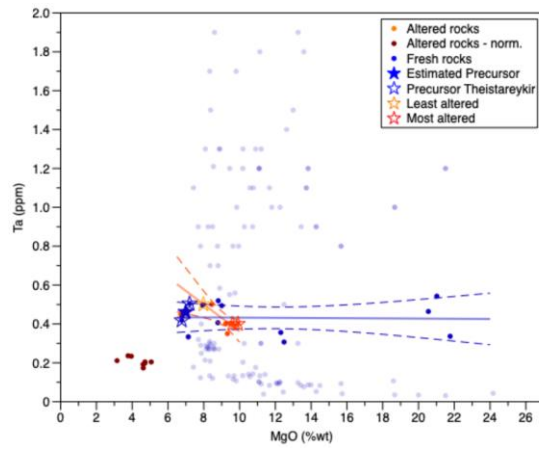












CONCLUSION

Magmatic-hydrothermal systems are sites of geothermal production of energy, but also areas where metals can accumulate over geological time to form exploitable ore deposits, particularly Cu-Au-Ag porphyry and epithermal ores. Understanding the origins of metals in these systems is a key part to find exploitable resources. However, despite decades of studies, there is still an ongoing debate concerning the origin of the metal load of an active magmatic-hydrothermal system between magma degassing sourcing and rock leaching, and their respective contributions for individual constituents. The main objective of this thesis was to resolve this debate by studying the active high-enthalpy magmatic-related convective geothermal field of Theistareykir in Northeastern Iceland. Theistareykir, located in an oceanic spreading ridge is the ideal candidate to study metal origins and element behaviour in a magmatic-hydrothermal system given its status as a pristine geothermal field where fluids have not been irremediably disturbed by exploitation through recovery of steam and brine re-injection. Furthermore, magma compositions show negligible disturbance by magma differentiation or crustal assimilation, which can add complexity to the metal sources and their redistribution. Finally, Theistareykir provides unique access to a full cross-section of a geothermal reservoir, from surface fluids and gases emitted from wells and natural manifestations, to deep reservoir fluids sampled down-well, to the altered rocks that host the fluids and the precursor basalts from which these formed.

The original aspect of this work is to combine noble gases and their isotopes with metal abundances. The noble gases are a class of volatiles which are inert and rare, and have distinct isotopic signatures for their sourcing reservoirs (e.g., Ballentine et al., 2002). They enable us to differentiate between the mantle (the source of heat, mantle-derived

isotopes and possibly metals); the atmosphere (sourcing meteoric water and atmospheric gases to the system); and the crust (releasing metals and radiogenic isotopes through water-rock interactions).

Thanks to this approach, we could discriminate the two above-mentioned sources of metals in the system, determine that both contribute to the metal load, and quantify their relative importance. The resulting geochemical tools can be transferred to other, more complex magmatic-hydrothermal systems, such as those within volcanic-arc settings which are normally the areas, within tectonic plates, where porphyry and epithermal associated ore deposits form.

It is well established that the fluids released by the magma are relatively enriched in metals compared to their host magma (Hedenquist et al., 1993), and that these fluids therefore sequester the metals and inject them into the hydrothermal system. However, it was not clearly defined whether a sufficient mass of metal can be released in this process to lead to the genesis of ore deposits (Yang and Scott, 2006). On the other hand, the mass balance on weathered rocks and their fresh counterparts shows a significant mobilization of metals, linked to the high temperatures of hydrothermal fluids and their high ligand concentrations such as halogens (Williams-Jones and Migdisov, 2014, Seward et al. al., 2014). Leaching of rocks therefore appears to be an effective mechanism for the concentration of metals in hydrothermal fluids.

Since fluids are the main carriers of metals, it is of primary importance to define the source(s) of water as well as its role in the dynamics of an active magmatic-hydrothermal system. For this, the use of noble gases as a tool for discriminating between sources of fluids has proved particularly interesting. The analysis of isotopes of noble gases, and more particularly of helium, makes it possible to constrain the sources of mantle-derived, atmospheric and crustal fluids, thanks to their distinct

isotopic signatures ($R/Ra = (^3\text{He}/^4\text{He}_{\text{sample}})/(^3\text{He}/^4\text{He}_{\text{air}})$) (Ballentine and Burnard, 2002; Saar et al., 2005; Mazor and Truesdell, 1984; Kennedy et al., 1991; Kennedy and Van Soest, 2007). The analysis of water isotopes ($\delta^{18}\text{O}$ and $\delta^2\text{H}$) makes it possible to further discriminate between the different water sources in the magmatic-hydrothermal system (Craig, 1961; Stefánsson et al., 2017).

In the first chapter of this thesis, noble gas and water stable isotopes were therefore combined, together with heat (Q), to develop a conceptual model of the fluid sources and mode of circulation within the geothermal area under study. The results showed the presence of four fluid sources in the system: a magmatic fluid, old recharge water under colder climate conditions, sub-modern regionally recharged water in the highlands, and a modern meteoric water component. The combined $^3\text{He}/^4\text{He}$ and the $Q/^3\text{He}$ signature of fluids allow for distinguishing the conduction/convection regimes of volatile transfer from the magma to the system in the different exploited areas of Theistareykir and confirm that little boiling affects the deep fluids. The $\delta^{18}\text{O}$ and $^3\text{He}/^4\text{He}$ ratios indicate a slight change in the chemistry of the original fluid caused by local water-rock interaction, which increase $\delta^{18}\text{O}$ and decrease the $^3\text{He}/^4\text{He}$ by adding radiogenically-produced ^4He . Noble gases ultimately provided us with information on specific wells affected by direct magma degassing, which is critical information for estimating both heat release and system chemical load.

After precisely determining the sources of fluids as well as the general dynamics of the Theistareykir hydrothermal system, it was possible to focus on analyzing the metal content of both fluids and rocks to discriminate the sources of metals, namely those from magmatic degassing or those from rock leaching (Chapter 2). For this, we were able to sample and analyze the fluids located at a depth of up to 1.6 km using a titanium sampler unique in the world (Simmons and Brown, 2006), and evaluate the metal content of these deep fluids compared to those sampled at the surface.

Metals present in active magmatic-hydrothermal systems are impacted by different processes between depth and surface. The decrease in pressure induces boiling and fluid partitioning between the high-density brine that remains in the deep system and the relatively light vapors that rise through the well to the surface (Hedenquist and Lowenstern, 1994). The drop in pressure and temperature (surface water cooling) higher in the hydrothermal system induces second boiling (Spycher and Reed, 1989; Hedenquist, 1991). The boiling process plays a key role in precipitating metals and other elements in scale and preferentially releasing the volatiles. Although it has long been assumed that metals precipitate entirely from aqueous fluids, several recent studies have shown that volatile metals can also be concentrated in and precipitated from the vapor phase (Nadeau et al, 2010, Williams-Jones & Heinrich, 2005; Hurtig & Williams-Jones, 2016).

The results of the analysis of deep and surface fluids confirmed that that the deep fluids are relatively enriched in base metals and (semi)-volatile metals (in particular Te, Hg, Re and Tl) compared to local basalt, and that this reflects element input from both magma degassing and water-rock interaction. Boiling of this deep fluid results in a well-head composition that is significantly depleted in most elements, and has a distinct elemental signature, including a characteristic depletion in Sb that is mirrored in the altered rocks, and a depletion in the base metals that shows their selective sequestration in scale minerals, likely sulfides. The element content and patterns in surface fluids can thus not be interpreted to reflect that of the deep fluid. The behavior of elements in Theistareykir and closely-located Krafla fluids is consistent, and largely agrees with similar data obtained for the Reykjanes geothermal system in SW Iceland, and we therefore posit that our results are representative for this geological setting and indicate a significant magmatic degassing input to deep fluids variably modified by water-rock interaction.

Finally, thanks to the combination of the study of noble gases as tracers of the contribution of magmatic fluids, of the alteration flux of the host rocks, and of the application of the emanation coefficient to the fresh rock composition, we were able to constrain the relative contributions of magma degassing and water-rock interaction to the deep reservoir fluid (Chapter 3). There is remarkable consistency between the predicted magmatic degassing fluid and the measured composition of deep Theistareykir geothermal fluids, with an estimated contribution of 80% of magma degassing and the remainder from water-rock interaction. The R_c/R_a ratio ($(^3\text{He}/^4\text{He})_{\text{sample}}/(^3\text{He}/^4\text{He})_{\text{air}}$) of surface wells has been used as a tracer of the relative contribution of magma degassing across the geothermal field, and presents a strong positive correlation with some of the most volatile metals (Hg and Bi). Helium isotopes indicate a contribution of mantle helium of 82.3%, thereby confirming the result obtained from the metal analyses, and indicating that the element load of Theistareykir geothermal reservoir fluids is dominated by magmatic input.

This work has brought important new insights regarding the behaviour of metals in active magmatic-hydrothermal systems hosted by basalt. Noble gases have been used with great success to better constrain sources and transport of volatile metals in these systems, which is of prime importance for both economic geology and for geothermal energy use, in order to explore and exploit these systems while respecting sustainability and the environment. Finally, this understanding gives a deeper insight into volcanic activity and eruptions, by providing information as to how gases and aqueous fluids evolve in magmatic systems.

BIBLIOGRAPHY

- Aiuppa, A., Baker, D.R. and Webster, J.D., 2009. Halogens in volcanic systems. *Chem Geol* 263, 1-18.
- Albarède, F., 1995. Introduction to geochemical modeling. Cambridge University Press, Cambridge, England, 543 pp.
- Allègre, C. J., Moreira M., and Staudacher T., 1995. $^4\text{He}/^3\text{He}$ dispersion and mantle convection. *Geophy Res Let* 22(17), 2325-2328.
- Alletti, M., Baker, D. R., Scaillet, B., Aiuppa, A., Moretti, R., & Ottolini, L., 2009. Chlorine partitioning between a basaltic melt and H₂O–CO₂ fluids at Mount Etna. *Chemical Geology*, 263(1-4), 37–50. doi:10.1016/j.chemgeo.2009.04.003
- Andrews, J.N., Kay, R.L.F., 1983. The U contents and $^{234}\text{U}/^{238}\text{U}$ activity ratios of dissolved uranium in groundwaters from some Triassic Sandstones in England. *Chem. Geol.* 41, 101-117.
- Ármannsson, H, Gíslason, G, Torfason, H, 1986. Surface exploration of the Theistareykir high-temperature geothermal area, Iceland, with special reference to the application of geochemical methods. *Appl. Geochem.* 1, 47-64.
- Ármannsson, H., 2015. The fluid geochemistry of Icelandic high temperature geothermal areas. *Appl. Geochem.* 66, 14-64.
- Arnaldsson, A., Halldórsdóttir, S., Kjarran S.P., Axelsson G., 2011. Computational model of the geothermal system at Theistareykir and initial capacity assessment. ÍSOR report: ÍSOR-2011/049, 58p. (In Icelandic).

- Árnason, B., 1977. Hydrothermal systems in Iceland traced by deuterium. *Geothermics* 5, 125–151.
- Arnórsson, S., Andrésdóttir, A., 1995. Processes controlling the distribution of boron and chlorine in natural waters in Iceland. *Geochim. Cosmochim. Acta* 59, 4125–4146.
- Arnórsson, S., Stefánsson, A., Bjarnason, J.O., 2007. Fluid-fluid interactions in geothermal systems. *Reviews in Mineralogy and Geochemistry* 65:259-312.
- Arnórsson, S. and Stefánsson, A., 2005. Wet-steam well discharges. II. Assessment of aquifer fluid.
- Audétat, A. and Edmonds, M., 2020. Magmatic-hydrothermal fluids. *Elements*, 16: 401-406.
- Audétat, A. and Pettke, T., 2003. The magmatic-hydrothermal evolution of two barren granites: a melt and fluid inclusion study of the Rito del Medio and Canada Pinabete plutons in northern New Mexico (USA). *Geochimica et Cosmochimica Acta*, 67(1): 97-121.
- Baker, E.T., Lupton, J.E. 1990. Changes in submarine hydrothermal ^3He /heat ratios as an indicator of magmatic/tectonic activity. *Nature* 346, 556-558.
- Bali, E., Aradi, L. E., Zierenberg, R., Diamond, L. W., Pettke, T., Szabo, A., et al., 2020. Geothermal energy and ore-forming potential of 600 °C mid-ocean-ridge hydrothermal fluids. *Geology*, 48(12), 1221–1225).
- Ballentine, C.J. and Burnard, P.G., 2002. Production, release and transport of noble gases in the continental crust. *Rev. Mineral. Geochem.* 47, 481-538.

- Ballentine, C.J., O’Nions, R.K., 1994. The use of natural He, Ne and Ar isotopes to study hydrocarbon-related fluid provenance, migration and mass balance in sedimentary basins. *Geol. Soc. London Spec. Publ.* 78, 347-361.
- Bangma P., 1961. The Development and Performance of a Steam-Water Separator for use on Geothermal Bores, Mechanical Engineer, Ministry of Works, Wairakei, New Zealand.
- Barnes, H. and Seward, T., 1997. Geothermal systems and mercury deposits. *Geochemistry of hydrothermal ore deposits*, 3: 699-736.
- Benson, B.B., Krause Jr, D., 1980. Isotopic fractionation of helium during solution: A probe for the liquid state. *J. Sol. Chem.* 9, 895-909.
- Berger, B.R. and Bethke, P.M., 1985. *Geology and geochemistry of epithermal systems.* Society of economic geologists.
- Berning, J., Cooke, R., Hiemstra, S. and Hoffman, U., 1976. The Rössing uranium deposit, south west Africa. *Economic Geology*, 71(1): 351-368.
- Birkle, P., Portugal Marín, E., Pinti, D.L. and Castro, M.C., 2016. Origin and evolution of geothermal fluids from Las Tres Vírgenes and Cerro Prieto fields, Mexico - Co-genetic volcanic activity and paleoclimatic constraints. *Appl. Geochem.* 65, 36-53.
- Bodnar, R.J., 1995. Fluid inclusion evidence for a magmatic source for metals in porphyry copper deposits. In: Thompson, J.F.H. (Ed.) *Magmas, Fluids and Ore Deposits.* Mineralogical Association of Canada Short Course Series Volume 23, pp. 139-152.
- Breddam K., Kurz, M.D., 2001. Helium isotope signatures of Icelandic alkaline lavas. *EOS Trans. Am. Geophys. Union* 82, F1315.

- Breddam, K., Kurz, M.D., Storey, M., 2000. Mapping out the conduit of the Iceland mantle plume with helium isotopes. *Earth Planet. Sci. Lett.* 176, 45-55.
- Brown, K.L., Simmons, S.F., 2000. Precious metals in high-temperature geothermal systems in New Zealand. *Geothermics* 32, 619–625.
- Burnard, P., 1999. The bubble-by-bubble volatile evolution of two mid-ocean ridge basalts. *Earth and Planetary Science Letters*, 174(1): 199-211.
- Burnard, P., 2001. Correction for volatile fractionation in ascending magmas: noble gas abundances in primary mantle melts. *Geochimica et Cosmochimica Acta*, 65(15): 2605-2614.
- Burnard, P., 2004. Diffusive fractionation of noble gases and helium isotopes during mantle melting. *Earth Planet. Sci. Lett.* 220, 287-295.
- Burnard, P., Graham, D. and Farley, K., 2004. Fractionation of noble gases (He, Ar) during MORB mantle melting: a case study on the Southeast Indian Ridge. *Earth and Planetary Science Letters*, 227(3): 457-472.
- Burnard, P.G. and Polya, D.A., 2004. Importance of mantle derived fluids during granite associated hydrothermal circulation: He and Ar isotopes of ore minerals from Panasqueira 1 Associate editor: R. Wieler. *Geochimica et Cosmochimica Acta*, 68(7): 1607-1615.
- Burnard, P.G., Hu, R., Turner, G., Bi, X.W., 1999. Mantle, crustal and atmospheric noble gases in Ailaoshan Gold deposits, Yunnan Province, China. *Geochim. Cosmochim. Acta*, 63(10): 1595-1604
- Burnham, C.W., 1979. Magmas and hydrothermal fluids. *Geochemistry of Hydrothermal Ore Deposits.*: 71-136.

- Candela, P. and Piccoli, P., 2005. Magmatic processes in the development of porphyry-type ore systems. *Economic Geology*, 100: 25-37.
- Candela, P., 1989. Magmatic ore-forming fluids: thermodynamic and mass-transfer calculations of metal concentrations. In ore deposition associated with magmas. *Rev. Econ. Geol.*, 4: 203-221.
- Candela, P.A. and Holland, H.D., 1984. The partitioning of copper and molybdenum between silicate melts and aqueous fluids. *Geochimica et Cosmochimica Acta*, 48(2): 373-380.
- Candela, P.A. and Holland, H.D., 1986. A mass transfer model for copper and molybdenum in magmatic hydrothermal systems; the origin of porphyry-type ore deposits. *Economic Geology*, 81(1): 1-19.
- Černý, P. and Ercit, T.S., 2005. The classification of granitic pegmatites revisited. *The Canadian Mineralogist*, 43(6).
- Chambeforet, I., & Stefansson, A., 2020. Fluids in Geothermal Systems. *Elements*, 16, 407–411
- Christenson, B. and Wood, C., 1993. Evolution of a vent-hosted hydrothermal system beneath Ruapehu Crater Lake, New Zealand. *Bulletin of volcanology*, 55(8): 547-565.
- Clark, I., 2015. *Groundwater Geochemistry and Isotopes*. Boca Raton: CRC Press, <https://doi.org/10.1201/b18347>
- Clark, J.R. and Williams-Jones, A.E., 1990. Analogues of epithermal gold–silver deposition in geothermal well scales. *Nature*, 346(6285): 644-645.

- Clarke, W. B., W. J. Jenkins and Z. Top, 1976. "Determination of tritium by mass spectrometric measurement of ^3He ." *The International Journal of Applied Radiation and Isotopes* 27: 515-522.
- Clarke, W.B., Jenkins, W.J., Top, Z., 1976. Determination of tritium by mass spectrometric measurement of ^3He . *Appl. Radiat. Isot.* 27, 515-522.
- Cline, J.S. and Bodnar, R.J., 1991. Can economic porphyry copper mineralization be generated by a typical calc-alkaline melt? *Journal of Geophysical Research: Solid Earth*, 96(B5): 8113-8126.
- compositions. *Proc. World Geother. Congr. 2005, Antalya, Turkey, 24-29 April.*
- Craig, H., 1961. Isotopic variations in meteoric waters. *Science* 133, 1702-1703.
- Craig, H., 1963. The isotopic geochemistry of water and carbon in geothermal areas, Nuclear geology on geothermal areas, Spoleto Conference Proceedings, 1963, pp. 17-53.
- Craig, H., Clarke, W.B., Beg, M.A., 1975. Excess ^3He in deep water on the East Pacific Rise. *Earth Planet. Sci. Lett.* 26, 125-132.
- Craig, H., Lupton J.E., Welhan J.A., Poreda R., 1978. Helium isotope ratios in Yellowstone and Lassen Park volcanic gases. *Geophys. Res. Lett.* 5, 897-900.
- Crowe, B. M., Finnegan, D. L., Zoller, W. H. and Boynton, W. V., 1987. Trace element geochemistry of volcanic gases and particles from 1983-1984 eruption episodes of Kilauea volcano. *J. Geophys. Res.* 92, 13,708-13,714.
- Darling, G, Ármannsson, H., 1989. Stable isotope aspects of fluid flow in the Krafla, Námafjall and Theistareykir geothermal systems of northeast Iceland. *Chem. Geol.* 76, 197-213.

- Dauphas, N., and Rouxel, O. 2006. Mass spectrometry and natural variations of iron isotopes. *Mass Spectrometry Reviews*, 25(4), 515–550. doi:10.1002/mas.20078
- Delmelle, P. and Bernard, A., 1994. Geochemistry, mineralogy, and chemical modeling of the acid crater lake of Kawah Ijen Volcano, Indonesia. *Geochimica et cosmochimica acta*, 58(11): 2445-2460.
- Edmonds, M., Mather, T.A. & Liu, E.J., 2018. A distinct metal fingerprint in arc volcanic emissions. *Nature Geosci* 11, 790–794, <https://doi.org/10.1038/s41561-018-0214-5>
- Eggertsson, G.H., Lavallée, Y., Kendrick, J.E., Markússon, S.H., 2020. Improving fluid flow in geothermal reservoirs by thermal and mechanical stimulation: The case of Krafla volcano, Iceland. *J. Volcanol. Geotherm. Res.* 391, 106351.
- Eichelberger, J.C., 1995. Silicic volcanism: ascent of viscous magmas from crustal reservoirs. *Annual Review of Earth and Planetary Sciences*, 23(1): 41-63.
- Einarsson, P., 2008. Plate boundaries, rifts and transforms in Iceland: *J kull*, v. 58, p. 35-58.
- Ellis, A., 1979. Explored geothermal systems. *Geochemistry of hydrothermal ore deposits*: 465-514.
- Fernández, D. P., Goodwin, A. R. H., Lemmon, E. W., Levelt Sengers, J. M. H., & Williams, R. C. (1997). A Formulation for the Static Permittivity of Water and Steam at Temperatures from 238 K to 873 K at Pressures up to 1200 MPa, Including Derivatives and Debye–Hückel Coefficients. *Journal of Physical and Chemical Reference Data*, 26(4), 1125–1166. doi:10.1063/1.555997
- Fischer, T.P., Sturchio, N.C., Stix, J., Arehart, G.B., Counce, D. and Williams, S.N., 1997. The chemical and isotopic composition of fumarolic gases and spring

discharges from Galeras Volcano, Colombia. *Journal of Volcanology and Geothermal Research*, 77(1): 229-253.

Füri, E., Hilton, D.R., Halldórsson, S.A., Barry, P.H., Hahn, D., Fischer, T.P., Grönvold, K., 2010. Apparent decoupling of the He and Ne isotope systematics of the Icelandic mantle: the role of He depletion, melt mixing, degassing fractionation and air interaction. *Geochim. Cosmochim. Acta* 74, 3307–3332.

Gamo, T., Ishibashi, J., Tsunogai, U., Okamura, K. and Chiba, H., 2006. Unique Geochemistry of Submarine Hydrothermal Fluids from Arc-Back-Arc Settings of the Western Pacific. *Back-arc spreading systems: geological, biological, chemical, and physical interactions*: 147-161.

Gamo, T., Okamura, K., Charlou, J.-L., Urabe, T., Auzende, J.-M., Ishibashi, J., Shitashima, K. and Chiba, H., 1997. Acidic and sulfate-rich hydrothermal fluids from the Manus back-arc basin, Papua New Guinea. *Geology*, 25(2): 139-142.

Gautason, B., Gudmundsson, Á., Hjartarson, H., Blischke, A., Mortensen, A.K., Ingimarsdóttir, A., Gunnarsson, H.S., Sigurgeirsson, M.Á., Árnadóttir, S., Egilson, Th., 2010. Exploration drilling in the Theistareykir high-temperature field, NE-Iceland: Stratigraphy, alteration and its relationship to temperature structure. *Proc. World Geother. Congr. 2010, Bali, Indonesia*, 5 pp.

Gena, K., Mizuta, T., Ishiyama, D. and Urabe, T., 2001. Acid-sulphate Type Alteration and Mineralization in the Desmos Caldera, Manus Back-arc Basin, Papua New Guinea. *Resource Geology*, 51(1): 31-44.

Giggenbach, W., 1992. Isotopic shifts in waters from geothermal and volcanic systems along convergent plate boundaries and their origin. *Earth and planetary science letters*, 113(4): 495-510.

Gíslason, G., and Arnórsson, S., 1976. Framvinduskýrsla um breytingar á rennsli og efnainnihaldi í borholum 3 og 4 í Kröflu (A progress report on flow and chemical

composition of fluids from boreholes 3 and 4 in Krafla). Orkustofnun, report OS-JHD-7640 (in Icelandic), 14 pp.

Graham, D.W., 2002. Noble gas isotope geochemistry of mid-ocean ridge and ocean island basalts: Characterization of mantle source reservoirs. *Rev. Mineral. Geochem* 47, 247-317.

Grant, J.A. Isocon analysis: A brief review of the method and applications, 2005. *Phys. Chem. Earth Parts A/B/C*, 30, 997–1004.

Guðmundsson A., Myer E. M., Pálmarsson S.O., 2015. Northeast - flow model revision. Engineer Vatnaskil, report 15.05. 98 p.

Guðmundsson, Á., Gautason, B., Axelsson, G., Lacasse, C., Thorgilsson, G., Ármannsson, H., Tulinius, H., Saemundsson, K., Karlsdóttir, R., Kjaran, S.P., Pálmarsson, S.Ó., Halldórsdóttir, S., 2008. A conceptual model of the geothermal system at Theistareykir and a volumetric estimate of the geothermal potential. Iceland GeoSurvey, Mannvit and Vatnaskil Consulting Engineers, report ÍSOR-2008/024 (in Icelandic): 57.

Guðmundsson, J.S., 1983. Geothermal electric power in Iceland: development in perspective. *Energy* 8, 491-513.

Gundfinnsson, G.H., 2014. Alteration in the Theistareykir Geothermal System. A Study of Drill Cuttings in Thin Sections. LV report: LV-2014-063, 110 pp.

Gunnlaugsson, E., Ármannsson, H., Thorhallsson, S., and Steingrímsson, B., 2014. Problems in geothermal operation – Scaling and corrosion. Presented at “Short Course VI on Utilization of Low- and Medium-Enthalpy Geothermal Resources and Financial Aspects of Utilization”, organized by UNU-GTP and LaGeo, in Santa Tecla, El Salvador, March 23-29, 2014. 18 pp.

- Hannington, M., Harðardóttir, V., Garbe-Schönberg, D. and Brown, K.L., 2016. Gold enrichment in active geothermal systems by accumulating colloidal suspensions. *Nature Geoscience*, 9(4): 299-302.
- Harðardóttir, S., Halldórsson, S.A., Hilton, D.R., 2018. Spatial distribution of helium isotopes in Icelandic geothermal fluids and volcanic materials with implications for location, upwelling and evolution of the Icelandic mantle plume. *Chem. Geol.* 480, 12-27.
- Hardardottir, V., Brown, K.L., Fridriksson, T., Hedenquist, J.W., Hannington, M.D. and Thorhallsson, S., 2009. Metals in deep liquid of the Reykjanes geothermal system, southwest Iceland: Implications for the composition of seafloor black smoker fluids. *Geology*, 37(12): 1103-1106.
- Harrison, D., Burnard, P.G., Tieloff, M., Turner, G., 2003. Resolving atmospheric contaminants in mantle noble gas analyses. *Geochem. Geophys. Geosyst.* 4, 1023.
- Hattori, K.H. and Keith, J.D., 2001. Contribution of mafic melt to porphyry copper mineralization: evidence from Mount Pinatubo, Philippines, and Bingham Canyon, Utah, USA. *Mineralium Deposita*, 36(8): 799-806.
- Hauksson T., 2018. Theistareykir, Krafla and Bjarnarflag performance of borehole and chemical content of water and steam in boreholes and production process in 2018. Landsvirkjun report LV-2019-026.
- Hauksson, T., and Gudmundsson, 2008: Krafla. Acid wells. Landsvirkjun, report, 17 pp.
- Hedenquist, J. W., S. Taguchi and H. Shinohara, 2018. "Features of Large Magmatic–Hydrothermal Systems in Japan: Characteristics Similar to the Tops of Porphyry Copper Deposits." *Resource Geology* 68(2): 164-180.

- Hedenquist, J.W. and Henley, R.W., 1985. Hydrothermal eruptions in the Waiotapu geothermal system, New Zealand; their origin, associated breccias, and relation to precious metal mineralization. *Economic geology*, 80(6): 1640-1668.
- Hedenquist, J.W. and Lowenstern, J.B., 1994. The role of magmas in the formation of hydrothermal ore deposits. *Nature*, 370(6490): 519-527.
- Hedenquist, J.W., 1998. The influence of geochemical techniques on the development of genetic models for porphyry copper deposits. *Rev. Econ. Geol.*, 10: 235-256.
- Hedenquist, J.W., Arribas, A. and Gonzalez-Urien, E., 2000. Exploration for epithermal gold deposits. *Reviews in Economic Geology*, 13(2): 45-77.
- Hedenquist, J.W., Arribas, A. and Reynolds, T.J., 1998. Evolution of an intrusion-centered hydrothermal system; Far Southeast-Lepanto porphyry and epithermal Cu-Au deposits, Philippines. *Economic Geology*, 93(4): 373-404.
- Hedenquist, J.W., Simmons, S.F., Giggenbach, W.F. and Eldridge, C.S., 1993. White Island, New Zealand, volcanic-hydrothermal system represents the geochemical environment of high-sulfidation Cu and Au ore deposition. *Geology*, 21(8): 731-734.
- Heinrich, C., Günther, D., Audétat, A., Ulrich, T. and Frischknecht, R., 1999. Metal fractionation between magmatic brine and vapor, determined by microanalysis of fluid inclusions. *Geology*, 27(8): 755-758.
- Heinrich, C.A., Ryan, C.G., Mernagh, T.P. and Eadington, P.J., 1992. Segregation of ore metals between magmatic brine and vapor; a fluid inclusion study using PIXE microanalysis. *Economic Geology*, 87(6): 1566-1583.
- Henley, R.W. and Ellis, A.J., 1983. Geothermal systems ancient and modern: a geochemical review. *Earth-science reviews*, 19(1): 1-50.

- Henley, R.W., Barton, P., Truesdell, A. and Whitney, J., 1984. Fluid-mineral equilibria in hydrothermal systems, 1. Society of Economic Geologists El Paso, TX.
- Hermannsson, S., Líndal, B., 1951. Chemical analysis of warm and hot springs. Jarðboranir Ríkisins, State Drilling Company (in Icelandic).
- Hermanská, M., Kleine, B.I., Stefánsson, A., 2020. Geochemical constraints on supercritical fluids in geothermal systems. *Journal of Volcanology and Geothermal Research* 394, doi:10.1016/j.jvolgeores.2020.106824
- Hilton, D.R., Grönvold, K., O'Nions, R.K., Oxburgh, E.R., 1990. Regional distribution of ^3He anomalies in the Icelandic crust. *Chem. Geol.* 88, 53-67.
- Hilton, D.R., Grönvold, K., Sveinbjörnsdóttir, A.E., Hammerschmidt, K., 1998. Helium isotope evidence for off-axis degassing of the Icelandic hotspot. *Chem. Geol.* 149, 173–187.
- Hinkley, T. K., 1991. Distribution of metals between particulate and gaseous forms in a volcanic plume. *Bull. Volcanol.* 53, 395– 400.
- Hinkley, T. K., Lamothe, P. J., Wilson, S. A., Finnegan, D. L. and Gerlach, T. M., 1999. Metal emissions from Kilauea, and a suggested revision of the estimated worldwide metal output by quiescent degassing of volcanoes. *Earth Planet. Sci. Lett.* 170, 315–325.
- Hjartardóttir, Á. R., Einarsson, P., Magnúsdóttir, S., Björnsdóttir, Þ., and Brandsdóttir, B., 2016, Fracture systems of the Northern Volcanic Rift Zone, Iceland: an onshore part of the Mid-Atlantic plate boundary, in Wright, T. J., Ayele, A., Ferguson, D. J., Kidane, T. & Vye-Brown, C., eds., Geological Society, London, Special Publication 420, p. 297-314.

- Horita, J., Wesolowski, D.J., 1994. Liquid-vapor fractionation of oxygen and hydrogen isotopes of water from the freezing to the critical temperature. *Geochim. Cosmochim. Acta* 58, 3425-3437.
- Hu, R., Burnard, P., Turner, G. and Bi, X., 1998. Helium and argon isotope systematics in fluid inclusions of Machangqing copper deposit in west Yunnan Province, China. *Chemical Geology*, 146(1): 55-63.
- Hu, R., Turner, G., Burnard, P., Zhong, H., Ye, Z. and Bi, X., 1998. Helium and argon isotopic geochemistry of Jinding superlarge Pb-Zn deposit. *Science in China Series D: Earth Sciences*, 41(4): 442-448.
- Huttrer, G.W., 2020. Geothermal power generation in the world 2015-2020 Update Report. Proceedings of the World Geothermal Congress 2020. <https://www.geothermal-energy.org/pdf/IGAstandard/WGC/2020/01017.pdf> , 17 pp
- John, D.A., 1991. Evolution of hydrothermal fluids in the Alta stock, central Wasatch mountains, Utah. US Department of the Interior, US Geological Survey.
- Juliusson, E., Markusson, S., Sigurdardottir, A., 2015. Phase-specific and phase-partitioning tracer experiment in the Krafla reservoir, Iceland. Proceedings, World Geothermal Congress.
- Kajugus, 2012. Updated reservoir analysis of the theistareykir high-temperature geothermal field, N-iceland. Geothermal training programme, Orkustofnun, Reykjavik, Iceland.
- Kelley, D. F., and Barton, M., 2008, Pressures of crystallization of Icelandic magmas: *Journal of Petrology*, v. 49, p. 465-492.

- Kendrick, M.A., Duncan, R. and Phillips, D., 2006. Noble gas and halogen constraints on mineralizing fluids of metamorphic versus surficial origin: Mt Isa, Australia. *Chem. Geol.* 235, 325-351.
- Kennedy, B. M., Holohan, E. P., Stix, J., Gravely, D. M., Davidson, J. R. J., and Cole, J. W., 2018, Magma plumbing beneath collapse caldera volcanic systems: *Earth-Science Reviews*, v. 177, p. 404-424.
- Kennedy, B.M., Fischer, T.P., Schuster, D.L., 2000. Heat and helium in geothermal systems, Twenty-Fifth Workshop on Geother. Reser. Engin., Standord University, Stanford, California, SGP-TR-165.
- Kennedy, B.M., Hiyagon, H., Reynolds, J.H., 1991. Noble gases from Honduras geothermal sites. *J. Volcanol. Geotherm. Res.* 45, 29–39.
- Kennedy, B.M., van Soest, M.C., 2007. Flow of mantle fluids through the ductile lower crust: helium isotope trends. *Science* 318, 1433–1436.
- Khodayar, M., Björnsson, S., Kristinsson, S.G., Karlsdóttir, R., Ólafsson, M., Víkingsson, S., 2018. Tectonic control of the Theistareykir geothermal field by rift and transform zones in North Iceland: a multi-disciplinary approach. *Open J. Geol.* 8, 543-584
- Kristinsson, S.G., Fridriksson, Th., Ólafsson, M., Gunnarsdóttir, S.H, Níelsson, S., 2013. The Theistareykir, Krafla and Námafjall high-temperature geothermal areas. Monitoring of surface activity and groundwater. Iceland GeoSurvey, report ÍSOR-2013/037 (in Icelandic), 152 pp.
- Kristmannsdóttir, H., & Ármannsson, H. 2003. Environmental aspects of geothermal energy utilization. *Geothermics*, 32(4-6), 451–461. doi:10.1016/s0375-6505(03)00052-x

- Kristmannsdóttir, H., 1989. Types of scaling occurring by geothermal utilization in Iceland. *Geothermics*, 18(1-2), 183–190. doi:10.1016/0375-6505(89)90026-6
- Krupp, R.E. and Seward, T.M., 1987. The Rotokawa geothermal system, New Zealand; an active epithermal gold-depositing environment. *Economic Geology*, 82(5): 1109-1129.
- Krupp, R.E. and Seward, T.M., 1990. Transport and deposition of metals in the Rotokawa geothermal system, New Zealand. *Mineralium Deposita*, 25(1): 73-81.
- Krupp, R.E., Seward, T.M., 1987. The Rotokawa geothermal system, New Zealand: an active epithermal gold depositing environment. *Economic Geology* 82: 1109-1129
- Kulongoski, J.T., Hilton, D.R., 2011. Applications of Groundwater Helium, *Handbook of Environmental Isotope Geochemistry*, Vol. 1, 1 ed. Springer Isotope Handbook, Reston, VA, pp. 285-304.
- Kurz, M. D., Jenkins, W. J., Hart, S. R. 1982. Helium isotopic systematics of oceanic islands and mantle heterogeneity. *Nature*, 297, 43.
- Lafarge, T., Possolo, A., 2015. The NIST Uncertainty Machine. *NCSLI Measure J Meas. Sci.* 10, 20-27.
- Landis, G.P. and Rye, R.O., 2005. Characterization of gas chemistry and noble-gas isotope ratios of inclusion fluids in magmatic-hydrothermal and magmatic-steam alunite. *Chemical Geology*, 215(1-4): 155-184.
- Langmuir, C.H., Vocke, R.D., Hanson, G.N., Hart, S.R., 1978. A general mixing equation with applications to Icelandic basalts. *Earth Planet. Sci. Lett.* 37, 380-392.

- Lee, B., Unsworth, M., Árnason, K., and Cordell, D., 2020. Imaging the magmatic system beneath the Krafla geothermal field, Iceland: A new 3-D electrical resistivity model from inversion of magnetotelluric data: *Geophysical Journal International*, v. 220, p. 541-567.
- Libbey, R. and Williams-Jones, A., 2016. Lithochemical approaches in geothermal system characterization: An application to the Reykjanes geothermal field, Iceland. *Geothermics*, 64: 61-80.
- Lowenstern J.B., van Hinsberg V., Berlo K., Liesegang M., Iacovino K., Bindeman I.N. and Wright H.M., 2018. Opal-A in Glassy Pumice, Acid Alteration, and the 1817 Phreatomagmatic Eruption at Kawah Ijen (Java), Indonesia. *Front. Earth Sci.* 6:11. doi: 10.3389/feart.2018.00011
- Lund, J.W., Boyd, T.L., 2016. Direct utilization of geothermal energy 2015 worldwide review. *Geothermics* 60, 66-93.
- Lupton, J., Baker, E., Embley, R., Greene, R., Evans, L., 1999a. Anomalous helium and heat signatures associated with the 1998 axial volcano event, Juan de Fuca ridge. *Geophys. Res. Lett.* 26, 3449-3452.
- Lupton, J.E., Baker, E.T., Massoth, G.J., 1999b. Helium, heat, and the generation of hydrothermal event plumes at mid-ocean ridges. *Earth Planet. Sci. Lett.* 171, 343-350.
- MacKenzie, J. M., and Canil, D., 2008. Volatile heavy metal mobility in silicate liquids: Implications for volcanic degassing and eruption prediction. *Earth and Planetary Science Letters*, 269(3-4), 488–496. doi:10.1016/j.epsl.2008.03.005
- MacLennan, J., M. Jull, D. McKenzie, L. Slater, Grönvold, K., 2002. The link between volcanism and deglaciation in Iceland, *Geochem Geophys Geosyst*, 3, 1062, doi:10.1029/2001GC000282.

- Macpherson, C.G., Hilton, D.R., Day, J.M.D., Lowry, D., Grönvold, K., 2005a. High- $^3\text{He}/^4\text{He}$, depleted mantle and low- $\delta^{18}\text{O}$, recycled oceanic lithosphere in the source of central Iceland magmatism. *Earth Planet. Sci. Lett.* 233, 411-427.
- Macpherson, C.G., Hilton, D.R., Mertz, D.F., Dunai, T.J., 2005b. Sources, degassing, and contamination of CO_2 , H_2O , He, Ne, and Ar in basaltic glasses from Kolbeinsey Ridge, North Atlantic. *Geochim. Cosmochim. Acta* 69, 5729-5746.
- Mamyrin, B.A., Tolstikhin, I.N., 1984. Helium isotopes in nature. Elsevier, Amsterdam.
- Manning, A.H. and Hofstra, A.H., 2017. Noble gas data from Goldfield and Tonopah epithermal Au-Ag deposits, ancestral Cascades Arc, USA: Evidence for a primitive mantle volatile source. *Ore Geology Reviews*, 89: 683-700.
- Mather, T. A., Witt, M. L. I., Pyle, D. M., Quayle, B. M., Aiuppa, A., Bagnato, E., et al., 2012. Halogens and trace metal emissions from the ongoing 2008 summit eruption of Kīlauea volcano, Hawaii. *Geochimica Et Cosmochimica Acta*, 83(C), 292–323. <http://doi.org/10.1016/j.gca.2011.11.029>
- Mazor, E., Truesdell, A., 1984. Dynamics of a geothermal field traced by noble gases: Cerro Prieto, Mexico. *Geothermics*, 13(1): 91-102.
- McKennedy, B.M., Fischer, T.P., Schuster, D.L., 2000. Heat and helium in geothermal systems, Twenty-Fifth Workshop on Geother. Reser. Engin., Standord University, Stanford, California, SGP-TR-165.
- Méjean, P., Pinti, D.L., Kagoshima, T., Roulleau, E., Demarets, L., Poirier, A., Takahata, N., Sano, Y., Larocque, M., 2020. Mantle helium in southern quebec groundwater: a possible fossil record of the New England hotspot. *Earth Planet. Sci. Lett.* In press.
- Migdisov, A.A., Williams-Jones, A.E., & Wagner, T., 2009. An experimental study of the solubility and speciation of the Rare Earth Elements (III) in fluoride- and

chloride-bearing aqueous solutions at temperatures up to 300 degrees C. *Geochimica Et Cosmochimica Acta*, 73(23), 7087–7109. <http://doi.org/10.1016/j.gca.2009.08.023>

Migdisov, A. A., Bychkov, A. Y., Williams-Jones, A. E., & van Hinsberg, V. J., 2014. A predictive model for the transport of copper by HCl-bearing water vapour in ore-forming magmatic-hydrothermal systems: Implications for copper porphyry ore formation. *Geochimica et Cosmochimica Acta*, 129, 33–53. doi:10.1016/j.gca.2013.12.024

Moreira, M., J. Kunz, Allègre, C., 1998. Rare gas systematics in Popping Rock: Isotopic and elemental compositions in the upper mantle. *Science* 279, 1178–1181.

Moune, S., Sigmarsson, O., Thordarson, T. and Gauthier, P.-J., 2006. Recent volatile evolution in the magmatic system of Hekla volcano, Iceland. *Earth and Planetary Science Letters*, 255(3-4): 373-389.

Moynier, F., Vance, D., Fujii, T., & Savage, P., 2017. The Isotope Geochemistry of Zinc and Copper. *Reviews in Mineralogy and Geochemistry*, 82(1), 543–600. doi:10.2138/rmg.2017.82.13

Mukhopadhyay, S., 2012. Early differentiation and volatile accretion recorded in deep-mantle neon and xenon. *Nature* 486, 101-124.

Nadeau, O., Stix, J. and Williams-Jones, A.E., 2016. Links between arc volcanoes and porphyry-epithermal ore deposits. *Geology*, 44(1): 11-14.

Nadeau, O., Williams-Jones, A.E. and Stix, J., 2010. Sulphide magma as a source of metals in arc-related magmatic hydrothermal ore fluids. *Nature Geoscience*, 3(7): 501-505.

Nieva, D., Quijano, L., Garfias, A., Barragán, R.M., Laredo, F., 1983. Heterogeneity of the liquid phase, and vapour separation in Los Azufres (Mexico) geothermal

reservoir, Ninth Workshop Geothermal Reservoir Engineering, Stanford University, California, USA, pp. 253-260.

Norton, D.L., 1984. Theory of Hydrothermal Systems. *Annu. Rev. Earth Planet. Sci.* 12, 155-177.

O'Nions, R.K., Oxburgh, E.R., 1983. Heat and helium in the Earth. *Nature* 306, 429-431.

Óskarsson, F., Ármannsson, H., Ólafsson, M., Sveinbjörnsdóttir, Á.E., Markússon, S.H., 2013. The Theistareykir geothermal field, NE Iceland: fluid chemistry and production properties. *Proc. Earth Planet. Sci.* 7, 644–647.

Oxburgh, R.E., O'Nions, R.K., 1987. Helium loss, tectonics and the terrestrial heat budget. *Science* 237, 1583-1588.

Ozima, M. and Podosek, F.A., 1983. *Noble Gas Geochemistry*. Cambridge University Press, Cambridge.

Paonita, A., 2005. Noble gas solubility in silicate melts: a review of experimentation and theory, and implications regarding magma degassing processes. *Annals of Geophysics*, 48(4-5).

Pedersen, R., Sigmundsson, F., Masterlark, T., 2009. Rheologic controls on inter-rifting deformation of the Northern Volcanic Zone, Iceland. *Earth Planet. Sci. Lett.* 281, 14–26.

Petrov, S., 2004. Economic deposits associated with the alkaline and ultrabasic complexes of the Kola Peninsula. Phoscorites and carbonatites from mantle to mine: the key example of the Kola Alkaline Province. *Mineral. Soc. Ser.* 10: 469-490.

- Pinti, D.L.; Haut-Labourdette, M.; Poirier, A.; Saby, M.; van Hinsberg, V.J.; Berlo, K.; Castro, M.C.; Gautason, B.; Sigurðardóttir, Á.K., 2022. $^{87}\text{Sr}/^{86}\text{Sr}$ Ratios and Atmospheric Noble Gases in Theistareykir Geothermal Fluids: A Record of Glacial Water. *Geosciences*, 12, 119. <https://doi.org/10.3390/geosciences12030119>
- Pinti, D. L., Castro, M. C., López-Hernández, A., Hernández Hernández, M. A., Richard, L., Hall, C. M., Shouakar-Stash, O., Flores-Armenta, M. and Rodríguez-Rodríguez, M. H., 2019. Cerro Prieto Geothermal Field (Baja California, Mexico) – A fossil system? Insights from a noble gas study. *J. Volcanol. Geother. Res.* 371: 32-45.
- Pinti, D.L., Castro, M.C., Lopez-Hernandez, A., Han, G., Shouakar-Stash, O., Hall, C.M. and Ramírez-Montes, M., 2017. Fluid circulation and reservoir conditions of the Los Humeros Geothermal Field (LHGF), Mexico, as revealed by a noble gas survey. *Journal of Volcanology and Geothermal Research*, 333: 104-115.
- Pinti, D.L., Castro, M.C., Shouakar-Stash, O., Tremblay, A., Garduño, V.H., Hall, C.M., Hélie, J.F. and Ghaleb, B., 2013. Evolution of the geothermal fluids at Los Azufres, Mexico, as traced by noble gas isotopes, $\delta^{18}\text{O}$, δD , $\delta^{13}\text{C}$ and $^{87}\text{Sr}/^{86}\text{Sr}$. *Journal of Volcanology and Geothermal Research*, 249: 1-11.
- Pokrovski, G. S., Roux, J., Harrichoury, J.-C. 2005. Fluid density control on vapor-liquid partitioning of metals in hydrothermal systems. *Geology*, 33, 657– 660
- Pokrovski, G.S., Borisova, A.Y. and Harrichoury, J.-C., 2008. The effect of sulfur on vapor–liquid fractionation of metals in hydrothermal systems. *Earth and Planetary Science Letters*, 266(3): 345-362.
- Pope, E.C., Bird, D.K., Arnórsson, S., Fridriksson, Th., Elders, W.A., Fridleifsson, G.Ó., 2009. Isotopic constraints on ice age fluids in active geothermal systems: Reykjanes, Iceland. *Geochim. Cosmochim. Acta*, 73, 4468–88.

- Pope, E.C., Bird, D.K., Arnórsson, S., Giroud, N., 2016. Hydrogeology of the Krafla geothermal system, northeast Iceland. *Geofluids* 16, 1–23.
- Poreda, R., Craig, H., Arnórsson, S. and Welhan, J., 1992. Helium isotopes in Icelandic geothermal systems: I. ^3He , gas chemistry, and ^{13}C relations. *Geochimica et cosmochimica acta*, 56(12): 4221-4228.
- Poreda, R.J., and Arnórsson, S., 1992a. Helium isotopes in Icelandic geothermal systems: II. Helium-heat relationships. *Geochim. Cosmochim. Acta* 56, 4229-4235.
- Poreda, R.J., Craig, H., Arnórsson, S., Welhan, J.A., 1992b. Helium isotopes in Icelandic geothermal systems: I. ^3He , gas chemistry, and ^{13}C relations. *Geochim. Cosmochim. Acta* 56, 4221–4228.
- Rae, A.J., Cooke, D.R., Brown, K.L., 2011. The trace metal chemistry of deep geothermal water, Palinpinon Geothermal Field, Negros Island Philippines: implications for precious metal deposition in epithermal gold deposits. *Economic Geology* 106:1425-1446
- Ragnarsson Á., Steingrímsson B., Thorhallsson S., 2020. Geothermal development in Iceland, 2015-2019. *Proc. World Geother. Congr. 2020*, paper 01063
- Reed, M.H. and Spycher, N.F., 1984. Calculation of pH and mineral equilibria in hydrothermal waters with application to geothermometry and studies of boiling and dilution. *Geochim. Cosmochim. Acta* 48, 1479–1492.
- Reeves, E.P., Seewald, J.S., Saccocia, P., Bach, W., Craddock, P.R., Shanks, W.C., Sylva, S.P., Walsh, E., Pichler, T. and Rosner, M., 2011. Geochemistry of hydrothermal fluids from the PACMANUS, Northeast Pual and Vienna Woods hydrothermal fields, Manus basin, Papua New Guinea. *Geochimica et Cosmochimica Acta*, 75(4): 1088-1123.

- Reimann, C., & de Caritat, P. (1998). *Chemical Elements in the Environment*. doi:10.1007/978-3-642-72016-1
- Ridley, J., 2013. *Ore deposit geology*. Cambridge University Press.
- Robb, L., 2005. *Introduction to ore-forming processes*. John Wiley & Sons.
- Rusk, B.G., Reed, M.H. and Dilles, J.H., 2008. Fluid inclusion evidence for magmatic-hydrothermal fluid evolution in the porphyry copper-molybdenum deposit at Butte, Montana. *Economic Geology*, 103(2): 307-334.
- Rusk, B.G., Reed, M.H., Dilles, J.H., Klemm, L.M. and Heinrich, C.A., 2004. Compositions of magmatic hydrothermal fluids determined by LA-ICP-MS of fluid inclusions from the porphyry copper–molybdenum deposit at Butte, MT. *Chemical Geology*, 210(1): 173-199.
- Saar, M.O., Castro, M.C., Hall, C.M., Manga, M., Rose, T.P., 2005. Quantifying magmatic, crustal, and atmospheric helium contributions to volcanic aquifers using all stable noble gases: implications for magmatism and groundwater flow. *Geochem. Geophys. Geosyst.* 6, Q03008. <http://dx.doi.org/10.1029/2004GC000828>.
- Saby, M., van Hinsberg V., Pinti, D.L., Berlo K., Gautason B., Sigurðardóttir Á., Brown K., Rocher O. *The Behaviour of Metals in Deep Fluids of NE Iceland*. Submitted to *Scientific Reports* (July 2022).
- Saby, M. Pinti, D.L., van Hinsberg, V., Gautason, B., Sigurðardóttir, Á., Castro, M.C., Hall, C., Óskarsson, F., Rocher, O., Hélie, J-F., Mejean, P., 2020. Sources and transport of fluid and heat at the newly-developed Theistareykir Geothermal Field, Iceland. *Journal of Volcanology and Geothermal Research*. 405. 107062. [10.1016/j.jvolgeores.2020.107062](https://doi.org/10.1016/j.jvolgeores.2020.107062).

- Saemundsson, K., 1974, Evolution of the axial rifting zone in northern Iceland and the Tj rnes Fracture Zone: Geological Society of America Bulletin, v. 85, p. 495-504.
- Saemundsson, K., 2007. The geology of Theistareykir. Iceland GeoSurvey, short report ÍSOR-07270 (in Icelandic): 23.
- Samson, I.M., Williams-Jones, A.E., Ault, K.M., Gagnon, J.E. and Fryer, B.J., 2008. Source of fluids forming distal Zn-Pb-Ag skarns: Evidence from laser ablation–inductively coupled plasma–mass spectrometry analysis of fluid inclusions from El Mochito, Honduras. *Geology*, 36(12): 947-950.
- Sano, Y. and Fischer T.P., 2013. The Analysis and Interpretation of Noble Gases in Modern Hydrothermal Systems. The Noble Gases as Geochemical Tracers. P. Burnard. Berlin, Heidelberg, Springer Berlin Heidelberg: 249-317.
- Sano, Y. and Wakita, H., 1985. Geographical Distribution of $^3\text{He}/^4\text{He}$ Ratios in Japan: Implications for Arc Tectonics and Incipient Magmatism. *Journal of Geophysical Research* 90, 8729-8741.
- Sano, Y., Takahata, N., Seno, T., 2006. Geographical Distribution of $^3\text{He}/^4\text{He}$ Ratios in the Chugoku District, Southwestern Japan. *Pure Appl. Geoph.* 163, 745-757.
- Sano, Y., Wakita, H., 1985. Geographical Distribution of $^3\text{He}/^4\text{He}$ Ratios in Japan: Implications for Arc Tectonics and Incipient Magmatism. *J. Geophys. Res.* 90, 8729-8741.
- Saunders, J.A., Hofstra, A.H., Goldfarb, R.J. and Reed, M.H., 2014. 13.15 - Geochemistry of Hydrothermal Gold Deposits A2 - Holland, Heinrich D. In: K.K. Turekian (Editor), *Treatise on Geochemistry (Second Edition)*. Elsevier, Oxford, pp. 383-424.

- Sawkins, F.J. and Scherkenbach, D.A., 1981. High copper content of fluid inclusions in quartz from northern Sonora: Implications for ore-genesis theory. *Geology*, 9(1): 37-40.
- Seewald J.F. and Seyfried W.E., 1990. The effect of temperature on metal mobility in subseafloor hydrothermal systems: constraints from basalt alteration experiments. *Earth and Planetary Science Letters*, 101 : 2–4, 388-403.
- Seo, J.H., Guillong, M. and Heinrich, C.A., 2009. The role of sulfur in the formation of magmatic–hydrothermal copper–gold deposits. *Earth and Planetary Science Letters*, 282(1): 323-328.
- Seward, T.M., 1989. The hydrothermal chemistry of gold and its implications for ore formation: Boiling and conductive cooling as examples. *Econ. Geol. Monogr.*, 6: 398-404.
- Seward, T.M., Williams-Jones, A.E. and Migdisov, A.A., 2014. *The Chemistry of Metal Transport and Deposition by Ore-Forming Hydrothermal Fluids*. 29-57.
- Shanks, W.C. and Thurston, R., 2012. *Volcanogenic massive sulfide occurrence model*. US Department of the Interior, US Geological Survey.
- Sheppard, S.M.F., Epstein, S., 1970. D/H and $^{18}\text{O}/^{16}\text{O}$ ratios of minerals of possible mantle or lower crustal origin. *Earth Planet. Sci. Lett.* 9, 232-239.
- Sheppard, S.M.F., Nielsen, R.L., and Taylor, H.P.Jr., 1969. Oxygen and hydrogen isotope ratios of clay minerals from porphyry copper deposits. *Econ. Geol.* 64, 755-777.
- Sherman, L.A. and Barak, P., 2000. Solubility and dissolution kinetics of dolomite in Ca–Mg–HCO/CO solutions at 25 C and 0.1 MPa carbon dioxide. *Soil Science Society of America Journal*, 64(6): 1959-1968.

- Sigmundsson, F., Einarsson, P., Hjartardóttir, A. R., Drouin, V., Jónsdóttir, K., Árnadóttir, T., Geirsson, H., Hreinsdóttir, S., Li, S., Ófeigsson, B.G., 2018. Geodynamics of Iceland and the signatures of plate spreading. *J. Volcanol. Geotherm. Res.* 391, 106436
- Sillitoe, R.H., 2010. Porphyry Copper Systems. *Economic Geology*, 105(1): 3.
- Simmons, S.F. and Brown, K.L., 2006. Gold in magmatic hydrothermal solutions and the rapid formation of a giant ore deposit. *Science*, 314(5797): 288-91.
- Simmons, S.F., Brown, K.L., Browne, P.R.L. and Rowland, J.V., 2016. Gold and silver resources in Taupo Volcanic Zone geothermal systems. *Geothermics*, 59: 205-214.
- Simmons, S.F., Sawkins, F. and Schlutter, D., 1987. Mantle-derived helium in two Peruvian hydrothermal ore deposits. *Nature*, 329(6138): 429-432.
- Simmons, SF, Brown, KL, Tutolo, B.M., 2016. Hydrothermal transport of Ag, Au, Cu, Pb, Te, Zn, and other metals and metalloids in New Zealand geothermal systems: spatial patterns, fluid-mineral equilibria, and implications for epithermal mineralization. *Economic Geology* 111: 589-618
- Simon, A.C., Pettke, T., Candela, P.A., Piccoli, P.M. and Heinrich, C.A., 2006. Copper partitioning in a melt–vapor–brine–magnetite–pyrrhotite assemblage. *Geochimica et Cosmochimica Acta*, 70(22): 5583-5600.
- Smith, S. P., Kennedy, B. M. 1983. The solubility of noble gases in water and in NaCl brine. *Geochim. Cosmochim. Acta.* 47, 503-515.
- Stefánsson, A., Arnórsson, S., 2002. Gas pressures and redox reactions in geothermal fluids in Iceland. *Chem. Geol.* 190, 251–271.

- Stefánsson, A., Arnórsson, S., Sveinbjörnsdóttir, Á.E., 2005. Redox reactions and potentials in natural waters at disequilibrium. *Chem. Geol.* 221, 289–311.
- Stefánsson, A., Hilton, D., Sveinbjörnsdóttir, Á.E., Torsander, P., Heinemeier, J., Barnes, J.D., Ono, S., Halldórsson, S.A., Fiebig, J., Arnórsson, S., 2017. Isotope systematics of Icelandic thermal fluids. *J. Volcanol. Geotherm. Res.* 337, 146–164.
- Stracke, A., Zindler, A., Salters, V. J. M., McKenzie, D., Blichert-Toft, J., Albarède, F. and Grönvold, K., 2003. Theistareykir revisited. *Geochemistry, Geophysics, Geosystems* 4(2).
- Stuart, F. M., Lass-Evans S., Godfrey Fitton J. and Ellam R. M., 2003. High $^3\text{He}/^4\text{He}$ ratios in picritic basalts from Baffin Island and the role of a mixed reservoir in mantle plumes. *Nature* 424(6944): 57-59.
- Stuart, F.M., Burnard, P.G., Taylor, R.P., Turner, G., 1995. Resolving mantle and crustal contributions to ancient hydrothermal fluids: He-Ar isotopes in fluid inclusions from Dae Hwa W-Mo mineralisation, South Korea. *Geochim. Cosmochim. Acta*, 59(22): 4663-4673.
- Stuart, F.M., Lass-Evans, S., Fitton, J.G., Ellam, R.M., 2003. High $^3\text{He}/^4\text{He}$ ratios in picritic basalts from Baffin Island and the role of a mixed reservoir in mantle plumes. *Nature* 424, 57-59.
- Sun, W., Arculus, R.J., Kamenetsky, V.S. and Binns, R.A., 2004. Release of gold-bearing fluids in convergent margin magmas prompted by magnetite crystallization. *Nature*, 431(7011): 975-978.
- Sveinbjörnsdóttir, Á., Ármannsson, H., Ólafsson, M., Óskarsson, F., Markússon, S., Magnúsdóttir, S., 2013. The Theistareykir geothermal field, NE Iceland. Isotopic characteristics and origin of circulating fluids. *Proc. Earth. Planet. Sci.* 7, 822-825.

- Sveinbjörnsdóttir, Á.E., Ármannsson, H., Óskarsson, F., Ólafsson, M., Sigurdardóttir, Á.K., 2015. A conceptual hydrological model of the thermal areas within the Northern neovolcanic zone, Iceland using stable water isotopes. *Proc. World Geother. Congr. 2015*, pp. 1–7.
- Symonds, R.B., Rose, W.I., Reed, M.H., Lichte, F.E. and Finnegan, D.L., 1987. Volatilization, transport and sublimation of metallic and non-metallic elements in high temperature gases at Merapi Volcano, Indonesia. *Geochimica et Cosmochimica Acta*, 51(8): 2083-2101.
- Tivey, M.K., 2007. Generation of seafloor hydrothermal vent fluids and associated mineral deposits. *Oceanography*, 20(1): 50-65.
- Toddsdal, R.M., Dilles, J.H. and Cooke, D.R., 2009. From Source to Sinks in Auriferous Magmatic-Hydrothermal Porphyry and Epithermal Deposits. *Elements*, 5(5): 289-295.
- Torgersen, T. and Jenkins, W., 1982. Helium isotopes in geothermal systems: Iceland, the geysers, raft river and steamboat springs. *Geochimica et Cosmochimica Acta*, 46(5): 739-748.
- Torgersen, T., 2010. Continental degassing flux of ^4He and its variability. *Geochem. Geophys. Geosyst.* 11, Q06002, doi:06010.01029/02009GC002930.
- Torgersen, T., Clarke, W.B., 1985. Helium accumulation in groundwater, I: an evaluation of sources and the continental flux of crustal ^4He in the Great Artesian Basin, Australia. *Geochim. Cosmochim. Acta* 49, 1211-1218.
- Torgersen, T., Kennedy, B.M., Hiyagon, H., Chiou, K.Y., Reynolds, J.H., Clarke, W.B., 1989. Argon accumulation and the crustal degassing flux of ^{40}Ar in the Great Artesian Basin. *Earth Planet. Sci. Lett.* 92, 43-56.

- Turner, G., Stuart, F., 1992. Helium/heat ratios and deposition temperatures of sulphides from the ocean floor. *Nature* 357, 581-583.
- van Hinsberg, V., Vigouroux, N., Palmer, S., Berlo, K., Mauri, G., Williams-Jones, A., et al., 2017. Element flux to the environment of the passively degassing crater lake-hosting Kawah Ijen volcano, Indonesia, and implications for estimates of the global volcanic flux. *Geological Society London Special Publications*, 1–26. <http://doi.org/10.6084/m9.figshare.c.2134359>
- Varekamp, J. C., Ouimette, A. P., Herman, S. W., Bermúdez, A., & Delpino, D., 2001. Hydrothermal element fluxes from Copahue, Argentina: A “beehive” volcano in turmoil. *Geology*, 29(11), 1059. doi:10.1130/0091-7613(2001)029<1059:heffca>2.0.
- Wahrenberger, C., Seward, T. and Dietrich, V., 2002. Volatile trace-element transport in high-temperature gases from Kudriavy volcano (Iturup, Kurile Islands, Russia). *Geochemical Society Special Publication*, 7: 307-327.
- Webster, J.D., 1992. Water solubility and chlorine partitioning in Cl-rich granitic systems: effects of melt composition at 2 kbar and 800 C. *Geochimica et Cosmochimica Acta*, 56(2): 679-687.
- Weiss, R.F., Lonsdale, P., Lupton, J.E., Bainbridge, A.E. and Craig, H., 1977. Hydrothermal plumes in the Galapagos Rift. *Nature*, 267: 600.
- Weissberg, B.G., Browne, P.R. and Seward, T.M., 1979. Ore metals in active geothermal systems. *Geochemistry of hydrothermal ore deposits*: 738-780.
- Williams-Jones, A. and Migdisov, A., 2014. Experimental constraints on the transport and deposition of metals in ore-forming hydrothermal systems. *Society of Economic Geologists*, 18: 77-96.

- Williams-Jones, A., & Heinrich, C., 2005. 100th Anniversary special paper: Vapor transport of metals and the formation of magmatic-hydrothermal ore deposits. *Economic Geology*, 100(7), 1287–1312.
- Williams-Jones, A.E., Migdisov, A.A., Archibald, S.M. and Xiao, Z., 2002. Vapor-transport of ore metals. *Water–Rock Interaction, Ore Deposits, and Environmental Geochemistry: A Tribute to David A. Crerar*: 279-306.
- Winter, J.D., 2001 *An introduction to igneous and metamorphic petrology*: Upper Saddle River. Prentice-Hall Inc., New Jersey.: 697.
- Witham, F., Blundy, J., Kohn, S. C., Lesne, P., Dixon, J., Churakov, S. V., & Botcharnikov, R., 2012. SolEx: A model for mixed COHSCl-volatile solubilities and exsolved gas compositions in basalt. *Computers & Geosciences*, 45, 87–97. doi:10.1016/j.cageo.2011.09.021
- Wu, L.-Y., Hu, R.-Z., Li, X.-F., Stuart, F.M., Jiang, G.-H., Qi, Y.-Q. and Zhu, J.-J., 2017. Mantle volatiles and heat contributions in high sulfidation epithermal deposit from the Zijinshan Cu-Au-Mo-Ag orefield, Fujian Province, China: Evidence from He and Ar isotopes. *Chemical Geology*.
- Yang, K. and Scott, S.D., 2006. Magmatic fluids as a source of metals in seafloor hydrothermal systems. *Back-arc spreading systems: geological, biological, chemical, and physical interactions*: 163-184.
- Yardley, B.W.D. and Bodnar, R.J., 2014. Fluids in the Continental Crust. *GeochemPersp* 3, 1-127; Harlov, D.E., Austrheim, H. (Eds.), *Metasomatism and the Chemical Transformation of Rock: The Role of Fluids in Terrestrial and Extraterrestrial Processes*. Springer Berlin Heidelberg, Berlin, Heidelberg).
- Zajacz, Z., Halter, W.E., Pettke, T. and Guillong, M., 2008. Determination of fluid/melt partition coefficients by LA-ICPMS analysis of co-existing fluid and silicate melt inclusions. *Geochimica et cosmochimica acta*, 72(8): 2169-2197.

Zajacz, Z., Seo, J.H., Candela, P.A., Piccoli, P.M. and Tossell, J.A., 2011. The solubility of copper in high-temperature magmatic vapors: a quest for the significance of various chloride and sulfide complexes. *Geochimica et Cosmochimica Acta*, 75(10): 2811-2827.

Zoller, W. H., Parrington J. R. and Phelan Kotra J. M., 1983. Iridium enrichment in airborne particles from Kilauea volcano – January 1983. *Science* 222, 1118–1121.